

Doctoral theses at NTNU, 2023:428

Anna Hesthagen

Expanding knowledge base for photovoltaic systems' integration by contributing to the development of an experimental testing method for evaluation of their performance as climate screens

Doctoral thesis

NTNU
Norwegian University of Science and Technology
Thesis for the Degree of
Philosophiae Doctor
Faculty of Engineering
Department of Civil and Environmental
Engineering



NTNU

Norwegian University of
Science and Technology

Anna Hesthagen

**Expanding knowledge base for
photovoltaic systems'
integration by contributing to
the development of an
experimental testing method
for evaluation of their
performance as climate screens**

Thesis for the Degree of Philosophiae Doctor

Trondheim, December 2023

Norwegian University of Science and Technology
Faculty of Engineering
Department of Civil and Environmental Engineering



Norwegian University of
Science and Technology

NTNU

Norwegian University of Science and Technology

Thesis for the Degree of Philosophiae Doctor

Faculty of Engineering

Department of Civil and Environmental Engineering

© Anna Hesthagen

ISBN 978-82-326-7556-2 (printed ver.)

ISBN 978-82-326-7555-5 (electronic ver.)

ISSN 1503-8181 (printed ver.)

ISSN 2703-8084 (online ver.)

Doctoral theses at NTNU, 2023:428

Printed by NTNU Grafisk senter

SUMMARY

This thesis aims to expand the knowledge base of solar cell systems called building-integrated photovoltaic (BIPV) systems, their climate screen function, and experimental investigation of wind-driven rain (WDR) exposure. BIPVs are a vital element of zero energy or zero emission buildings (ZEB). BIPV systems are integrated into the building envelope and generate electricity on-site during the expected service lifetime of a system of around 25-30 years. The primary function of a BIPV system is seen as electricity production. Hence, factors that affect it are usually in focus when systems are evaluated and monitored after installation. While its function as a building envelope component is usually not appropriately evaluated, neither before nor after installation. One of the main functions of building envelope components is weather protection of inner building structures. A significant impact of precipitation on the building envelope is represented by WDR (wind-driven rain), a simultaneous occurrence of wind and rain.

Most wind-driven rain testing is done for façade systems, wall-windows, and wall-doors, while much less is published on WDR testing for roof systems. Furthermore, BIPV systems are barely studied as climate screens. In the standard EN 50583-2 “Photovoltaics in buildings. Part 2: BIPV systems”, it is stated that BIPV systems, especially for a roof integration, should be tested to evaluate their performance under exposure to a locally expected wind-driven rain intrusion and water leakages that occur during testing should be quantified. However, no published information can be found on quantifying water leakages for BIPV systems intended for roof integration. Additionally, even though the standard EN 50583-2 states that a water intrusion should be quantified, neither information on a methodology, for that matter, nor details for constructing a water collection system for testing is provided. This thesis bridges this knowledge gap and contributes to the research on WDR testing by investigating selected BIPV systems for roof integration with means of quantitative measurements.

This thesis presents results from experimental testing of a water collection system for quantification of WDR intrusion and provides extensive information on the design and application of BIPV systems designed for roof integration. As a result, a framework is presented, which includes a step-by-step test methodology and a detailed description of the construction of the water collection system. Climate conditions in northern Europe can be quite extreme regarding wind speeds and precipitation. Therefore, it was decided to apply wind speed

ranges from 12.9 m/s (strong breeze) to 35.3 m/s (hurricane), which are extreme levels, but they occur from time to time in Norway, and building components should be able to withstand them. Even though the amount of precipitation can be extreme as well, it was not implemented into the experimental conditions, and the water spray and runoff water rate were left constant during laboratory testing.

This methodology was applied to three BIPV systems designed for roof integration: solar shingles system integrated along metal roof plates, solar roof tiles integrated along dummy roof tiles produced by the same manufacturer, and large glass-glass solar modules integrated along steel roof plates. The watertightness level was determined for all the tested systems. The systems can be ranked according to their watertightness level, i.e., the maximum level of air pressure applied simultaneously with water spray and runoff water when no water leakages occur on the tested system's inner side.

Additionally, quantifying water leakages can provide vital information on changes in the building envelope elements that happen over time. Such changes are usually studied and identified during accelerated ageing testing. Thus, using the present test methodology before and after accelerated aging testing might provide comprehensive information on how the watertightness of tested systems will change over time, what design elements need to be improved, and what changes will occur during a system's service lifetime of 25-30 years.

ACKNOWLEDGEMENTS

My experience with working on PhD thesis was like my experience from a marathon run. Both took me through various stages like excitement, not giving up, “the wall”, pain, wanting to stop and never do it again, and then the last stage when I kept running just because the finish line was too close and giving up was not an option because I invested so much energy, time, and resources into the processes before the marathon. In my case, PhD “marathon” became more like an ultrarun, which was not easy at all, and I had to “run” far more to the final finish line. But as I have been told, when a way is more difficult, it just makes you more resilient and prouder of the result, which I totally agree with. I want to sincerely thank everyone who has given their feedback, comments, and advice on my thesis and the work I have done.

I would like to express my gratitude to my supervisor, professor Bjørn Petter Jelle, for seeing the potential in me and giving me the opportunity to pursue a PhD degree at NTNU (Norges Teknisk Naturvitenskapelige Universitet). His support along the way, ideas, and questions were inevitable for this thesis. Thank you for giving me the freedom to find my own way in research.

I am also extremely grateful for my supervisor, associate professor Bozena Dorota Hrynyszyn, who became a finishing and so needed piece of a puzzle in my PhD. Your willingness to join the work, enthusiasm, and a fresh view on my work improved it tremendously. It almost seemed we were destined to get to work together. Without you, I would not have finished my thesis.

I would like to thank Dr. Stig Geving for giving useful inputs on parameters and important aspects of wind-driven rain testing and for collaborative work on papers.

I would also like to thank NTNU and SINTEF Byggforsk employees for their willingness to help and guide me when it was needed. I want to especially thank Jan Ove Busklein and Ole Aunrønning. Jan Ove was working with me during all laboratory tests in the RAWI box. His help with fixing any problem that occurred was inevitable. Ole was always there to help with lab work, to arrange material supply, to discuss testing of systems, building them and teaching me various technical things. I would not cope with all the work without these two incredible people.

I am very grateful for the support from Jørgen Young from Isola and Karstein Lomundal from Orkla elektronikk. Thank you for helping with aquation of BIPV systems for testing and guidance in installing them. Another person, whom I want to thank is Dr. Gaute Stokkan, thank

you for inviting me to take a look at BIPV installation at your home, for sharing information and experience with your BIPV installation, and for providing me with contacts of BIPV distributor. It was very insightful and gave me a better understanding of BIPV, which additionally boosted my motivation for the subject.

I want to thank “Building integrated Photovoltaics (BIPV) for Norway” team for discussions, meetings, and traveling, for showing me what working in Norway is. I especially want to thank Dr. Tore Kålas for his work and dedication to managing this project. It was a pleasure to work with you all; thank you for being so hospitable and willing to help whenever it was needed.

I want to thank the team of IEA (International Energy Agency) PVPS Task 15 and especially Subtask C for the work and time we spent discussing various aspects of BIPV technologies and how to promote the use of BIPV.

I want to thank the former heads of the department of Civil and Environmental Engineering, Carl and Vikas, for their wise advice and endless encouragement.

I want to sincerely thank the few people who became essential in finishing this thesis. Bozena, Gabriele, Elin, Borgny, Tove, Olav, Kjerstina, and Vikas, thank you for all the help, encouragement, and boost at the last stage of my PhD journey. In my opinion, it is the toughest and the most vital stage of all. Without you, this thesis would not be finished.

This journey would not be the same without two incredible people, Kristoffer and Elida, who have always been there for me, even before I moved to Norway. Thank you for all the walks, talks, celebrations, and movie nights. Thank you for supplying me with a 2,5 kg package of Kvikkklunsj chocolate that you sent me prior to my move to Norway. It made waiting time easier and made me feel like I was already in Norway. You have been through all the ups and downs along the way, and I am forever grateful to have you in my life. During my time in Trondheim, I was fortunate to meet many amazing people. I want to thank Charly, Torgeir, Tanja, Elisa, and Roar for being so nice and welcoming, for your advice, and for our talks about life in Norway, life in general, and so much more. I also want to thank my former office-mate Amin, who gave me particularly useful advice about research, which helped me a lot at the beginning of my PhD study.

My deepest gratitude goes to my parents, who encouraged me to pursue my dreams.

There is one special person whom I am forever grateful for. Vegard, you brighten my every day and make me the luckiest and happiest woman. I cannot imagine my life without you, and

this Ph.D. and my delay with it made it in a way possible for us to meet. But without you, I would not be here wrapping up this thesis. Thank you for all your love, support, jokes, positive outlook on life, and constantly reminding me to focus on the good.

It was a truly indescribable journey of learning, growing, and becoming the person I am now. Even though it was the most demanding thing I have ever done in my life, I look back with enormous gratitude for this experience.

Trondheim 01.09.2023

ACRONYMS AND NOMENCLATURE

Acronyms

a-Si	Amorphous silicon
BAPV	Building-applied photovoltaics
BIPV	Building-integrated photovoltaics
CdTe	Cadmium telluride
CIGS	Copper indium gallium selenide
DRWP	Driving rain wind pressure
LCC	Life cycle cost
mono c-Si	Mono-crystalline silicon cells
poly c-Si	Poly-crystalline silicon cells
PV	Photovoltaics
WDR	Wind-driven rain
ZEB	Zero energy building or zero emissions building
ZEN	Zero emissions neighbourhood

Nomenclature

ΔP	Pa	Air pressure difference
P_d	Pa	Cyclic (pulsating) air pressure
U	m/s	Wind speed
U_{max}	m/s	Maximum wind speed
Q	L/ (min x m)	Runoff rate
	L/ (min x m ²)	Water spray rate
$W_{absorbed}$	L	Absorbed water
$W_{adhered}$	L	Adhered water
$W_{evaporated}$	L	Evaporated water
$W_{impinging}$	L	Impinging water
$W_{infiltrated}$	L	Infiltrated water
W_{runoff}	L	Runoff water
W_{splash}	L	Water splash

APPENDED PAPERS

- I. Anna Fedorova, Bjørn Petter Jelle. *“Building integration of photovoltaics at Nordic climate conditions”* ABS 2017 conference proceeding, 1216-1225.

Presented at Advanced Building Skins conference 2017 in Switzerland and published in the conference proceeding.

- II. Anna Fedorova, Bożena Dorota Hrynyszyn, Bjørn Petter Jelle. *“Building-Integrated Photovoltaics from Products to System Integration – A Critical Review”* IOP: Materials Science and Engineering, 2020.

Presented at 5th World Multidisciplinary Civil Engineering – Architecture – Urban planning symposium WCAUM 2020.

- III. Anna Fedorova, Bjørn Petter Jelle, Bożena Dorota Hrynyszyn, Stig Geving. *“A testing methodology for quantification of wind-driven rain intrusion for building-integrated photovoltaic systems”* Building and Environment, 199, 107917, 2021.

- IV. Anna Fedorova, Bjørn Petter Jelle, Bożena Dorota Hrynyszyn, Stig Geving. *“Quantification of wind-driven rain intrusion in building-integrated photovoltaic systems”* Solar Energy, 230, 376-389, 2021.

CONTENTS

Summary	i
Acknowledgements.....	iii
Acronyms and nomenclature	vii
Appended papers.....	ix
List of figures.....	xiii
List of tables.....	xvii
1 Introduction	1
1.1 Project aim, research question and objectives.....	5
1.2 Structure of the thesis.....	6
1.3 Limitations	7
2 Building-integrated photovoltaic (BIPV) systems: design, integration, standardization, and maintenance.....	9
2.1 Design of BIPV systems and integration ways	9
2.2 BIPV standardization	20
2.2.1 BIPV related standards	21
2.2.2 PV related standards	22
2.2.3 Building related standards.....	23
2.3 Maintenance of BIPV systems	24
3 Testing methodology	29
3.1 Wind-driven rain impact on the roof cladding	29
3.2 Tests to evaluate waterproofing	33
3.3 Principals and standards of wind-driven rain testing	37
3.4 Wind-driven rain intrusion test examples	42
3.5 Background of wind-driven rain exposure testing of BIPV systems	50
3.6 Comparison of testing methodologies of wind-driven rain exposure on BIPV systems	52
3.7 Designing A water collection SYSTEM for quantification of water intrusion.....	54
4 Laboratory investigation results	67
4.1 Overview of tested BIPV systems.....	67
4.2 Installation of BIPV systems.....	68
4.2.1 BIPV system 1 details.....	68
4.2.2 BIPV system 2 details.....	70

4.2.3	BIPV system 3 details	71
4.3	Testing of BIPV systems.....	73
4.3.1	Testing of BIPV system 1	73
4.3.2	Testing of BIPV system 2	77
4.3.3	Testing of BIPV system 3	79
4.4	Comparison of tested BIPV systems	83
5	Discussion of learning points	85
6	Conclusions regarding the research question and objectives	87
7	Outlook and suggestions for further research.....	93
	References	95
	Scientific papers	103
	Papers overview and their interconnection	103
	I. “Building integration of photovoltaics at Nordic climate conditions”	105
	II. “Building-integrated photovoltaics from products to system integration – a critical review”	117
	III. “A testing methodology for quantification of wind-driven rain intrusion for building-integrated photovoltaic systems”	131
	IV. “Quantification of wind-driven rain intrusion in building-integrated photovoltaic systems”	145

LIST OF FIGURES

Figure 1. (left) Off-grid PV system installed on the façade of a mountain cabin, (middle) building-applied PV (BAPV) system attached on the roof tiles and (right) PV tiles system (BIPV) integrated into the roof. (Photos by Anna Fedorova and Bozena Dorota Hrynyszyn) [14].2

Figure 2. BIPV categories as defined in EN 50583 [17,20]. (A) Sloped, roof-integrated, not accessible from within the building. (B) Sloped, roof-integrated, accessible from within the building. (C) Non-sloped (vertically) mounted, not accessible from within the building. (D) Non-sloped (vertically) mounted, accessible from within the building. (E) Externally integrated, accessible, or not accessible from within the building.9

Figure 3. Examples of BIPV systems according to categories defined in EN 50583 [17,20]. 10

Figure 4. Examples of PV-integration as part of the building skin [21]. 11

Figure 5. Examples of fully integrated in roofs BIPV solutions, as they cover all the surface of the roof (a) [24], (b) [25], (c) [26] and (d) [27]. 12

Figure 6. Examples of in-roof mounting BIPV systems [28]. 13

Figure 7. Examples of PV membranes and metal plates [29]. 13

Figure 8. Examples of solar skylight and glazing [29]. 14

Figure 9. Examples of solar shading and falling protection (i.e. balustrades) [29]. 14

Figure 10. (left) Example of traditional slate roofing tiles [34] and (right) solar shingles installation along traditional slate roofing tiles [35]. 19

Figure 11. Solar shingles installed on pitched roofs [25]. 19

Figure 12. Roof tiles colour variations: antacid, cooper red, light grey, natural red and black [36]. 19

Figure 13. (left) Solar tile made of a ceramic material [37] and (right) their installation on a roof [38].20

Figure 14. (left) Solar tile made of a concrete material and (right) their installation on a roof [39].20

Figure 15. Side section of a sloped ventilated roof structure [64,65].30

Figure 16. A roof construction with (left) a separate wind barrier and an underlayer roof and (right) a combined wind barrier and underlayer roof [19].31

Figure 17. Rainfall impact on roof cladding [74,75].32

Figure 18. Schematic representation of roof cladding response to rainfall impact before raindrop impact – the impinging WDR intensity and the response of the roof at and after raindrop impact (ventilated pitched roof structure [64,65] redrawn based on [67,68]).32

Figure 19. Thermograms captured at (a) 8:00 AM, (b) noon, and (c) 5:00 PM [87].35

Figure 20. Location of points of dry area and area affected by humidity on the subjected wall [87].35

Figure 21. Water monitoring and collection setup. (a) Complete setup with camera and plastic ceiling, (b) the test specimen from bird’s view, (c) leaked water through the roof layer and (d) water collection [104].43

Figure 22. The apparatus for watertightness tests of discontinuous coverings (a) plan and section and (b) isometric drawing [106].44

Figure 23. The apparatus used for waterproofing tests, the transparent box under the sample is visible [106].45

Figure 24. View of the front side of the specimen during testing of tile covering [106].45

Figure 25. View of the specimen of a traditional stone roof carried out by Fasana and Nelva (a) front side of the specimen and (b) back side of the same specimen [106].45

Figure 26. (a) Schematic drawing of the gutter system placed beneath the test specimen showing two points of water collection. (b) Photo of the gutters A3 and A5 placed in the mock-up with the tube connections for the drainage of collected water to the buckets [111].49

Figure 27. Photo of the laboratory setup of the rear face of the mock-up. The collection trays are connected with plastic tubes to buckets placed on weighting scales, which measure the water ingress [111]......49

Figure 28. Roof system tested by Breivik [114].51

Figure 29. Roof systems tested by Andenæs, (a) solar roof tiles and conventional roof tiles, (b) solar shingles in two configurations with four solar shingles and (c) seven solar shingles surrounded by dummy shingles from the same manufacturer [115].52

Figure 30. Large-scale turnable box for rain and wind tightness testing of sloping building surfaces (RAWI box), while test is running (left) and RAWI box without a test sample (right) [114]. Schematic drawing of RAWI box is shown in Figure 29.55

Figure 31. Outline of the water collection system [116].59

Figure 32. The BIPV system during trial runs viewed from the outside (left) and inside (right) of the RAWI box [116].60

Figure 33. The water collection sections viewed from the back side of the BIPV system [116].60

Figure 34. Schematic drawing of sealing tapes layering [116].61

Figure 35. Sealing the edges of the BIPV system using sealing tapes and polyethylene foil (view from the frontside). On the right photo a tube used to measure the differential air pressure is visible lying on the black module [116].61

Figure 36. View of a complete taping from the frontside (left) and from the backside (right) [116].61

Figure 37. (1) Triangle wooden profile covered by duct tape built on the underlayment. (2) Waterproof tape sealing the gap between the underlayment and the triangle wooden profile, and (3) double-sided tape sealing area between the triangle wooden profile and (4) plastic foil [116].62

Figure 38. Schematic drawing of rain tightness test setup with four water collecting sections connected by tubes to four containers where the leakage water was collected. Additionally, a set of 3 tubes was used to measure air pressure difference. Tube 1 for measuring the differential air pressure by the RAWI box, and tubes 2 and 3 for measuring the differential air pressure connected to the external micromanometer. Dimensions of the water collection system are given in Figure 22. Upper sketch depicts a cross section top view of the RAWI box, whereas the lower sketch shows the front face of the RAWI box (see e.g., right photo in Figure 21 for front face of the RAWI box with additional details) [116].63

Figure 39. Rain tightness test setup in the laboratory. The set of 3 tubes to measure air pressure difference are marked. Tube 1 for measuring the differential air pressure by the

RAWI box, and tubes 2 and 3 for measuring the differential air pressure connected to the external micromanometer [116].....64

Figure 40. Summary of the present test methodology [116].65

Figure 41. (left) BIPV system 1 installed on an actual building roof. (middle) Metal plates completing BIPV system at edges. (right) Range of solar shingles: 1 – basic solar shingle; 2 – solar shingle bottom; 3 – solar shingle top; 4 – solar shingle left (photo and drawing by Anna Fedorova).69

Figure 42. Rubber element on upper part of the solar shingle (schematically shown on the drawing to the left and how they are attached on the real roof shown on the photo in the middle) and (right) lower part of the solar shingle. 1 – basic solar shingle, 3 – solar shingle top and 5 – matching glass-glass triangle element on an actual building roof (photo and drawing by Anna Fedorova).69

Figure 43. (left) Front view of the outline of the BIPV system 1. To distinguish components of the system and to make connecting points better visible, solar shingles are left transparent, grey parts are metal plates, and black parts are glass-glass parts without PV cells. (right) BIPV system with completed taping before laboratory testing. View from the bottom of the exterior BIPV system side (photo and drawing by Anna Fedorova).70

Figure 44. (a) Complete solar tile system on an actual building roof [126], (b) solar tile and matching non-solar tile with dimensions, and (c) actual solar tile and dummy tile [126]. The matching tile may seem more of a greyish colour here, but in reality, it is the same black colour as solar tile.70

Figure 45. Front view of the outline of the BIPV system 2 on the left. To distinguish solar tiles from matching tiles they are coloured in dark grey and black (solar tiles) and light grey (matching tiles). In reality, both types of tiles have the same black colour, as shown in BIPV system with completed taping, front view of the exterior BIPV system side, before laboratory testing on the right (photo and drawing by Anna Fedorova).71

Figure 46. (left) BIPV system with vertically orientated modules and (right) horizontally orientated modules installed on an actual building [127].72

Figure 47. BIPV system with horizontally orientated modules integrated with metal roof plates on the left. Steel roof plates installed on an actual building roof on the right [127,128].72

Figure 48. (a) Front view of the outline of the BIPV system and steel roof plates on the left. The BIPV modules are coloured in dark grey, whereas the steel roof plates are coloured in light grey. (b) BIPV system integrated with steel roof plates with completed taping before laboratory testing on the right. (c) Schematic illustration of BIPV module and metal plate. View from the bottom of the exterior BIPV system side (drawings by Anna Fedorova).73

Figure 49. Location of water leakage points for the BIPV system 1 with corresponding colours as given in Table 4. (a) First test phase (inclination 30°); (b) second test phase (inclination 15°). View from the backside of the BIPV system (drawings by Anna Fedorova).75

Figure 50. Location of water leakage points for the BIPV system 1 with corresponding colours as given in Table 11. Second test phase ran for the second time with the BIPV system inclined to 15°. All screws were loosened by three turns each. View from the backside of the BIPV system (drawing by Anna Fedorova).76

Figure 51. Quantitative measurements of water amounts collected during wind-driven rain testing in the RAWI box for the BIPV system 1. 76

Figure 52. Location of water leakage points for the BIPV system 2 with corresponding colours as given in Table 12. (a) first test phase (inclination 30°); (b) second test phase (inclination 15°). View from the backside of the BIPV system (drawings by Anna Fedorova). 78

Figure 53. Quantitative measurements of water amounts collected during wind-driven rain testing in the RAWI box for the BIPV system 2. 79

Figure 54. The rubber sealant profile (marked with white rectangles) between pairs of BIPV modules during wind-driven rain testing in the RAWI box with 30° inclination. A major difference in water leakage intensity between left pairs (no leakage) and right pairs (intense leakage) of the BIPV modules could be observed (photo by Anna Fedorova). 80

Figure 55. The rubber sealant profiles (marked with white rectangles) between the BIPV modules during wind-driven rain testing in the RAWI box with 15° inclination. A major difference in water leakage intensity between left pairs (no leakage) and right pairs (intense leakage) of the BIPV modules could be observed (photo by Anna Fedorova). 81

Figure 56. The rubber profile between the pairs of BIPV modules (marked with white rectangles) inspected after wind-driven rain testing in the RAWI box for the BIPV system 3 installed with steel roof plates. The rubber profile between right pair of modules was dislocated and had lost its sealing function, while the rubber profile between the left pair of modules was still in place and thus no water leaked through it (photo by Anna Fedorova). .. 81

Figure 57. Location of water leakage points for the BIPV system 3 installed with steel roof plates with corresponding colours as given in Table 6. A – first test phase (inclination 30°); b – second test phase (inclination 15°). View from the backside of the BIPV system (drawings by Anna Fedorova). 82

Figure 58. Quantitative measurements of water amounts collected during wind-driven rain testing in the RAWI box for the BIPV system 3 installed with steel roof plates. Note that some of the water collected here has erroneously run through the sealing tape system. 83

Figure 59. The fourth BIPV system that was received for testing but was not tested due to severely damaged during transportation. 85

LIST OF TABLES

Table 1. Categorization by the type of BIPV products [22].	11
Table 2. Categorization by the way BIPV systems could be integrated [23].	11
Table 3. BIPV categorization by BIPV category, type of product (module) and type of system integration.	15
Table 4. BIPV related standards [14].	22
Table 5. Standards of PV industry [14].	23
Table 6. Standards of building industry applicable to BIPV [14].	24
Table 7. Test parameters from EN 50583-2:2016 [20].	39
Table 8. Test parameters from NT Build 421 [100].	40
Table 9. Test parameters from EN 12865:2001 [101].	41
Table 10. Comparison of wind-driven rain exposure test methodologies used for the tested BIPV systems for roof integration [116].	53
Table 11. Test parameters of NT Build 421 [100] compared to parameters used in BIPV systems testing [116].	56
Table 12. Parameters used during wind-driven rain testing [116].	57
Table 13. Parameters of tested BIPV systems.	67
Table 14. Qualitative observations of water leakages during wind-driven rain tightness testing in the RAWI box for the Sunstyle BIPV system.	75
Table 15. Qualitative observations of water leakages during wind-driven rain tightness testing in the RAWI box for the BIPV system 2.	78
Table 16. Qualitative observations of water leakages during wind-driven rain tightness testing in the RAWI box for the BIPV system 3 installed with steel roof plates.	82
Table 17. Watertightness level of tested BIPV systems.	84

1 INTRODUCTION

This chapter briefly introduces to the subject and the research motivation for this doctoral thesis. It further presents the aim and scope of the study, the research questions, and objectives that were set for the research work. The thesis structure and limitations of the study are given at the end of the chapter.

According to the data from the United Nations Environment Programme (UNEP), up to 40% of global energy is consumed by buildings, and they emit approximately 1/3 of greenhouse gas (GHG) emissions [1]. Due to an expected population increase projected to reach 9.7 billion in 2050 [2] and the continuation of its growth in the future, the global energy system will experience additional pressure. With growing energy needs, the issue of GHG emissions exceeding a sustainable level is one of the most significant our society faces, and there is a need to find solutions to cope with it.

Among other ways, GHG emission mitigation could be achieved by energy efficiency and using renewable energy sources. These two measures will be used to achieve decarbonization of the energy system and the building stock by 2050 according to the European Directive (EU) 2018/2001 on the promotion of the use of energy from renewable sources [3] and Directive 2018/844 [4], which amended Directive 2010/31/EU on the energy performance of buildings [5] and Directive (EU) 2012/27/EU on energy efficiency [6]. This perspective is also supported by the United Nations (UN) sustainability goals: 7 “Affordable and clean energy” and 11 “Sustainable cities and communities” [7].

To make the building sector more sustainable, concepts such as zero energy and zero emission buildings (ZEB) [8–10], plus houses [11], and zero emission neighbourhoods (ZEN) [12] have been introduced and actively developed [8]. A promising on-site renewable energy source for buildings is solar energy, particularly photovoltaic (PV) technology, as it provides direct electricity production and can be integrated into the building envelope. In this way, buildings could be converted from energy consumers only to both energy producers and consumers. What is more, the energy produced on the site will already have a lower environmental impact, and if the source of energy is renewable, it will bring additional benefits. Therefore, it will significantly improve the energy balance of ZEB and give economic and environmental benefits [13].

PV modules have been successfully used in the built environment for many decades. PV systems have two main distinctions in the built environment: building-applied PV (BAPV) and building-integrated PV (BIPV). Figure 1 left shows BAPV, where standard PV modules are used at a cabin in a remote area. As there is no connection to the electricity grid, the PV system supplies cabin users with electricity. Figure 1 middle shows another example of a BAPV system utilized on a detached house, and Figure 1 right shows BIPV installation.



Figure 1. (left) Off-grid PV system installed on the façade of a mountain cabin, (middle) building-applied PV (BAPV) system attached on the roof tiles and (right) PV tiles system (BIPV) integrated into the roof. (Photos by Anna Fedorova and Bozena Dorota Hrynyszyn) [14].

In cities, PV systems are usually connected to the electricity grid; this way, excess produced electricity can be supplied to the grid according to an agreement with an electricity provider or distributed among houses in the neighbourhood.

To understand the intended meaning of the terms “BIPV module” and “BIPV system” and to distinguish them from the BAPV term, it referred to the definitions proposed by members of IEA-PVPS Task 15, Subtask C report “International definitions of BIPV” [15]. Definitions are quoted here.

“BIPV modules

A BIPV module is a PV module and a construction product together, designed to be a component of the building. A BIPV module is the smallest (electrically and mechanically) non-divisible photovoltaic unit in a BIPV system, which retains building-related functionality.

PV modules are considered to be building-integrated if the PV modules form a construction product providing a function as defined in the European Construction Product Regulation CPR 305/2011 [16]. Thus, the BIPV module is a prerequisite for the integrity of the building’s functionality. If the integrated PV module is dismantled (in the case of structurally bonded modules, dismantling includes the adjacent construction product), the PV module would have to be replaced by an appropriate construction product.

The building's functions in the context of BIPV are one or more of the following:

- Mechanical rigidity or structural integrity.
- Primary weather impact protection: rain, snow, wind, hail.
- Energy economy, such as shading, daylighting, thermal insulation.
- Fire protection.
- Noise protection.
- Separation between indoor and outdoor environments.
- Security, shelter, or safety.

BIPV system

A BIPV system is a photovoltaic system in which the PV modules satisfy the definition above for BIPV products. It includes the electrical components needed to connect the PV modules to external AC or DC circuits and the mechanical mounting systems needed to integrate the BIPV modules into the building.

PV systems are considered to be building-integrated if the PV modules they utilize fulfil the criteria for BIPV modules as defined in EN 50583 Part 1 [17] and thus form a construction product providing a function as defined in the European Construction Product Regulation CPR 305/2011 [16].

BAPV modules

PV modules are considered to be building-attached if the PV modules are mounted on a building envelope and do not fulfil the above-listed criteria for building integration.

BAPV systems

PV systems are considered to be building-attached if the PV modules they utilize do not fulfil the criteria for BIPV modules as defined in EN 50583 Part 1 [17].”

The building is a multi-complex structure; various materials and building elements are coupled to construct a weather protection screen – the building envelope. Roof and façade systems create the climate screen, protecting the inner building structures and the environment from various climate exposures. The primary layer of a sloped ventilated roof structure, viewed from the outside, is composed of various roof coverings, such as shingles or tiles, whose primary function is to keep as much precipitation out of the inner roof structure as possible [18].

As BIPVs are functional elements of the building envelope, they should maintain the weather protection function on the same level as conventional building elements. One of the primary climate exposures that affect the building envelope is precipitation. All kinds of precipitation, such as horizontal rain, wind-driven rain (WDR), hail, and snow, significantly affect the hygrothermal performance of the building envelope. To ensure that components and systems of the building envelope can sufficiently withstand exposure to various precipitations, they are subjected to numerous tests. Assessment of BIPV systems' watertightness is especially crucial in coastal regions like Nordic regions. It is therefore recommended to test BIPV systems' ability to withstand WDR and have documented performance in order to know strains of what magnitude will be experienced by the roof underlayment [19].

WDR is a significant source of moisture load on the building envelope. The building envelope systems' ability to withstand WDR exposure or finding their watertightness level can be examined in laboratories. Even though primary weather impact protection is stated in CPR No 305/2011 [16] as one of the building envelope functions, there are no requirements for obligatory testing of construction products' watertightness levels in the EU. Therefore, the watertightness testing for the building envelope systems is voluntary and is not required for them to be sold on the market. Such tests may provide valuable information that might be further used to predict product performance and compare various products in the same product range or future product development.

The watertightness level can also be expressed by the limit for water leakage intruding through the system. For BIPV systems intended for roof integration, this aspect is mentioned in the standard EN 50583-2 "Photovoltaics in buildings. Part 2: BIPV systems" in annexe A "Resistance to wind-driven rain of BIPV roof coverings with discontinuously laid elements – test method" [20]:

- "A water collector shall be provided, capable of recording the amount of leakage water during any pressure step in the test."
- "Reference leakage rate $(10 \text{ g/m}^2)/5 \text{ min}$, 5 min being the duration of a single test step in the sub-test."
- "The cases in which leakages exceeding fine spray and wetting on the underside occur are considered as being too severe for the application. In any case, the reference leakage rate of $(10 \text{ g/m}^2)/5 \text{ min}$ shall not be surpassed."

There are four sub-tests (A, B, C, and D) defined in the standard EN 50583-2 [20]; each specifies a WDR combination appropriate to specific climate zones. Sub-test A: low wind speed with severe rainfall rate; Sub-test B: low wind speed with high rainfall rate; Sub-test C: severe wind speed with low rainfall rate; Sub-test D: maximum rainfall rate with no wind (deluge).

As no structural details or drawings of the water collection system are given in EN 50583-2 [20], it is unclear how water collection should be executed. Thus, the research in this thesis focused on designing a water collection system and applying it for water leakage quantification, providing a detailed step-by-step testing methodology. If data on quantified water leakages is available, it may be used to evaluate various systems and rank them according to their watertightness level. It might be beneficial for BIPV systems that are planned to be used in areas with harsher climates and where wind speeds and precipitation levels are excessively varying.

1.1 PROJECT AIM, RESEARCH QUESTION AND OBJECTIVES

This thesis aims to gather a knowledge base of BIPV systems design and technical aspects of integrating PV systems specifically designed for utilizing them in the building envelope, further investigating how they perform as climate screens, concerning wind-driven rain (WDR) exposure. Even though there is a wide variety of BIPV systems on the market, roof-integrated solutions were chosen for investigation. This type of BIPV is the most used for commercial and private buildings, and its market share is the biggest. Thus, it was anticipated to be able to test more systems and collect more data.

The following research question and objectives were formulated:

When integrated into the building envelope, how do BIPV systems perform as climate screens?

- Understanding ways BIPV systems are evaluated nowadays.
- Assessing the possibility of evaluating watertightness of BIPV systems by quantifying wind-driven rain (WDR) intrusion.
- Designing and implementing a water collection system to quantify WDR intrusion during testing.
- Testing BIPV of diverse designs and configurations according to the developed testing methodology.
- Reporting on results and failures during testing in the laboratory.

1.2 STRUCTURE OF THE THESIS

Chapter 1 (the present chapter) introduces the topic of this study. The main research question, with the following objectives, is formulated, which determines the outline and stages of the work.

Chapter 2 gives an overview of BIPV systems design and ways of integration into the building envelope, and a standardization framework is presented. This part of Chapter 2 is published as a review article (Paper II). Additionally, the maintenance of BIPV systems is discussed.

The main body of the thesis begins in Chapter 3, where roof structures typical for BIPV integration are shown, and wind-driven rain impact on the roof cladding is described and illustrated. Tests that can be used to evaluate the watertightness of building components are briefly discussed. Principles of watertightness testing methodology are provided, further presenting an overview of the WDR exposure testing methodologies reviewed and adapted from previous studies. Then, the design of a testing setup and procedure for quantification of water intrusion is explained, suggesting a framework for evaluating BIPV systems as climate screens. It includes a step-by-step test methodology, a detailed description of constructing a water collection system, and a laboratory test setup. The chapter ends with a comparison of the present study to previous studies, highlighting the main improvements. Results from this part of the research were published in a scientific article (Paper III).

Chapter 4 contains data from laboratory experiments, where three BIPV systems for roof integration were investigated. The chapter starts with an overview of the tested BIPV system. Continuing with information about the installation of the systems and then presenting the main results of the present study, these parts are divided into three subchapters that correspond with each tested BIPV system. The chapter ends with a comparison of the tested systems. This chapter represents the central part of the research published as a scientific article (Paper IV).

In Chapter 5, learning points are highlighted and discussed.

Chapter 6 summarises the achievements of the thesis.

In Chapter 7, directions for future research are discussed.

Published papers that formed this thesis's basis are included after Chapter 7 and References.

1.3 LIMITATIONS

Laboratory investigation of large-scale systems takes a considerable amount of time and resources. As the primary goal of the present study was to implement quantification of water intrusion into the test methodology, certain limitations had to be set to optimize the research work. The following limitations were set:

1. BIPV systems with the potential to be integrated into a typical sloped roof construction in cold climate conditions were chosen.
2. The size of a specimen with the BIPV system was limited by the frame size of the RAWI box to around 7.5 m^2 (2.75 m x 2.75 m).
3. Laboratory investigations were limited to quantification of wind-driven rain intrusion.
4. Wind pressure was manipulated during testing, while the amount of water applied was constant.

2 BUILDING-INTEGRATED PHOTOVOLTAIC (BIPV) SYSTEMS: DESIGN, INTEGRATION, STANDARDIZATION, AND MAINTENANCE

This chapter encloses information on BIPV systems' design and variations of their integration into the building envelope. A table with several BIPV products, chosen from the market and illustrations are presented to highlight examples. A comprehensive analysis of primary standards related to BIPV products is presented, including special BIPV standards and construction and photovoltaic sector standards. Maintenance of BIPV systems is discussed, and a causes diagram for decision-making in changing BIPV system elements is presented.

2.1 DESIGN OF BIPV SYSTEMS AND INTEGRATION WAYS

As explained in the introduction, PV systems can be considered building-integrated if they replace building components by providing functions defined in CPR 305/2011 [16]. Integrated BIPV systems cover conventional building components functions, primarily as climate screens, for the layering underneath or the whole building envelope. Part of the requirements in CPR 305/2011 [16] concern designing and building mechanical resistance and stability, safety in case of fire, hygiene and health of people, safety and accessibility in use, protection against noise, as well as energy economy and sustainable use of natural resources.

BIPVs are multi-functional technologies which can be used in both new constructions and existing building projects. BIPV systems can be integrated into roofs, façades or they can be used as shading devices. BIPV can be categorized into five groups according to categories given in the standard EN 50583 [17,20], which explains several ways of BIPV integration into the building envelope. These groups are (A) Sloped, roof-integrated, not accessible from within the building; (B) Sloped, roof-integrated, accessible from within the building; (C) Non-sloped (vertically) mounted, not accessible from within the building; (D) Non-sloped (vertically) mounted, accessible from within the building; (E) Externally integrated, accessible, or not accessible from within the building. Examples are shown in Figure 2.

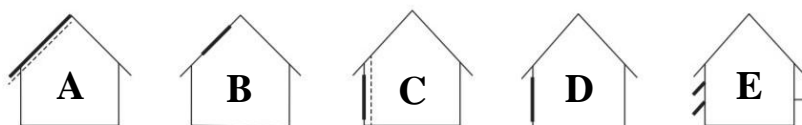


Figure 2. BIPV categories as defined in EN 50583 [17,20]. (A) Sloped, roof-integrated, not accessible from within the building. (B) Sloped, roof-integrated, accessible from within the building. (C) Non-sloped (vertically) mounted, not accessible from within the building. (D) Non-sloped (vertically) mounted, accessible from within the building. (E) Externally integrated, accessible, or not accessible from within the building.

mounted, accessible from within the building. (E) Externally integrated, accessible, or not accessible from within the building.

EN 50583 does not provide examples of BIPV categories; therefore, information about examples and illustrations is given here. BIPV category A includes opaque roof elements such as roof tiles, shingles, PV membranes and metal plates. Category B is mostly represented by skylights and semi-transparent elements; Category C – is by opaque façade elements (cladding systems), or cold façade systems; Category D – is by semi-transparent and transparent façade elements (windows or curtain walls) or warm façade systems; Category E – is by falling protection (i.e., balustrades) and shading devices (either for daylighting or solar control). Figure 3 illustrates these BIPV categories.

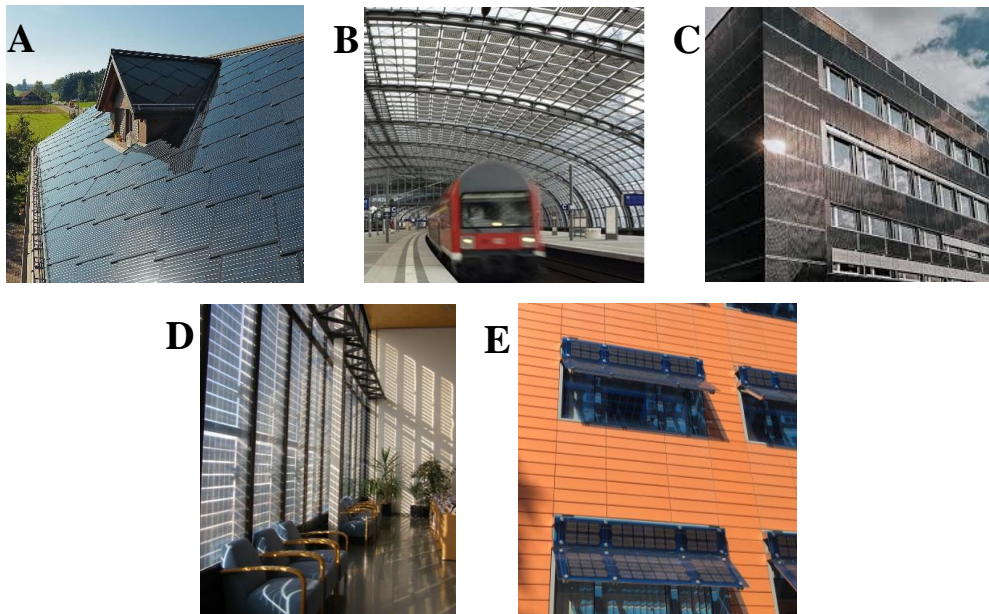


Figure 3. Examples of BIPV systems according to categories defined in EN 50583 [17,20].

Various ways in which BIPV systems can be used in the built environment are summarised and illustrated in Figure 4.

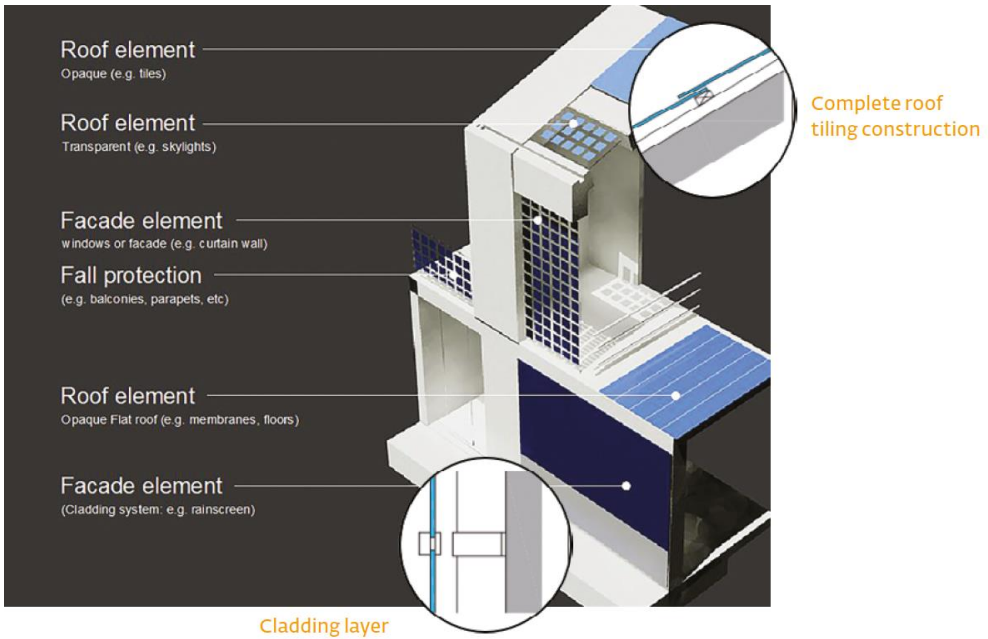


Figure 4. Examples of PV-integration as part of the building skin [21].

BIPV can be additionally categorized by the type of BIPV products [22] (Table 1) and by the type of BIPV systems [23] (Table 2). Examples of BIPV products are shown in Table 3.

Table 1. Categorization by the type of BIPV products [22].

Product type	BIPV foil products	BIPV tile products	BIPV module products	Solar cell glazing products
Specification	Lightweight and flexible, often made from thin-film cells	Normally arranged in modules with the appearance and properties of standard roof tiles	Similar to conventional PV modules, but made with protective weather skin solutions	Utilized in windows, glazing, tiles, facades and roofs, and skylights

Table 2. Categorization by the way BIPV systems could be integrated [23].

System integration	Roof	Façade
Type of integration	Full roof BIPV solutions In-roof mounted system PV membrane, Metal panels	Solar glazing/skylight Cold façade Warm façade Accessories

BIPV solutions fully integrated into a roof can be described as an integrated BIPV system which covers a whole roof area by BIPV products only or by BIPV products and dummy

products (elements that have the same or similar design but do not contain PV elements), preferably manufactured by the same producer. Examples of fully integrated into roofs BIPV solutions are shown in Figure 5.

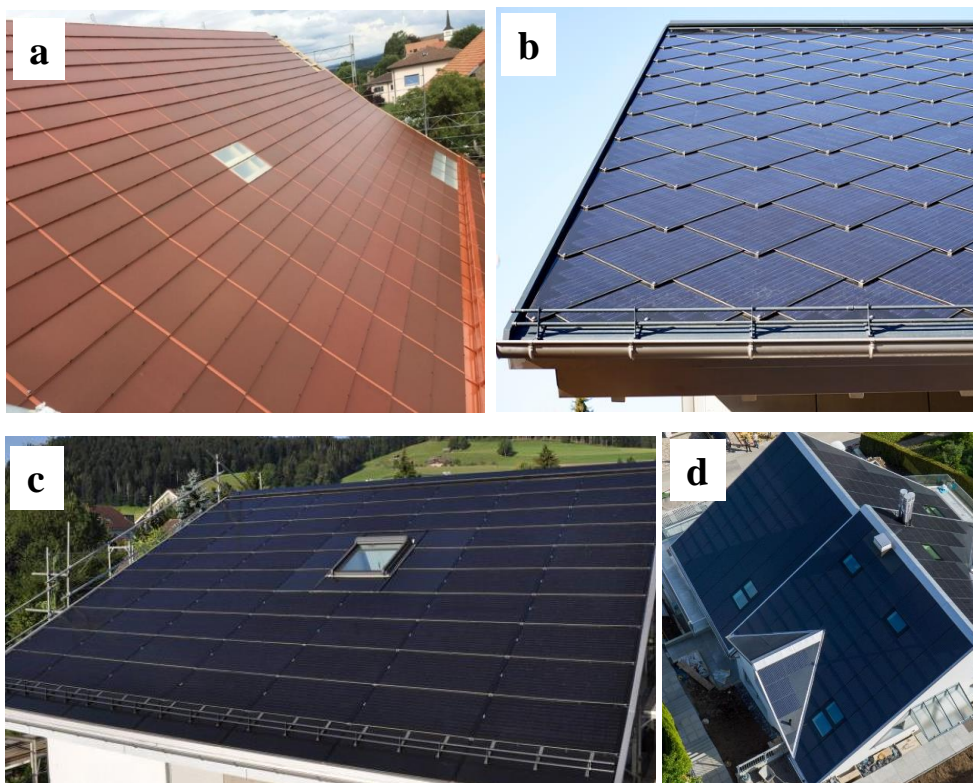


Figure 5. Examples of fully integrated in roofs BIPV solutions, as they cover all the surface of the roof (a) [24], (b) [25], (c) [26] and (d) [27].

In-roof BIPV systems cover part of the whole roof area and are installed along conventional roof coverings. Mounting systems can be used to provide a more seeming connection between BIPV systems and roof coverings. These BIPV systems are especially useful for retrofitting roofs or when a building owner wants to change part of the roof with BIPV system but also wants to retain part of conventional roof coverings. Mounting systems may be designed in two ways: 1 – the mounting system is designed to be installed on the roof first, and then BIPV modules are installed on it; 2 – fastening system is integrated with PV modules, so-called prefabricated BIPV system, and then the installed directly on the roof. Examples of in-roof mounting BIPV systems are shown in Figure 6.



Figure 6. Examples of in-roof mounting BIPV systems [28].

PV membranes and metal plates are usually applied to finished and waterproofed roof structures. Examples are shown in Figure 7.

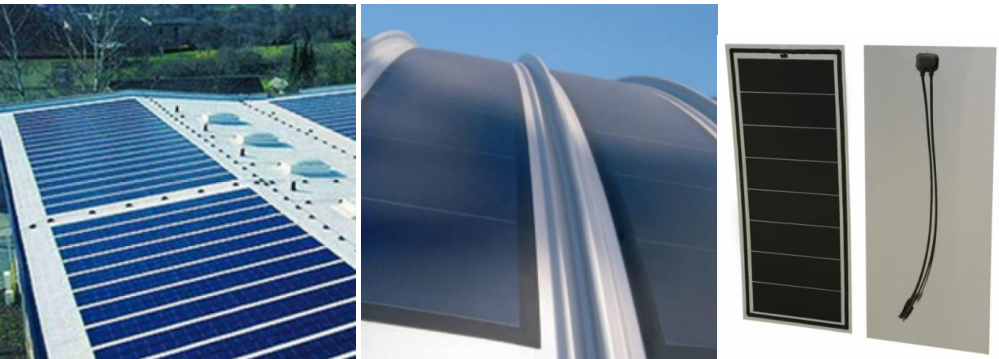


Figure 7. Examples of PV membranes and metal plates [29].

Solar skylight, glazing, and solar shading and falling protection are reminiscent of glass-glass elements used in buildings, as they are PV cells laminated between two safety glass layers and encapsulated within glazed panes. Solar skylight and glazing are often utilized in envelope systems with extruded aluminium frames (but also steel, wood, etc.), similar to a curtain wall. Skylight, a semi-transparent roof, replaces a transparent functional glass façade element with PV glazed panes, whilst the load-bearing part is equipped for the electric wirings' passages. Choosing the optimal cell pattern and assembly provides Solar and daylighting control. Skylights can be used in flat roofs, pitched roofs, and sometimes also in curved surfaces". Solar shading may replace the traditional external louvers. Solar skylight, glazing, and solar shading usually combine glass-glass PV laminates with adjustable light transmission, stimulating the architectural design of light and shadow and performing a fundamental role for the energy

balance of the building [21]. Examples of solar skylight and glazing are shown in Figure 8, and solar shading and falling protection are shown – in Figure 9.



Figure 8. Examples of solar skylight and glazing [29].



Figure 9. Examples of solar shading and falling protection (i.e. balustrades) [29].

PV cell technologies that lead the existing BIPV market are the first-generation PV cells (wafer-based), are similar to the primary PV market of free-standing and rooftop PV applications. These technologies include mono-crystalline silicon cells (mono c-Si) and polycrystalline silicon cells (poly c-Si). A smaller part of the market is shared by the second-generation PV cells (also called thin-film solar cells), i.e., amorphous silicon (a-Si), cadmium telluride (CdTe) and copper indium gallium selenide (CIGS). The third-generation PV cells are not included, as their market share is minimal [30].

Additionally, BIPV products may be subcategorized into two groups: designed and produced for integration and customizable. In Table 3, various selected commercial BIPV products specially designed for integration are presented. Categorizations presented in Figure 3, Tables 1 and 2, are used in Table 3. Such products have lower costs, are available for purchase right away and can be compared with each other. Customizable BIPV products must be designed for each project separately, which leads to higher cost and time constraints; however, they still have an unbeatable advantage. If a project they are anticipated to be part of is large enough,

the cost may be less critical. Furthermore, the building may obtain a unique appearance and be better integrated into the surrounding built environment, as the aesthetics of this type of product is usually of high importance. Companies such as, e.g. Onyx solar, Ertex, and Issol offer a wide range of customizable BIPV products. The substantial similarity of glass-glass PV modules to laminated glass panes simplifies their application as a construction product. Therefore, an extensive amount of glass-glass PV modules is presented on the market. Moreover, large parts of the existing standardization procedures for glass-based construction products can easily be adapted for glass-glass PV modules [31].

Table 3. BIPV categorization by BIPV category, type of product (module) and type of system integration.







Illustration	BIPV category [17,20]	Type of product [22]	Type of system [23]	Type of PV	Specific features	Source
	A	BIPV foil	metal panels	CIGS	Glass-free, suitable for both roofs and facades	https://www.fli-som.com/
	A	solar tile	full roof solution	mono c-Si	Made of composite materials, has a unique tile form that enables water drainage	http://www.or-klaelektronikk.com/new/heda-solar/
	not BIPV	roof tile		no PV	Made of composite materials, compatible tile is produced by the same manufacturer	http://www.or-klaelektronikk.com/new/heda-solar/
	A	solar tile	full roof solution, in-roof	mono c-Si	Beton roof tiles designed with intention to integrate PV cells on them	https://sun-net.no/
	not BIPV	roof tile		no PV	Beton roof tiles compatible to the ones with PV cells	https://www.sk-arpnes.com/
	A	solar tile	full roof solution	poly c-Si	5 colours	https://www.enfsolar.com/pv-panel-datasheet/crystalline/34338

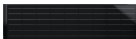



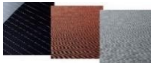
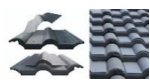







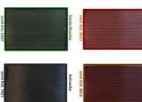



Illustration	BIPV category [17,20]	Type of product [22]	Type of system [23]	Type of PV	Specific features	Source
	A	solar tile	full roof solution	mono c-Si		https://solarstone.ee/en/tiled-roofs/
	A	BIPV tile	full roof solution	mono c-Si	Solar tile that equals to width of four compatible conventional roof tiles	https://www.solinso.nl/
	A	BIPV tile	full roof solution	mono c-Si	Solar tile that equals to width of two compatible conventional roof tiles	https://www.solinso.nl/
	not BIPV	roof tile		no PV	Conventional roof tiles compatible to the ones with PV cells	https://www.solinso.nl/
	A	solar shingle	full roof solution,	mono c-Si	Compatible rubber sealant elements are provided with the Sunstyle solar shingles	https://www.sunstyle.com/en/Home.html
	A	BIPV tile	solar tiles-shingles	not specified	Available in four colours: brown, graphite, red and black	https://www.nelskamp.de/index.php/en/
	A	BIPV tile	solar tiles-shingles	mono c-Si	Compatible roof tiles are available from the same manufacturer	https://www.nelskamp.de/index.php/en/
	A	BIPV module	in-roof system	mono c-Si	Frameless modules specially designed for integration into the rooftop	https://www.solitek.eu/en/products
	C	BIPV module	cold facade	poly c-Si	The series of frameless glass-glass PV panels created for rooftop and BIPV applications	https://www.solitek.eu/en/products

Illustration	BIPV category [17,20]	Type of product [22]	Type of system [23]	Type of PV	Specific features	Source
	A, D	BIPV module	in-roof system, cold facade	CIGS	Only one module size and one colour are available	http://solibro-research.com/en/technology/
	C	BIPV module	cold facade	CIGS	Frameless modules and modules with frame are available	https://www.manz.com/en/markets/solar/cigs-fab/
	B, D	BIPV module, solar cell glazing	solar glazing/skylight	mono and poly c-Si	Can be customized in size and shape of the module	https://mlsystem.pl/bipv-modules/?lang=en
	A	BIPV module	in-roof system	mono c-Si	Capillary system for roof integration, enables water drainage	http://www.sunage.ch/prodotti/
	A, C	BIPV module	in-roof system, warm facade	mono c-Si	Can be customized in size and shape of the module	http://www.sunage.ch/prodotti/
	A, C	BIPV module	in-roof system, warm facade	CdTe	Modules provided already with installation system attached to modules and compatible rubber sealant elements	https://ennogie.com/documentation_uk-2/
	E	Solar cell glazing	solar glazing/skylight	Bi-facial	SOLID Bifacial, created for rooftops and BIPV applications	https://www.solitek.eu/en/products
	E	Solar shading	façade accessories	-	PVSD product from SOLARLAB	[32]

Research presented in this thesis focuses on BIPV systems integrated into sloped roofs. Therefore, it was decided to include a short comparison of BIPV tiles and shingles to conventional roof coverings, which apply in this case.

Solar tiles and shingles are usually designed to resemble conventional roof tiles and shingles as much as possible. It concerns shape, size, and colour of elements. Solar tiles usually consist of a flat roof tile (made of concrete or composite materials) and PV cells encapsulated under the glass that is placed on the roof tile. Solar tiles can be glazed (glass sub/superstrate) or foil-based, i.e., polymer membranes. The tile height is usually equal to the roof tile's row height. The width of the solar tiles varies from small to large (the width of one solar tile equals the width of one or multiple conventional roof tiles). These aspects ensure that the solar tiles will blend in perfectly with the traditional roof tiles. Aesthetics is one of the principal aspects considered in architecture. Regarding the tile size, smaller tiles have the advantage of greater roof filling, providing a better aesthetical look. Larger tiles may potentially cost less, although this has not yet been demonstrated in any of the surveys [21]. Solar shingles are usually constructed with two layers of safety glass with PV cells encapsulated between them. They can be installed with rubber sealant materials or without them. Sealant materials will provide better waterproofness to the system. However, due to the lack of information from manufacturers and the research community on durability and maintenance aspects, it is not evident how these elements will perform during the service life of the BIPV system and whether they need to be changed at some point.

Figure 10 left shows examples of roof installations using traditional slate roofing tiles, while the picture on the right demonstrates solar shingles installed along the same type of slate roofing tiles. Separated parts of the roof are covered either with solar shingles or slate tiles. From an aesthetical point it could be beneficial to choose solar shingles of similar colour. However, then power output is expected to be decreased as the efficiency of coloured BIPV is lower than that of not coloured ones [33]. In Figure 11 full roof installation utilizing solar shingles is demonstrated.



Figure 10. (left) Example of traditional slate roofing tiles [34] and (right) solar shingles installation along traditional slate roofing tiles [35].



Figure 11. Solar shingles installed on pitched roofs [25].

Examples of solar tiles are demonstrated in Figures 13 and 14. Here, ceramic, and concrete roof tiles were used to compound solar tiles. Separate manufacturer produces the original roof tiles, and PV cells are attached afterwards. The roof tile has a flat profile that enables it to cover the front side with a PV element. These tiles are used for sloped roof integration. There are five colours originally available: antacid, cooper red, light grey, natural red and black (shown in Figure 12). However, black ceramic roof tiles with PV elements are available only. Considering emerging interest in coloured PV cells, other colour variations than black is foreseen. Examples of installed systems are presented in Figures 13 and 14.



Figure 12. Roof tiles colour variations: antacid, cooper red, light grey, natural red and black [36].



Figure 13. (left) Solar tile made of a ceramic material [37] and (right) their installation on a roof [38].

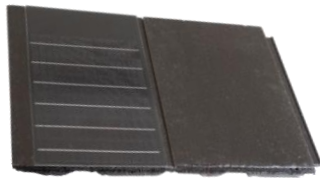


Figure 14. (left) Solar tile made of a concrete material and (right) their installation on a roof [39].

2.2 BIPV STANDARDIZATION

Building integration of PV must always comply with two different standardization and regulation schemes. The first scheme refers to requirements of the building industry, often regulated by local building codes and international (ISO) standards; the second – is to the electrical industry and international (IEC) standards, as well as mandatory local regulations [40]. All PV products must be approved by testing certification authorities and laboratories according to current international standards. At the same time, as PV products designed specifically for building integration still represent a niche market, no harmonized standards for actual testing of these products exist [41]. The first BIPV standard EN 50583 [17,20] was released in 2016, which became a starting point for further work on BIPV standardization. The standard is now under review, and there have been debates whether the watertightness aspect and WDR testing should be in the revised version. There was a meeting within IEA-PVPS Task 15 where several manufacturers of BIPV systems participated. They had concerns about WDR testing; they already have an extensive list of testing and expenses associated with them, and

additional testing was seen as more of an obstacle than an advantage for their products. The information provided by manufacturers is still insufficient for BIPV to fully enter the building sector, as they can only provide primary electrical performance data and standard module durability certification. In contrast, technical requirements for building integration are provided in the installation manuals that are not always readily available and they still might lack some key details [42]. Besides, the information provided in BIPV product data sheets has no defined form, making it harder to compare various products.

2.2.1 BIPV related standards

EN 50583 [17,20] standard classifies BIPV into specific categories and defines a series of requirements for the BIPV products to satisfy building specifications. However, there have also been published studies with BIPV categorizations. This standard applies to photovoltaic systems used as construction products integrated into the building envelope. EN 50583 consists of “Part 1: BIPV modules” and “Part 2: BIPV systems” due to the need to address the photovoltaic modules and their mounting and electrical systems. The focus of EN 50583 is on general, electrical, and building-related requirements, along with requirements for building products with and without glass panes, labelling, system documentation, commissioning tests and inspection requirements. EN 50583 includes an initial list of “basic requirements” for BIPV, and part 2 of this standard includes information about watertightness testing of BIPV systems intended for roof integration however, additional qualities such as durability and reliability, and seismic resistance should also be included when BIPV products are evaluated [40]. An international standard for glass in buildings, ISO 18178 [43], specifies requirements for appearance, durability, and safety as well as test methods and designation for laminated solar photovoltaic (PV) glass for use in buildings, which is defined as laminated glass that integrates the function of photovoltaic power generation. The standard IEC 62980 PV modules for building curtain wall applications were cancelled and incorporated into the new IEC 63092 "Photovoltaics in buildings" (former IEC 63092 "Photovoltaics on the roof") restructured in 2017. For further detailed information on BIPV standardization, refer to the report IEA-PVPS T15-08: 2019 “Analysis of requirements, specifications and regulation of BIPV” [40] and the standards themselves. All currently applicable BIPV standards are presented in Table 4 [14].

Table 4. BIPV related standards [14].

Number	Name
EN 50583-1 [17]	Photovoltaics in buildings. Part 1: BIPV modules.
EN 50583-2 [20]	Photovoltaics in buildings. Part 2: BIPV systems.
ISO 18178 [43]	Glass in buildings - Laminated solar PV glass for use in buildings.
IEC 63092-1 [44]	Photovoltaics in buildings - Part 1: Building integrated photovoltaics modules.
IEC 63092-2 [45]	Photovoltaics in buildings - Part 2: Building integrated photovoltaics systems.

For further BIPV product development, there is a need to define of complementary tests for cases when existing test standards are suitable only for some of the BIPV system types. The results of the existing standards analysis are described in a Tecnia report [41], and the review of standards for BIPV façade and roof integration is given by Rehde et al. [46].

2.2.2 PV related standards

As PV production is a global industry, test centres use common international standards to evaluate PV panels. While the existing standards focus on PV panel quality, performance, and safety to some extent, product reliability must also be considered. Likewise, long-term system performance and energy produced over the system’s service life should also be addressed [47]. The existing primary standards for PV modules are the International Electrotechnical Commission (IEC) standards and the European Standards (EN). IEC and EN standard test requirements initially address the qualification characteristics of PV modules [41]. National standards should also be considered when applying BIPV products in specific countries. From the viewpoint of PV, BIPV should comply with the standards for conventional PV modules such as IEC 61215 (design qualification, etc.) and IEC 61730 (construction requirements, etc.). The commercial success of conventional PV is based on the well-studied long-term reliability of the modules, which was achieved due to PV product qualification and certification, according to IEC 61215. Existing primary standards for PV are presented in Table 5 [14].

Table 5. Standards of PV industry [14].

Number	Name
PV design and performance	
IEC 61215-1 [48] (equal to EN 61215-1)	Terrestrial photovoltaic (PV) modules - Design qualification and type approval - Part 1: Test requirements.
IEC 61215-1-1 [49] (equal to EN 61215-1-1)	Terrestrial photovoltaic (PV) modules - Design qualification and type approval - Part 1-1: Special requirements for testing of crystalline silicon photovoltaic (PV) modules.
IEC 61215-1-2 [50] (equal to EN 61215-1-2)	Terrestrial photovoltaic (PV) modules - Design qualification and type approval - Part 1-2: Special requirements for testing of thin-film Cadmium Telluride (CdTe) based photovoltaic (PV) modules.
IEC 61215-1-3 [51] (equal to EN 61215-1-3)	Terrestrial photovoltaic (PV) modules - Design qualification and type approval - Part 1-3: Special requirements for testing of thin-film amorphous silicon based photovoltaic (PV) modules.
IEC 61215-1-4 [52] (equal to EN 61215-1-4)	Terrestrial photovoltaic (PV) modules - Design qualification and type approval - Part 1-4: Special requirements for testing of thin-film Cu (In, GA) (S, Se) (CIGS) based photovoltaic (PV) modules.
PV safety	
IEC 61730-1 [53]	Photovoltaic (PV) module safety qualification - Part 1: Requirements for construction.
IEC 61730-2 [54]	Photovoltaic (PV) module safety qualification - Part 2: Requirements for testing.

2.2.3 Building related standards

Many building industry standards can apply to BIPV products, but it still needs to be determined which of them must be obligatory and which should be voluntary. Standards concerning various aspects of safety and resistance to load impact must be of high priority. Resistance to rain penetration could be classified as the second priority, as for most buildings a satisfactory rain tightness would be considered obligatory. Two standards that are of particular use for BIPV are ISO 15392 [55] and ISO 15686-1 [56]. ISO 15392 “Sustainability in building construction” could be a roadmap that will help to reach the objectives of sustainable development in buildings, like information on environmental impact, environmental product declaration, the life cycle of the building or construction work, service life and performance requirements, life cycle cost, life cycle environmental assessment, and inclusion of use-phase concerns in project planning. ISO 15686-1 “Buildings and construction assets – service life planning” could be particularly useful when predicting service life and estimation using reference service life and data from practical experience. The service life prediction could be especially challenging for innovative components like the BIPV products. The building industry standards that can be applied to BIPV are presented in Table 6 [14].

Table 6. Standards of building industry applicable to BIPV [14].

Number	Name
ISO 12543 [57]	Glass in building — Laminated glass and laminated safety glass.
IEC TR 63226 [58]	Solar photovoltaic energy systems - Managing fire risk related to photovoltaic (PV) systems on buildings.
ISO 15392 [55]	Sustainability in building construction – general principals.
ISO 15686-1 [56]	Buildings and construction assets – service life planning – part 1: general principals and framework.

Even though BIPV standardization has started to form a durable base for a better representation of BIPV products on the market, there is still a need for further development and work on more harmonized standardization. The necessity and suitability of international standardization for BIPV were defined in the IEA report “Analysis of requirements, specifications and regulation of BIPV” by Berger et al. [40]. In this report, three categories of standardization to be addressed at the international level were proposed: “internationally mandatory “, “useful to design BIPV “, and “useful to characterize BIPV, but no need for pass/fail criteria “.

2.3 MAINTENANCE OF BIPV SYSTEMS

Maintenance is a vital part of keeping a building resilient so that it the building will sufficiently perform its main function during its whole lifetime. The term resilience refers to the capacity of the object to absorb disturbances and retain its basic function [59]. It can also be applied to buildings. Resilience is included in the Sustainable Development Goals (SDGs) number 11 “Make cities and human settlements inclusive, safe, resilient and sustainable”, which focuses on future cities, infrastructure, and buildings [7].

As mentioned earlier, there needs to be more harmonized standards and testing methodologies for BIPV. BIPV systems must comply with the requirements of building construction regulations and building codes, which may vary from country to country [41]. That also affects maintenance as it is not feasible to predict BIPV systems’ behaviour under prolonged exposure to climate conditions in all possible locations. Thus, more attention should be paid when they are applied.

The maintenance of BIPV systems is not usually considered or suggested by the manufacturers, as typically, BIPV systems need little maintenance during their expected service life of 25–30 years. BIPV systems intrinsically have no moving parts. During certification, the BIPV products must withstand various mechanical loads therefore, mechanical stability is ensured before installation. Moreover, if BIPV systems are installed correctly according to the manuals

they are expected to work without mechanical failures. Rarely is it possible to find a maintenance section in the installation or technical documentation supplied with the systems. Firstly, it could be due to the system's operational lifetime. A few system components require replacement during BIPV system service life: an inverter, which requires replacement every ten years, and rubber sealant elements, whose replacement frequency needs to be studied. The rest of the system is expected to work sufficiently during the whole period of operation. It is important to note that producers mainly consider sufficient energy production as the primary function of BIPV. In contrast, building integrity protection should be considered the primary function and, therefore, evaluated in the first place.

Secondly, the cost of maintenance is foreseen to be very low. The costs of repair and replacement of BIPV during the systems lifetime are usually not considered in the lifecycle cost (LCC) of the building [60,61] because calculations represent the economic balance between costs and benefits, and it is difficult to predict whether a part or the entire system will need to be changed. If parts of the system or the entire system are being replaced it could be considered a new system with a new lifecycle and, therefore, a new lifecycle cost. However, special consideration should be made when correcting the LCC of an old system with replaced parts. The building envelope cost, the average maintenance cost of the building envelope, the BIPV cost (including material and mounting) and the average BIPV maintenance cost in the life cycle are calculated in the total cost of initial investment for the building envelope. The life span of the whole building is taken in calculations here. However, prediction of the BIPV system behaviour over period of 20-30 years is still complex. No one can estimate how many parts of the system will need to be replaced. Two possible situations can occur. One is when the BIPV system operates properly, producing the expected amount of electricity with no parts needing replacement – another situation - is when an element or the entire system must be replaced. The replacement cost lies on the shoulders of the installation owner.

The manufacturers ask for a periodic system check usually not specified by any period. The only maintenance operation recommended is installation cleaning, which can increase installation energy production. The need to clean BIPV systems is highly dependent on their location of installation and the meteorological conditions (rain, humidity, wind, dust, etc.), the tilt angle of the system, and the surface morphology. However, as BIPV is a part of the building envelope, it is usually cleaned by rain most of the year, and there is almost no need for extra cleaning. But again, it strongly depends on the location and climate of the installation area. If

the installation requires a more frequent cleaning due to extraordinary climatic conditions, it should be planned in advance and regularly done.

As roof integration was chosen for investigation, maintenance of the roofing cladding is important to include. The maintenance of the roofing cladding can be planned and mostly optimized according to defects occurring during the roof's lifetime. As BIPV roof systems replace existing roofing, it is vital to analyse defects and their causes in usual roofing cladding. The defects in external claddings of roofs could be caused by [62]:

- Design/execution defects – defects in the connections or tail-ends, lack or deterioration of sealants, too little or too much overlap, defects in the thermal insulation, and defects in the ventilation system.
- Cladding degradation – corrosion, spalling/peeling/exfoliation, vegetation growth, colour change/unevenness, disaggregation (ageing), cracking/fracture.
- Condensation.
- Displacement/deformation – significant deformation, misalignment or loosening of cladding elements.

The building's degradation behaviour is strongly influenced by exposure to various environmental stresses. Environmental stresses on roofing can be divided into the following climate exposure factors [63]:

- Solar radiation, including ultraviolet (UV) radiation.
- Mechanical loads (wind, snow loads).
- High and low temperatures.
- Temperature changes/cycles.
- Moisture ingress, relative air humidity, rain, and wind-driven rain.
- Salt water.
- Pollution.
- Erosion.
- Corrosion.
- Abrasion.

Two main groups of defect causes can be identified. Direct causes when the defects are induced by actions in a direct manner. They include mechanical actions and environmental actions. The direct causes are more challenging to predict, as it needs results from climate ageing testing

that is expensive and very time-consuming. Otherwise, prediction can be made according to data collection of existing roofing installation defects. In the second group, indirect causes are assembled, which need an additional force to trigger the pathological process. They comprise design, execution, and use/maintenance errors [62]. Therefore, in contradiction to direct causes, indirect causes induced mainly by people are more accessible to predict and avoid.

The causes of defects in roofing cladding and other building envelope parts can occur due to [62]:

- Design errors – missing or incorrect design of the support structure, errors in the design of the elements and components.
- Execution errors – errors in mounting, installation, and connection of the roofing elements.
- Mechanical actions – deformation of the roof support structure, movement of people or loads over cladding, heavy equipment on the roof.
- Environmental actions – intense winds, solar radiation, rain/snow, chemical action of pigeon-related pollution, biological action.
- Use/maintenance errors – absence/inadequate maintenance, replacement of elements with other or different shapes or colours, change of the initially predicted in-service conditions.

Maintenance of roofing cladding should include diagnosing roofing materials before and during installation. Therefore, design and execution errors can be avoided. Then, periodical inspection (for example, two times a year in spring and autumn, as they come after the most extreme seasons, winter and summer) can identify the starting stages of defects caused by mechanical and environmental actions. If during service life replacement is required, special attention should be paid to choosing the exact same or maximum similar roofing elements to the old ones.

3 TESTING METHODOLOGY

This chapter defines the applied research methods. It describes wind-driven rain impact on the building envelope components, roof cladding response to rainfall impact, and watertightness testing principles. Previous investigations of BIPV systems for roof integration are analysed. It also summarises the experimental setup and analytical analysis used to obtain the answers to the research questions.

3.1 WIND-DRIVEN RAIN IMPACT ON THE ROOF CLADDING

BIPV systems require ventilation underneath them as when they are in service, they heat up, and if no ventilation is present, their power production will significantly decrease [40,46]; at the same time, ageing of the materials under the BIPV systems can be accelerated due to high temperatures [63]. Therefore, a pitched ventilated roof structure is well suited for BIPV systems to be installed on them. The more modern and cost-effective ventilated pitched wooden roof type is when the drainage and ventilation are combined and directly under the roofing (Figure 15) [64]. The primary layer of the pitched ventilated roof structure, viewed from the outside, comprises of various roof coverings, for example shingles or tiles, whose main function is to keep as much precipitation out of the inner roof structure as possible. Under this layer first lies a ventilated air cavity and then the underroof. The underroof is a secondary water barrier - a layer of a wind and waterproof membrane, which ensures that the water that went through the primary layer would not enter the next layers of the roof structure [65]. However, it was found that 50% of building defects with this type of roof structure come from precipitation [64].

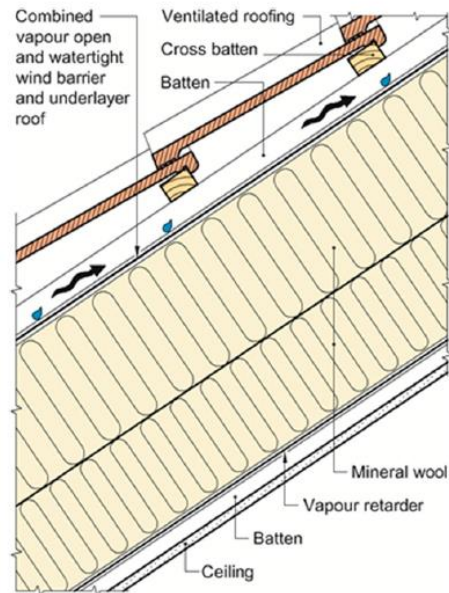


Figure 15. Side section of a sloped ventilated roof structure [64,65].

Figure 16 shows two variations of how roof ventilation may be built [19]. On the left, the underlayer roof is separated from the wind barrier by the air cavity. The underlayer roof is usually vapour tight and the wind barrier is vapour open, so the roof is vented between the underlayer roof and the wind barrier. Such roof construction may also require aeration between the roofing and the underlayer roof. This variation was the traditional way of building ventilated pitched roofs. More modern construction of ventilated pitched roof system (Figure 16 right) utilizes materials that combine the underlayer roof and the wind barrier functions. In this case, the underlayer roof consists of a watertight and vapour open wind barrier and is separated from a rain tight roofing by the ventilation cavity. This more modern way of roof construction is a more environmental conscious and cost effective, as it requires less materials, but it seems that the construction sector prefers previous way of roof construction as it is viewed as more robust [19]. The WDR testing of roofing systems can provide valuable information on rain tightness, promoting the use of more modern roof construction.

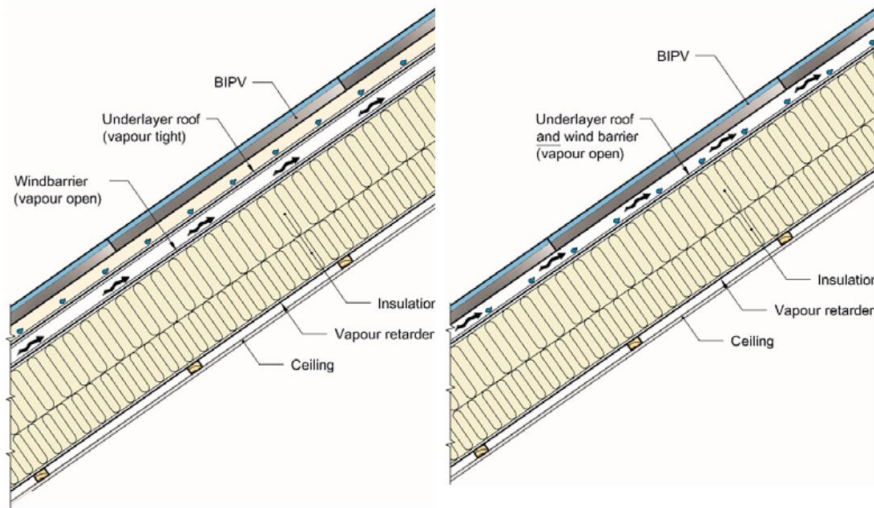


Figure 16. A roof construction with (left) a separate wind barrier and an underlayer roof and (right) a combined wind barrier and underlayer roof [19].

When rain falls on the roof, roof cladding experiences the impact of raindrops and responds to this impact (Figure 17). Raindrops move and distribute as they fall from the clouds while being carried by the wind in the atmospheric boundary layer until they impinge on the building envelope [66,67]. When atmospheric precipitation and wind act simultaneously, it is called wind-driven rain (WDR). Investigation of WDR impact on the building envelope usually consists of two parts: 1 - assessment of the impinging WDR intensity (before raindrop impact) and 2 -assessment of the response of the roof (at and after raindrop impact) [66]. The impinge WDR is the total amount of rainwater that meets the roof surface [68]. Raindrops impinging the roof cladding and collide with the solid surface of the cladding, where several surface phenomena happen, such as spreading, splashing, bouncing, adhesion and absorption of raindrops, film forming, runoff, evaporation, film absorption and the distribution of the moisture in the roofing (wetting-drying), if the material is porous and can absorb water [69–72], and infiltration through the cladding. In this sense, it is assumed that when a raindrop collides with the roof surface, a part of the impinging water is lost by splash, absorption, and immediate evaporation; a part creates the runoff film along the inclined plane, a part remains adhered to the surface of the roofing, and a part is infiltrated. Forces that apply to rainwater penetration mechanisms are hydrostatic pressure, wind pressure, surface tension and gravity [73]. Schematic representation of the WDR impact on the roof before raindrop impact – the impinging WDR intensity and the response of the roof at and after raindrop impact is schematically shown in Figure 18 (based on [67,68]).



Figure 17. Rainfall impact on roof cladding [74,75].

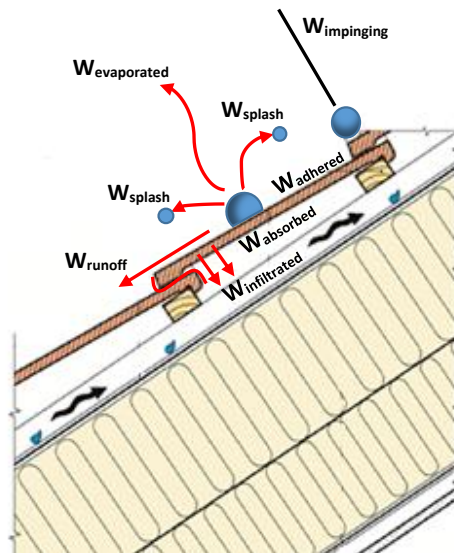


Figure 18. Schematic representation of roof cladding response to rainfall impact before raindrop impact – the impinging WDR intensity and the response of the roof at and after raindrop impact (ventilated pitched roof structure [64,65] redrawn based on [67,68]).

To investigate how roofing performs as the climate screen, a quantification of the water infiltration on the system's backside may be evaluated. The most common way to do it is laboratory investigations of WDR impact on roofing by watertightness testing. Hence, the study of WDR impact could now be extended to three parts instead of two: before raindrop impact, during the wetting process (during raindrop impact and immediately after raindrop impact) and after the wetting process (infiltration). The investigation would now cover the assessment of the response of the roof cladding during all stages of impinging rain impact: contact and surface phenomena, rainwater runoff, and rainwater infiltration. The WDR infiltration loads into the building envelope represent the moisture loads to which the enclosure system is subjected during a rain event and must be managed. It may be possible to calculate

the proportion of the impinging rain that infiltrates through the enclosure to identify WDR infiltration loading.

Other parameters that may be considered during investigations are the impact velocity of the drop, drop diameter and the impact angle. The impact angle affects the water splashing. “At 15°, the splash occurs clearly on both sides of the droplet. However, unbalanced splashing is observed with spreading distance, and splash height in the downhill direction is larger than in the uphill direction. As the inclination angle increases to 30°, the magnitude of splashing is much weaker and only occurs in the downhill direction. Again, the displacement is much larger in the downhill direction. At 45°, the splashing is nearly eliminated, but with significantly higher overall spreading displacement downhill.” [70].

Rain penetration into the building envelope can create problems affecting building materials' durability, such as material degradation, mould growth, and wood decay. Rainwater can reach inner roof structures through the areas where nails and staples fasten the roofing underlayment. To predict moisture damage, rain penetration through roof tiles may be quantified [76]. Several studies investigated WDR exposure on building facades in different countries [77–81], which shows the importance of risk mitigation associated with moisture-related problems.

Another crucial aspect is that it is often not feasible to access information on the methodology and results used for watertightness testing of the building envelope components and systems available on the market. Laboratory investigations are usually carried out by laboratories on assignment by manufacturers, where the results usually are not available to the public. Thus, the building envelope components and systems cannot be compared according to their watertightness quality. In international standards, watertightness is mainly addressed on material or component level [82]. Therefore, a testing methodology that includes the quantification of water intrusion for roof systems would give the opportunity to compare (a) various conventional roof systems with each other, (b) BIPV systems with traditional (non-BIPV) roof systems, and (c) different BIPV systems with each other. Also, developing new BIPV systems may be challenging without a knowledge base of documented performance of such systems and the same information on conventional roof systems.

3.2 TESTS TO EVALUATE WATERPROOFING

There are several test techniques that are used to evaluate waterproofing of building envelope materials: infrared thermography, nuclear moisture testing, electrical impedance testing, electric field vector mapping and wind-driven rain exposure.

Infrared Thermography (IRT) is a non-contact, non-destructive and remote temperature mapping technique to identify causes of deterioration in materials and structures. IRT is the easiest and quickest technique that can be used for the evaluation of large surfaces [83]. The detectors collect infrared radiation emitted by the studied surface. The surface temperature is noted, and results are expressed in a thermal image where measured temperature ranges have each corresponding colour. The obtained thermal images can be evaluated quantitatively or qualitatively [84,85]. The surface temperature distribution can be obtained either by a passive or an active approach. IRT uses a camera with an infrared detector, which absorbs the IR energy emitted by the object, measures surface temperature, and converts it into electrical current. The detection of emitted energy depends on the tested surface's emissivity and the environment. "The thermal energy propagates under the surface by conduction, while the infrared camera monitors surface temperature variations. The temperature distribution is uniform in the case of uniform heating and homogeneous material; the presence of a defect at a certain layer interferes with the propagation of the thermal energy and causes a localised temperature difference. Generally, a deep defect becomes visible later than a subsurface one, and a large defect produces a larger temperature difference than a smaller one. The evolution of the phenomenon can be observed by acquiring sequences of images, which, by means of postprocessing procedures, give information about the size, depth, and thermal resistance of defects." [83].

Even though IRT has much potential in various areas of engineering, its application in building science meets some issues. The Emissivity parameter was identified as essential by Barreira and Freitas [86] as it greatly influences thermographic measurements and may restrict the application of IRT in building science. However, emissivity value is less critical if the investigation aims to analyse results qualitatively.

Surface temperature changes are related to changes in moisture content in building materials and can be identified by IRT due to three physical phenomena: cooling due to evaporation at the surface induces a decrease in the surface temperature, reduces thermal resistance as the heat flow through dry materials is lower than through wet materials, wet materials has increased heat storage capacity and the surface temperature of wet materials responses slower to changes in the air temperature [85].

While studies [83–86] present IRT used in laboratory conditions, Rocha et al. [87,88] presented a field investigation on IRT use for detecting humidity coming from precipitation on existing

buildings. The article showed images of surface temperature during a day in the rainy season (Figures 19 and 20).

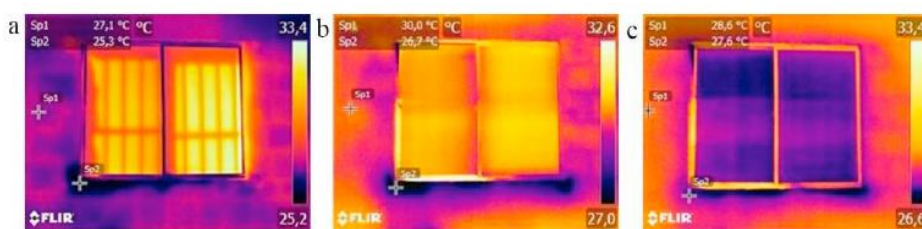


Figure 19. Thermograms captured at (a) 8:00 AM, (b) noon, and (c) 5:00 PM [87].



Figure 20. Location of points of dry area and area affected by humidity on the subjected wall [87].

While the above mentions studies mainly provide qualitative results, Gomes Barbosa et al. [89] presented both qualitative and quantitative results of the façade degradation degree. Qualitative analyses provide the visual difference in the temperature in the thermogram image and identify the thermal image's hot and cold points by colour difference. Quantitative analysis classifies the importance of an anomaly that requires intervention to solve pathological manifestations of defects caused by moisture [89].

Nuclear magnetic resonance (NMR) is a non-destructive testing technique for building materials [90]. Porosity, water content, hydration and damage mechanisms were investigated by quantification and localization of moisture and its bonding state analysis. An NMR tomograph determines moisture contents and hydration processes in building materials. “The tomograph allows measurements along the entire sensitive length of the coils, as well as layer-selective and 2- or 3-dimensional (2D or 3D) measurements” [90]. Kruschwitz et al. [90] measured moisture content in 19 sandstone types in the laboratory. Samples were fully and partially saturated and included oven-drying at 40°, 60°, 70° and 105°. Results showed that NMR tomograph has a high sensitivity and enables detection of low moisture contents. The signal could be measured, and thus, moisture content was identified, even in oven-dried samples [90].

Electrical impedance (EI) testing is another non-destructive method. It is based on the principle that the electrical impedance (the amount of opposition to alternating current (AC)) varies in proportion to the moisture content in the material. A moisture meter is used to conduct EI. Zhang et al. [91] investigated the EI of carbon fibre-reinforced cement-based sensors. AC electrochemical impedance spectroscopy provides reliable and fundamental physicochemical characterizations of materials in terms of pore structures and hydration [91]. The instrument measures the EI of the material by creating a low-frequency AC between two electrodes that are attached to the tested material. Moisture content is read from the surface and further into the material or materials if there are layers of various materials (for example, insulation and membrane material). Dry material creates greater EI than wet [91].

Electric field vector mapping (EFVM) is a non-destructive method of electronic leak detection in roof membranes by tracing an electric current flow across the roof surface [92]. “EFVM is a low-voltage test method that creates an electrical potential difference between a non-conductive membrane surface and conductive structural deck or substrate, which is earthed or grounded” [93]. This method detects leaks in low-slope roofing and waterproofing systems to ensure quality. Unlike other methods like infrared or nuclear testing, vector mapping detects membrane faults directly [92]. This method is used for quality assurance of green (vegetative) and ballasted roofs [92], as EFVM can evaluate leaks through the overburden and ballast while still providing accurate results [93].

Wind-driven rain (WDR) exposure testing evaluates the response of the building to WDR loads [66,77,78]. WDR is characterized by the cooccurrence of rain and wind that causes oblique rain [66]. WDR test is usually done in controlled laboratory conditions. Equipment that is used consists of either a pressure chamber or wind tunnel where wind speed/air pressure can be controlled and changed. Nozzle arrays simulate rain employing water spray and runoff water. The building envelope component is installed on a specimen and placed in the equipment. There are usually transparent windows built in such equipment so the tested system can be viewed from different angles. The inner side of the tested system is visually inspected to identify water intrusion points [66,77,78].

IRT, NMR and EI techniques may be the most useful for porous building materials and materials that absorb some moisture. EFVM technique is usually used for flat or low slope roof cover with membrane. Research in this thesis utilises the WDR test technique as testing of BIPV systems is in focus. BIPV usually consists of PV cells encapsulated between two glass

layers. Water is usually not absorbed by most BIPV systems. Thus, to evaluate the watertightness of such systems, WDR testing is the most suitable method.

3.3 PRINCIPALS AND STANDARDS OF WIND-DRIVEN RAIN TESTING

The principle of the watertightness test for roof coverings is to apply a certain quantity of water spray at various ranges of air pressure differences at various slopes at defined conditions concerning the exterior surface of a roof specimen to observe if water leakages occur [82,94,95]. It is usual to apply a combination of runoff water on an upper side of the tested system and water spray distributed along the test specimen surface area. Simultaneously, a specific level of air pressure difference (ΔP) is reached between the outer and inner surfaces of the tested specimen [95]. A range of air pressure is applied and increased stepwise. The test specimen is inspected for water passages into its inner surface, and water leakage points are registered. As a result, a limit of watertightness can be identified for the tested systems. The limit of watertightness may be described as the maximum level of air pressure applied simultaneously with water spray and runoff water when no water leakages occur on the tested system's inner side. Test parameters from watertightness test standards are water spray and runoff water rates, air pressure and the duration of these parameters [96]. Standards focus on manipulating air pressure ranges, while water spray and runoff water rates are usually kept constant. It could be beneficial to manipulate both parameters to simulate WDR exposure more closely to the one in real conditions. However, this manipulation may be challenging, and more research is needed before implementing it in the laboratory investigation.

The air pressure loads at which water leakages occur and their locations, along with corresponding water leakage intensities, have so far been recorded with the main aim of identifying a qualitative description of the water leakages and the limit of watertightness for the tested building envelope systems. However, to be able to classify tested systems, additional test parameters and measurements should be included. More specifically, the watertightness could be characterized by a measured quantity of water leakages, enabling a comparison between an extensive range of different roof (and facade) products in general and BIPV systems in particular. Thus, in the testing methodology of WDR intrusion for BIPV systems presented herein, a water leakage quantification method is proposed and evaluated.

Several standards provide a methodology for testing the building components against wind-driven rain exposure. The specific standards for BIPV EN 50583-2:2016 "Photovoltaics in buildings. Part 2: BIPV systems" [20] and IEC 63092-2-2020 "Photovoltaics in buildings –

Part 2: Requirements for building-integrated photovoltaic systems” [45] in part describing wind-driven rain exposure testing, refer to the standard CEN/TR 15601:2012 “Hygrothermal performance of buildings – Resistance to wind-driven rain of roof coverings with discontinuously laid small elements – Test method” [97]. The standard 15601 [97] is unfortunately not accessible through the NTNU library system, nor it was possible to purchase access due to excessive cost; therefore, information from this standard cannot be compared to other standards or included in this thesis. The mentioned BIPV standards provide information on test methods that include test conditions for climate zones such as northern Europe (coastal), central Europe, and southern Europe, and four sub-tests for climate zone. These four sub-tests (A, B, C, and D) specify a WDR combination for the mentioned climate zones. Sub-test A: low wind speed with severe rainfall rate; Sub-test B: low wind speed with high rainfall rate; Sub-test C: severe wind speed with low rainfall rate; Sub-test D: maximum rainfall rate with no wind (deluge). According to these BIPV standards, a wind-driven rain test should consist of a set that includes sub-tests B and D and optionally sub-tests A and C. However, there is no explanation or reference to what these test parameters are based on and how they represent real weather conditions.

A table with test conditions provides wind speed and rainfall rates for each climate zone and each sub-test and is modified for roof pitches 15°, 17,5°, 20°, 25°, 30°, 35°, 40° and 45°. Table 7 presents test parameters for coastal climate in Northern Europe. The duration of a step in the sub-tests (A, B and C) is 5 minutes ± 10 seconds, during which wind speed and rainfall rates are kept the same, but they change when roof inclination is changed. In the sub-test (D), the rainfall and runoff were applied without wind for 2 minutes ± 10 seconds. An equation to calculate runoff water from rainfall rate is provided, but it is unclear whether only runoff should be applied at the top of the test specimen or if water spray will be included. This test method also requires quantifying of water leakage that might occur, but no details or examples of a system for water collection are provided.

Blocken and Carmeliet [98,99] investigated an optimal time step of the driving rain load on the building envelope. The experimental time step of 10 minutes was estimated to represent the corresponding driving rain load. EN 50583-2:2016 has time intervals of 5 minutes for sub-tests A, B and C and 2 minutes for sub-test D, which may be too short to be representative of driving rain load.

Table 7. Test parameters from EN 50583-2:2016 [20].

Climate zone	Sub-test	Test conditions				
		Wind speed U (m/s)	Rainfall Rh (mm/h)	Roof pitch α (°)	Wind speed on roof surface u_s (m/s)	Rainfall on roof surface Rt (mm/h)
Northern Europe, coastal	A	5	110	15,5	4,3 ± 0,5	124
				17,5	4,1 ± 0,5	126
				20,0	4,0 ± 0,5	127
				25,0	3,8 ± 0,5	129
				30,0	3,6 ± 0,5	130
				35,0	3,4 ± 0,5	129
				40,0	3,0 ± 0,5	128
				45,0	2,7 ± 0,5	126
	B	13	60	15,5	11,1 ± 0,5	85
				17,5	10,5 ± 0,5	89
				20,0	10,4 ± 0,5	92
				25,0	9,9 ± 0,5	99
				30,0	9,2 ± 0,5	104
				35,0	8,7 ± 0,5	109
				40,0	7,8 ± 0,5	113
				45,0	7,0 ± 0,5	116
	C	25	6	15,5	21,3 ± 0,5	13
				17,5	20,3 ± 0,5	14
				20,0	20,0 ± 0,5	15
				25,0	19,0 ± 0,5	17
				30,0	17,8 ± 0,5	19
				35,0	16,8 ± 0,5	20
				40,0	15,0 ± 0,5	22
				45,0	13,5 ± 0,5	23
	D	0	225	15,5	0 ± 0,5	217
				17,5	0 ± 0,5	215
				20,0	0 ± 0,5	211
				25,0	0 ± 0,5	204
30,0				0 ± 0,5	195	
35,0				0 ± 0,5	184	
40,0				0 ± 0,5	172	
45,0				0 ± 0,5	159	

The standard used in this study is NT Build 421 "Roofs: watertightness under pulsating air pressure" [100] and is described in detail in sub-section 3.7 in this thesis. It is a common standard used at the SINTEF Building construction laboratory in Trondheim, Norway, where

the laboratory investigation for this thesis was performed when roof systems are being tested with wind-driven rain exposure. This method applies to all components and sections of roofs made of any material to be fitted in roofs at any slope between 0° (horizontal) and 90° (vertical) at their normal operating conditions for which they were designed and installed according to the manufacturer's recommendations in a finished building. In short, a test specimen is exposed to constant runoff water applied at the top of the specimen and water spray applied across the specimen using a moving beam while pulsating air pressure intervals are increased in steps according to a load level for 10 minutes each. The amount of runoff water is 1,7 L/min x m ± 0,3 L/min x m, and driving rain is 0,3 L/min x m² ± 0,05 L/min x m². Each pressure pulse lasts 15 ± 6 sec. and consists of four stages: an increasing pressure of 3 ± 1 sec., a maximum pressure of 5 ± 2 sec., and a decreasing pressure 2 ± 1 sec. and a zero pressure of 5 ± 2 sec. Test parameters are provided in Table 8.

Table 8. Test parameters from NT Build 421 [100].

Angle of slope:		90°-60°	59°-40°	39°-0°
Wind pressure coefficient:		100%	75%	50%
Load level	Duration min.	Pulsating air pressure intervals, Pa		
1	10	0-200	0-150	0-100
2	10	0-400	0-300	0-200
3	10	0-600	0-450	0-300
4	10	0-800	0-600	0-400
5	10	0-1100	0-825	0-550

A similar test methodology is described in EN 12865:2001: “Hygrothermal performance of building components and building elements - Determination of the resistance of external wall systems to driving rain under pulsating air pressure” [101]. Pulsating air pressure is increased in similar steps that are given in NT Build 421 for slope angle 59°-40°; both runoff water and water spray are applied. There are two procedures given in EN 12865:2001, “procedure A for qualitative short time testing and procedure B for quantitative testing where water absorbed by the test specimen or penetrating the test specimen during the test has to be determined” [101]. Test parameters are provided in Table 9. Time intervals for procedure A are 20 minutes for the application of runoff and driven rain without air pressure, then 10 minutes for each step of load level. For procedure B, each load level lasts for 60 minutes. Amount of runoff water is 1,2 L/min x m ± 0,3 L/min x m and driving rain is 1,5 L/min x m² ± 0,5 L/min x m². Each pressure pulse lasts of 15 ± 4 sec. and is consists of four stages: an increasing pressure of 3 ± 1 sec., a

maximum pressure of 5 ± 1 sec., a decreasing pressure of 2 ± 1 sec. and a zero pressure of 5 ± 1 sec.

Table 9. Test parameters from EN 12865:2001 [101].

Load level	Procedure A	Procedure B	Pressure difference Pa
	Duration min.	Duration min.	
1	20	60	0
2	10	60	0-150
3	10	60	0-300
4	10	60	0-450
5	10	60	0-600
6	10	60	$600 + i \times 150$ $i=1,2, 3 \dots n$

Laboratory tests of building elements could have different purposes [102]:

- Quality assurance.
- Product performance prediction.
- Comparison of different products' performance.
- Data for product design development.

WDR testing covers the abovementioned purposes and can provide useful data for building elements assessment and improvement.

To thoroughly test the building envelope systems as the climate screen, it is crucial to test a large-scale model, as the most vital here is to investigate how the connection of elements of such systems affects the performance. There are three basic experimental methods that can be used in building science: (a) full-scale models, (b) test cells or (c) experimental modules and large-scale model tests [103]. Full-scale model means that a whole building in full-scale is taken as a model for test, which usually is performed outdoors [104]. Such test aims to collect data on the building performance in real outdoor conditions. Test cells means that a part of a building, a cell, is tested in outdoor conditions, while the necessary indoor conditions are controlled [105], while outdoor conditions are present as they are. The test cells test may be a connecting point between the full-scale test and the scale model test. Large-scale model means a model, constructed of elements and modules of real size, but the tested fragment of the building envelope fitted to a test specimen. The large-scale model test enables the evaluation

of various building envelope systems under close-to-identical laboratory conditions, as these conditions can be easily replicated in indoor laboratories using similar equipment and methodology.

Compared to the other two basic experimental methods the large-scale model test (c) has both economic and time-related advantages, but the exact scale is to be chosen for each specific test case. While full-scale and test-cells testing of the building envelope systems can provide extensive information and understanding of how various building envelope components work together [104], the large-scale model test was found most appropriate for the present study and thus employed in the investigations.

3.4 WIND-DRIVEN RAIN INTRUSION TEST EXAMPLES

Bitsuamlak et al. [104] present a full-scale testing apparatus, the Wall of Wind (WoW), and a testing methodology that can be adopted for assessing wind-driven-rain intrusion through the building envelope. A full-scale 2-fan and 6-fan WoW facility is described. The first is used for testing small structures and assemblies, and the second one can test a full-scale low-rise building model; therefore, any building envelope system (facades, wall assemblies, roofs, doors, and windows) can be tested there. 6-fan WoW can generate sustained wind speeds up to 56 m/s, representing hurricane-like winds. The researchers assessed how effective a roof secondary water barrier (no primary roof covering such as shingles or tiles) prevents water intrusion. This case represents a worst-case scenario when the main roofing has been blown off by a hurricane.

A water-intrusion test was conducted for a roof sample size of 3 m × 2,4 m. Six roof secondary water barriers were investigated: light asphalt-based, heavy asphalt-based, self-adhered asphalt based, light synthetic, heavy synthetic, and self-adhered synthetic. Testing of light asphalt-based secondary water barrier was conducted for three slopes 9,46°, 18,43° and 26,57°, which represent typical Florida roof slopes. Water-intrusion test for the six secondary water barriers was carried out for 9,46° slope. The following test parameters were used: water rate 224 mm/h., wind speed 24.6 m/s, and test duration 3 minutes. “Artificial seams were introduced on the plywood sheathing underneath the secondary water barrier at every 0.3 m to enable the collection of infiltrated water using the clear plastic sheet covering the ceiling of the roof deck.” [104] (Figure 21 c and d).

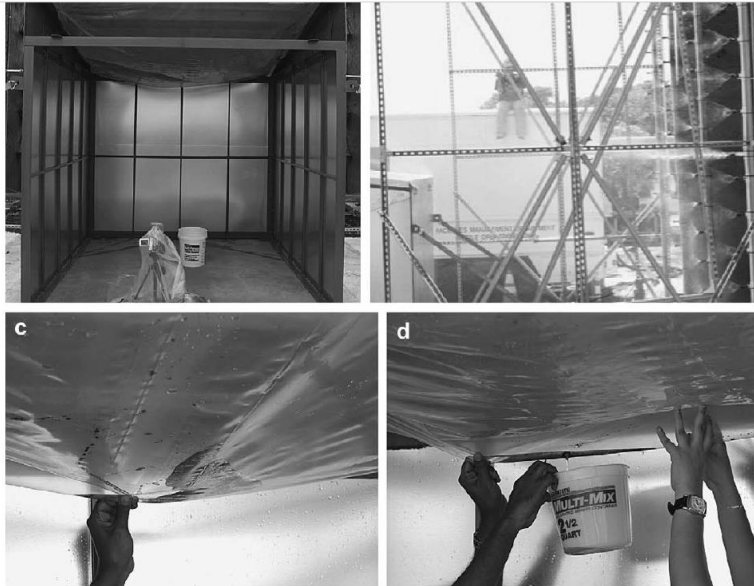


Figure 21. Water monitoring and collection setup. (a) Complete setup with camera and plastic ceiling, (b) the test specimen from bird's view, (c) leaked water through the roof layer and (d) water collection [104].

The test results for the light asphalt-based secondary water barrier showed that wind-driven rain intrusion through the roof underlayment is lower at the steeper slope than the lower slopes. The wind affects the secondary water barrier at the lower slope, and the overlapping lining between two consecutive secondary water barrier layers was flipped, allowing the wind-driven rain to migrate upward along the slope to penetrate through. “Furthermore, the pressure type that develops on the roof deck (i.e., negative versus positive) influences the amount of water intrusion. It can be explained by the external pressure distribution generated on the $9,46^\circ$ roof deck is dominantly negative, causing separation and pulling the membrane upwards from the roof surface, eventually facilitating the leaked water to run under the secondary water barrier and over the plywood deck, and leak through the plywood seams. On the other hand, for the steepest roof slope $26,57^\circ$, the mean pressure generated was positive. In this case, the membrane was pressed down and stuck with the roof deck, making the whole system act as a unit, thus leading to a minor amount of seepage and hence less leakage. In addition, it was relatively complex for the wind to push the rain to migrate up a steeper slope compared to a gentler slope. As the slope gets steeper, pressure tends to be less negative, and the flipping at the overlaps is reduced, with the reduced intrusion of wind-driven rain” [104]

Watertightness of stone roof slates was investigated by Fasana and Nelva [106]. They described what may influence watertightness of traditional stone roofing, possible weak points of roofing (clay tiles, concrete tiles, metal profiled sheets, fibre-cement profiled sheets, stones, slates, etc.) tested previously to help improve stone roof slates' watertightness by changing a shape of slate sides and changing how these slates overlap.

A sloping closed-jet wind tunnel (Figures 22 and 23) was used for watertightness testing of roofing. This equipment can fit specimen size 1,5 m × 1,75 m. Under the roof specimen, a transparent box is placed to regulate the static pressure difference by a fan. Roofing was tested at slopes 40%, 45% and 50% (45° equals to 100%). Test parameters included water spray rate 2 L/min x m² and runoff 10 L/min x m, wind speed 14 m/s, air pressure difference from -60Pa to 40Pa with 5Pa increase to the next increase of air pressure, increasing static air pressure difference and test duration. Figures 24 and 25 show two roof systems during testing.

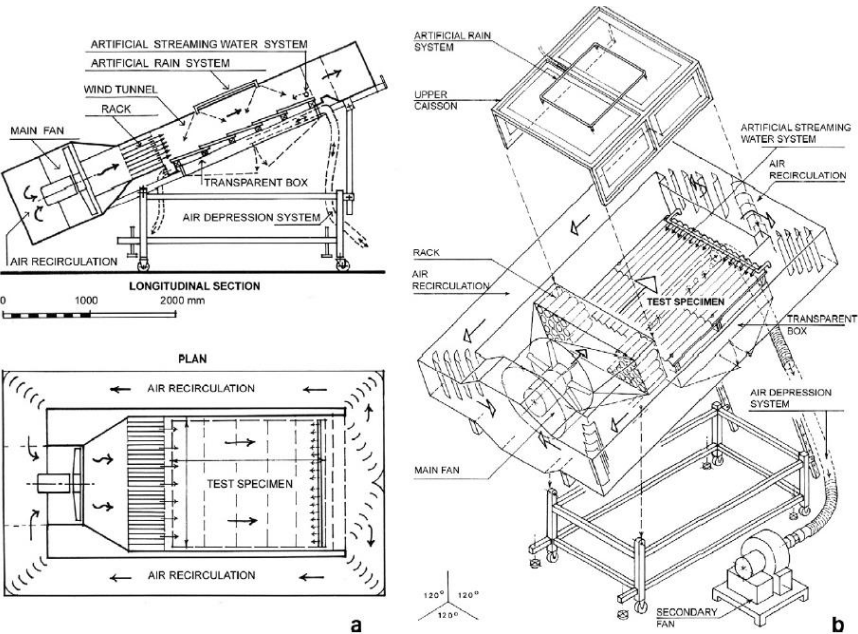


Figure 22. The apparatus for watertightness tests of discontinuous coverings (a) plan and section and (b) isometric drawing [106].



Figure 23. The apparatus used for waterproofing tests, the transparent box under the sample is visible [106].

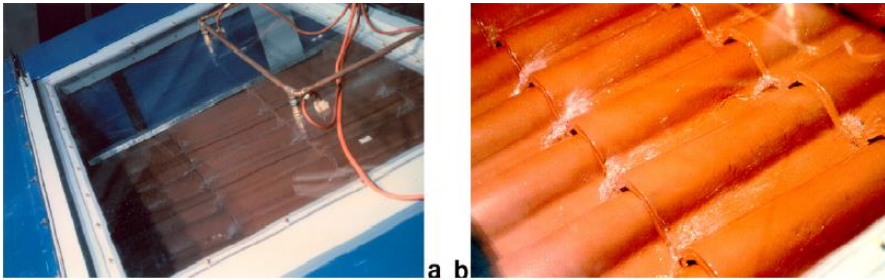


Figure 24. View of the front side of the specimen during testing of tile covering [106].

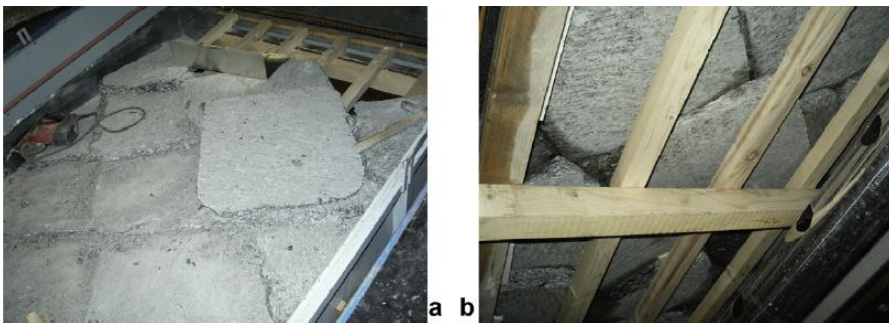


Figure 25. View of the specimen of a traditional stone roof carried out by Fasana and Nelva (a) front side of the specimen and (b) back side of the same specimen [106].

Qualitative observation of water infiltration is presented. The roof slope had the most influence on the occurrence of water infiltration. At low inclinations water infiltration points appeared at the head-on overlaps (the action of the wind influences it); at higher inclinations infiltration points were in the side overlaps (the gravity and the water streaming down influences the most). The value of the overlap of the roof slates and the dimension of the side joint between the roof slates affected the watertightness of the roof slates the most. It was also highlighted that the inclination of the installed roof system plays a critical role, and an angle at which the system is the most watertight can be found [106].

A study done by Olsson [107] investigated the expected rain intrusion rate at façade details based on four laboratory studies. EN 12865 “Determination of the resistance of external wall systems to driving rain under pulsating air pressure” [101] was partially used for the experiments, but additional load combinations and repetitions were included.

Façade systems that were tested: ventilated facades with façade layer of render on fibre cement board, fibre cement board, composite board, and wood panel, 29 window-wall interfaces with three different façades or wall constructions (where some of the window-wall interfaces had intentionally not well-performed joints so they could be compared to well-performed joints). The specimen size was 3×3 m and represented a full-scale wall. Test parameters included water rate $1,5 \text{ L/min} \times \text{m}^2$ and runoff $1,2 \text{ L/min} \times \text{m}$ (in some of the experiments, the rain load was reduced to simulate lower driving rain intensity), dynamic pressure loads of 0 Pa, 0-75 Pa, 0-150 Pa, 0-300 Pa, 0-450 Pa and 0-600 Pa. Type of equipment and test steps duration were not presented in the article. However, as it utilizes the standard EN 12865 and rain intrusion was quantified, test steps duration should be 60 minutes each. Rain intrusion was quantified by measuring the amount of water in collection funnels that were placed under each façade detail on the rear of the façade. Unit of water infiltration is given in L/min and % of total water amount applied.

The results showed that leakages of significant volumes appeared in small invisible deficiencies in the façade. The leakage rates depend on the deficiency’s size, position and geometry, cumulative runoff rates, surface properties and size of the projecting details. Testing of 29 window-wall interfaces with the best possible installations showed no noticeable difference in watertightness and leakage rate compared to the same interfaces with man-made flaws [107].

Lacasse et al. evaluated and compared laboratory tests from several studies on driving rain load and the risk of rain infiltration through various types of wall assemblies [108]. It was concluded that the risk of rain ingress entirely depends on the nature and material of the cladding or wall surface, the presence of openings or deficiencies in the wall that water can infiltrate through, and pressure differences across openings. It is not uncommon that water infiltrates through the plane of the exterior cladding, but it is not seen as typical either. Thus, details of each cladding can be associated with potential risk for water infiltration. Such details are windows (i.e., fenestration products), ventilation ducts, and electrical outlets, but most of the risk should be considered for water infiltration through joints in the cladding [108]. “The hydrostatic pressure of the runoff is an important parameter for water infiltration to occur. A higher spray rate, i.e. a thicker runoff film, results in a higher water entry rate. The applied wind pressure difference over the exterior surface of the wall assembly has an impact on the water entry rate. A reduced airtightness of the air barrier causes an increase in the pressure difference over other layers of the wall assembly, resulting in an increased impact of wind-driven rain and increased water entry rates. If the cavity behind the rainscreen is not pressure equalized or if no cavity is apparent, the water entry rate will increase for increasing pressure difference. Cyclic test sequences resulted in lower pressure equalization values, especially for wall assemblies with low pressure equalization and small openings in the rainscreen. Water ingress was therefore recorded at lower pressure differences and higher water entry rates” [108].

WDR testing of the curtain wall was conducted with both static and cyclic pressure. Results showed that the amount of infiltrated water did not show any correlation with pressure difference. This indicates that the hydrostatic pressure exerted by runoff film is the main force for water infiltration. Results from the cyclic test showed greater rates of water ingress at lower pressure differences compared to the results from the static test [108]. “Cyclic pressure fluctuations resulted in lower pressure equalization values, resulting in water ingress into the interior at lower pressure differences than to static pressure differences” [108].

Evaluation of ventilated facades gave the following results: “49.7% of the sprayed water splashed back, 22.5% created a runoff film along the exterior surface, 27.3% infiltrated into the air cavity, and 0.54% reached the exterior surface of the thermal insulation layer” [108]. Results for window products installed in various wood-frame wall assemblies pinpointed that water intrusion occurred even when no pressure was applied. This can be explained by gravity action. “The water infiltration rates increased with increasing spray rate, increasing pressure difference, and reduced airtightness of the air barrier” [108].

Equipment, systems tested, sample/test specimen size, tilt angles (if sloped roof), test parameters water rate L/min x m², wind speed, and test duration.

A comprehensive study of the water management of a ventilated façade system and quantification of water intrusion through joints was carried out by Arce-Recatala et al. [109–111]. Three rear-ventilated façade systems were chosen based on the type of fixing method and the vertical and horizontal joints design [109]. Rear-ventilated facades are pressure-equalized rainscreen systems. This type of façade is not load-bearing; external cladding consists of an outer skin of panels fixed to a framework which is mechanically fixed to an airtight, insulated wall [109]. A ventilated, drained, and pressure-moderated cavity is left between the outer skin of the panels and the airtight wall. A pressure-moderated rainscreen cladding is designed so that wind pressure acting on the face of the rainscreen is balanced by the pressure created at the joint. Water ingress in facades is induced due to the kinetic energy of raindrops, surface tension, gravity action, pressure difference, local air current, hydrostatic pressure and capillary forces [109]. Even though the rear-ventilated facades are designed to control these forces, water ingress may occur if the forces are not sufficiently considered in the joint design and construction details. The test was carried out using water spray and pressure differences applied in steps (150, 300, 450, 600 and 750Pa); the test duration was 15 minutes, during which a constant film of water at a rate of 2 L/min × m² was supplied. Results are presented as the water infiltration rates (%) as a function of applied pressure differences. Water infiltration rates into the cavity were constant for all pressure difference levels. “These results evidence that there is no driving pressure acting on the water infiltration through the test specimens as it would have been expected for a pressure-equalized façade system” [109].

Arce-Recatala et al. provided descriptions and schematic illustrations of water intrusion collection during WDR testing of a façade system [111]. The water ingress was studied at laboratory conditions and measured at each differential pressure load level using a gutter system (Figure 26), where a full-scale mock-up of the ventilated façade system was built. The complete laboratory setup of this study is shown in Figure 27, showing how water intrusion was collected and measured. The gutter system was connected to buckets that were placed on scales. Pressure difference was applied in 10 steps ranging from 50 to 800 Pa, first applied across the test specimen in over-pressure (+ ve) and later in under-pressure (- ve; suction).

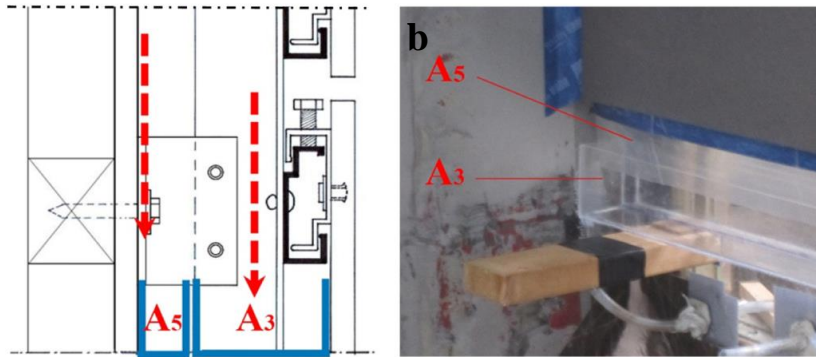


Figure 26. (a) Schematic drawing of the gutter system placed beneath the test specimen showing two points of water collection. (b) Photo of the gutters A3 and A5 placed in the mock-up with the tube connections for the drainage of collected water to the buckets [111].



Figure 27. Photo of the laboratory setup of the rear face of the mock-up. The collection trays are connected with plastic tubes to buckets placed on weighing scales, which measure the water ingress [111].

Sai Vutukuru et al. [112] investigated water intrusion for shuttered and impact-resistant windows to evaluate quantitatively wind-driven rain exposure. 12 fan Wall of Wind (WoW) was used, which is twice as powerful that used by Bitsuamlak et al. [104]. Wind speed for up to category five hurricane-force on the Saffir-Simpson scale (almost 70 m/s) can be simulated. Full-scale window assemblies were installed on a large-scale building model. “The building was constructed from Structurally Insulated Panels (SIPs) for all four walls and roof and has dimensions of 2.75 m. (length) x 2.44 m. (width) x 3.00 m. (height) covered by a gable roof of 5:12 slope with a 0.3m overhang on all sides” [112].

Van Linden and Van Den Bossche [113] also evaluated window-wall interfaces but chose drained and face-sealed systems. The wall type, cladding and window type varied due to the type of window-wall system tested. Wall specimens' sizes were: "2,39 m high and 1,07 m wide, incorporating a window with a height of 1,01 m and a width of 0,56 m.; window frame (1,48 m high by 1,23 m wide) was installed in a brick cavity wall of 2,28 m high by 1,96 m wide; a non-operable wooden window (1,55 m high and 1,23 m wide) was installed in a typical wood frame wall of 2,28 m high and 1,96 m wide" [113]. The test was carried out according to EN 12865 [101] cyclic and static test sequence. "The results of the static and cyclic test corresponded well. From a scientific point of view, it may be advisable to conduct both tests to determine the threshold values for water leakage, but a static test is simple and typically a conservative approach" [113].

3.5 BACKGROUND OF WIND-DRIVEN RAIN EXPOSURE TESTING OF BIPV SYSTEMS

Even though WDR testing of the building envelope components is well studied and documented, more studies should be done on BIPV performance under WDR exposure. A few large-scale experiments with WDR exposure for the BIPV systems were conducted by Breivik et al. [114] and Andenæs et al. [115] for their master theses. These studies are conducted in the same laboratory that the study in this thesis was conducted, therefore for easier reference, they are named Study 1 (experiments done by Breivik et al. [114]) and Study 2 (experiments done by Andenæs et al. [115]). Both studies were based on the test method standard NT Build 421 "Roofs: watertightness under pulsating air pressure" [100] and used the same equipment rain and wind (RAWI) box at the NTNU and SINTEF Building construction laboratory in Trondheim, Norway. The RAWI box was also used for investigations in this thesis, and detailed information about this equipment is given in subsection 3.4. NT Build 421 was used in the present study as this is the standard used at the SINTEF Building construction laboratory for evaluating WDR exposure on roofs.

In Study 1, large BIPV modules were tested. Two modules were surrounded by tailor-made (tailor-made meaning that they are designed for this type of BIPV modules) steel fittings, and steel plate roofing was installed around the BIPV modules. The BIPV modules and steel fitting were produced by the same manufacturer, DuPont, steel plate roofing Isola Powertekk tile was manufactured by Isola and cut at the laboratory to fit on the specimen. This BIPV system and surrounding roofing were market-available at the time; it is not a prototype. The transparent

polycarbonate (Lexan) board underlayment was used under the BIPV system (Figure 28 left). Areas between the steel roofing and steel fitting were sealed with self-adhering siliconized paper.

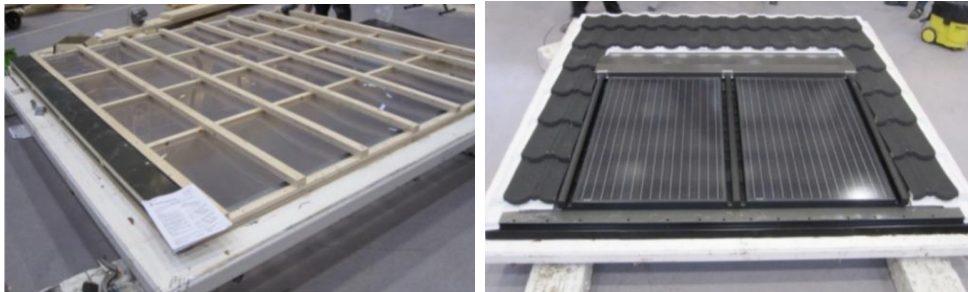


Figure 28. Roof system tested by Breivik [114].

Throughout the test, the differential air pressure occurred over the underlayment. The test required that the differential air pressure occurred over the BIPV roof sample, so a hole (37 cm x 43 cm) was cut in the underlayment (2.75 m x 2.75 m). During further testing, difficulties in maintaining the desired level of air pressure difference were encountered. To solve to this problem, it was decided to seal the initial hole and cut a smaller hole (7 cm x 43 cm). However, the desired differential air pressure levels still were not reached, and as it was a study for a master thesis with limited time, testing was stopped at this stage.

In Study 2, solar tiles and solar shingles systems were tested; all were available on the market at the time and are not prototypes. Compared to Study 1, no underlayment was used in Study 2, which was due to time constraints associated with a study for a master thesis. The underlayment provides a certain amount of resistance against WDR intrusion due to an air cushion accumulating in the ventilated air gap behind the elements of an actual roof or façade structure. Therefore, water leakages were expected to occur quite early in the test and a test procedure with lower load levels was used. In Study 2, the BIPV systems did not cover the whole test frame area; thus, areas between these BIPV systems, roof tiles and the rest of the frame were sealed using duct tape and a 0.15 mm thick polyethylene foil (Figure 21).

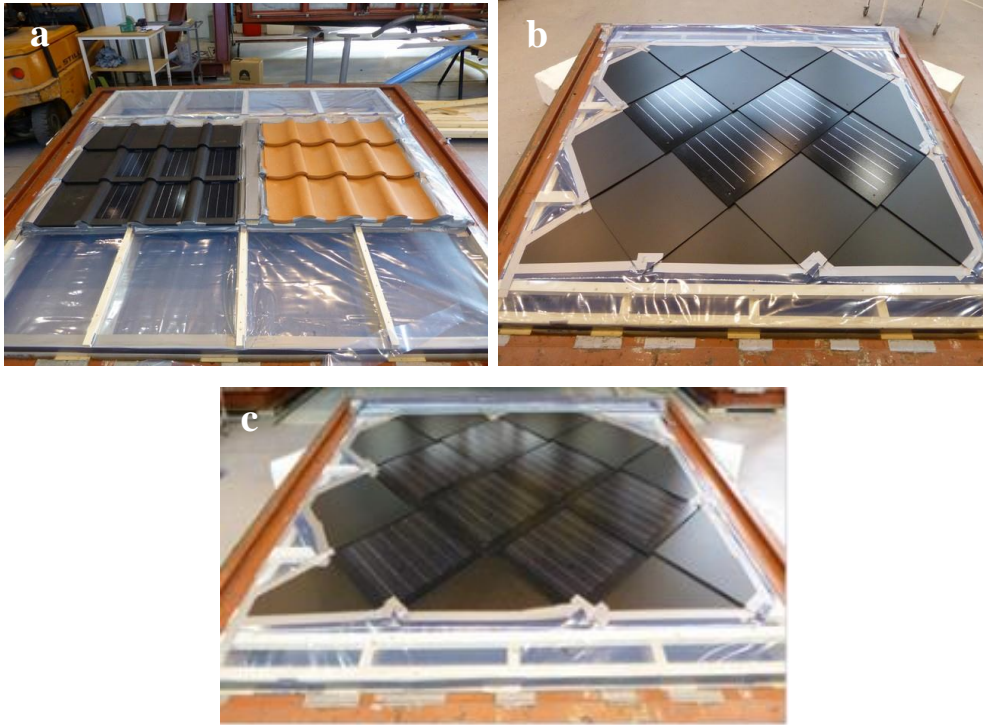


Figure 29. Roof systems tested by Andenaes, (a) solar roof tiles and conventional roof tiles, (b) solar shingles in two configurations with four solar shingles and (c) seven solar shingles surrounded by dummy shingles from the same manufacturer [115].

In Study 1, the inclination angle was changed more times during the test than in the present study and Study 2. It was found to be more time-efficient to adjust the inclination angle once from 30° in phase 1 to 15° in phase 2. Additionally, drying the test systems between test phases could be shortened. In Study 1, heating fans were used; in Study 2, the test systems were left to air-dry overnight; in the present study, the test systems were left to air-dry for a couple of hours. It must be noted that in the present study, the preparation time before the test and trial testing took a considerable amount of time. Taping a large area with sealing tapes was challenging, and the tape had to be fixed multiple times during trial test runs. Then, once the tape was fixed, the test procedure was straightforward.

3.6 COMPARISON OF TESTING METHODOLOGIES OF WIND-DRIVEN RAIN EXPOSURE ON BIPV SYSTEMS

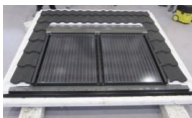

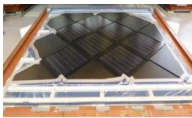

The present test methodology and methodologies from Study 1 and 2 are summarised in Table 10. Studies 1 and 2 laid the ground for research in this thesis. The experience and lessons

learned from these two previous studies were very valuable and helped to save precious time during Ph.D. period

The main distinctions of the present study can be highlighted as follow:

- Water intrusion quantification using the underlayment was implemented.
- Holes of optimal size that were cut in the underlayment were found.
- Layering of sealing tapes was used to cover areas around the BIPV systems.
- Time between test phases was shortened.

Table 10. Comparison of wind-driven rain exposure test methodologies used for the tested BIPV systems for roof integration [116].

Study reference	Tested system	Photo of the BIPV system	Pulsating (cyclic) air pressure intervals	Underlayment (Lexan plate)	Water intrusion quantification	Test procedure
Study 1	Large BIPV modules		Runoff water (0 Pa), 100 Pa, 200 Pa, 300 Pa, 400 Pa, 500 Pa, 600 Pa, 750 Pa	Yes	No	3 phases of test: 1. runoff water applied at 30° to 15° inclinations; 2. runoff water, water spray, and range of pulsating air pressure applied to underlayment at 30° then the system was dried, and range of pulsating air pressure was applied at 15°; 3. An attempt to apply pulsating air pressure to BIPV system (terminated)
Study 2a	Roof tiles		Runoff water (0 Pa), 10 Pa, 20 Pa, 30 Pa, 40 Pa, 50 Pa, 60 Pa, 70 Pa, 80 Pa, 90 Pa, 100 Pa, 120 Pa, 150 Pa	No	No	2 phases of test: 1. runoff water, water spray, and lower range of pulsating air pressure applied to BIPV system at 30° inclination; 2. runoff water, water spray, and lower range of pulsating air pressure applied to BIPV system at 15° inclination. Phase 2 was carried out on the next day after phase 1.
Study 2b	Roof shingles		Runoff water (0 Pa), 100 Pa, 200 Pa, 300 Pa, 400 Pa, 500 Pa, 600 Pa, 750 Pa	No	No	2 phases of test: 1. runoff water, water spray, and a range of pulsating air pressure applied to BIPV system at 30° inclination; 2. runoff water, water spray, and a range of pulsating air pressure applied to BIPV system at 15° inclination. Phase 2 was carried out on the same day after phase 1.
The present study	Roof shingle Roof tiles Large BIPV modules		Runoff water (0 Pa), 100 Pa, 200 Pa, 300 Pa, 400 Pa, 500 Pa, 600 Pa, 750 Pa	Yes	Yes	2 phases of test: 1. runoff water, water spray, and a range of pulsating air pressure applied to BIPV system at 30° inclination; 2. runoff water, water spray, and a range of pulsating air pressure applied to BIPV system at 15° inclination. Phase 2 was carried out on the same day after phase 1.

The present study's main aim was to quantify water intrusion during WDR testing in the RAWI box. The underlayment was used as a part of the water collection system, the optimal size of holes was found, and water was collected during WDR experiments. While Study 1 also used underlayment, no holes were cut at first. Even though air pressure intervals of the same magnitude as in the present study were applied in Study 1, with no holes in the underlayment, differential air pressure was applied to the underlayment and not to the tested BIPV system. The author of Study 1 cut a hole 37 cm × 43 cm in the underlayment (Lexan wind barrier) and attempted to apply the same differential air pressure as before. However, they could not be reached inside the RAWI box as it was concluded that the hole was too large. That hole was then sealed, and a smaller 7 cm × 43 cm hole was cut in the underlayment. However, the desired differential air pressure levels were still not reached.

The author of Study 1 concluded that both holes cut were too large, that the study was a master thesis study with strict time and budget constraints, and that further testing was terminated. Qualitative data on the placement of water intrusion obtained in Study 1 may differ from data that can be obtained if the same system is tested according to the test methodology from the present study. Therefore, data from Study 1 cannot be compared to data from the present study. Data obtained in Study 2 also cannot be compared to data from the present study. No underlayment was used in Study 2, and air pressure intervals of a lower range were used. Therefore, qualitative data on the placement of water intrusion obtained in Study 2 (a and b) may differ from data obtained if the same systems are tested according to the test methodology from the present study. In conclusion, qualitative data from Study 1 and Study 2 cannot be compared to qualitative data from the present study. However, testing methodologies can be compared (Table 10), and this comparison helped to improve the present testing procedure. It must be noted that in the present study, the preparation time before the test and trial testing took a considerable amount of time. Taping a large area with sealing tapes was challenging, and the tape had to be fixed multiple times during trial tests. Then, once the tape was fixed, the test procedure was straightforward.

3.7 DESIGNING A WATER COLLECTION SYSTEM FOR QUANTIFICATION OF WATER INTRUSION

In the present study and previous studies [96, 97], WDR was simulated in a specially designed rain and wind (RAWI) box (Figure 30) at the NTNU and SINTEF Building construction laboratory in Trondheim, Norway. A roof sample is mounted on a test frame that is fitted in

the RAWI box. Runoff water is applied from a row of tubes placed above the top of the test sample. WDR is simulated by air tubes that supply pulsating air velocities mounted on to a horizontal boom and a set of nozzles spraying water across the entire test specimen. A horizontal boom (row) with water nozzles is mounted on rails inside the box and moves up and down at a velocity of 0.2 m/s along the sample 0.6 m above the exterior roof surface, spraying WDR at a rate of 0.3 L/min x m². The runoff water and WDR spray rates are the same in NT Build 421 [100]. The nozzle boom sprays water, and air pressure is supplied in pulses onto a test sample, simulating gusts of wind and rain. “Both the velocity of pulsating air from the tubes and the pulsating positive pressure (overpressure) inside the RAWI box was increased” [114]. The RAWI box allows step-less tilting between 0 and 95 degrees from the horizontal plane, controlled pulsating air pressure across the test specimen and runoff water at a constant rate of 1.7 L/min x m at the top of the test area [114].



Figure 30. Large-scale turnable box for rain and wind tightness testing of sloping building surfaces (RAWI box), while test is running (left) and RAWI box without a test sample (right) [114]. Schematic drawing of RAWI box is shown in Figure 29.

The boom inside the RAWI box, which delivers WDR across the sample area, consists of tubes that supply water down to transparent vertical cylinders, where it hits the air stream that blows out of horizontal air tubes and is blown onto the sample area [114].

The duration of the water spray and air pressure exposure are combined in NT Build 421 [100] and last for 10 min for each increase of air pressure, while the water spray rate stays constant. The parameters given in NT Build 421 [100] and the parameters used in the present study are given in Table 11. All parameters used in the current study are presented in Table 12. Air pressures provided in Table 12 and related to weather conditions and wind speeds, do not









consider the building’s geometry and its’ effect on air pressure. The load level 0 (0 Pa air pressure, runoff water) was added along additional levels 6 (600 Pa) and 7 (750 Pa) compared to the parameters given in NT Build 421 [100]. It was decided to have additional load levels as potential worst-case scenarios when wind speeds are of more extreme levels. The test is initiated at load level 0, when the nozzle boom is inactive, and only runoff water is applied. At load levels 1-7 (between 100 Pa and 750 Pa, depending on the load level), air pressure inside the box is increased and decreased in cycles (pulses) lasting 5 seconds for 10 minutes.

15° and 30° roof inclinations were used in the present study, which is based on typical roof constructions found in Wooden Houses book that describes traditional Norwegian buildings [65]. Roof inclinations of 15°, 30°, and 45° are typical; however, 45° is considered a very high inclination [117] and is therefore less typical. A pitched roof that is covered with roof tiles should have the inclination of at least 14 - 15° [65] “The SINTEF Building Design Guides (Byggforskserien) [118] sets the minimum roof pitch to 10-15°. 15° is the lowest and 45° is the highest roof inclinations specified in the standards for BIPV EN 50583-2-2016 “Photovoltaics in buildings. Part 2: BIPV systems” [20] and IEC 63092-2-2020 “Photovoltaics in buildings – Part 2: Requirements for building-integrated photovoltaic systems” [45]. The optimal tilt angle for PV installation for power output in Norway is set to around 40° [119]. A software tool, PVsyst, designed for the solar energy industry, simulates and analyses solar energy systems of various types. The optimal tilt for PV systems in Trondheim when simulated in PVsyst, is 45°. However, it may not always be feasible to change and adapt the tilt angle to the optimal tilt angle for PV systems. Then building traditions and local, building guidelines are prioritised.

Table 11. Test parameters of NT Build 421 [100] compared to parameters used in BIPV systems testing [116].

NT Build 421			The present study		
Angle of slope		39°- 0°	Angle of slope		30° and 15°
Load level	Duration (min)	Pulsating air pressure intervals (Pa)	Load level	Duration (min)	Pulsating air pressure intervals (Pa)
1	10	0-100	0	10	0 Runoff water
2	10	0-200	1	10	0-100
3	10	0-300	2	10	0-200
4	10	0-400	3	10	0-300
5	10	0-550	4	10	0-400
			5	10	0-500
			6	10	0-600
			7	10	0-750

Table 12. Parameters used during wind-driven rain testing [116].

Load level	Colour mark	Pulsating (cyclic) air pressure intervals (Pa)	Weather condition description	Maximum wind speed (m/s)	Duration (min)
0		0, runoff water	-	0	10
1		0-100	Strong breeze	12.9	10
2		0-200	Fresh gale	18.2	10
3		0-300	Strong gale	22.3	10
4		0-400	Storm	25.8	10
5		0-500	Violent storm	28.8	10
6		0-600	Violent storm	31.6	10
7		0-750	Hurricane	35.3	10

The maximum applied wind speed was 35.3 m/s, which corresponds to extreme weather conditions such as hurricanes. This level is identified as a red danger warning; inhabitants usually receive messages from municipalities about prognoses, weather conditions, hazards associated with it and recommendations on how to behave during the period while this condition lasts. Norwegian Meteorological Institute (MET) issues reports with information concerning extreme weather conditions, which are available on their website.

In January 2021, middle and north parts of Norway (Trøndelag and Nord-Norge) experienced extreme wind speeds of 35-50 m/s and even 40-50 m/s [120]. In October 2008, other parts of Norway, more to the south and middle part, experienced extreme wind conditions. Wind speeds of 30-37 m/s were measured in Sogn and Fjordalen, Møre and Romsdal and Trøndelag [121]. In September 2020 the northern part of Norway (Lofoten, Vesteraalen and Troms) experienced wind speeds of 27-35 m/s and up to 40 m/s [122]. MET also sends warnings about extreme precipitation loads. In November 2020, Helgeland and north Trøndelag, the prognosis was expected to be 80-100 millimetres (mm) in 24 hours and locally up to 120 mm; actual measurements were around 60 mm in 24 hours. For Hordaland and Sogn prognosis was 120-150 mm in 24 hours; no information about actual measurements was presented [123,124].

Therefore, it is of significant importance to test the building envelope systems applying extreme weather conditions to test and ensure that installed systems can withstand such conditions without creating hazardous situations.

Studies 1 and 2 were analysed to identify possible improvements. Firstly, it was concluded that the underlayment must be used along with finding an optimal hole size cut into it to achieve the desired air pressure difference. The underlayment was also needed for water collection, i.e.,

quantifying the water leakages. A water collection system was used for the first time in the RAWI box when roof components were exposed to WDR. Thus, it took many trials and failures to make this system work properly; ultimately, the system proved feasible to build and use. A transparent polycarbonate (Lexan) board was applied as the underlayment so water leakages could be observed (and collected).

Study 1 [114] found that the underlayment must be punctured so that the air pressure will be applied to the tested system and the desired levels of air pressure difference can be reached. Hence, four holes (each with a size of 5 cm x 40 cm) were cut in the upper part of the underlayment. During the underlayment evaluation, an idea to cover these holes with a breathable, waterproof material was assessed prior to testing. If water that would go through the connecting points of a tested system would be drained through holes in the upper part of the underlayment, they must have been covered to collect all the water. After the first test trials, no water was draining through the holes in the underlayment, and they were left uncovered for the duration of the experiments.

The underlayment was fitted into the frame (2.75 m x 2.75 m) and was mounted on the wooden structure secured by screwing wooden battens to it. The wooden battens were spaced 0.6 m from each other and formed four separate sections. As the main frame of the test specimen was wider than the width of these four sections, two small sections were left along section 4 and section 1 (Figure 31). The two smaller sections were not a part of the water collection system, as water was only collected from the four main sections.

At the bottom of the frame, a water collection system was built. Following the already built four sections, four water collection sections were formed, where one round hole was cut in each section, and a tube was connected to each hole. A triangle profile of wooden battens was built near each hole and taped to the underlayment with duct tape. An outline of the water collection system is shown in Figure 39.

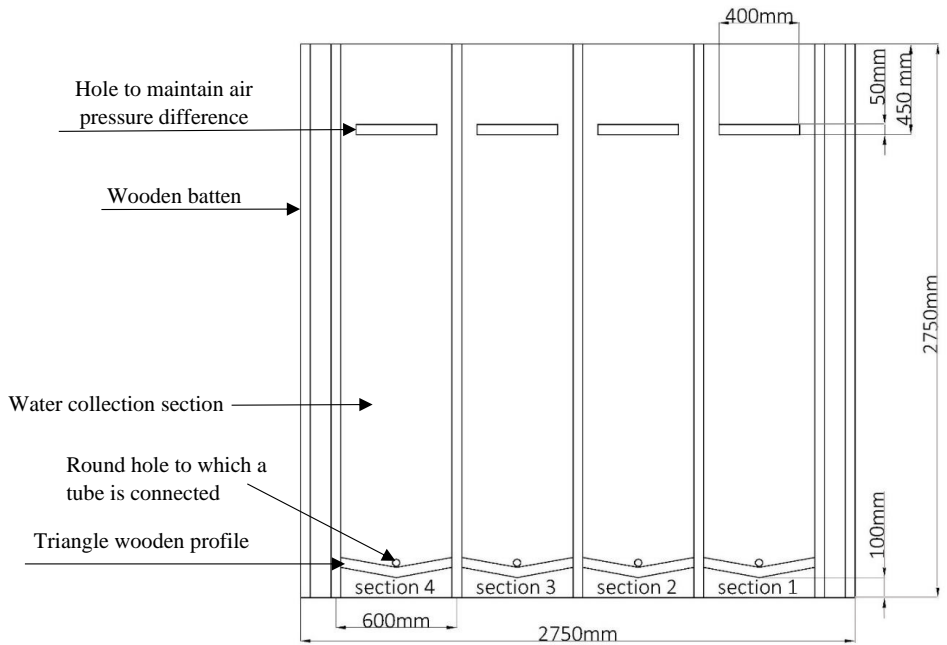


Figure 31. Outline of the water collection system [116].

The four water collection sections were numbered, and respective containers for water collection were placed at the end of each tube connected to their section. The tubes were partially filled with water so that the air pressure measurements would not be interfered with, which was suggested by laboratory staff. The four sections with the water collection system at the bottom of the sections are shown in Figure 32 (except the water collection containers), with some details depicted in Figure 33. See also Figures 38 and 39 that show the water collection containers. In Figure 32 left, one of the four holes cut in the underlayment's upper part is marked with a white rectangle.

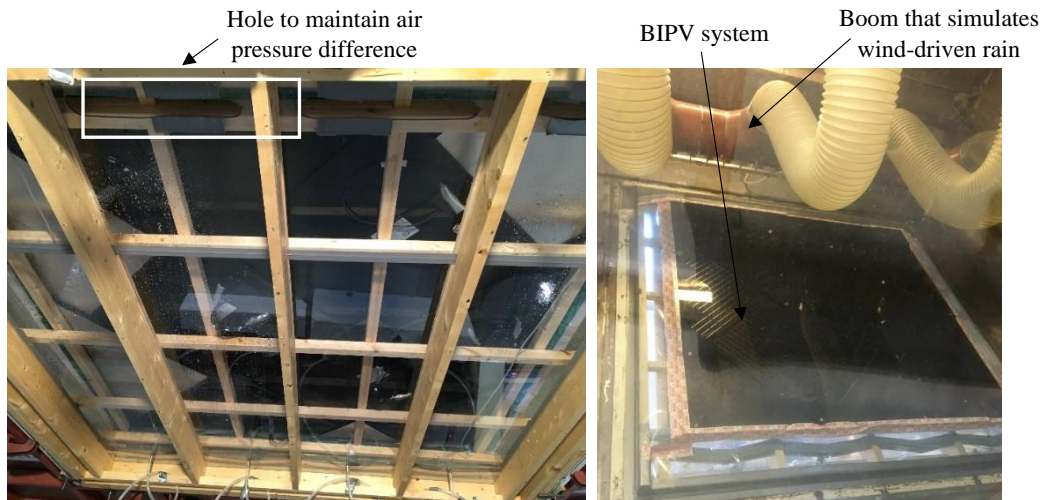


Figure 32. The BIPV system during trial runs viewed from the outside (left) and inside (right) of the RAWI box [116].

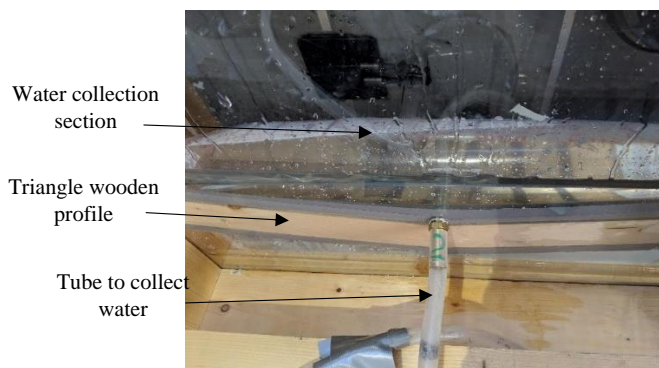


Figure 33. The water collection sections viewed from the back side of the BIPV system [116].

The remaining fragments of the surrounding frame were covered with 0.15 mm thick polyethylene foil to create a watertight barrier around the BIPV systems, which was sealed to the test frame using duct tape. Edges of the BIPV system were sealed using three types of sealing tape. The first layer was Halotex Flex Tape 60 mm, following the polyethylene foil. Then, Halotex Delta Tape 60 mm was placed over the plastic foil, following Halotex Delta Tape 100 mm (Figures 34, 35 and 36). Examples of a complete taping are depicted in Figure 36, from the front point of view before a trial testing and from the back-side point of view during testing. It was decided to try to apply sealing tapes that are usually used in underroof structures, as they had proven to be durable enough for prolonged periods [125].

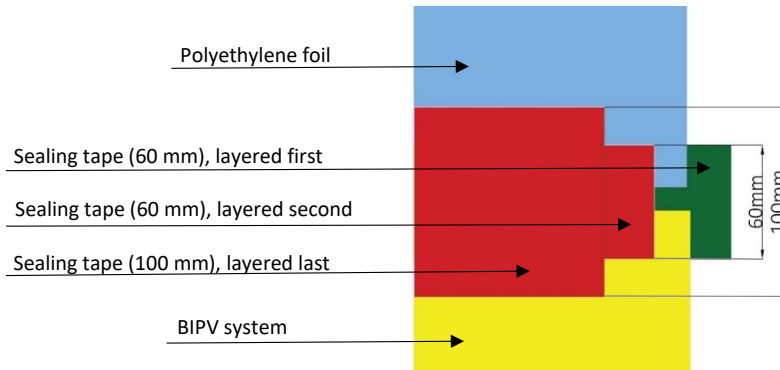


Figure 34. Schematic drawing of sealing tapes layering [116].

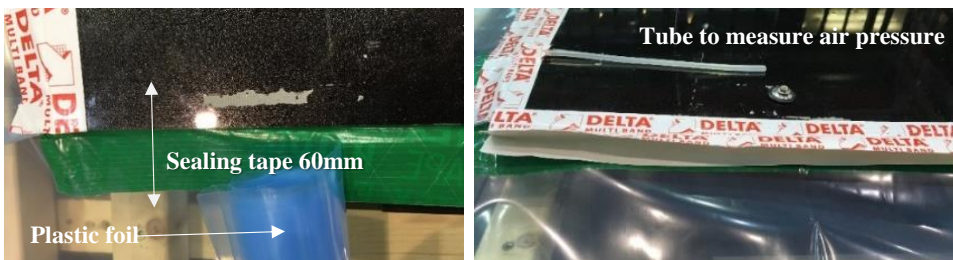


Figure 35. Sealing the edges of the BIPV system using sealing tapes and polyethylene foil (view from the frontside). On the right photo a tube used to measure the differential air pressure is visible lying on the black module [116].



Figure 36. View of a complete taping from the frontside (left) and from the backside (right) [116].

Wooden triangle profiles were covered on the top and the bottom side with duct tape (marked with number 1 on Figure 37 left), while on the side part of each triangle profile where they were connected to the underlayment, Haloproof multi xtreme flex tape was attached (marked with number 2 on Figure 37 left) to seal the gap and ensure that all the water would be collected. Then, double-sided sealing tape was attached to the upper part of each triangle profile. Later, plastic foil was attached to this double-sided tape (marked with number 3 on Figure 37 right). The step-by-step procedure of the present methodology is summarized in Figure 40.

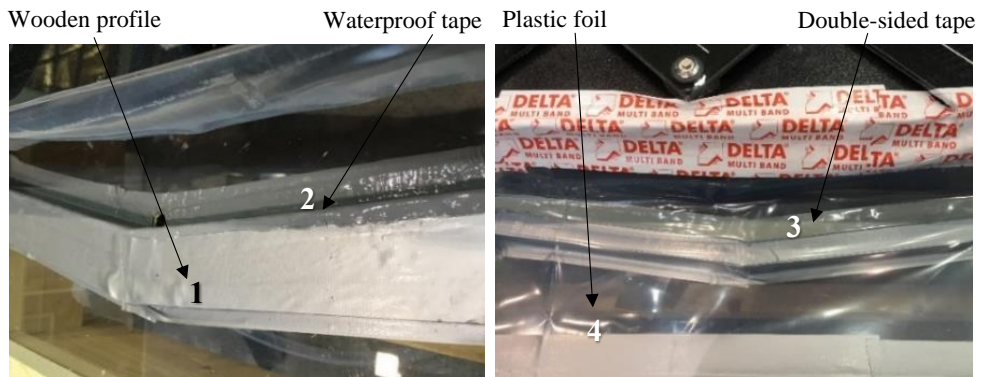


Figure 37. (1) Triangle wooden profile covered by duct tape built on the underlayment. (2) Waterproof tape sealing the gap between the underlayment and the triangle wooden profile, and (3) double-sided tape sealing area between the triangle wooden profile and (4) plastic foil [116].

As in the case of this test method, the air pressure difference must be set concerning the air pressure over and underneath the tested BIPV system. A tube (Figures 38 and 39) was placed under the BIPV system in the upper left corner, and the other end of the tube was then connected to the RAWI box. Along with this measurement, it was advised by the laboratory staff decided to measure the air pressure difference externally. One tube of the same diameter was installed during the taping stage on top of the BIPV system in the upper right corner (Figure 35 right). Later, this tube was connected to the external micromanometer, and another tube of the same diameter was placed underneath the BIPV system (Figures 38 and 39). Both the RAWI box and external micromanometer measured the air pressure difference over and under BIPV systems. Measurements were taken at each load level at the beginning of each, monitored during each load level and compared to the level of air pressure measured by the RAWI box. All load levels provided in Table 11 and measured by the external micromanometer and measurements in the RAWI box during all test runs reached the desired values of 100, 200, 300, 400, 500, 600 and 750 Pa. Once it was confirmed that the desired air pressure level was reached, the focus was on monitoring water leakages, their intensities if they occurred, monitoring that no water leakages occurred under the sealing tapes or water collection system surrounding that are not associated with leakages through BIPV systems.

Cross section A-A

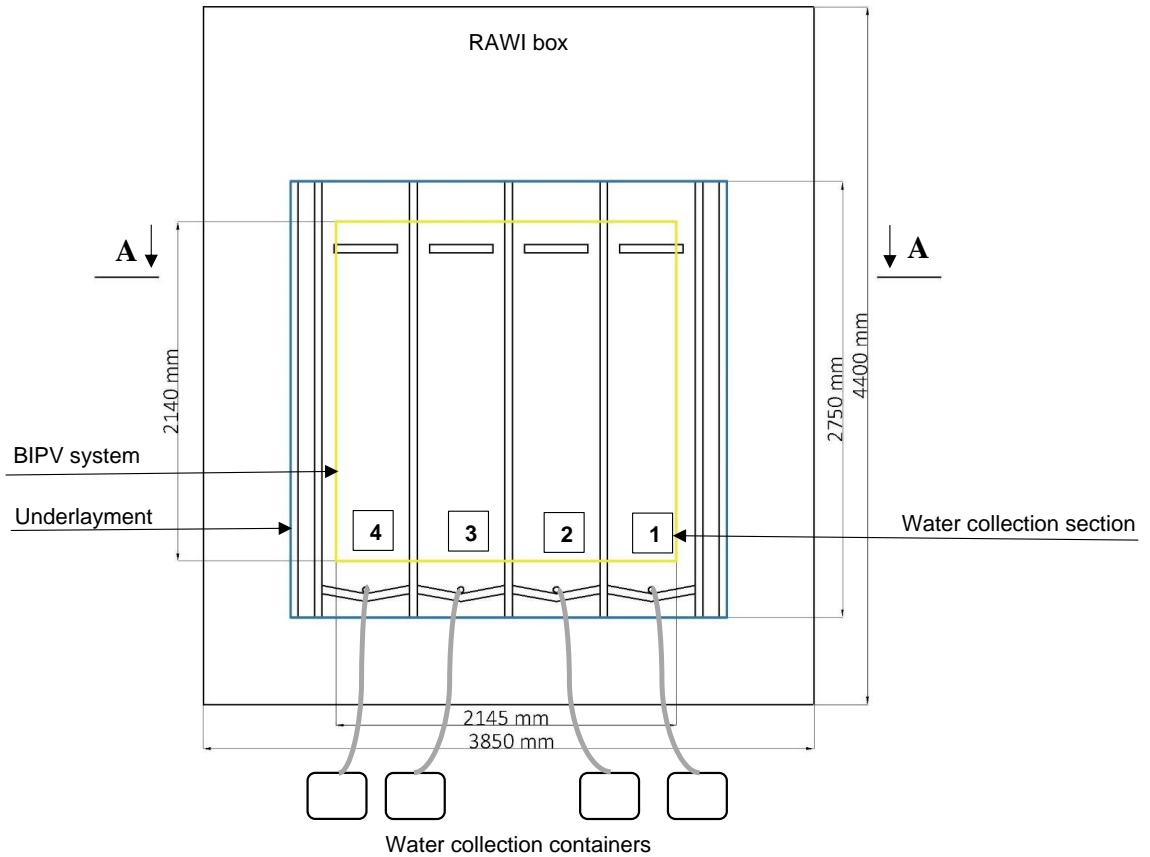
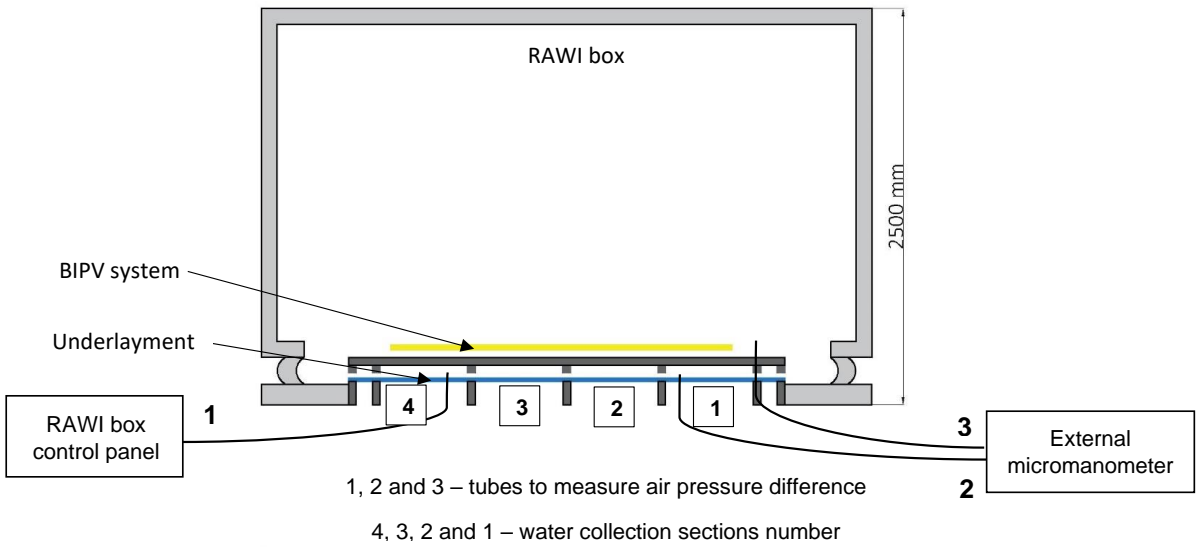


Figure 38. Schematic drawing of rain tightness test setup with four water collecting sections connected by tubes to four containers where the leakage water was collected. Additionally, a set of 3 tubes was used to measure air pressure difference. Tube 1 for measuring the differential air pressure by the RAWI

box, and tubes 2 and 3 for measuring the differential air pressure connected to the external micromanometer. Dimensions of the water collection system are given in Figure 22. Upper sketch depicts a cross section top view of the RAWI box, whereas the lower sketch shows the front face of the RAWI box (see e.g., right photo in Figure 21 for front face of the RAWI box with additional details) [116].

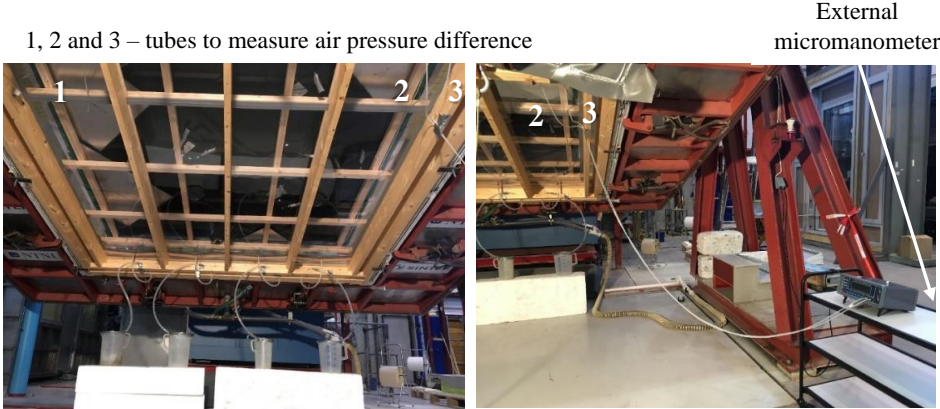


Figure 39. Rain tightness test setup in the laboratory. The set of 3 tubes to measure air pressure difference are marked. Tube 1 for measuring the differential air pressure by the RAWI box, and tubes 2 and 3 for measuring the differential air pressure connected to the external micromanometer [116].

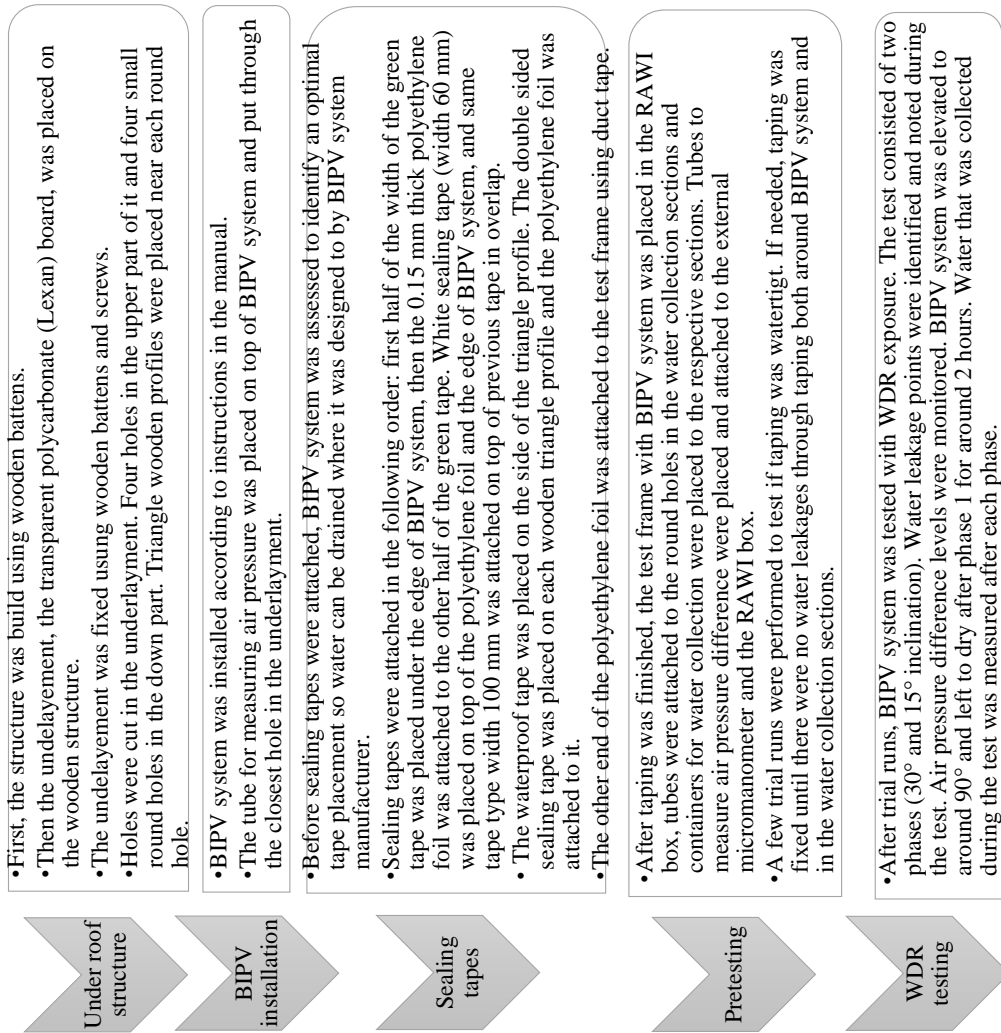


Figure 40. Summary of the present test methodology [116].

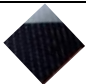


4 LABORATORY INVESTIGATION RESULTS

This chapter summarizes the main research outcomes from applying the methodology to quantify of water intrusion. It presents information on the design and installation of tested BIPV systems and the results of laboratory investigations. All information provided in this chapter is currently under review as a research paper.

4.1 OVERVIEW OF TESTED BIPV SYSTEMS

Three BIPV systems were tested in this study. The first (BIPV system 1) one constructed by fish-scale solar shingles resembling the skin of a fish. Each solar shingle is a compound of two layers of safety glass with solar cells laminated between them. Therefore, such modules are called glass-glass modules. The BIPV system can be complemented to fit the roof shape using colour-matching aluminium composite plates, which can be cut to diverse sizes and forms. The second BIPV system (BIPV system 2) is composed of flat solar tiles and their matching tiles. Rectangular-shaped tiles are made of a ceramic compound, and the tiles with solar cells are covered with tempered glass. The matching tile is half of the size of the solar tile. Finally, the third tested system (BIPV system 3) is constructed by large-size BIPV modules, reminiscent of standard PV modules. Glass-glass BIPV modules are installed on coated steel rails attached to each module's left and right sides, easing the installation. The parameters of these BIPV systems are summarized in Table 13.

Table 13. Parameters of tested BIPV systems.

System number	Type of PV	Illustration	BIPV product category	BIPV system category	BIPV integration category (Fig. 1)	Weight (kg/m ²)	Materials
BIPV system 1	mono c-Si		Solar tile	Full roof solution	A	19.5	Laminated glass-glass module without a frame.
BIPV system 2	mono c-Si		Solar tile	Full roof solution	A	17.1	Tile is made of a ceramic compound; solar cells are covered with glass.
BIPV system 3	CdTe		BIPV module	In-roof system/warm facade	A, C	18	Laminated glass-glass module with steel profile on the left and right side of each module.

4.2 INSTALLATION OF BIPV SYSTEMS

The tested BIPV systems were installed according to the manufacturers' manuals. The manuals are available on the manufacturers' websites or could be requested from the manufacturers or BIPV system resellers. The same frame, 2.75 m x 2.75 m (Figure 23), built of wooden beams, was used for all the tested BIPV systems.

4.2.1 BIPV system 1 details

The BIPV system's installation on an actual building roof is depicted in Figure 41 left. Glass-glass BIPV shingles of four shapes are presented on the market (marked with 1, 2, 3, and 4 on Figure 41 right) and can cover roof of diverse sizes using only solar shingles and additional triangle glass-glass parts (Figure 42 middle, marked with 5).

When needed, this system can be complemented by metal plates. However, these metal plates have a significantly smaller thickness and different stiffness from their BIPV counterparts and could thus cause additional water leakages, as anticipated and demonstrated during testing. It must also be noted that it needed to be more obvious how these metal plates should be installed. The manufacturer provided only BIPV shingles and small glass-glass triangle parts made of the same materials and do not contain solar cells. The squared-shaped metal plates are provided when the BIPV system is purchased from a reseller. These metal plates should be cut, but no instructions, sizes or shapes were given. Thus, no specific manuals and precise details were given for installing metal plates with the BIPV system. In Figure 41 middle of the metal plates are fixed using small screws, which differ from the screws used for the BIPV system 1. When the system was delivered to the laboratory, both types of screws were provided. The final recommendation from the reseller was to use the same screws as used for the BIPV system; holes of the same size as on BIPV modules were cut in the metal plates. However, that led to metal plates not being screwed as tight as they would when screwed with the smaller screws. It could have been beneficial to install new metal plates and use smaller screws, but the metal plates provided were all used and cut to fit around the BIPV system, and as the holes were cut to use the bigger screws, it was not possible to reuse the same metal plates. Due to time and budget constraints, new metal plates were not purchased.

A few rubber elements provided with the Sunstyle BIPV system are attached to each solar shingle (Figure 42). Reverse anchor-like components are attached to the upper part of the BIPV shingles, with a line of rubber sealing the gap between shingles (Figure 42, illustrated on the

left picture and shown in the middle photo, marked with white rectangles). Additionally, rubber gaskets are used under each screw (Figure 42 right).

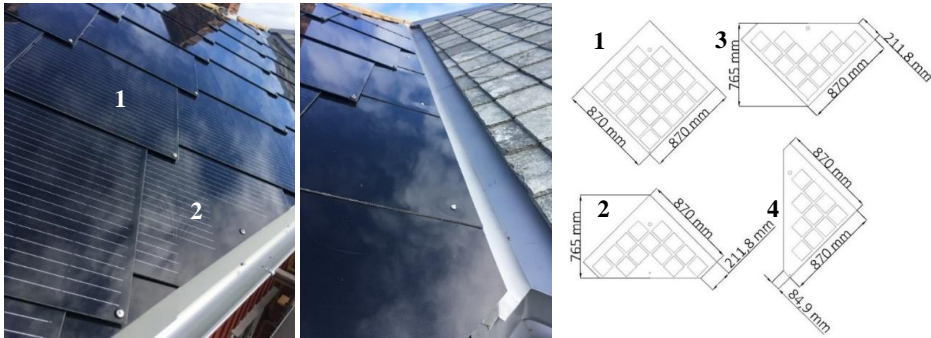


Figure 41. (left) BIPV system 1 installed on an actual building roof. (middle) Metal plates completing BIPV system at edges. (right) Range of solar shingles: 1 – basic solar shingle; 2 – solar shingle bottom; 3 – solar shingle top; 4 – solar shingle left (photo and drawing by Anna Fedorova).



Figure 42. Rubber element on upper part of the solar shingle (schematically shown on the drawing to the left and how they are attached on the real roof shown on the photo in the middle) and (right) lower part of the solar shingle. 1 – basic solar shingle, 3 – solar shingle top and 5 – matching glass-glass triangle element on an actual building roof (photo and drawing by Anna Fedorova).

The tested BIPV system consisted of three whole and three half solar shingles (one solar shingle top, one solar shingle bottom and one solar shingle left), four glass-glass elements shaped to the system profile and provided with the system. Four metal plates, also shaped to fit the remaining parts of the profile, were cut in the laboratory. The BIPV system with completed taping is depicted in Figure 43. The BIPV system 1 outline (Figure 43) shows how the solar shingles and complementing elements are connected.

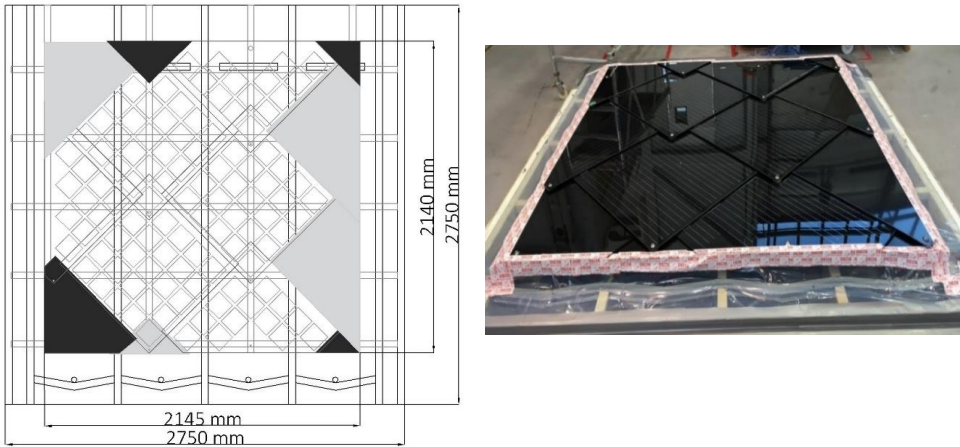


Figure 43. (left) Front view of the outline of the BIPV system 1. To distinguish components of the system and to make connecting points better visible, solar shingles are left transparent, grey parts are metal plates, and black parts are glass-glass parts without PV cells. (right) BIPV system with completed taping before laboratory testing. View from the bottom of the exterior BIPV system side (photo and drawing by Anna Fedorova).

4.2.2 BIPV system 2 details

The installation of flat solar tiles and matching tiles on an actual building roof is depicted in Figure 44. The number of roof tiles with solar cells used on the roof will depend on the building's electricity demand, where the rest of the roof area can be covered with the matching tiles. Solar tiles have a unique design that provides drainage of water. Their mounting is similar to the mounting of conventional roof tiles. Tiles are placed on wooden beams and secured with hurricane clip nails (hooks) on each tile's right side, which is also standard for conventional roof tiles. Additionally, solar tiles are secured with three screws and matching tiles with two screws on top of each tile.

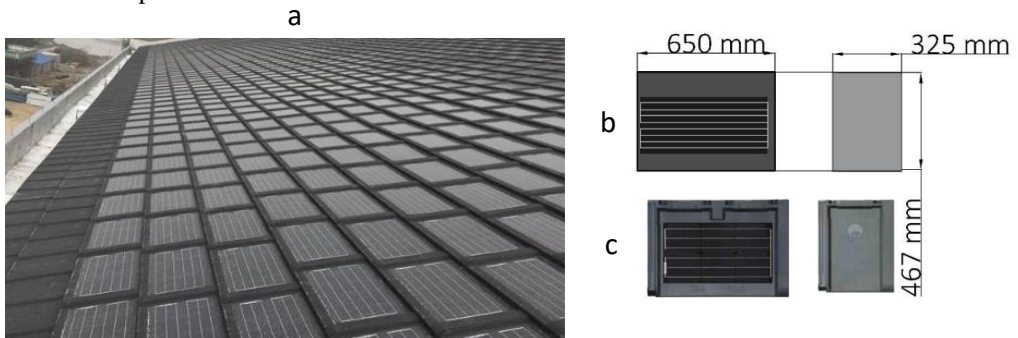


Figure 44. (a) Complete solar tile system on an actual building roof [126], (b) solar tile and matching non-solar tile with dimensions, and (c) actual solar tile and dummy tile [126]. The matching tile may seem more of a greyish colour here, but in reality, it is the same black colour as solar tile.

The tested BIPV system consisted of four BIPV roof tiles with eight matching tiles (one cut in two). There needed to be a better understanding with the provider of this BIPV system; tiles two the size were initially considered. A minimal number of tiles were requested and received, and when they came to the laboratory and laid out, tiles covered only part of the test specimen. After several discussions, it was decided to keep the BIPV system as it is, and no more tiles were received. The BIPV system with completed taping and an outline of the BIPV system, which shows how the tiles are connected, are depicted in Figure 45. The solar tiles are coloured in dark grey with black rectangles with stripes illustrating the solar cells, whereas matching non-solar tiles are coloured in light grey for visualization purposes in Figure 45; in reality, they have the same colour.

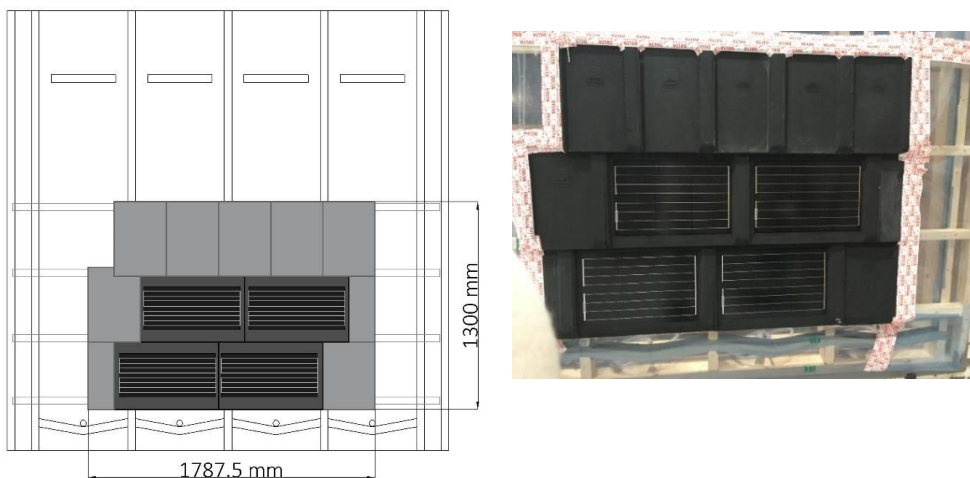


Figure 45. Front view of the outline of the BIPV system 2 on the left. To distinguish solar tiles from matching tiles they are coloured in dark grey and black (solar tiles) and light grey (matching tiles). In reality, both types of tiles have the same black colour, as shown in BIPV system with completed taping, front view of the exterior BIPV system side, before laboratory testing on the right (photo and drawing by Anna Fedorova).

4.2.3 BIPV system 3 details

BIPV systems 3 glass-glass modules can be installed in two ways: orientated vertically (Figure 46 left) or horizontally (Figure 46 right). The manufacturer’s website, has there is a portfolio of buildings where BIPV modules were used. Most of the realized projects utilize BIPV modules only, covering the roof’s whole area with BIPV modules. Depending on the energy needs of a particular building, it may not be necessary to cover the roof’s entire area with solar modules. One design shown on the website combines BIPV modules with metal roofing plates (Figure 47).



Figure 46. (left) BIPV system with vertically orientated modules and (right) horizontally orientated modules installed on an actual building [127].



Figure 47. BIPV system with horizontally orientated modules integrated with metal roof plates on the left. Steel roof plates installed on an actual building roof on the right [127,128].

In the current study, BIPV system 3 was integrated with steel roof plates (Figure 48). These two roof systems have not been designed to be installed together but were used for experimental purposes. Steel rails attached to each module's left and right side were not only helpful to ease the installation of the BIPV modules but also made it uncomplicated to couple them with steel roof plates. Both BIPV modules and steel roof plates were fixed to the wooden beams with screws. The tested system consisted of four BIPV modules with six rows of steel roof plates. The BIPV modules are coloured in dark grey, whereas the steel roof plates are coloured in light grey, similar to systems' colours in real life.

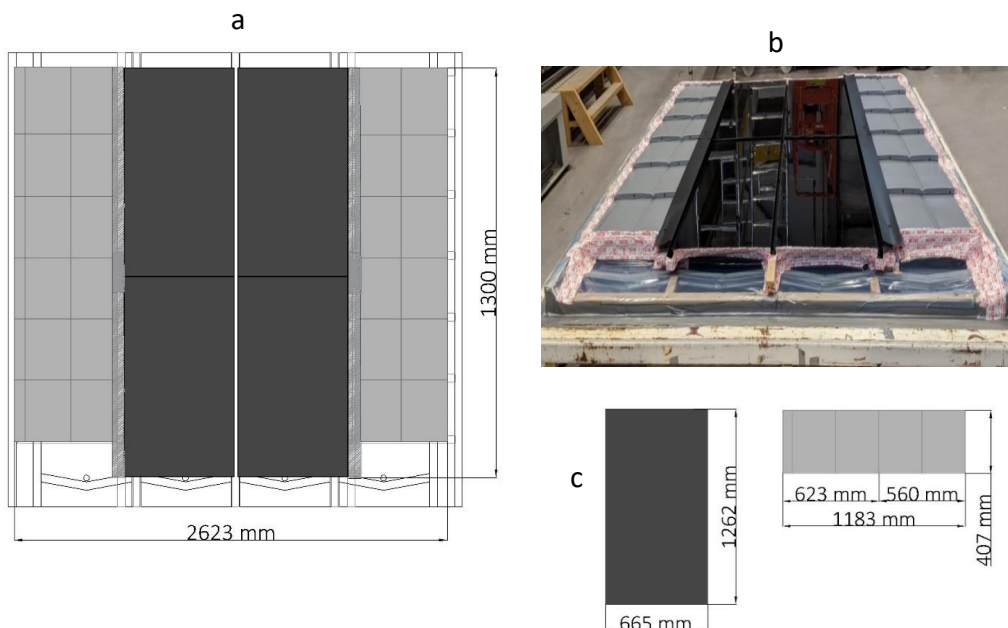


Figure 48. (a) Front view of the outline of the BIPV system and steel roof plates on the left. The BIPV modules are coloured in dark grey, whereas the steel roof plates are coloured in light grey. (b) BIPV system integrated with steel roof plates with completed taping before laboratory testing on the right. (c) Schematic illustration of BIPV module and metal plate. View from the bottom of the exterior BIPV system side (drawings by Anna Fedorova).

4.3 TESTING OF BIPV SYSTEMS

Before data on the water collection was aggregated, several trial tests were conducted to ensure that the water collection system was ready for testing and that sealing tapes were sufficient. The data sets gathered are presented in the order in which the BIPV systems were tested.

4.3.1 Testing of BIPV system 1

The WDR tightness test of the BIPV system 1 started with the system being inclined at 30° and load level 0. After 10 minute of applying runoff water, a differential air pressure of 100 Pa (load level 1) was used, moving in 10 minutes periods to load levels 2 and 3. No water leakages were detected up to load level 4 (400 Pa). Water droplets started to occur in two areas where the Sunstyle BIPV full shingles overlapped with the metal plates (all points of water leakage are shown in Figure 41). New points of water droplets occurred at load levels 5 (500 Pa) and 6 (600 Pa). No new leakages were detected at the last load level 7 (750 Pa). Leakages that occurred had been intensifying at each next load level. When the test for 30° inclination was over, the system was elevated to nearly 90° inclination to drain water droplets that were on the transparent underlay. After two hours, the underlay was inspected, and as no water droplets were seen, the containers with collected water were weighed, and data was noted. The water

was collected at the end of the test for the inclination, after all load levels were applied, and not after each load level as desired.

For the next stage of the test, the system was inclined to 15°. The same procedure was followed, starting at load level 0 and finishing with load level 7 (750 Pa). Water leakages began to occur one load level earlier than at the previous stage, but only at the point where the metal plates were screwed together. A small number of droplets occurred at load level 4 (400 Pa) at the points where the Sunstyle BIPV shingles overlapped with the metal plates, following water leakages along the overlapping area at load level 5 (500 Pa) (the same area where water leakages occurred at load levels 4 (400 Pa) and 6 (600 Pa) at the previous stage). Small water leakages were visible on the overlap of the Sunstyle BIPV half-shingle lower tile, glass-glass triangle, and metal plate. The first water leakage between the Sunstyle BIPV shingles (the whole shingle and the half-shingle right tile) occurred at the last load level. After this stage was finished, the system was again lifted to nearly 90° and left for two hours to drain water droplets from the underlay; water collected was weighed and noted.









The BIPV system 1 was initially tested at two inclinations (30° and 15°). As the system showed a high level of watertightness, it was advised to conduct an additional testing stage as a possible worst-case scenario where all screws were loosened by three full turns each. The system was inclined to a 15° angle, as the impact of the WDR is expected to be more forceful on lower inclined roof systems. During this stage of the test, no water leakages occurred until load level 2 (200 Pa). Water droplets appeared at the points where metal plates were screwed together and at the overlapping point of them and where the half-shingle right was screwed with the glass-glass part. At the next load level, new points with water leakages emerged at overlaps of Sunstyle whole shingles and metal plates. Following new leakage points at load levels 4 (400 Pa) and 5 (500 Pa) (various overlapping points of solar shingles, glass-glass parts, and metal plates). At the last load level, 7 (750 Pa), droplets appeared on the glass-glass part where it overlapped with the metal plate. After this stage was finished, the system was again lifted to nearly 90° and left for two hours to drain water droplets from the underlay; water collected was weighed and noted.

Observations are summarized in Table 14, and water leakage points are marked in Figures 49 and 50.

During the first two WDR testing at 30° and 15° inclination, before the test where the fastening screws were loosened, it was observed that the metal plates were slightly bending from the

BIPV shingles when the air pressure was pulsating due to a difference in stiffness in the metal plates and their BIPV counterparts (and possible differences in distance between fastening screws), thus causing larger water leakages at these locations, which lead to considerably larger water leakages collected in section 3 and 4 as compared with sections 1 and 2 for both inclinations as depicted in Figure 51.

Table 14. Qualitative observations of water leakages during wind-driven rain tightness testing in the RAWI box for the Sunstyle BIPV system.

Load level	Pulsating air pressure (Pa)	Colour mark	Inclination 30° (Figure 49 a)	Inclination 15° (Figure 49 b)	Inclination 15°* (Figure 50)
0	0 (runoff water)		No water leakages	No water leakages	No water leakages
1	0-100		No water leakages	No water leakages	No water leakages
2	0-200		No water leakages	No water leakages	Leakages occurred
3	0-300		No water leakages	Leakages occurred	New leakages occurred
4	0-400		Leakages occurred	New leakages occurred	New leakages occurred
5	0-500		New leakages occurred	New leakages occurred	New leakages occurred
6	0-600		New leakages occurred	New leakages occurred	No new leakages
7	0-750		No new leakages	New leakages occurred	New leakages occurred

*All screws of the tested system were loosened by three turns.

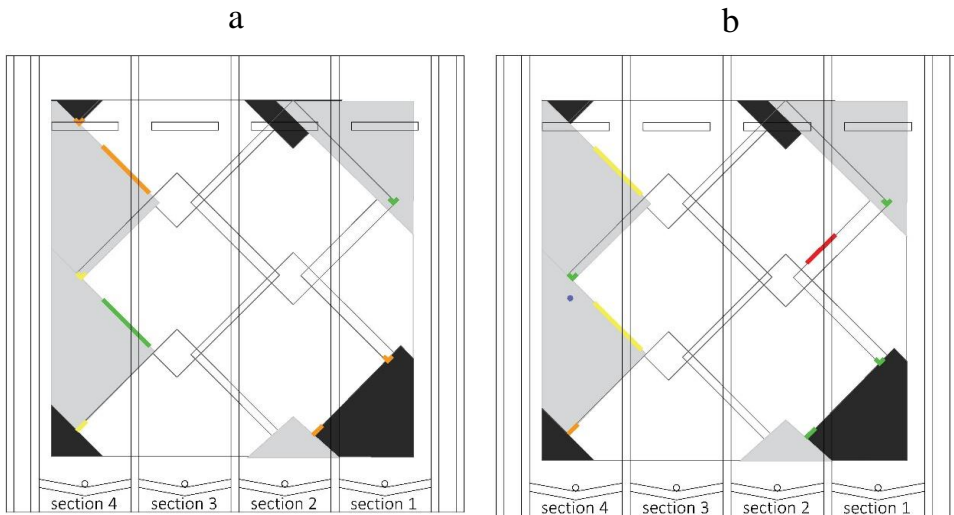


Figure 49. Location of water leakage points for the BIPV system 1 with corresponding colours as given in Table 4. (a) First test phase (inclination 30°); (b) second test phase (inclination 15°). View from the backside of the BIPV system (drawings by Anna Fedorova).

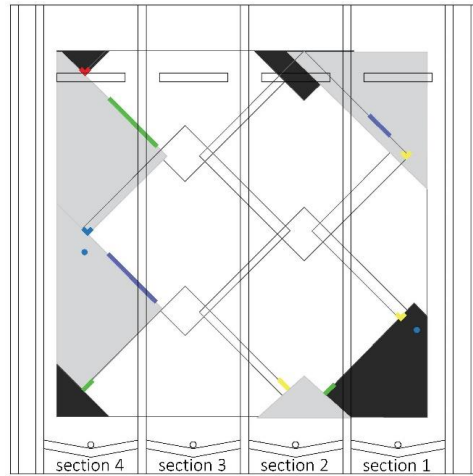


Figure 50. Location of water leakage points for the BIPV system 1 with corresponding colours as given in Table 11. Second test phase ran for the second time with the BIPV system inclined to 15°. All screws were loosened by three turns each. View from the backside of the BIPV system (drawing by Anna Fedorova).

Water collected from the respective four sections was weighed on a scale after each test phase. The amount of water did not exceed 3 L (5 L containers for each collection section were used when the BIPV system 1 was tested), so it could be measured once per test phase. The quantified results of these water leakage measurements for the BIPV system 1 are collected in Figure 51.

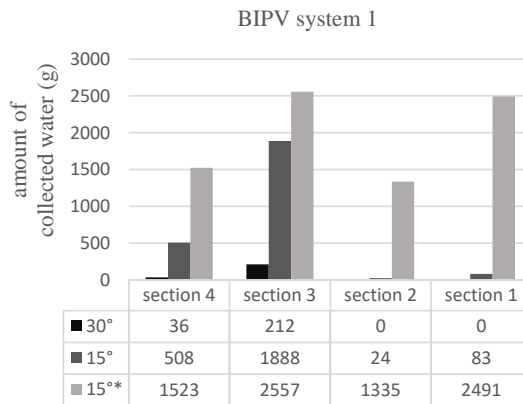


Figure 51. Quantitative measurements of water amounts collected during wind-driven rain testing in the RAWI box for the BIPV system 1.

From Table 14, it is evident that the first water infiltration occurred at 30° at load level 4, at 15° at load level 3 and at 15° with loosen screws at load level 2. Water leakages occurred one load level earlier as the roof inclination was lower. The amount of water follows the same path.









The amount of water infiltration increases at lower roof inclination. These observations are coherent with observations from other studies. Rain intrusion is higher at lower slopes than the steeper ones; that might be because runoff film and water amount on the surface is higher as water runs faster from steeper slopes due to the gravity force. The roof slope has the most influence on the occurrence of water infiltration. The water leakage points occurred in the overlap area of the BIPV module and the metal plate where the metal plate lay under the BIPV module. It was observed that metal plates are much thinner and more flexible than BIPV modules. Metal plates were bent and pushed down a little during testing, allowing water infiltration. However, no leakages were observed associated with the overlap of BIPV modules by each other.

4.3.2 Testing of BIPV system 2

The BIPV system 2 did not cover the whole testing frame. Due to time and economic constraints, obtaining more tiles from the manufacturer was not feasible, and the testing was thus run with the initially provided components. Two stages of WDR tightness testing were conducted for 30° and 15° angle inclinations, following the same procedure as for the BIPV system 1 testing. Before the experiment with water collection started, a few trials to test the sealing tape were carried out. More severe water leakages occurred already at load level 1 (100 Pa), compared to the leakages in the BIPV system 1, and hence, 5 L containers were changed to 10 L containers for each collection section.

At the first phase (30° inclination), water leakages appeared at load level 1 (100 Pa) at four locations: two leakage points between matching tiles and two leakage points between solar tiles connected to matching tiles. More leakages started appearing with higher intensities during the next load level. Only one more leakage point occurred during load level 3 (300 Pa). During the following load levels, no new leakages occurred. All earlier leakage points remained, and each water leakage's intensity was increasing with each next load level. At the second test phase (15° inclination), leakages occurred at the same load levels and approximately at the same points but at a higher rate. At load level 1 (100 Pa), six water leakage points occurred (compared to the four leakage points in the first phase), and at load level 2 (200 Pa), thirteen leakage points occurred (compared to the six points in the first phase). More leakages appeared at load level 3 (300 Pa), all along the downside of the lower row of tiles of the BIPV system. Observations of both phases of the test are summarized in Table 15. All leakage points are shown in Figures 52 and 52 b.

Table 15. Qualitative observations of water leakages during wind-driven rain tightness testing in the RAWI box for the BIPV system 2.

Load level	Pulsating air pressure (Pa)	Colour mark	Inclination 30° (Figure 43 a)	Inclination 15° (Figure 43 b)
0	0 (runoff water)		No water leakages	No water leakages
1	0-100		Leakages occurred	Leakages occurred
2	0-200		New leakages occurred	New leakages occurred
3	0-300		New leakages occurred	New leakages occurred
4	0-400		No new leakages	No new leakages
5	0-500		No new leakages	No new leakages
6	0-600		No new leakages	No new leakages
7	0-750		No new leakages	No new leakages

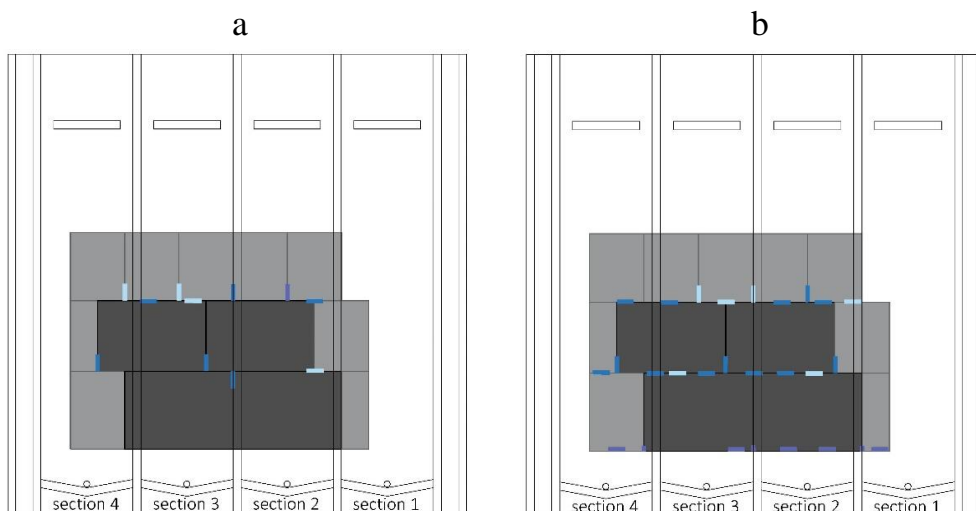


Figure 52. Location of water leakage points for the BIPV system 2 with corresponding colours as given in Table 12. (a) first test phase (inclination 30°); (b) second test phase (inclination 15°). View from the backside of the BIPV system (drawings by Anna Fedorova).

While testing the BIPV system 2, it was first attempted to weigh the leakage water amount at each load level. It was then decided to proceed with weighing the water amount from each water collection section summarized for each phase. After each phase, the system was lifted to nearly 90° and left for two hours to drain water droplets from the underlay; the water collected was then weighed and noted. The quantified results of these water leakage measurements for the BIPV system 2 are collected in Figure 53. As shown in this figure, the amounts of water collected at the 30° inclination from sections 4 and 3 are higher than those collected from the same sections at the 15° inclination. However, data collected for sections 2 and 1 showed the opposite, i.e., the water amounts collected at the 15° inclination were slightly higher than at the

30° inclination, where the observed differences are larger than the estimated uncertainties in the water collection measurements.

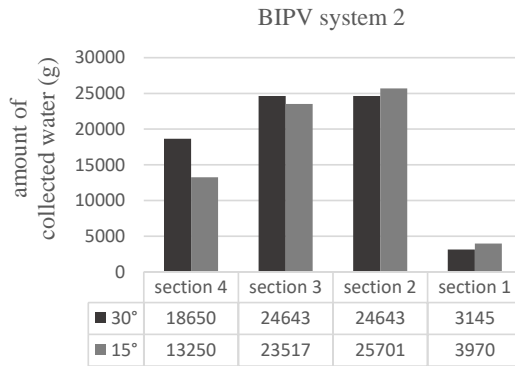


Figure 53. Quantitative measurements of water amounts collected during wind-driven rain testing in the RAWI box for the BIPV system 2.

Table 15 shows that water leakages started to occur at the same load level of 100 Pa at both 30° and 15°. Moreover, the leakage occurrence pattern is the same for both inclinations. The amount of water infiltration collected was close to each other for both inclinations. It can be concluded that this BIPV system performs similarly at 30° and 15° roof inclinations. However, there were more leakage points at 15°, where more leakages occurred at horizontally oriented joints. It may happen because, at lower slopes, the pressure is negative. Thus, roof tiles may be pulled a bit up, and leakages may occur at exactly horizontal joints.

4.3.3 Testing of BIPV system 3

The third tested system was constructed with large BIPV modules and installed with steel roof plates. The BIPV system consisted of two pairs of modules (four modules in total). One module overlapped with the second module in each pair, and a rubber sealant profile was placed between them to fill in the gap. The two lower modules were installed first, and then pieces of the rubber profile were placed on top of each module, followed by the installation of the two upper modules. The rubber sealant profile was not visible from the front side of the BIPV system and could, therefore, not be inspected for correct placement during installation. When the system was later placed in the RAWI box and inclined at 30° for the test, it was possible to observe the rubber sealant profiles. However, no visible difference in the placement of the sealant profile between the left pair and the right pair of modules was observed.

At the first test phase (30° inclination) of the WDR testing, no water leakages were detected at load levels 0 and 1. However, the rubber profile between the right pair of modules had started to move/dislocate, and at load level 2 (200 Pa), water began to run through it. New leakages occurred at load level 4 (400 Pa) at points where the metal plates overlapped, the parts close to the BIPV modules. A few water droplets appeared on the rubber profile between the left pair of modules. Water leakage points remained the same during all the following load levels, increasing in intensity with each next load level.

At the second test phase (15° inclination), water leakages appeared at the same locations but at lower load levels: between the right pair of modules at load level 1 (100 Pa), at metal plate overlaps, and between the left pair of modules at load level 3. As the BIPV system was mounted and sealed with waterproof tapes, it was not feasible to correct the sealing profile placement between the right pair of BIPV modules. Therefore, it was decided to run the test as it was and investigate how much leakages would occur if the sealing profile was dislocated. Additionally, moderate water leakages occurred between the upper modules at the last load level. The difference in the amount of water leakage through the rubber profile between the left and right pair of BIPV modules at 30° inclination can be observed in Figure 54 and at 15° inclination in Figure 55. A comparison of the rubber profile between the left and right pairs of the modules after the WDR test was fully finished is shown in Figure 56.

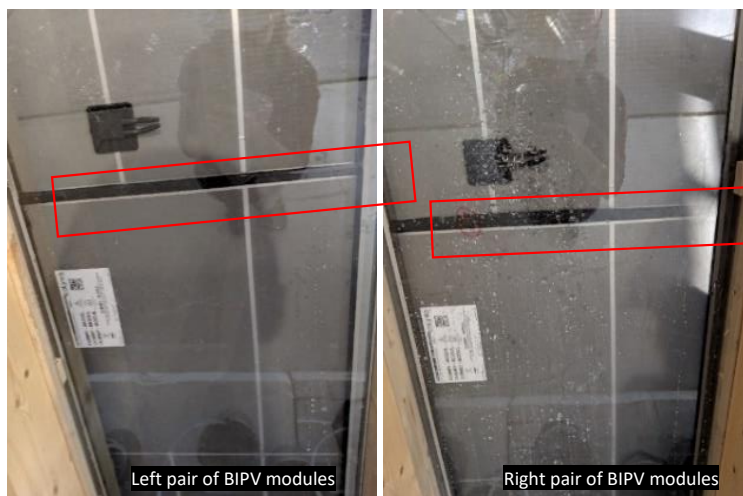


Figure 54. The rubber sealant profile (marked with white rectangles) between pairs of BIPV modules during wind-driven rain testing in the RAWI box with 30° inclination. A major difference in water leakage intensity between left pairs (no leakage) and right pairs (intense leakage) of the BIPV modules could be observed (photo by Anna Fedorova).

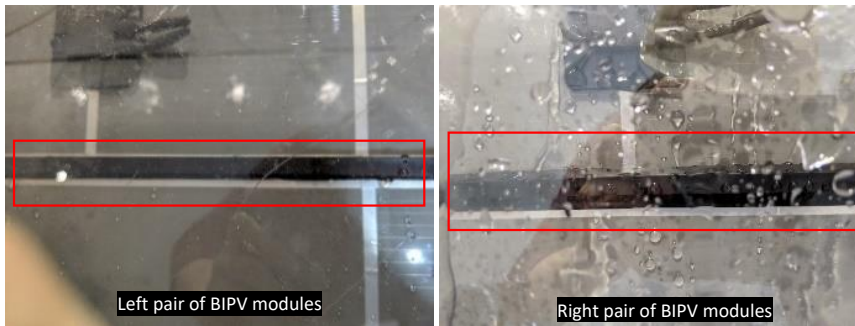


Figure 55. The rubber sealant profiles (marked with white rectangles) between the BIPV modules during wind-driven rain testing in the RAWI box with 15° inclination. A major difference in water leakage intensity between left pairs (no leakage) and right pairs (intense leakage) of the BIPV modules could be observed (photo by Anna Fedorova).

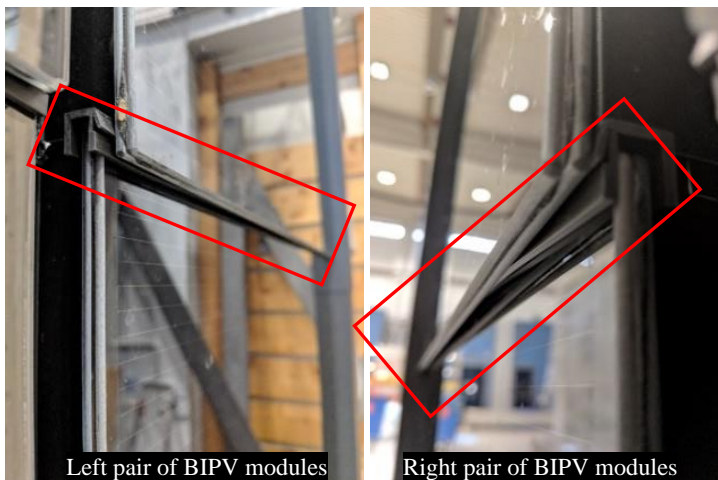

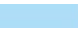








Figure 56. The rubber profile between the pairs of BIPV modules (marked with white rectangles) inspected after wind-driven rain testing in the RAWI box for the BIPV system 3 installed with steel roof plates. The rubber profile between right pair of modules was dislocated and had lost its sealing function, while the rubber profile between the left pair of modules was still in place and thus no water leaked through it (photo by Anna Fedorova).

Observations of both phases of the test are summarized in Table 13. All water leakage points are shown in Figures 57 a and 57 b. The quantified results of these water leakage measurements for the BIPV system 3 integrated with steel roof plates are collected in Figure 58.

Table 16. Qualitative observations of water leakages during wind-driven rain tightness testing in the RAWI box for the BIPV system 3 installed with steel roof plates.

Load level	Pulsating air pressure (Pa)	Colour mark	Inclination 30° (Figure 48 a)	Inclination 15° (Figure 48 b)
0	0 (runoff water)		No water leakages	No water leakages
1	0-100		No water leakages	Leakages occurred
2	0-200		Leakages occurred	No new leakages
3	0-300		No new leakages	New leakages occurred
4	0-400		New leakages occurred	No new leakages
5	0-500		No new leakages	No new leakages
6	0-600		No new leakages	No new leakages
7	0-750		No new leakages	New leakages occurred

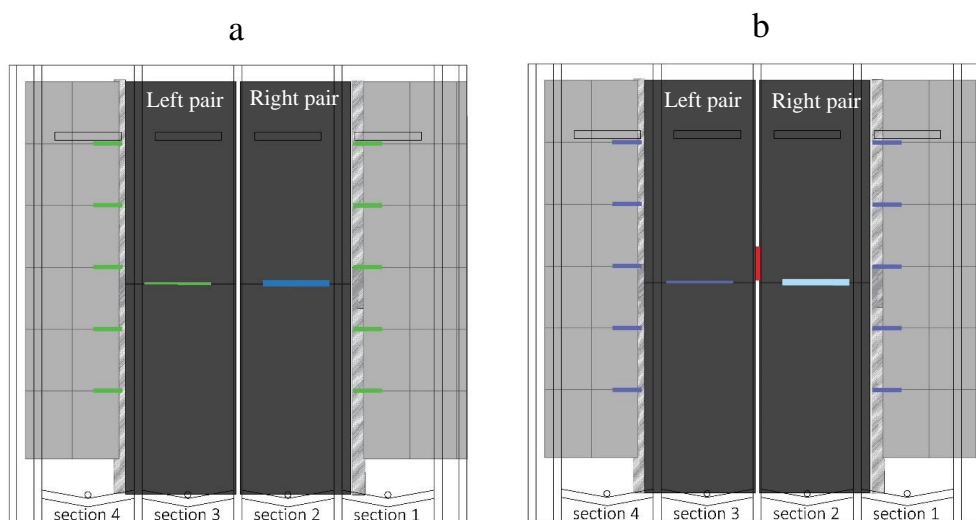


Figure 57. Location of water leakage points for the BIPV system 3 installed with steel roof plates with corresponding colours as given in Table 6. A – first test phase (inclination 30°); b – second test phase (inclination 15°). View from the backside of the BIPV system (drawings by Anna Fedorova).

Even though data on leakage water collected during WDR testing of the BIPV system 3 is provided, it must be noted that an utterly watertight tape sealing was not achieved for this system (see Figure 40 b). Thus, the amount of water in Figure 58 also contains some water that ran through the sealing tape system. The test was run anyway to study the behaviour of this system under WDR exposure. The amount of water collected from section 3 corresponds to a small water leakage between the left pair of BIPV modules. In contrast, the water amount collected in section 2 is approximately 21 and 16 (for 30° and 15° inclination, respectively) times larger than in section 3.

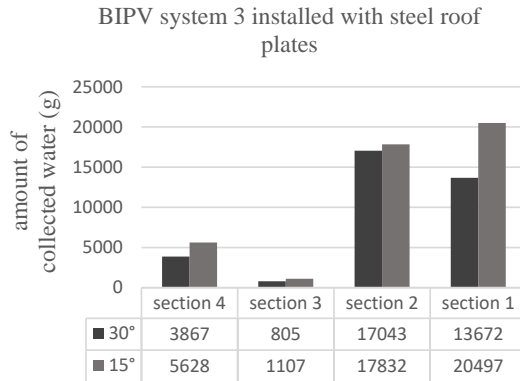


Figure 58. Quantitative measurements of water amounts collected during wind-driven rain testing in the RAWI box for the BIPV system 3 installed with steel roof plates. Note that some of the water collected here has erroneously run through the sealing tape system.

Such a significant difference occurred due to the rubber sealant profile's displacement between the right pair of the BIPV modules. Therefore, it can be advisable to include information about the importance of properly placing the sealant profile in the installation manual. Additionally, a solution for fixing this rubber profile on the module may be found to avoid displacement. Water collection sections 4 and 1 collected water leakage from the points connecting the BIPV system with steel roof plates. The steel rails attached to the left and right sides of BIPV modules are designed for water drainage, and steel roof plates on both sides of the BIPV system were placed over the steel rails. The distance from the roof plates placed to the right pair of BIPV modules was wider than the distance from the left pair of BIPV modules to the roof plates. Consequently, the amount of leakage water on the right side of the BIPV modules (section 1) was approximately 3.5-3.6 times larger than on the left side of the BIPV modules (section 4), for inclination 30° and 15°, respectively. Therefore, it can be concluded that the steel roof plates should be placed closer to the BIPV modules to minimize water leakage.

Similarly, the results obtained for BIPV system 1, leakages started to occur at load level 4 at 30° inclination and one load level earlier for 15° inclination. It is coherent with both results from BIPV system 1 and results from WDR testing of roof systems reviewed for this thesis.

4.4 COMPARISON OF TESTED BIPV SYSTEMS

As was anticipated before the experiment, test results showed that the most watertight BIPV system among the tested ones was the BIPV system 1, with respect to short-time wind-driven rain exposure tests. Multiple rubber sealing elements used during the system installation provided reliable waterproofing. However, if after installation, the BIPV system needs

adjustment or the cabling needs to be checked, it should be advised to change the used sealing elements to new ones. The BIPV shingles are screwed quite tightly, and sealing elements are hence squeezed. Thus, they might be deformed and thereby lose waterproofing ability to some degree. Careful use of a rubber sealing profile was also necessary for the BIPV system 3. If the sealing profile is placed correctly and stays in place, the watertightness level is quite close to the BIPV system 1.

However, more investigations of the long-term performance of the rubber sealing profiles should be carried out, as the durability of these materials may be much shorter than the service lifetime of the BIPV system. The BIPV system 2 resembles conventional roof tiles and was expected to be less watertight than the other two BIPV systems. As no sealing materials were used in the BIPV system 2, it should be compared to data on the watertightness of conventional roof tiles. From the graph in Figure 53, it can be concluded that the BIPV system 2 has an advantage when it comes to a lower inclination angle. The BIPV system 2 performed almost as good or even better at 15° than at 30° inclination, whereas the two other BIPV systems were less watertight at 15° than at 30° when compared to themselves. The watertightness level of the tested BIPV systems is provided in Table 17.

Table 17. Watertightness level of tested BIPV systems.

BIPV system	Angle of inclination		Weather condition equivalent of air pressure
	30°	15°	
	Watertight at air pressure level		200 Pa ≡ fresh gale 18.2 m/s
BIPV system 1	300 Pa	200 Pa	300 Pa ≡ strong gale 22.3 m/s
BIPV system 3	300 Pa	200 Pa	
Metal roof plates	300 Pa	200 Pa	
BIPV system 2	0 Pa (runoff water)	0 Pa (runoff water)	

Even though the watertightness level may be identified without quantifying the water leakage, it is an influential parameter supporting a more precise classification of the tested BIPV systems. In this study, water leakage was quantified, and water was weighed at the end of each test phase but not at each load level as desired or done in other studies.

5 DISCUSSION OF LEARNING POINTS

In this chapter learning points are highlighted.

Through the work with PhD project and thesis writing, I have found several valuable learning points I wish I had known when I started my research.

Acquisition of BIPV systems

One of the most significant critical issues was the acquisition of BIPV systems for testing. It was attempted to find manufacturers willing to collaborate and provide BIPV systems for the testing. It was also an approach used by Andenæs for his thesis [115], and even though it was successful in the end, acquiring relevant contributors was time-consuming. At the end, three relevant systems could be chosen and used for testing: the BIPV system 1 was purchased from a reseller in Norway, the BIPV system 2 was provided by another reseller in Norway who had a direct supply from a manufacturer in China, the BIPV system 3 was provided by a manufacturer through the “BIPV for Norway” project participant. A fourth BIPV system originating from Italy was considered for testing, but unfortunately, during transportation, the system was severely damaged and could not be used.



Figure 59. The fourth BIPV system that was received for testing but was not tested due to severely damaged during transportation.

There are pros and cons to involving manufacturers and resellers in research and laboratory work. When manufacturers/resellers are involved and agree to collaborate, there are benefits in terms of saved budget for both them and researchers. What is important is that manufacturers/resellers can guarantee that installation was done correctly and without errors, provide a critical review of obtained results, and participate in discussion of possible iterations in test methodology and parameters. They can also provide inputs on locations of systems, usually used inclinations or various technical details related to integrating BIPV systems with building envelopes. For research purposes, any results are beneficial, positive, or negative, and it is vital to use them and present them objectively. However, manufacturers/resellers can be

reserved when publishing results showing that products perform not as well as expected. When systems for testing are chosen by researchers/research projects independently, it can provide the freedom needed to publish any outcomes and results obtained.

Installation of BIPV systems

BIPV systems 1 and 3 were installed by the author of this study with help from the laboratory staff. The BIPV system 2 was installed with help from a reseller of this system in Norway, which was immensely helpful and the recommended way to use it. However, installation of all the tested BIPV systems was done according to installation manuals recommended for each system and provided by their manufacturers. If questions or issues were encountered before, during, or after installation or testing, they were attempted to be discussed with the manufacturer or reseller. Ideally, professional installers or manufacturers' representatives who are familiar with installation should be involved when systems are installed in the laboratory, such as it was possible to ensure in case of the BIPV system 2.

Test results

Results of water intrusion from wind-driven rain (WDR) testing are usually presented in infiltration rate (%) as a function of air pressure difference and normalised so the length of joints can be related to collected water (cm of joint/ml of rain). When these are not normalised to account for joint length, it might promote that large modules perform better as there are fewer joints and potential points for water infiltration. It was considered to measure the length of joints for this study. However, it was unclear whether it should be done from the front side or the back side, as there is an overlap of elements of the tested systems that are not always visible and accessible from the front side. The measurement of joint length from underneath was problematic due to the transparent underlay that cannot be removed after the tested system is installed onto the wooden structure. Values of overlaps and joints must be measured, especially when water leakages are going to be quantified.

Water leakages that occurred during testing were quantified, but they were measured at the end of each test phase, which included all load levels of air pressure for each inclination tested. It should be beneficial to measure it after each load level is applied, but there is a time shift for water collection from when water leakage occurs. Therefore, results from the quantification of water leakages obtained in this study should be seen as for worst-case weather scenarios.

6 CONCLUSIONS REGARDING THE RESEARCH QUESTION AND OBJECTIVES

This chapter summarizes answers to the raised research question and following objectives, highlights the obtained results and the overall contribution of this PhD thesis.

The research in wind-driven rain (WDR) exposure regarding building-integrated photovoltaic (BIPV) systems is complex and broad. It spreads from a micro-scale, covering the investigation of WDR exposure itself, its intensity, and field measurements, to a macro scale, when the subject of study explores how the WDR intrusion affects building envelope systems or entire buildings.

This thesis aims to expand knowledge of using BIPV systems in the building envelope and contribute to developing an experimental testing method for evaluating BIPV systems' performance as climate screens. One research question is formulated in the thesis:

When integrated into the building envelope, how do BIPV systems perform as climate screens?

The research question is addressed through literature reviews, market analysis, and mainly – experimental investigation in a laboratory. Objectives are set to help find answers to the main question.

- Understanding ways BIPV systems are evaluated nowadays.

This objective is addressed through a literature review and BIPV market analysis in Chapter 2, where BIPV systems design and integration ways are reviewed. There are five categories of BIPV: (A) Sloped, roof-integrated, not accessible from within the building; (B) Sloped, roof-integrated, accessible from within the building; (C) Non-sloped (vertically) mounted, not accessible from within the building; (D) Non-sloped (vertically) mounted, accessible from within the building; (E) Externally integrated, accessible, or not accessible from within the building. There is a wide variety of BIPV systems available on the market. It includes variations in the type of BIPV (foil, tile, module, or solar cell glazing products), type of solar cells, and ways systems could be integrated (full roof solutions, in-roof mounted systems, PV membrane, metal panels, solar glazing/skylight, cold facade, warm facade, or facade accessories in the form of fall protection). Additionally, BIPV products may be subcategorized into two groups: designed and produced for integration and customizable.

When evaluating the characteristics of BIPV systems, they must comply with requirements from two different standardization and regulation schemes: the electrical industry and the building industry. Primary standards for PV modules are the International Electrotechnical Commission (IEC) standards and the European Standards (EN), which test requirements initially address the qualification characteristics of PV modules. IEC standards evaluate the design qualification of each solar cell technology type that ensures PV design and performance quality and that they will operate without failures. IEC standards also evaluate PV safety.

Standards from the building industry evaluate aspects of safety and resistance to load impact, resistance to rain ingress (watertightness), safety in case of fire, durability, and reliability in use. BIPV standard EN 50583-2 contains the testing methodology for evaluating watertightness for systems intended for roof integration (BIPV category A). Wind-driven rain exposure testing is one of the methods to evaluate the watertightness of building envelope systems in a controlled laboratory environment.

- Assessing the possibility of evaluating watertightness of BIPV systems by quantifying wind-driven rain (WDR) intrusion.

Watertightness testing methodology is the focus of Chapter 3. At the beginning of this chapter, information on roof constructions typical for Norwegian building tradition, wind-driven rain impact on the roof cladding, and parameters of this impact that are valuable for wind-driven rain exposure testing sets a starting point for evaluation of watertightness testing.

BIPV systems heat up when operating; thus, ventilated building envelope systems are preferable for integration. PV systems should be installed with a certain tilt so that the electricity output will be sufficient. Therefore, widely used in Norway, a pitched ventilated roof is well suited for BIPV integration. Two variations of roof construction may be built: an old traditional variant where the underlay roof is separated from the wind barrier by the air cavity and a more modern variation where the underlayer roof consists of a watertight and vapour open wind barrier and is separated from a rain tight roofing by the ventilation cavity. This more modern way of roof construction is more environmentally conscious and cost-effective, but it is viewed as less robust. Watertightness evaluation of BIPV can ensure that the tested system is safe to use in such modern roof construction.

Wind-driven rain (WDR) is a cooccurrence of precipitation and wind, where rain intensity and wind speeds characterize exposure. Impinging WDR intensity is the total amount of rainwater that meets the roof surface where several surface phenomena happen. The ones influencing

watertightness are film forming, runoff, rain infiltration, wetting-drying, adhesion, and absorption if the material is porous. Forces that apply to rainwater penetration mechanisms are hydrostatic pressure, wind pressure, surface tension and gravity.

Tests that are usually used to evaluate the waterproofing of building envelope systems include infrared thermography, nuclear moisture testing, electrical impedance testing, electric field vector mapping, and wind-driven rain exposure. The first three methodologies are used for detecting absorbed water by porous materials. Electric field vector mapping is usually used to detect if water is present in porous materials, indicating leakage points in the membrane on a flat or low-slope roof. Water is usually not absorbed by most BIPV systems. Both the quality and quantity of rain infiltration rates can be measured. Thus, the WDR exposure test is the most suitable for evaluating the watertightness of BIPV systems.

- Designing and implementing a water collection system to quantify WDR intrusion during testing.

Usually, WDR exposure testing is done to collect qualitative data on rain infiltration points. Studies where quantitative data is collected in addition to qualitative evaluation are provided in subsection 3.4. Most of these studies utilize quantitative evaluation of façade systems and window-wall assemblies. Roof coverings and structures are studied less with means of rain infiltration quantification. To be able to quantify rain infiltration through building envelope systems, a transparent board or cavities must be installed in a way that rain infiltration can be collected from the whole area of the specimen (to get the result of the total amount of infiltrated water), but it can be separated in sections if it suits construction of roof, façade, or window-wall system best. It can be, for example, utilized to measure rain infiltration through particular details of these systems, like vertical or horizontal joints that are in question or details that have high rain infiltration assessed visually that need a better understanding of mechanisms that induce infiltration. Wind-driven rain exposure testing is one of the methods to evaluate the watertightness of building envelope systems in a controlled laboratory environment.

For this thesis, WDR simulation is done in a specially designed rain and wind (RAWI) box at the NTNU and SINTEF Building construction laboratory in Trondheim, Norway. A roof sample is mounted on a test frame (2.75 m x 2.75 m) that is fitted in the RAWI box. A transparent polycarbonate (Lexan) board is mounted on the wooden structure and secured by screwing wooden battens to it. The wooden battens are spaced 0.6 m from each other and form four separate sections. At the bottom of the frame, a water collection system is built. Following

the already built four sections, four water collection sections are formed, where one round hole is cut in each section, and a tube is connected to each hole. A triangle profile made of wooden battens is built near each hole and taped to the underlayment with duct tape. The four water collection sections are numbered, and respective containers for water collection are placed at the end of each tube connected to their section.

The wooden frame area not covered by the BIPV systems must be watertight; therefore, the remaining fragments of the surrounding frame are covered with thick polyethylene foil, which is sealed to the test frame using duct tape. Edges of the BIPV systems are sealed to the polyethylene foil using three types of sealing tape (60 mm and 100 mm).

- Testing BIPV of diverse designs and configurations according to the developed testing methodology.

The principal of the watertightness test for building envelope systems is to apply a certain quantity of water spray at various ranges of air pressure differences at defined conditions with respect to the exterior surface of a roof specimen. Usually, a combination of two water sources is used: runoff water applied on an upper side of the tested system and water spray that is distributed along the test specimen surface area. Differential air pressure between the outer and inner surfaces of the tested specimen is usually increased stepwise. When roof systems are tested, they are tilted to various slopes. The test specimen is inspected for water passages into its inner surface and water leakage points are registered (qualitative data). As a result, a limit of watertightness can be identified for the tested systems. The limit of watertightness may be described as the maximum level of air pressure applied simultaneously with water spray and runoff water when no water leakages occur on the tested system's inner side. Acquired data on the rain infiltration rates provides a ground for comparing different systems. Systems can be ranked according to their watertightness level.

The testing methodology is based on the standard NT Build 421 "Roofs: watertightness under pulsating air pressure". Other two European standards on wind-driven testing for building envelope systems are reviewed: EN 50583-2:2016 "Photovoltaics in buildings. Part 2: BIPV systems" (Annex A "Resistance to wind-driven rain of BIPV roof coverings with discontinuously laid elements – Test method") and EN 12865:2001 "Hygrothermal performance of building components and building elements - Determination of the resistance of external wall systems to driving rain under pulsating air pressure".

The following test parameters are used in this thesis for WDR testing in the RAWI box: runoff at a rate 1.7 L/min x m, water spray at a rate 0.3 L/min x m², cyclic air pressure intervals ranging from 0 Pa to 750 Pa (each load level is increased in steps of 100 Pa and last load level increased in 150 Pa step), duration of each load level is set to 10 minutes. Tilt angles are 15° and 30° roof inclinations.

Three different BIPV systems for roof integration are evaluated: the BIPV system 1 (solar shingles), the BIPV system 2 (solar tiles), and the BIPV system 3 (glass-glass solar modules installed with steel roof plates). BIPV system 1 is constructed with fish-scale solar shingles (glass-glass modules with solar cells laminated between them). Solar shingles have four shapes to fit on the roof (full squared shingles and three half shingles that fit the roof's edges), and the rest of the roof area is covered using colour-matching aluminium composite plates (cut to diverse sizes and forms). BIPV system 2 is composed of flat rectangular-shaped solar tiles (PV cells are covered with tempered glass) and their matching tiles without PV cells, all made of a ceramic compound. The matching tile is half of the size of the solar tile. BIPV system 3 is constructed by large-size BIPV modules, reminiscent of standard PV modules. Glass-glass BIPV modules are installed on coated steel rails attached to each module's left and right sides, which eases the installation. Four BIPV modules are installed, and the remaining specimen area is covered with steel roof plates.

- Reporting on results and failures during testing in the laboratory.

All three tested BIPV systems have proven to be mechanically stable under even hurricane wind speed conditions. The BIPV system 1 (solar shingles) and the BIPV system 3 (glass-glass solar modules installed with steel roof plates) are watertight at the same wind pressure levels: 300 Pa at 30° inclination and 200 Pa at 15° inclination. Both systems are integrated with the use of rubber sealant elements, which improved the systems' watertightness. Quantification of rain infiltration shows higher amount of water infiltrated in BIPV systems 1 and 3 at lower inclination.

To conclude this thesis, the research question: “When integrated into the building envelope, how do BIPV systems perform as climate screens?” can be answered as follows: BIPV systems show a high level of watertightness when tested using wind-driven rain exposure testing. Based on visual assessment (qualitative data), BIPV systems seem more watertight than conventional roof coverings.

7 OUTLOOK AND SUGGESTIONS FOR FURTHER RESEARCH

This chapter proposes perspective on further research.

The assessment of watertightness and wind-driven rain (WDR) impact on BIPV systems for roof integration and systems for a building envelope integration, in general, still contains a lot of room for further investigations. This study focuses on assessing performance of BIPV systems for roof integration under exposure to WDR, including the quantification of water intrusion during testing. This measurement helps to identify a watertightness level of a tested system and can provide useful data for a design improvement of the system. Future work can include the investigation of following problems:

- Testing of systems with various inclinations, typical for specific localisations and climate zones.
- Testing may run with the duration of application of each air pressure load level (the duration of a single test step in the sub-test) shortened down from 10 minutes to 5 minutes by a step, i.e., so that water leakage measurements can be compared to a reference leakage rate of 10 g/m²/5 minutes. Then measurements collected for 5 minutes, and 10 minutes steps can be compared to see if shorter test duration is sufficient.
- Changing rates of water spray to simulate heavier rain, for example as it is described in the sub-tests in EN 50583 Part 2.
- Testing parameters used in this study are standard parameters for WDR tests in Norway. Ideally, test parameters could be calculated from information on intensities of driving rain, wind pressure rates, water droplet sizes that are likely to occur for specific local climate conditions where systems are supposed to be installed and used.
- More systems could be tested and compared to the performance of conventional roof systems.
- When choosing an outline of systems to test it should be of the same size, so the WDR exposure could relate to the same area.
- The quantification of water intrusion can provide vital information on changes occurring during the ageing process of building envelope components. Thus, using the presented test methodology and recommended procedures before and after accelerated ageing tests might give comprehensive information on how the watertightness of tested systems is supposed to change over time. In turn, it might contribute to making decisions regarding design of building integrated components basing on information about changes which are

supposed to occur during a system's service lifetime of 25-30 years, which should be considered.

Further development and verification of the presented test procedure might form a basis for evaluating various BIPV systems that can be tested under similar conditions worldwide in different laboratories and hence be directly compared.

Results from this study can be useful for both the scientific community, and for the development of BIPV products to be integrated in roofs in the near future. Firstly, the methodology can be used by certifying institutions giving quality assurance for products available on the market. Secondly, such data may provide some directions for manufacturers and designers developing products. Then, it could be easier for customers and resellers to choose optimal-suited systems to be used for particular locations.

REFERENCES

- [1] UNEP 2009 annual report, U. N. Environ. Programme. (2009).
- [2] World Population Prospects 2019: Ten Key Findings., U. N. Dep. Econ. Soc. Aff. Popul. Div. (2019).
- [3] The European Parliament and the European Union, Directive (EU) 2018/2001 on the promotion of the use of energy from renewable sources, (2018).
- [4] The European Parliament and the European Union, Directive (EU) 2018/844 amending Directive 2010/31/EU on the energy performance of buildings and Directive 2012/27/EU on energy efficiency, (2018).
- [5] The European Parliament and the European Union, Directive 2010/31/EU on the energy performance of buildings, (2010).
- [6] The European Parliament and the European Union, Directive 2012/27/EU on energy efficiency, (2012).
- [7] The United Nations, The Sustainable Development Goals, (2015).
- [8] K. Peterson, P. Torcellini, R. Grant, A Common Definition for Zero Energy Buildings, Natl. Inst. Build. Sci. (2015).
- [9] S.M. Fufa, R.D. Schlanbusch, K. Sørnes, M.R. Inman, I. Andersen, A Norwegian ZEB Definition Guideline, Res. Cent. Zero Emiss. Build. (2016).
- [10] J. Stene, M.J. Alonso, Ø. Rønneseth, L. Georges, State-of-the-art analysis of nearly zero energy buildings. Country report IEA HPT Annex 49 Task 1 – Norway, SINTEF Acad. Press. (2018).
- [11] E. Rodriguez-Ubinas, C. Montero, M. Porteros, S. Vega, I. Navarro, M. Castillo-Cagigal, E. Matallanas, A. Gutiérrez, Passive design strategies and performance of net energy plus houses, Energy Build. 83 (2014) 10–22.
- [12] S. Backe, A.K. Kvellheim, Zero emission neighbourhoods. Drivers and barriers towards future development, N Res. Cent. Zero Emiss. Neighb. Smart Cities FME ZEN. (2020).
- [13] M. van der Hoeven, Transition to Sustainable Buildings. Strategies and Opportunities to 2050, Int. Energy Agency IEA. (2013).
- [14] A. Fedorova, B.D. Hrynyszyn, B.P. Jelle, Building-integrated photovoltaics from products to system integration – a critical review, IOP Mater. Sci. Eng. (2020).
- [15] K. Berger, A. Cueli Belen, S. Boddaert, M. Del Buono, V. Delisle, A. Fedorova, F. Frontini, P. Hendrick, H. Ishii, K. Kapsis, J.-T. Kim, P. Kovacs, N.M. Chivelet, L. Maturi, M. Machado, A. Schneider, H.R. Wilson, International definitions of “BIPV”. Report IEA-PVPS T15-04: 2018, Int. Energy Agency. (2018).
- [16] The European Parliament and the European Council, the Construction Product Regulation (CPR) 305/2011, Off. J. Eur. Union. (2011).
- [17] European Committee for Electrotechnical Standardization, EN 50583-1. Photovoltaics in buildings - Part 1: BIPV modules, (2016).
- [18] M.L. Mehta, W. Scarborough, D. Armpriest, Building construction: principles, materials, and systems, 3rd edition, Pearson. (2017).
- [19] L. Gullbrekken, T. Kvande, B. Time, Roof-integrated PV in Nordic climate - building physical challenges, 6th Int. Build. Phys. Conf. - IBPC 2015 Energy Procedia. 78 (2015) 1962–1967.
- [20] European Committee for Electrotechnical Standardization, EN 50583-2. Photovoltaics in buildings. Part 2: BIPV systems, (2016).
- [21] I. Zanetti, P. Bonomo, F. Frontini, E. Saretta, Building integrated photovoltaics: product overview for solar building skins. Status report 2017., Univ. Appl. Sci. Arts South. Switz. SUPSI.

- [22] B.P. Jelle, C. Breivik, H.D. Røkenes, Building integrated photovoltaic products: A state-of-the-art review and future research opportunities, *Sol. Energy Mater. Sol. Cells*. 100 (2012) 69–96.
- [23] G. Verberne, P. Bonomo, F. Frontini, M.N. van den Donker, A. Chatzipanagi, K. Sinapis, W. Folkerts, BIPV products for facades and roofs: a market analysis, 29th EU-PVSEC Amst. (2014).
- [24] <http://www.issol.eu/solarterra/>, accessed 03.05.21, accessed 05.05.21.
- [25] https://www.sunstyle.com/The_projects.html, accessed 05.05.21.
- [26] <http://www.bipv.ch/index.php/en/residential-side-en/item/948-housegrosshoechstetten-eng.>, accessed 05.05.21.
- [27] <http://www.bipv.ch/index.php/en/residential-side-en/item/1102-primagneerach-eng.>, accessed 05.05.21.
- [28] <http://www.bipv.ch/index.php/en/residential-side-en/item/894-einfamilienhaus-mettmenstetten.>, accessed 05.05.21.
- [29] <http://www.bipv.ch/index.php/en/products-en-top/bipv-modules>, accessed 05.05.21.
- [30] S. Philipps, W. Warmuth, Photovoltaics report, updated: 18 May 2020, Fraunhofer Inst. Sol. Energy Syst. ISE Support PSE GmbH. (2020).
- [31] C. Ferrara, H.R. Wilson, W. Sprenger, The performance of photovoltaic (PV) systems. Modelling, measurement and assessment. Part three: Maximising photovoltaic (PV) system performance. 8 - Building-integrated photovoltaics (BIPV), Woodhead Publ. (2017).
- [32] E. Taveres-Cachat, G. Lobaccaro, F. Goia, G. Chaudhary, A methodology to improve the performance of PV integrated shading devices using multi-objective optimization, 247 (2019) 731–744.
- [33] A. Røyset, T. Kolås, B.P. Jelle, Coloured building integrated photovoltaics: Influence on energy efficiency, *Energy Build*. 208 (2020).
- [34] <https://www.altaskifer.com/produkter/tak>, accessed 07.05.21.
- [35] <https://susoltech.no/solar-panel-map/>, accessed 07.05.21.
- [36] <https://www.skarpnes.com/taktegl/domino/>, accessed 07.05.21.
- [37] <https://sun-net.no/produkter/tegl-teglstein-med-integrert-solcelle/>, accessed 07.05.21.
- [38] <https://sun-net.no/referanser/>, accessed 07.05.21.
- [39] <https://sun-net.no/produkter/solstein-betongtakstein-med-integrert-solcelle/>, accessed 07.05.21.
- [40] K. Berger, S. Boddaert, M. Del Buono, A. Fedorova, F. Frontini, S. Inoue, H. Ishii, K. Kapsis, J.-T. Kim, P. Kovacs, M. Machado, N.M. Chivelet, A. Schneider, H.R. Wilson, Analysis of requirements, specifications and regulation of BIPV. Report IEA-PVPS T15-08: 2019, Int. Energy Agency. (2019).
- [41] CEA, Tecnalía, CTCV, Standardization needs for BIPV, PVSITES. (2016).
- [42] P. Bonomo, A. Chatzipanagi, F. Frontini, Overview and analysis of current BIPV products: new criteria for supporting the technological transfer in the building sector, *Vitr. - Int. J. Archit. Technol. Sustain*. 0 (2015) 67–85.
- [43] International Organization for Standardization, ISO 18178. Glass in buildings - Laminated solar PV glass for use in buildings, (2018).
- [44] International Electrotechnical Commission, IEC 63092-1. Photovoltaics in buildings - Part 1: Building integrated photovoltaics modules., (2020).
- [45] International Electrotechnical Commission, IEC 63092-2. Photovoltaics in buildings - Part 2: Building integrated photovoltaics systems., (2020).
- [46] F. Rehde, T. Szacsavay, A. Peppas, Review of standards for integrating BIPV-modules in building facade and roof, Fraunhofer ISE. (2016).

- [47] B.P. Jelle, Building integrated photovoltaics: a concise description of the current state of the art and possible research pathways, *Energies*. 9 (2015).
- [48] International Electrotechnical Commission, IEC 61215-1. Terrestrial photovoltaic (PV) modules - Design qualification and type approval - Part 1: Test requirements, (2016).
- [49] International Electrotechnical Commission, IEC 61215-1-1. Terrestrial photovoltaic (PV) modules - Design qualification and type approval - Part 1-1: Special requirements for testing of crystalline silicon photovoltaic (PV) modules, (2016).
- [50] International Electrotechnical Commission, IEC 61215-1-2. Terrestrial photovoltaic (PV) modules - Design qualification and type approval - Part 1-2: Special requirements for testing of thin-film Cadmium Telluride (CdTe) based photovoltaic (PV) modules, (2016).
- [51] International Electrotechnical Commission, IEC 61215-1-3. Terrestrial photovoltaic (PV) modules - Design qualification and type approval - Part 1-3: Special requirements for testing of thin-film amorphous silicon based photovoltaic (PV) modules, (2016).
- [52] International Electrotechnical Commission, IEC 61215-1-4. Terrestrial photovoltaic (PV) modules - Design qualification and type approval - Part 1-4: Special requirements for testing of thin-film Cu(In,Ga)(S,Se) (CIGS) based photovoltaic (PV) modules, (2016).
- [53] International Electrotechnical Commission, IEC 61730-1. Photovoltaic (PV) module safety qualification - Part 1: Requirements for construction, (2016).
- [54] International Electrotechnical Commission, IEC 61730-2. Photovoltaic (PV) module safety qualification - Part 2: Requirements for testing, (2016).
- [55] International Organization for Standardization, ISO 15392. Sustainability in building construction – general principals, (2008).
- [56] International Organization for Standardization, ISO 15686-1. Buildings and construction assets – service life planning – part 1: general principals and framework, (2011).
- [57] International Organization for Standardization, ISO 12543. Glass in building — Laminated glass and laminated safety glass, (2011).
- [58] International Electrotechnical Commission, IEC TR 63226. Solar photovoltaic energy systems - Managing fire risk related to photovoltaic (PV) systems on buildings, (2020).
- [59] Building Resilience | WBDG Whole Building Design Guide., accessed 13.04.21. <https://www.wbdg.org/resources/building-resiliency>.
- [60] K. Fath, A. Hartmann, H.R. Wilson, C. Hemmerle, T.E. Kuhn, J. Stengel, F. Schultmann, B. Weller, Life-cycle cost assessment of photovoltaic facade panels, *Conf. Proc. ENERGY FORUM Sol. Build. Ski*. (2011).
- [61] P. Eiffert, Guidelines for the economic evaluation of building-integrated photovoltaic power systems, *Natl. Renew. Energy Lab*. (2003).
- [62] N. Garcez, N. Lopes, J. de Brito, J. Silvestre, System of inspection, diagnosis and repair of external claddings of pitched roofs, *Constr. Build. Mater.* 35 (2012) 1034–144.
- [63] B.P. Jelle, Accelerated climate ageing of building materials, components and structures in the laboratory, *J. Mater. Sci.* 47 (2012) 6475–6496.
- [64] L. Gullbrekken, T. Kvande, B.P. Jelle, B. Time, Norwegian pitched roof defects, *Buildings*. 6 (2016) 24.
- [65] K. Edvardsen, T. Ramstad, *Trehus håndboka 5 (Wooden houses handbook No5)*, SINTEF Build. Infrastruct. Oslo Nor. (2014).
- [66] B. Blocken, J. Carmeliet, A review of wind-driven rain research in building science, *J. Wind Eng. Ind. Aerodyn.* 92 (2004) 1079–1130.

- [67] B. Blocken, D. Derome, J. Carmeliet, Rainwater runoff from building facades: a review, *Build. Environ.* 60 (2013) 339–361.
- [68] B. Blocken, J. Carmeliet, Impact, runoff and drying of wind-driven rain on a window glass surface, 84 (2015) 170–180.
- [69] M. Rein, Phenomena of liquid drop impact on solid and liquid surfaces, *Fluid Dyn. Res.* 12 (1993) 61–93.
- [70] J. Liu, H. Vu, S.S. Yoon, R. Jepsen, G. Aguilar, Splashing phenomena during liquid droplet impact, *At. Sprays.* 20 (2010) 297–310.
- [71] R. Rioboo, M. Marengo, C. Tropea, Time evolution of liquid drop impact onto solid, dry surfaces, *Exp. Fluids.* 33 (2002) 112–124.
- [72] Y. Yu, C. Hopkins, Experimental determination of forces applied by liquid water drops at high drop velocities impacting a glass plate with and without a shallow water layer using wavelet deconvolution, *Exp. Fluids.* 59:84 (2018).
- [73] B. Blocken, J. Carmeliet, A simplified numerical model for rainwater runoff on building facades: possibilities and limitations, *Build. Environ.* 53 (2012) 59–73.
- [74] <https://pixabay.com/photos/raindrop-inject-rain-splashes-61919/>, accessed 11.05.21.
- [75] <https://www.pikist.com/free-photo-ismye>, accessed 11.05.21.
- [76] H. Saito, Application of the wood degradation model to an actual roof assembly subjected to rain penetration, *Energy Procedia.* 132 (2017) 399–404.
- [77] M. Abuku, B. Blocken, S. Roels, Moisture response of building fasades to wind-driven rain: field measurements compared with numerical simulations, *J. Wind Eng. Ind. Aerodyn.* 97 (2009) 197–207.
- [78] J.M. Pérez-Bella, J. Domínguez-Hernández, B. Rodríguez-Soria, J.J. del Coz-Díaz, E. Cano-Suñén, Combined use of wind-driven rain and wind pressure to define water penetration risk into building façades: The Spanish case, *Build. Environ.* 64 (2013) 46–56.
- [79] C. Giarma, D. Aravantinos, On building components' exposure to driving rain in Greece, *J. Wind Eng. Ind. Aerodyn.* 125 (2014) 133–145.
- [80] J. Dominguez-Hernandez, J.M. Perez-Bella, M. Alonso-Martinez, E. Cano-Suñén, J.J. del Coz-Díaz, Assessment of water penetration risk in building facades throughout Brazil, *Build. Res. Inf.* 45 (2016) 492–507.
- [81] T. Qian, H. Zhang, Assessment of long-term and extreme exposure to wind-driven rain for buildings in various regions of China, *Build. Environ.* 189 (2021).
- [82] N. Van Den Bossche, M.A. Lacasse, A. Janssens, A uniform methodology to establish test parameters for watertightness testing: Part I: A critical review, *Build. Environ.* 63 (2013) 145–156.
- [83] C. Meola, R. Di Maio, N. Roberti, G.M. Carlomagno, Application of infrared thermography and geophysical methods for defect detection in architectural structures, *Eng. Fail. Anal.* 12 (2005) 875–892.
- [84] E. Barreira, R.M.S.F. Almeida, Drying Evaluation Using Infrared Thermography, *Energy Procedia.* 78 (2015) 170–175.
- [85] E. Barreira, R.M.S.F. Almeida, J.M.P.Q. Delgado, Infrared thermography for assessing moisture related phenomena in building components, *Constr. Build. Mater.* 110 (2016) 251–269.
- [86] E. Barreira, V.P. de Freitas, Evaluation of building materials using infrared thermography, *Constr. Build. Mater.* 21 (2007) 218–224.
- [87] J.H.A. Rocha, C.F. Santos, Y.V. Póvoas, Detection of precipitation infiltration in buildings by infrared thermography: a case study, *Procedia Struct. Integr.* 11 (2018) 99–106.

- [88] J.H.A. Rocha, C.F. Santos, Y.V. Póvoas, Evaluation of the infrared thermography technique for capillarity moisture detection in buildings, *Procedia Struct. Integr.* 11 (2018) 107–113.
- [89] M.T.G. Barbosa, V.J. Rosse, N.G. Laurindo, Thermography evaluation strategy proposal due moisture damage on building facades, *J. Build. Eng.* 43 (2021) 102555.
- [90] S. Kruschwitz, S. Munsch, M. Telong, W. Schmidt, T. Bintz, M. Fladt, L. Stelzner, The NMR core analyzing tomograph: a multi-functional tool for non-destructive testing of building materials, *Magn. Reson. Lett.* 3 (2023) 207–219.
- [91] J. Zhang, A. Heath, H.M.T. Abdalgadir, R.J. Ball, K. Paine, Electrical impedance behaviour of carbon fibre reinforced cement-based sensors at different moisture contents, *Constr. Build. Mater.* 353 (2022) 129049.
- [92] IR Analyzers, Electric field vector mapping, accessed 06.11.23.
- [93] International leak detection, Electric field vector mapping technology, accessed 06.11.23.
- [94] N. Van Den Bossche, M.A. Lacasse, A. Janssens, A uniform methodology to establish test parameters for watertightness testing part II: Pareto front analysis on co-occurring rain and wind, *Build. Environ.* 63 (2013) 157–167.
- [95] J.M. Perez-Bella, J. Dominguez-Hernandez, E. Cano-Suñén, J.J. del Coz-Díaz, F.J. Suárez-Domínguez, A comparison of methods for determining watertightness test parameters of building façades, *Build. Environ.* 78 (2014) 145–154.
- [96] N. Sahal, M.A. Lacasse, Proposed method for calculating water penetration test parameters of wall assemblies as applied to Istanbul, Turkey, *Build. Environ.* 43 (2008) 1250–1260.
- [97] European Committee for Standardization, CEN/TR 15601:2012 “Hygrothermal performance of buildings – Resistance to wind-driven rain of roof coverings with discontinuously laid small elements – Test method,” (2012).
- [98] B. Blocken, J. Carmeliet, Driving rain on building envelopes- I. numerical estimation and full-scale experimental verification, *J. Build. Phys.* 24 (2000).
- [99] B. Blocken, J. Carmeliet, Driving rain on building envelopes— II. representative experimental data for driving rain estimation, *J. Build. Phys.* 24 (2000).
- [100] Nordtest Standard, NT Build 421. Roofs: watertightness under pulsating air pressure, (1993).
- [101] European Committee for Standardization, EN 12865. Hygrothermal performance of building components and building elements - Determination of the resistance of external wall systems to driving rain under pulsating air pressure, (2001).
- [102] R.P. Brown, D. Kockott, W. Ketola, J. Shorthouse, A review of accelerated durability tests. VAMAS Technical Report No 18, Teddington. Natl. Phys. Lab. (1995).
- [103] J.M. Lirola, E. Castañeda, B. Lauret, M. Khayet, A review on experimental research using scale models for buildings: Application and methodologies, *Energy Build.* 142 (2017) 72–110.
- [104] G.T. Bitsuamlak, A. Gan Chowdhury, D. Sambare, Application of a full-scale testing facility for assessing wind-driven-rain intrusion, *Build. Environ.* 44 (2009) 2430–2441.
- [105] G. Cattarin, F. Causone, A. Kindinis, L. Pagliano, Outdoor test cells for building envelope experimental characterisation – A literature review, *Renew. Sustain. Energy Rev.* 54 (2016) 606–625.
- [106] S. Fasana, R. Nelva, Improvement of the performance of traditional stone roofs by wind driven rain experimental tests, *Constr. Build. Mater.* 25 (2011) 1491–1502.
- [107] L. Olsson, Rain intrusion rates at façade details - a summary of results from four laboratory studies, in: *Energy Procedia*, Trondheim, Norway, 2017: pp. 387–392.

- [108] M.A. Lacasse, N.V.D. Bossche, S.V. Linden, T.V. Moore, A brief compendium of water entry results derived from laboratory tests of various types of wall assemblies, *MATEC Web Conf.* 282 (2019) 02050.
- [109] M. Arce-Recatala, S. Garcia-Morales, N. Van Den Bossche, Quantifying wind-driven rain intrusion - a comparative study on the water management features of different types of rear-ventilated facade systems, *E3S Web Conf.* 172 (2020).
- [110] M. Arce-Recatala, Proposal for a new test methodology for assessing the performance of rear-ventilated facades against wind-driven rain (WDR) and driven rain wind pressure (DRWP), Doctoral thesis, Technical University of Madrid, 2017.
- [111] M. Arce-Recatala, S. Garcia-Morales, N. Van Den Bossche, Experimental assessment of rainwater management of a ventilated facade, *Build. Phys.* 42 (1) (2017) 38–67.
- [112] K.S. Vutukuru, M. Moravej, A. Elawady, A.G. Chowdhury, Holistic testing to determine quantitative wind-driven rain intrusion for shuttered and impact resistant windows, *J. Wind Eng. Ind. Aerodyn.* 206 (2020) 104359.
- [113] S. Van Linden, N. Van Den Bossche, Watertightness performance of face-sealed versus drained window-wall interfaces, *Build. Environ.* 196 (2021) 107824.
- [114] C. Breivik, B.P. Jelle, B. Time, Ø. Holmberget, J. Nygård, E. Bergheim, A. Dalehaug, Large-scale experimental wind-driven rain exposure investigations of building integrated photovoltaics, *Sol. Energy.* 90 (2013) 179–187.
- [115] E. Andenæs, Wind-driven rain exposure and assessment of building integrated photovoltaic systems MSc thesis, Norwegian University of Science and Technology, Trondheim. (2016).
- [116] A. Fedorova, B.P. Jelle, B.D. Hrynyszyn, S. Geving, A testing methodology for quantification of wind-driven rain intrusion for building-integrated photovoltaic systems, *Build. Environ.* (2021).
- [117] N.S. Bunkholt, T. Säwén, M. Stockhaus, T. Kvande, L. Gullbrekken, P. Wahlgren, J. Lohne, Experimental Study of Thermal Buoyancy in the Cavity of Ventilated Roofs, *Buildings.* 10 (2020) 8. <https://doi.org/10.3390/buildings10010008>.
- [118] SINTEF Byggforsk, SINTEF Building Research Design Guides, bks.byggforsk.no, n.d.
- [119] M.Z. Jacobson, V. Jadhav, World estimates of PV optimal tilt angles and ratios of sunlight incident upon tilted and tracked PV panels relative to horizontal panels, *Sol. Energy.* 169 (2018) 55–66. <https://doi.org/10.1016/j.solener.2018.04.030>.
- [120] E.M. Samuelsen, O. Bakke Aashamar, G. Haugen, J. Mamen, A.C. Berger, T. Lien, Extreme weather conditions report. METinfo. Hendelserapport. Ekstremværet Frank 21. og 22. januar 2021., *Meteorol. Inst.* (2021).
- [121] A.-M. Olsen, A. Haaland Simonsen, T. Lien, Extreme weather conditions report. Ekstremvaerrapport NR 4/2008 “Ulrik,” *Meteorol. Inst.* (2008).
- [122] E.M. Samuelsen, T. Lien, H. Thorset, J. Mamen, A.C. Berger, G. Haugen, Extreme weather conditions report. Metinfo. Hendelserapport. Svaert kraftige vindkast i Lofoten, Besteraalen og Troms onsdag 23. september 2020, *Meteorol. Inst.* (2020).
- [123] M. Granerød, S. Gulbrandsen, G. Livik, A. Solveig Andersen, T. Nipen, H. Nordlien Berg, Extreme weather conditions report. Metinfo. Hendelserapport. Svaert mye nedbør paa Helgeland og nord i Trøndelag 6. og 7. november 2020, *Meteorol. Inst.* (2020).
- [124] G.O. Fagerlid, A. Solveig Andersen, H. Nordlien Berg, Extreme weather conditions report. Metinfo. Hendelserapport. Svaert mykje regn i Hordaland og Sogn 18. november 2020, *Meteorol. Inst.* (2020).
- [125] S.M. Fufa, N. Labonnote, S. Frank, P. Rüter, B.P. Jelle, Durability evaluation of adhesive tapes for building applications, *Constr. Build. Mater.* 161 (2018) 528–538.
- [126] <https://www.orklaelektronikk.com/new/heda-solar/>, (n.d.).

- [127] <https://ennogie.com/>, accessed 07.05.21.
- [128] <https://www.isola.com/>, accessed 07.05.21.

PAPERS OVERVIEW AND THEIR INTERCONNECTION

Paper I

In Paper I, a brief overview of the solar market in Norway is given along potential of using building-integrated photovoltaics (BIPV) and building-applied photovoltaics (BAPV). Even though Norway and Nordic countries could seem not an obvious choice for use of solar energy, it has been shown that there is a great potential for solar energy in these countries. The number of projects realized and planned where either BIPV or BAPV are used increases every year and the numbers are expected to grow in the years to come. Among challenges of using BIPV and BAPV at Nordic climate conditions are higher level of precipitations like rain, wind-driven rain, snow, and ice formation. Weather is extremely varied in the Nordic region, due to a long coastline, and extreme events like storms and heavy rainfalls occur frequently. It concerns especially BIPV systems, as they must withstand weather constraints at the same level as conventional envelope systems. Snow and ice covering should also be considered, as they lead to loss in energy production and might affect durability of PV system components. Several buildings with BIPV and BAPV installations in Norway are presented.

Paper II

Paper I provided the ground to continue studying BIPV systems, as there is an immense potential and interest for these systems in Nordic countries. It was also identified that the aspect of watertightness of such systems should be one of the focus areas for the research work. Thus, in Paper II, BIPV products and systems are studied more in depth. BIPV standardization and market analysis were critically reviewed to identify what are the requirements for BIPV systems, how they are certified, what products can be found on the market, and what represent the critical aspects of the BIPV market. As BIPV systems are the building envelope elements producing electricity, they must comply with standardization of both the electrical and building industries. Electricity production is still viewed as the primary function of such systems; hence the building function does not get the attention it should get. The main function of the building envelope is to form a weather protection screen that shields the building inner structures from various outdoor climate strains as e.g., various precipitations and thus provide the desired indoor environment.

Paper III

After analysis of information gathered in Paper II, it was evident that the aspect of watertightness should be studied further, especially for roof integrated BIPV systems. In Paper III, we have therefore proposed an update to the testing methodology to evaluate the watertightness of BIPV systems integrated into the roof, which is a vital aspect for roof coverings. A quantitative measure is implemented in the wind-driven rain exposure testing, which provides additional information for evaluation of tested systems. Aspect of quantification of water intrusion is a part of the standard for BIPV systems, however there is lack of information on the design of the water collection system and the procedure. A novel framework is presented, which includes a step-by-step test methodology and a detailed description of the construction of a water collection system. A BIPV system comprised of solar shingles for roof integration was tested according to the methodology and collected water amounts.

Paper IV

In Paper IV, the presented methodology was used to evaluate the watertightness of two other BIPV systems for roof integration, additionally to previously studied solar shingle BIPV system in Paper III. The second system was built using solar roof tiles and the same roof tiles without PV, and the third system was a combination of large glass-glass BIPV modules and steel roof plates. The BIPV system that used solar shingles and large modules installed along steel roof plates showed the same level of watertightness (maximum air pressure level applied onto the tested system when no water leakages occurred). The system that used solar roof tiles was less watertight but should be compared to conventional roof tiles system, as their design is the most alike.

I. “BUILDING INTEGRATION OF PHOTOVOLTAICS AT NORDIC CLIMATE CONDITIONS”

Anna Fedorova, Bjørn Petter Jelle.

Published in the conference proceeding of Advanced Building Skins conference 2017, 1216-1225.

Building integration of photovoltaics at Nordic climate conditions

Anna Fedorova ^{a*}, Bjørn Petter Jelle ^{ab}

^a Norwegian University of Science and Technology (NTNU),

Department of Civil and Environmental Engineering, NO-7491 Trondheim, Norway.

^b SINTEF Building and Infrastructure,

Department of Materials and Structures, NO-7465 Trondheim, Norway.

*Corresponding author: anna.fedorova@ntnu.no

Abstract

Future buildings are foreseen to be energy-efficient and to have lower environmental impact, as these steps are of importance to reduce greenhouse gas (GHG) emissions. In this context, the concepts of zero energy and zero emission buildings have been established that require energy supply from renewable energy sources. Solar energy, and particularly photovoltaics (PV), could be used as integrated into the building skin solution. Such systems could simultaneously serve the dual function of a climate screen and electricity power generator. Integration of photovoltaic systems into the build environment could be challenging. Building skin components experience extensive degradation and damages caused by various environmental exposures. Severe climates, like the Nordic climate, are not an obvious choice for photovoltaics integration, nevertheless they could have their benefits. This work will present an overview of solar market and photovoltaics integration into buildings at Nordic climate conditions, where an overview of existing projects will be conducted. As environmental aspect of building integrated photovoltaics (BIPV) is highly important and is of interest for international research community, therefore possible environmental benefits of BIPV will be described.

Keywords: Building integrated photovoltaics, BIPV, Solar cell, Nordic climate, Climate exposure, Environmental benefits.

1. Introduction

The crucial level of greenhouse gas (GHG) emissions in the atmosphere is one of the most significant issues our society have to cope with nowadays, and initiatives, like the Kyoto Protocol [1], have put a target for significant reduction of GHG emissions. For instance, approximately 1/3 of GHG emissions is emitted by the building sector [2]. Consequently, this sector should be one of the main to focus on in regard to GHG emissions mitigation. The Nordic countries (including Norway, Sweden, Denmark, Finland, Iceland, Greenland, Faroe Islands and Åland Islands) are at the forefront for developing and implementing climate mitigation policies, where an active area is the reduction of GHG emissions. Even though energy use per capita in the residential sector in the Nordic region remains high, GHG emissions are at a low level [3]. Recent years GHG emissions from the Norwegian territory have decreased by 1% [4]. However, the commitment under the Kyoto protocol, which requires lowering the GHG emissions level in Norway, has not been reached yet [5] and work in this direction is still ongoing. Among other policy initiatives, in the building sector stricter building codes have gradually been introduced and used progressively [6]. They require reduction in energy use alongside energy production from renewable sources.

A wide range of renewable energy sources to provide energy include: wind power, hydropower, biomass and solar energy [7]. The solar photovoltaic (PV) technology has reached a considerable degree of maturity but yet economic viability [8]. Its development is still greatly dependent on the support policies of government and the European Union (EU) itself [9], but also higher electricity prices can be a trigger for installing more PV systems. The turn toward renewable energies in the building sector is vital. Solar energy offers a sustainable and economic alternative to electricity

generated from fossil fuels. Providing the energy needs of a building with a clean energy source will lead to environmental, economical and social benefits [10]. These are milestones on the way towards sustainability in the building sector. Buildings of the future will require a holistic approach to energy. The demand on energy production, as well as on energy consumption and savings, will continue to grow and step by step we need to change how we use buildings. In this regard, the concepts of zero energy and zero emission buildings (ZEB) have been established [11].

Buildings are huge consumers of energy but at the same time that can be changed by introducing on-site renewable energy sources. By that, buildings will become energy producers and will provide the needed amount of energy from clean energy source. The price of PV and building integrated PV (BIPV) systems costs have been decreasing and their application is becoming more feasible. Moreover, if during design and planning phases of new constructions, the buildings would be made “solar-ready”, it would add almost no additional costs [12], hence application of this approach would be beneficial to all new constructions. For example, in 2009 the US National Renewable Energy Laboratory (NREL) had made Solar Ready Building Planning Guide [13] so that buildings would be designed with possibility to install PV or other solar systems even after construction was finished.

According to the reports [14, 15], Nordic countries have a chance to be part of solar energy market. It might not be an obvious place for solar production, but solar irradiance and altitude have greater potential in this region. In 2016 Norway had significant increase in PV installations [15] that shows growing interest from government and public, giving a positive perspective on future development of the solar market in the country. The large amount of PV and BIPV installations are located in the southern regions of Norway [16] that is due to more suitable solar radiation availability for solar energy harvesting. However, other regions also have buildings with PV installations and their performance sufficiently show possibility to use more PV and BIPV systems in Norway. The main aim of the present research is to prove that Nordic countries, and Norway in particular, have potential for implementation of PV and BIPV technology alongside other countries. Another aim is to provide data update on PV and BIPV installations in Norway, alongside with challenges of PV technology implementation in the Nordic region. Environmental impact related to PV systems production and end-use phases would also be essential to look at.

2. Brief overview of renewables in Europe

Renewable electricity generation have been of major importance not only in Europe, but in the US and elsewhere. In Europe, hydropower is the largest source of electricity production from renewable energy sources. The second largest electricity generator is wind power, while solar power electricity generation is on the third place with rapid increase up to 12% of all renewable electricity production [17]. Electricity generation production by various sources and its changes during 1990-2015 is depicted in Fig. 1.

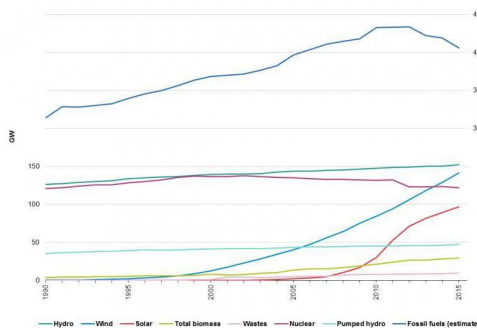


Figure 1: Electricity generation capacity, EU-28, 1990-2015 [17].

3. Solar market in Norway

In Norway, the main source of electricity is hydropower [18]. It could be argued that in Norway PV system installations are not necessary as hydropower is available and easily accessible. Moreover, areas with higher solar irradiation and electricity grids based on fossil energy should be of high priority for PV and BIPV systems installation [19] that is not applicable for Norway. In addition, feed-in tariffs (FIT) for domestic and corporate PV generation, similar to those in Germany, have not been introduced in Norway so far. Therefore, implementation of PV and BIPV [20, 21] technologies in Norway are still relatively slow. Climate policies in Nordic and European regions demand on development and increasing use of renewable energy sources (REC) to achieve lower GHG emissions level. PV market in Norway is still greater related to off-grid installations. Norwegians use PV modules for stand-alone applications, mostly at remote cottages and cabins in the mountains (one example of PV installation is shown in Fig. 2), forests and on the coast, or leisure boats. However, moderate number of grid-connected PV installations in large buildings and private houses are present [14]. Compared to 2015, by the end of 2016 the Norwegian solar market grew by 366% with installed solar panels capacity over 11 MWp. Approximately 10 MW from overall 11.4 MW of new capacity are grid-connected PV systems. Total cumulative PV installed capacity almost reached 27 MWp, where more than half of it supplies from grid-connected installations [15]. Mostly this rapid growth was possible due to the solving of two issues in the beginning of 2016: the rules on self-consumption and green electricity certificates. Alongside, subsidies from the government sector supports up to 30% of the total project investments.



Figure 2: PV installation on the highest mountain in Scandinavia – Galdhøpiggen (2469 m), which is located in the Jotunheimen mountain area, Norway (photo: Anna Fedorova).

3.1 Potential of solar energy in Nordic countries

For both grid- and off-grid connected PV and BIPV systems one of the most considerable parameters that influence the system performance is solar radiation. The quantity of solar radiation received by PV module greatly depends on the following factors: (a) geographical location, (b) position and orientation of PV, and (c) angle tilt of the panel [22]. The energy conversion efficiency of photovoltaic (PV) modules rely upon external factors as: (a) total amount of solar radiation at the site of installation, (b) wavelength of the solar radiation (will affect the light conversion efficiency), (c) variation of the type of PV efficiency, (d) efficiency decrease with time caused by long-term solar radiation and/or high temperature exposure, (e) temperature of surrounding air, (f) the solar radiation intensity, and (g) local wind speed. Energy output from PV or BIPV systems would significantly dependent on location of installation. Regions with horizontal solar radiation up to 2500 kWh/m² yearly have greater potential for energy production from solar source. For comparison, in Norway yearly solar radiation

vary from 700 kWh/m² in north to 1000 kWh/m² in south [23]. Among top European countries for energy production from the solar radiation are Germany, Italy, Spain, France and United Kingdom [7]. Data on yearly global solar irradiation in cities in closest neighboring countries like Denmark, Sweden and Germany show that Norwegian cities in southern part of the country, for instance Oslo, receive similar amount of solar radiation, which is shown in Fig. 3.

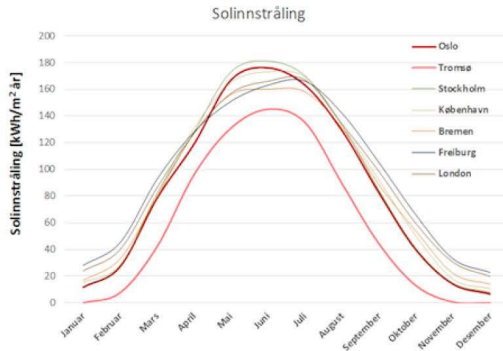


Figure 3: Yearly global solar irradiation (“solinnstråling”, år = year) for a horizontal surface for 7 cities in Europe [23].

The distribution of solar irradiation in the northern region vary greatly throughout the year, while in the southern part of the Nordic countries it remains more stable. For instance, the monthly averaged horizontal global irradiance in Oslo varies from 26.3 – 63.8 W/m² during November, December and January and rise up to 683 W/m² in June. Therefore, the energy production from PV installations in city of Oslo, southern Norway, would be mostly reliable from February to October [24]. Yearly global irradiance values on horizontal and optimally inclined surfaces for Norway [25–27] are depicted in Fig. 4.

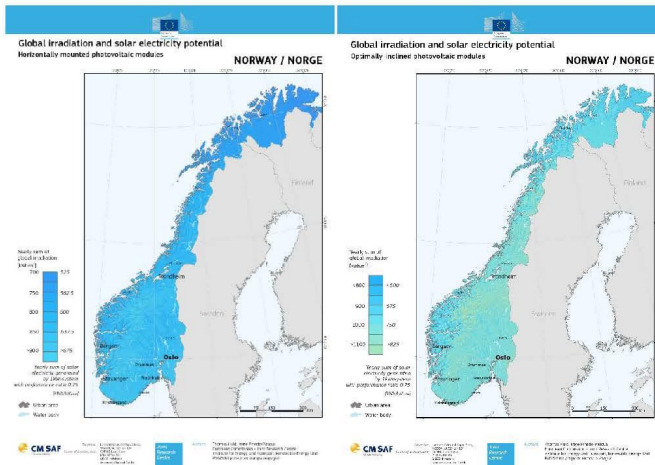


Figure 4: Global irradiation and solar electricity potential for horizontally (left) and optimally inclined (right) PV modules [25–27].

3.2 Challenges and benefits of using BIPV technology in Nordic countries

All PV panels can operate both in hot and cold climates, generating energy, while their efficiency would differ. In order for PV panels to function efficiently, it is vital to know latitude and optimum tilt angle of the area or region [22] and adapt PV system installation to the current location. Specific climate exposures that are present at the specific location would affect modules efficiency when causing degradation of PV module materials or covering BIPV modules' surfaces, for example with snow.

3.2.1 Type of PV technology

At cold climate conditions the most reliable and recommended type of PV panel is poly-crystalline Si, due to high efficiency and longer life span [22]. Especially when considering both efficiency, payback time and economical aspects poly-crystalline Si PV modules might be given a priority. However, all PV module types could effectively operate in cold climates and different types of modules could be combined and used jointly to achieve the highest energy output.

3.2.2 Degradation of BIPV module components

PV and BIPV systems are designed to harvest solar energy but due to the degradation of PV module components, while being exposed to various climate exposures, module efficiency gradually decreases. Mainly, degradation of PV modules could be grouped in five categories: (a) degradation of packaging materials, (b) loss of adhesion, (c) degradation of cell/module interconnects, (d) degradation caused by moisture intrusion, and (e) degradation of semiconductor device. Most PV modules' degradation observed by Chattopadhyay et al. [28] was found in modules installed in hotter and more humid climate locations. Discolouration of encapsulant was found in most PV modules including those installed in regions with cold climates. This damage occurred in 67% of 11-20 years old PV modules, compared to 90% of 11-20 years old PV modules exposed to hot and humid climate conditions. Colder climate conditions cause less degradations in PV modules. Hence, using PV technology in colder climates could have its advantages.

3.2.3 Watertightness of BIPV systems

When BIPV systems replace traditional building envelope elements, the weather resistance must be maintained. Water is the hardest climate factor for materials [29] while the main moisture source affecting the hydrothermal performance and durability of the building envelope is wind-driven rain [30]. As not all of the BIPV products are designed specifically for building envelope integration they must be extensively investigated for watertightness before being applied at large in buildings [31]. It is especially important for the Norwegian climate [32], as weather is extremely varied in this region due to a long coastline where extreme events, i.e. storms and rainfalls occur frequently during the autumn- and winter seasons [33].

3.2.4 Snow and ice covering BIPV

Snow and ice formation on BIPV systems would cause decrease in PV panel energy production [34, 35] likewise lower cost effectiveness [32]. However, during the winter period the Nordic region experiences low solar insolation and the potential for solar harvesting is relatively low [32]. Southern part of Norway experiences lighter winters compared to other parts of the country, hence periods with snow covering are relatively short here [36]. Number of snow days in the highly populated cities in Norway is comparable to the city of Munich in Germany where PV module energy production loss due to snow covering was estimated to 0.3-2.7% [37]. Thus, loss in energy production is not extremely large but still desirable to avoid.

3.3 PV and BIPV installations in Norway

Norwegian grid-connected BIPV and building attached photovoltaics (BAPV) systems range from small residential systems (1-10 kWp) to large commercial systems (up to 370 kWp). In total, there are more than 100 installations. Shortlist of existing BIPV and BAPV systems that were chosen and evaluated by Imenes [16] and Hauman [38] are presented in the Table 1. Basic information about the systems, i.e. type of integration, type of technology, purpose of the building, location and year of commissioning, is provided. Most of the installations are represented by BAPV systems, but number

of BIPV projects are growing. BIPV systems are so far mainly used in public buildings. Both mono- and poly-crystalline Si modules were installed.

Table 1: BIPV and BAPV installations in Norway [16, 38].

Name	Location	Building purpose	Integration	Type	Commissioned
Oseana Arts and Cultural Centre	Bergen	Culture centre	BIPV (curved façade)	mono-Si	2011-Nov
Kiwi Auli	Aulifeltet	Foodstore	BIPV (pitched roof)	mono-Si	2014-Nov
Skarpnes	Arendal	Detached house	BIPV (pitched roof)	mono-Si	2015-Jan/Nov
Haakonsvern	Bergen	Offices	BAPV (flat roof)	mono-Si	2015-Nov
Kjørbo	Sandvika	Offices	BAPV (flat roof)	mono-Si	2014-Apr/Aug
Solsmaragden	Drammen	Offices	BIPV (façade), BAPV (flat roof)	mono-Si, poly-Si	2015-Nov
Pastor Fangen	Oslo	Care homes	BIPV (pitched roof)	poly-Si	2015-Nov
Haldenterminalen	Halden	Warehouse	BIPV (façade), BAPV (flat roof)	poly-Si	2015-Sep
Evenstad	Hedmark	College	BAPV (pitched roof)	poly-Si	2013-Nov
Asko Vestby	Lillesand/Vestby	Warehouse	BAPV (flat roof)	poly-Si	2014-Sep
Økern	Oslo	Nursing home	BAPV (flat roof)	poly-Si	2014-Jun
Agder Energi	Kristiansand	Offices	BAPV (flat roof)	poly-Si, a-Si	2011-May
Lerkendal	Trondheim	Offices	BAPV (façade)	poly-Si	2012-Sep
Grøndalen Gård	Auli	Detached house	BAPV (pitched roof)	CIGS	2015-Dec

The largest PV installation in Norway (Agder Energi, Table 1) is located in the southern region in the city of Agder [39], one of the richest region for solar energy production in the country. PV modules cover 4500 m² of the building roof. The overall yearly energy capacity of the installation is estimated at 720 000 kWh. Another example of BIPV installation that presents high architectural quality is Oseana Arts and Cultural Centre (Table 1, Fig. 4 (left)). Coloured BIPV are used relatively rarely, for instance coloured BIPV façade safety glass modules were used in the Solsmaragden building (Table 1, Fig. 4 (right)). To emphasize environmental mindfulness a green colour of the PV was chosen, where panels were made by screen printing, and 26 mono-Si modules of various shapes were produced to construct the façade system [40].



Figure 4: (left) Oseana Arts and Cultural Centre [41]; (right) Solsmaragden [40].

3.4 Environmental benefits of BIPV technology

Comparison of three rooftop technologies, such as white roof, green roof and roof-mounted PV systems, at cold climate conditions revealed beneficial environmental impact especially from PV installation. Negative environmental impact from PV installation is 1 to 3 times lower than from the alternative rooftop technologies [42]. The mounting structures have significant contribution to the emissions from the BIPV systems. Proper integration of BIPV products could reduce the use of building materials. Therefore, emissions associated with used materials will decrease. Resources used for PV systems manufacturing are of a high value. Usually, materials used for production are semiconductor materials such as crystalline Si or CdTe, glass, plastics, rubber laminates and metals [43]. At the end of the modules' service life all these components could be reused when separated from the others and recycled [44]. A recovery rate could reach more than 90%, when 1 kg of semiconductor material can be reused 41 times, before it becomes insufficient for the manufacturing new panels [45]. As discussed by Kristiansdottir et al. [19], emissions from modules made with reused PV cells were lower. The end of life benefits from recycling, especially glass and aluminium, can have a significant influence on the overall life cycle of PV modules [46].

4. Discussion

The potential for the BIPV market to expand is promising, and an increase in building projects and designs implementing BIPV technology is expected. In the Nordic countries, the interest in BIPV technology is also growing and is anticipated to increase in the future. PV and BIPV installations in Norway increase in number rapidly during 2016 also due to the solving of two significant issues: the rules on self-consumption and green electricity certificates. Solar installation projects in Norway are receiving more and more subsidy support from the governmental sector each year. Overall interest in expansion of Norwegian solar market is present. Even though, the Nordic region receives less solar radiation than southern European countries it has potential for solar energy production. Yearly global solar irradiance in southern parts of Norway, Denmark and Sweden is comparable to the amount received in Germany. While most of the yearly amount of global solar irradiance received in Norway is stable and remain on a sufficient level, winter months could represent various challenges for BIPV installations. For instance, energy production from BIPV and PV systems drop significantly during this period, additionally snow covering may lead to even greater reduction in energy output from these systems. However, installation of BIPV products at Nordic climate conditions could also be beneficial. Any type of PV technology would work well in cold climates but priority may be currently given to polycrystalline Si modules, as they are more efficient and have a longer life span being exposed to colder climate conditions. BIPV systems should tolerate cold climate conditions with great performance but it has not been sufficiently proven yet. Degradation of PV module components is expected to be slower and to have less damage consequences, than PV installed in hotter and more humid climates. One important climate strain should be noted: wind-driven rain, as Nordic countries, and Norway in particular, have a long coastline and experience heavy precipitation events. Due to these aspects, all new technologies used in the building envelope systems should be evaluated and sufficient water tightness must be proven.

The PV market in Norway is mostly represented by off-grid installations, which are used for stand-alone applications, mainly in cabins in the mountains or at leisure boats. If looking at grid-connected systems in overall more than 100 installations could be found across Norway, at both private houses and public buildings. Performance of these installations was proven by various studies, however data from these ones is not present in this work. Mostly, BAPV installations are present, while BIPV systems are mainly installed in public buildings. Thus, number of BIPV installations is expected to grow in the nearest future. Mono- and poly-crystalline Si modules are the main PV types used till now.

Development and expansion of BIPV technology is vital for the building sector not only in Norway but also around the world. The Nordic countries have always been in forefront for climate mitigation policy implementation and use of renewable energy sources. Therefore, the solar market in the Nordic region is expected to grow extensively in the future.

5. Conclusions

The building integrated photovoltaics (BIPV) technology represents a profitable solution for the future buildings. As BIPV are replacing the building envelope elements it may lead to cost profits and building energy balance improvement, and will be an investment in building energy supply. BIPV systems have great potential also in Norway, especially if requirements for using them in Norway will be evaluated and applied to this technology. The BIPV systems must be well designed and approved by testing laboratories according to Norwegian building requirements and standards. This study discusses the current situation for the Norwegian solar market, solar power potential of Norway, and recent building attached photovoltaics (BAPV) and BIPV installations. In future work, evaluation of most suitable BIPV products on the world market should be conducted. The choice of the most suitable BIPV products and systems is strongly dependent on the environmental exposure conditions at the given installation site. Implementation of BIPV products and systems that are chosen specifically for Nordic climate conditions will reduce the lifetime costs and increase their potential as a building element in terms of a reliable investment choice.

6. Acknowledgments

This work has been supported by the Research Council of Norway within the ENERGIX program (project number 244031) and several partners through the research project "Building Integrated Photovoltaics for Norway" (BIPV Norway).

7. References

- [1] UN Framework Convention on Climate Change (UNFCCC), "Kyoto Protocol," Kyoto, 1998.
- [2] United Nations Environment Programme, "Buildings and Climate Change. Summary for Decision-Makers," UNEP SBCL, Paris, 2009.
- [3] Nordic Council of Ministers, "Nordic Climate Policy. A Case Study on Efficient Policy Measures," Copenhagen, 2014.
- [4] "Greenhouse Gas Emissions Decreased Last Year," ssb.no. [Online]. Available: <http://www.ssb.no/en/natur-og-miljo/artikler-og-publikasjoner/greenhouse-gas-emissions-decreased-last-year>. [Accessed: 07-Jul-2017].
- [5] Norwegian Ministry of the Environment, "Norway's Report on Demonstrable Progress under the Kyoto Protocol," Norwegian Ministry of the Environment, Oslo, Status report, 2005.
- [6] A. K. Amble, "Hva Betyr TEK 15, TEK 10/rev 2017," Trondheim, 2017.
- [7] European Environment Agency, "Renewable Energy in Europe 2017. Recent Growth and Knock-on Effects," Luxembourg, 2017.
- [8] P. Ly, Ban-Weiss G., Finch N., Wray C., Ogburn M., Delp W., Akbari H., Smaby S., Levinson R. and Gean B., "Building Integrated Photovoltaic (BIPV) Roofs for Sustainability and Energy Efficiency," Naval Facilities Engineering and Expeditionary Warfare Center, California, 2013.
- [9] P. Bonomo, A. Chatzipanagi, and F. Frontini, "Overview and Analysis of Current BIPV Products: New Criteria for Supporting the Technological Transfer in the Building Sector," *VITRUVIO - International Journal of Architectural Technology and Sustainability*, vol. 0, no. 1, pp. 67–85, 2015.

- [10] M. van der Hoeven, "Transition to Sustainable Buildings. Strategies and Opportunities to 2050." International Energy Agency (IEA), 2013.
- [11] K. Peterson, P. Torcellini, and R. Grant, "A Common Definition for Zero Energy Buildings," The National Institute of Building Sciences, 2015.
- [12] IRENA, "Renewable Energy in Cities," International Renewable Energy Agency (IRENA), Abu Dhabi, 2016.
- [13] L. Lisell, T. Tetreault, and A. Watson, "Solar Ready Buildings Planning Guide," National Renewable Energy Laboratory, Colorado, NREL/TP-7A2-46078, 2009.
- [14] L. Bugge and F. Salvesen, "National Survey Report of PV Power Applications in Norway 2007," International Energy Agency, Oslo, 2008.
- [15] Ø. Holm, "Press release of National Survey Report (NSR) of PV Power Applications in Norway 2017," International Energy Agency.
- [16] A. G. Imenes, "Performance of BIPV and BAPV Installations In Norway," in *IEEE 43rd Photovoltaic Specialists Conference*, 2016.
- [17] "Energy from renewable sources - Statistics Explained." [Online]. Available: http://ec.europa.eu/eurostat/statistics-explained/index.php/Energy_from_renewable_sources. [Accessed: 10-Jun-2017].
- [18] International Energy Agency, "Energy Policies of IEA Countries. Norway," IEA Publications, France, 2017.
- [19] T. F. Kristjansdottir, C. S. Good, M. R. Inman, R. D. Schlanbusch, and I. Andresen, "Embodied Greenhouse Gas Emissions from PV Systems in Norwegian Residential Zero Emission Pilot Buildings," *Solar Energy*, vol. 133, pp. 155–171, 2016.
- [20] B. P. Jelle, C. Breivik, and H. Drolsum Røkenes, "Building Integrated Photovoltaic Products: A State-of-the-Art Review and Future Research Opportunities," *Solar Energy Materials and Solar Cells*, vol. 100, pp. 69–96, 2012.
- [21] B. P. Jelle and C. Breivik, "State-of-the-art Building Integrated Photovoltaics," *Energy Procedia*, vol. 20, pp. 68–77, Jan. 2012.
- [22] M. M. Osman and H. Z. Alibaba, "Comparative Studies on Integration of Photovoltaic in Hot and Cold Climate," *Scientific Research Journal*, vol. 3, no. 4, 2015.
- [23] "Solenergi - NVE." [Online]. Available: <https://www.nve.no/energiforsyning-og-konsesjon/solenergi/>. [Accessed: 17-Jul-2017].
- [24] A. Kyllili and P. A. Fokaides, "Investigation of Building Integrated Photovoltaics Potential in Achieving the Zero Energy Building Target," *Indoor Built Environment*, vol. 23, no. 1, pp. 92–106, 2014.
- [25] "JRC's Institute for Energy and Transport - PVGIS - European Commission." [Online]. Available: <http://re.jrc.ec.europa.eu/pvgis/cmmaps/eur.htm>. [Accessed: 10-Jul-2017].
- [26] M. Sári, T. A. Huld, E. D. Dunlop, and H. A. Ossenbrink, "Potential of Solar Electricity Generation in the European Union Member States and Candidate Countries," *Solar Energy*, vol. 81, no. 10, pp. 1295–1305, 2007.
- [27] T. Huld, R. Müller, and A. Gambardella, "A New Solar Radiation Database for Estimating PV Performance in Europe and Africa," *Solar Energy*, vol. 86, no. 6, pp. 1803–1815, 2012.
- [28] S. Chattopadhyay et al., "Visual Degradation in Field-Aged Crystalline Silicon PV Modules in India and Correlation With Electrical Degradation," *IEEE Journal of Photovoltaics*, vol. 4, no. 6, pp. 1470–1476, Nov. 2014.
- [29] J. M. P. Q. Delgado, *New approaches to building pathology and durability*. Springer, 2016.
- [30] B. Blocken and J. Carmeliet, "A Review of Wind-driven Rain Research in Building Science," *Journal of Wind Engineering and Industrial Aerodynamics*, vol. 92, no. 13, pp. 1079–1130, 2004.
- [31] C. Breivik, B. P. Jelle, B. Time, Ø. Holmberget, J. Nygård, E. Bergheim and A. Dalehaug, "Large-Scale Experimental Wind-Driven Rain Exposure Investigations of Building Integrated Photovoltaics," *Solar Energy*, vol. 90, pp. 179–187, 2013.
- [32] L. Gullbrekken, T. Kvande, and B. Time, "Roof-integrated PV in Nordic Climate - Building Physical Challenges," *Energy Procedia*, vol. 78, pp. 1962–1967, 2015.
- [33] V. Nordvik and K. R. Lisø, "A Primer on the Building Economics of Climate Change," *Construction Management and Economics*, vol. 22, pp. 765–775, 2004.
- [34] B. P. Jelle, "The Challenge of Removing Snow Downfall on Photovoltaic Solar Cell Roofs in order to Maximize Solar Energy Efficiency - Research Opportunities for the Future," *Energy and Buildings*, no. 67, pp. 334–351, 2013.
- [35] P.-O. Andersson, B. P. Jelle, Z. Zhang, T. Gao, S. Ng, J. Selj, S. E. Foss, E. S. Marstein and T. Kolås, "A Review of Possible Pathways for Avoiding Snow and Ice Formation on Building

- Integrated Photovoltaics," *Proceedings of 1st International Conference on Building Integrated Renewable Energy Systems (BIRES 2017)*, Paper 29, Dublin, Ireland, 6–9 March, 2017.
- [36] A. G. Imenes, H. G. Beyer, K. Boysen, J. O. Odden, and R. E. Grundt, "Performance of Grid-connected PV System in Southern Norway," in *2015 IEEE 42nd Photovoltaic Specialist Conference (PVSC)*, 2015, pp. 1–6.
- [37] G. Becker, B. Schiebelsberger, W. Weber, C. Vodermayr, M. Zehner, and G. Kummerle, "An Approach to the Impact of Snow on the Yield of Grid Connected PV Systems," *Proceedings of European PVSEC 2006*, Dresden, 2006.
- [38] T. Hauman, "A Brief Look at the Performance of PV in Norway," Master thesis, The Arctic University of Norway, 2016.
- [39] S. Bratland Roksvåg, "Her Kommer Norges Største Solcelleanlegg," *agderposten*. [Online]. Available: <http://www.agderposten.no/Nyheter/1.1482324>. [Accessed: 07-Jul-2017].
- [40] "Colorful PV Facade Solsmaragden for Union Bryggen in Oslo, Norway," ISSOL | Architecture - BIPV. [Online]. Available: <http://www.issol.eu/solsmaragden-union-brygge-drammen/>. [Accessed: 02-Jul-2017].
- [41] "Oseana Kunst og Kultursenter | Ei verd av inspirasjon." [Online]. Available: <http://www.oseana.no/nb>. [Accessed: 26-Jul-2017].
- [42] E. Cubi, N. F. Zibin, S. J. Thompson, and J. Bergerson, "Sustainability of Rooftop Technologies in Cold Climates: Comparative Life Cycle Assessment of White Roofs, Green Roofs, and Photovoltaic Panels," *Journal of Industrial Ecology*, vol. 20, no. 2, pp. 249–262, 2016.
- [43] M. Poliskie, *Solar Module Packaging: Polymeric Requirements and Selection*. Boca Raton: CRC Press, 2011.
- [44] E. Roman, J. Lopez, I. Eisenschmid, P. Melo, J. Rousek, and T. Tsoutsos, *Potential and Benefits of BIPV*. DG Energy and Transport, 2008.
- [45] "First Solar Recycling Program." [Online]. Available: <http://www.firstsolar.com/Modules/Recycling>. [Accessed: 04-Jul-2017].
- [46] S. Weckend, A. Wade, and G. Heath, "End-Of-Life Management. Solar Photovoltaic Panels," International Renewable Energy Agency (IRENA), 2016.

II. “BUILDING-INTEGRATED PHOTOVOLTAICS FROM PRODUCTS TO SYSTEM INTEGRATION – A CRITICAL REVIEW”

Anna Fedorova, Bożena Dorota Hrynyszyn, Bjørn Petter Jelle.
The Institute of Physics (IOP): Materials Science and Engineering, 2020.

PAPER • OPEN ACCESS

Building-Integrated Photovoltaics from Products to System Integration – A Critical Review

To cite this article: Anna Fedorova et al 2020 *IOP Conf. Ser.: Mater. Sci. Eng.* **960** 042054

View the [article online](#) for updates and enhancements.

Building-Integrated Photovoltaics from Products to System Integration – A Critical Review

Anna Fedorova ¹, Bozena Dorota Hrynyszyn ¹, Bjørn Petter Jelle ^{1,2}

¹ Norwegian University of Science and Technology (NTNU), Department of Civil and Environmental Engineering, NO-7491 Trondheim, Norway

² SINTEF Community, Department of Materials and Structures, NO-7465 Trondheim, Norway

anna.fedorova@ntnu.no

Abstract. This review brings together research on the integration aspect of photovoltaic technologies in the building sector. Buildings are among the significant contributors of negative, yet not avoidable, environmental impact. Two primary drivers are pushing the building industry toward sustainability: a goal of lowering the emission levels emitted by the industry, and new norms and regulations on a zero-energy building. The zero-energy building concept is primarily based on the principle that the amount of renewable energy created on the site will be equal to the total amount of energy used by the building during its operational phase throughout its entire lifetime. As a result, the photovoltaic technology was introduced to the building sector, and from there started a rapid research and development of a merged field, building-integrated photovoltaics (BIPV). The market of BIPV is still young and is hence constantly changing. A few BIPV product manufacturers are steadily represented on the market, while new products and manufacturers are emerging and others disappearing now and then. A critical review presented herein provides technical information on existing BIPV products and systems, considering their multi-functionality as a climate screen, energy generator and aesthetic component. Therefore, this paper aims to help to understand BIPV products and systems as well as possibilities and challenges associated with their integration into the built environment of today, thus also giving guidelines for the development and design of BIPV components for the future.

1. Introduction

A building-integrated photovoltaic (BIPV) market is a young but fast-developing merged field of two industries – photovoltaic and building. According to the data from the United Nations Environment Programme (UNEP), up to 40% of global energy is consumed by buildings, and they emit approximately 1/3 of greenhouse gas (GHG) emissions [1]. Due to an expected population increase of 2.5×10^9 people by 2050 and the continuation of its growth in the future, the global energy system will experience additional pressure [2]. With growing energy needs, and as energy production nowadays is primarily based on fossil fuels [1] that release GHG emissions, the level of emissions will steadily continue to grow unless severe action is taken. The issue of GHG emissions, exceeding a sustainable level, is one of the most significant our society faces, and there is a need to find solutions to cope with it. Among other possible ways, GHG emissions mitigation could be achieved by applying energy efficiency approaches and using renewable energy sources [1]. In this regard, the concepts of zero-energy and zero-emission buildings (ZEB) have been established, also mentioned in sustainability in construction standards [3]. According to the European Parliament and the European Union Directive 2010/31/EU



Content from this work may be used under the terms of the [Creative Commons Attribution 3.0 licence](https://creativecommons.org/licenses/by/3.0/). Any further distribution of this work must maintain attribution to the author(s) and the title of the work, journal citation and DOI.

Published under licence by IOP Publishing Ltd

1

(EPD 2010/13 EU) [4] on the energy performance of buildings, by the end of the year 2020, all new buildings should be “nearly zero-energy buildings.”. This directive is one of the key market drivers, along with the opinion that BIPV is most applicable to ZEB. Challenges of the BIPV market include among others the following: cost reduction, performance, service life, product availability and flexibility, better aesthetics, standardization across industry, construction details, and energy field regulations, mentioned in order of priority [5]. Additional drivers of BIPV technologies are the United Nations (UN) sustainability goals: 7 “Affordable and clean energy” and 11 “Sustainable cities and communities” [6].

Initially, photovoltaic (PV) systems were implemented into the built environment in remote areas to supply buildings with electricity off the grid (an example of such an installation is shown in figure 1, left). Then, grid-connected PV installations have gained popularity among various users (an example of this type of installation is shown in figure 1, middle). Further advancement in the PV field has led to the design and extensive production of various PV products for integration into a building envelope (an example of PV integrated into the roof is shown in figure 1, right).



Figure 1. Off-grid PV system installed on the façade of a mountain cabin, building applied PV (BAPV) system attached on the roof tiles, PV tiles system (BIPV) integrated into the roof. (Source: authors’ photos)

The main objective of the present study is to provide a critical overview of existing BIPV products, illuminating significant obstacles of the market, after its analysis, and to find solutions for further market development. Only in 2016 internationally agreed definitions for the BIPV industry were presented, which boosted the standardization base and better structured market.

To understand the intended meaning of the terms “BIPV module” and “BIPV system”, it is referred to the definitions proposed by members of IEA-PVPS Task 15, Subtask C report “International definitions of BIPV” [7]. Definitions are quoted here: “A *BIPV module* is a PV module and a construction product together, designed to be a component of the building. A *BIPV module* is the smallest (electrically and mechanically) non-divisible photovoltaic unit in a *BIPV system*, which retains building-related functionality. If the *BIPV module* is dismantled, it would have to be replaced by an appropriate construction product. A *BIPV system* is a photovoltaic system in which the PV modules satisfy the definition above for BIPV products. It includes the electrical components needed to connect the PV modules to external AC or DC circuits and the mechanical mounting systems needed to integrate the BIPV modules into the building.”. The term “BIPV product” is mainly equal to the term “BIPV module” but can also mean the full “BIPV system”.

2. Method

The information presented in this study was collected from various sources, mainly based on a review of relevant scientific publications and projects as well as communication with BIPV manufacturers, installers, users, and researchers. Years 2013-2020 were in the focus as the BIPV market and technologies are developing fast, and information is quickly getting outdated. The review presented here is not intended to be a complete list of all BIPV products represented on the market, but rather to provide a critical overview of the market giving examples of BIPV products.

3. BIPV standardization

Building integration of PV must always comply with two different standardization and regulation schemes. The first scheme refers to requirements of the building industry, often regulated in local building codes and international (ISO) standards; the second - to the electrical industry and international (IEC) standards as well as mandatory, local regulations [8]. All PV products must be approved by testing centres and laboratories according to current international standards. At the same time, as PV products designed specifically for building integration still represent a niche market, no harmonized standards for actual testing of these products exist [9]. The first BIPV standard EN 50583 [10,11] had been realized in 2016, which became a starting point for further work on BIPV standardization. The information provided by manufacturers is still insufficient for BIPV to fully enter the building sector, as they can only provide primary electrical performance data and standard module durability certification, while technical requirements for building integration are still missing [12]. Besides, the information provided in BIPV product data sheets has no defined form, making it harder to compare various products.

3.1. BIPV related standards

EN 50583 [10,11] standard, which was released in January 2016 classifies BIPV in specific categories and defines a series of requirements for the BIPV products to satisfy building specifications, although there has also been published earlier studies with BIPV categorizations. This standard applies to photovoltaic systems used as construction products integrated into the building envelope. EN 50583 consists of "Part 1: BIPV modules" and "Part 2: BIPV systems" due to the need to address the photovoltaic modules, and their mounting, and electrical systems. The focus of EN 50583 is on general, electrical, and building-related requirements, along with requirements for building products with and without glass panes, labelling, system documentation, commissioning tests and inspection requirements. EN 50583 includes an initial list of "basic requirements" for BIPV, however additional qualities such as durability and reliability, water- and airtightness, and seismic resistance should also be included when BIPV products are evaluated [8]. International standard for glass in buildings ISO 18178 [13] specifies requirements for appearance, durability, and safety as well as test methods and designation for laminated solar photovoltaic (PV) glass for use in buildings, which is defined as laminated glass that integrates the function of photovoltaic power generation. The International Code Council (ICC) has established criteria for BIPV as a roofing material that dictates its performance in terms of stability, wind resistance, durability, and fire safety. Building product test requirements are set in the acceptance criteria AC 365 [14]. The standard IEC 62980 PV modules for building curtain wall applications was cancelled and incorporated into the new IEC 63092 "Photovoltaics in buildings" (former IEC 63092 "Photovoltaics on the roof") restructured in 2017. For further detailed information on BIPV standardization, it is referred to the report IEA-PVPS T15-08: 2019 "Analysis of requirements, specifications and regulation of BIPV" [8] and standards themselves. All currently applicable BIPV standards are presented in table 1.

Table 1. BIPV related standards.

Number	Name
EN 50583-1 [10]	Photovoltaics in buildings. Part 1: BIPV modules.
EN 50583-2 [11]	Photovoltaics in buildings. Part 2: BIPV systems.
ISO 18178 [13]	Glass in buildings - Laminated solar PV glass for use in buildings.
AC 365 [14]	Acceptance criteria for building-integrated photovoltaic (BIPV) roof covering systems.
IEC 63092-1*	Photovoltaics in buildings - Part 1: Building integrated photovoltaics modules.
IEC 63092-2*	Photovoltaics in buildings - Part 2: Building integrated photovoltaics systems.

*on June 2020 seem still in progress

For further BIPV product development, there is a need for the definition of complementary tests for cases when existing test standards are suitable only for some of the BIPV system types. The results of the existing standards analysis are described in a Tecnalia report [9], and the review of standards for BIPV façade and roof integration is given by Rehde et al. [15].

components, like the BIPV products. The building industry standards that can be applied to BIPV are presented in table 3.

Table 3. Standards of building industry applicable to BIPV.

Number	Name
ISO 12543 [25]	Glass in building — Laminated glass and laminated safety glass.
IEC TR 63226 [26]	Solar photovoltaic energy systems - Managing fire risk related to photovoltaic (PV) systems on buildings.
ISO 15392 [27]	Sustainability in building construction – general principals.
ISO 15686-1 [28]	Buildings and construction assets – service life planning – part 1: general principals and framework.

Even though BIPV standardization has started to form a strong base for a better representation of BIPV products on the market, there is still a need for further development and work on more harmonized standardization. The necessity and suitability of international standardization for BIPV were defined in the IEA report “Analysis of requirements, specifications and regulation of BIPV” by Berger et al. [8]. In this report three categories of standardization to be addressed at the international level were proposed: “internationally mandatory”, “useful to design BIPV” and “useful to characterize BIPV, but no need for pass/fail criteria”.

The building element’s functions applicable to BIPV are given in the European Construction Product Regulation (CPR 305/2011) [29] and are following: mechanical resistance and stability (rigidity or structural integrity); safety in case of fire; safety and accessibility in use; protection against noise; primary weather impact protection: rain, snow, wind, and hail; separation between indoor and outdoor environments; energy economy, such as shading, daylighting and thermal insulation; sustainable use of natural resources; security, shelter, or safety; hygiene, health, and the environment.

The same categories are listed in IEA report “Analysis of requirements, specifications and regulation of BIPV” IEA report “Analysis of requirements, specifications and regulation of BIPV” [8] as the ones that should be prioritized. Other categories recognized in the report, like technical requirements, will continue to be addressed best at the national or local level, as such requirements are not of immediate urgency or that some non-technical requirements are beyond the scope of the standardization efforts. Additionally, there should also be other functions to fulfil or to consider like aspects of user needs identified by Boddaert et al. [30] that complement the functions listed above. Needs concerning BIPV performance as a building component: water and air tightness, comfort during operation of a building. Needs concerning BIPV as an electrical generator: electricity for local use (self-consumption), energy self-sufficiency, applying simulation for reliable prediction of generated power. Needs concerning long-term BIPV operation: durability and reliability, ease of maintenance, protection against theft and vandalism. Needs concerning visual impact and interaction with the environment: aesthetically pleasing building appearance, flexibility in module dimensioning, visible expression of “green” values (corporate image), minimisation of disturbing reflection.

4. BIPV market analysis and discussion

To better understand the BIPV market, it is vital to start with its drivers and obstructions. As was mentioned in the introduction, there are two primary drivers of the building industry towards sustainability and hence drivers of a rapid BIPV market development. The first one – to meet the goal of lowering the emission levels emitted by the industry and second one is the new norms and regulations on zero-energy and zero-emission buildings. However, the BIPV market is still inconsistent and represents a niche market. Several barriers are causing this. Firstly, the use of BIPV is currently greatly complicated in the planning of the construction process. As such installations can be costly—it may be quite complicated to add BIPV systems later in the construction projects and therefore BIPV installations are rarely included at the beginning of the design process, budget calculation and life cycle cost (LCC). Secondly, the recently approved BIPV standard EN 50583 is not yet widely known in the building

industry. Only a few BIPV products certified as construction products and no easy installation methods (e.g. such as plug and play, plug and function) for BIPV exist [16,31]. What is more, BIPV products have not yet been integrated into widely available construction product catalogues (preferably online ones) and planning tools such as computer-aid design (CAD) and building information modeling (BIM) software. A valuable online catalogue [32] has been created by the Swiss BIPV Competence Centre at the University of Applied Science and Arts of Southern Switzerland (SUPSI). As the BIPV market is constantly changing product catalogues need consistent updating. The effort on planning, designing, and installation of BIPV is high. Additionally, specialists with knowledge of electrical design and wiring are needed [31]. For example, one may ask who has or should be given the responsibility for a multi-functional system like a BIPV roof system, e.g. the roofer or the electrician? This question would give several different answers depending who you ask. Only a small number of planners, building project managers, architects, and engineers are aware of the variety of BIPV technologies, their potential, and advantages when installed in the building envelope. Given these points, BIPV must be included in the early design phase of the construction process along with informing all the actors of the building construction industry about BIPV market products.

4.1. Critical aspects of BIPV market

A few critical aspects should be considered to support the BIPV market from the different actors involved in the decision process. These aspects are cost, reliability (including performance, output guarantee and product warranty), availability, aesthetics, maintenance, application of BIPV in the renovation of existing buildings and new constructions [5]. Some of the aspects are amplified below.

4.1.1. Cost of BIPV

The cost of PV technologies is gradually declining, while this fact has not directly resulted in lower BIPV product prices. BIPV could still be considered as a high cost investment. Therefore, BIPV product cost is the first and main obstacle for the BIPV market growth. It is promising that Renken [33] identified that the costs of BIPV modules per m² replacing facade elements are similar to common cladding materials. Similar cost of facade cladding and BIPV modules for facades can be explained by the fact that large BIPV modules reminiscent of standard PV modules hence can be produced by existing PV manufacturers without much changes in the production process. Frontini et al. [34] attained similar results for facades but found a difference in the cost of BIPV for roof integration of roughly 200 €/m² compared to conventional roofing materials. The Fraunhofer Institute for Solar Energy Systems ISE has developed a life-cycle cost model for BIPV systems. This model considers three main phases of the system lifetime and views the systems from the owner point of view: the investment/installation phase, the operation phase, and the demolition/disposal phase. Nowadays, BIPV prices are often calculated and published as €/W_p, or €/kWh; while in the future, €/m² will be more important to conform with construction industry practices [35], and should simultaneously increase the interest of architects and planners.

As mentioned earlier, to achieve a cost-effective production of PV modules, a highly automated technical process is required. PV manufacturers' primary market is the production of cost-competitive PV modules used for freestanding PV plants or rooftop PV applications (BAPV) [31]. In contrast, every construction product in the EU needs to satisfy the Construction Products Regulation (CPR), which leads to an extensive number of additional requirements for the PV modules, such as higher demands on fire safety or post-breakage behaviour. Furthermore, some basic properties of PV modules, especially the dimensions, need to be adapted to the different situations of the specific buildings. Due to their primary market, the automated processes required to produce PV modules do not allow the size of the PV modules to be changed arbitrarily. Consequently, only a few PV modules manufacturers can produce PV modules designed for building integration and in a range of customized dimensions. Furthermore, their automation process does not always allow PV modules to be manufactured with the appropriate mechanical specifications that construction products need to have.

4.1.2. Reliability of BIPV

The reliability of BIPV products is the second major aspect of slow BIPV market development [36]. For BIPV manufacturers, it is of major importance that standardized testing procedures are developed to evaluate the suitability of their products to defined applications. Additionally, at the moment there is not enough collaboration between the construction industry and the PV industry regarding the product optimization and application. Currently, it can often be seen that BIPV products are designed and developed from a PV point of view, instead of optimizing the products based on a construction point of view. The application should be simplified and better match the regular construction systems. A major advancement of the BIPV market could be achieved by the inclusion of architects in BIPV product development. Two more aspects that could be of interest for the BIPV products reliability, are (i) wind-driven rain intrusion and occurring water leakage problems, and (ii) various durability issues. Performance aspects could be expressed not only in amount of energy production, but also in need of easily understandable specific product performance information, technical drawings, installation details collected in a defined document form and available for a wide variety of specific BIPV products, which is collected into an extensive product database. Additionally, to ease BIPV installation, a verification of a long term guarantees of electricity output and a warranty of a proper BIPV product function of the as a building component are needed.

4.1.3. Availability

The availability of BIPV products is yet another aspect of the BIPV market. The products of compatible size and form must be consistently available on the market so that if there is a need to replace the system elements during the BIPV system service life, it will be possible to find replacement of the installed BIPV products. The market lacks large companies' representation and related marketing of BIPV products that could widely promote BIPV solutions, along with a database of BIPV products available on the market. All actors of the building sector should be informed about sources like BIPV database where they can find a suitable system for a building project. Further, all the data could be used in CAD and BIM software tools, which will guide architects to find the best suitable BIPV solution. An understandable ranking that could ease comparison of products could be useful to include in such libraries so that various market actors could easily understand a database without in-depth knowledge of PV and BIPV technologies. In Europe, each country still has its own legal procedures for building products. For BIPV, this is a serious constraint due to the limited demand for BIPV products within the as for today still limited market of each country.

4.1.4. Aesthetics

The aesthetics of BIPV may be relatively important as on the one hand more variations of coloured BIPV modules appear on the market that may make them more attractive to include in a building project, but on the other hand their cell efficiency is significantly reduced [37]. All so-called new technologies (dye-sensitized solar cell (DSSC), organic photovoltaics (OPV), and perovskite solar cell (PSC)) have the intrinsic potential for different colours. The materials of thin-film and crystalline technologies may be coloured to a limited extent, or the appearance changed using coloured front covers, either polymer sheets or glass [31]. Another alternative to BIPV appearance is semi-transparent modules. Semi-transparent thin-film based BIPV modules apply transparent conductive oxides instead of metals for the electrodes and are coloured in a neutral grey tone. Another possibility is to vary the distance between the PV-active areas and enhance the transparency of the BIPV module which hence simultaneously reduces the area-specific efficiency. Due to the limited space on roof and facade areas, the BIPV system efficiency should be as high as possible. Still, from an architectural point of view, it could be worth losing some degree of PV cell efficiency to gain a more aesthetically pleasing appearance. Aesthetics of a building may be also improved by reducing the complexity of mounting systems and increasing the flexibility in shapes and forms.

4.1.5. Maintenance

The maintenance of BIPV systems is not usually considered or suggested by the manufacturers, as typically, BIPV systems need little maintenance during its expected service life of 25–30 years. BIPV systems intrinsically have no moving parts. During certification, the BIPV products must withstand various mechanical loads and therefore mechanical stability is ensured before installation. Moreover, if BIPV systems installed correctly according to manuals they are expected to work without mechanical failures. The need to clean BIPV systems is highly dependent on their geographical location of installation and the meteorological conditions (rain, humidity, wind, dust, etc.), the tilt angle of the system, and the surface morphology. The only maintenance aspect that is vital to address is rubber sealant elements used for a better water tightness of BIPV systems. These elements could age tremendously in a much shorter period than 25-30 years and may need replacement by new sealant elements, thus research on the durability of such elements is needed

4.1.6. Application of BIPV in new constructions and renovation of existing ones

Application of BIPV in new constructions may seem easier as any of the BIPV systems represented on the market or specially designed BIPV products may be used. While in renovation of existing buildings it may be more difficult to find BIPV systems of suitable shape and colors. Regulations for compulsory use of BIPV products in new construction projects, and specific components development, which are adapted to application in renovation projects could be useful.

4.2. BIPV market overview

PV cell technologies that lead the existing BIPV market are the first generation PV cells (wafer-based), which are similar to the primary PV market of free-standing and rooftop PV applications. Among these technologies are mono-crystalline silicon cells (mono c-Si) and poly-crystalline silicon cells (poly c-Si). A smaller part of the market is shared by the second generation PV cells (also called thin-film solar cells), i.e. amorphous silicon (a-Si), cadmium telluride (CdTe) and copper indium gallium selenide (CIGS). The PV market share can be expressed by the percentage of global annual electricity production by each PV cell technology. The market share of the first-generation PV technologies is the biggest: poly c-Si – 60.8% and mono c-Si – 32.2%; followed by the second generation PV technologies thin-film solar cells – 4.5%, where the share is distributed between CdTe – 2.3%, CIGS – 1.9% and a-Si – 0.3% (data from a market analysis in 2017) [38]. The third generation PV cells are not included in the present study, as their market share is minimal.

All BIPV products can be categorized by the type of BIPV products [36], by the type of BIPV systems, and by the way of integration into the building envelope [39] and by the BIPV categories given in the standard EN 50583 [10,11]. These three categorizations are presented in table 4, table 5, figure 2, and summarized in table 6.






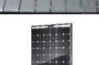






Table 4. Categorization by BIPV product type [36].

Product type	BIPV foil products	BIPV tile products	BIPV module products	Solar cell glazing products
Specification	Lightweight and flexible, often made from thin-film cells	Normally arranged in modules with the appearance and properties of standard roof tiles	Similar to conventional PV modules, but made with protective weather skin solutions	Utilized in windows, glazing, tiles, facades and roofs, and skylights

Table 5. Categorization by the way BIPV systems could be integrated [39].

System integration	Roofing	▲ Solar glazing/skylight ▲	Façade
Type of integration	Solar tiles-shingles In-roof mounted systems Full roof BIPV solution PV membrane Metal panels		Cold façade Warm façade Accessories

Table 6. Continue

Producers	Illustration	BIPV product category (table 4)	BIPV system category (table 5)	BIPV integration category (figure 2)	Type of PV	Special features	Source
Solarteg		solar tile	solar tiles-shingles	A	poly c-Si	Might be out of the BIPV market, had 5 different colours	https://www.enf-solar.com/pv/pa-nel-datasheet/crystalline/34338
Solinso		BIPV tile	solar tiles-shingles	A	mono c-Si	Solar tile that equals to width of four two compatible conventional roof tiles	https://www.solinso.nl/
Solinso		-	-	-	-	Dummy roof tile without PV	https://www.solinso.nl/
Sunstyle		solar shingle	solar tiles-shingles	A	mono c-Si	Compatible rubber sealant elements are provided with the Sunstyle solar shingles	https://www.sunstyle.com/en/Home.html
Nelskamp		BIPV tile	solar tiles-shingles	A	not specified	Available in four colours: brown, graphite, red and black	https://www.nelskamp.de/index.php/en/
Nelskamp		BIPV tile	solar tiles-shingles	A	mono c-Si	Compatible roof tiles are available from the same manufacturer	https://www.nelskamp.de/index.php/en/
Solitek		BIPV module	in-roof system	A	mono c-Si and poly c-Si	Frameless modules specially designed for integration	https://www.solitek.eu/en/products
Solibro		BIPV module	in-roof system, cold facade	A, C	CIGS	Only one module size and one colour are available	http://solibro-research.com/en/technology/
Sunage		BIPV module	in-roof system	A	mono c-Si	Capillary system for roof integration, enables water drainage	http://www.sunage.ch/prodotti/
Sunage		BIPV module	in-roof system, warm facade	A, C	mono c-Si	Can be customized in size and shape of the module	http://www.sunage.ch/prodotti/
Ennogie		BIPV module	in-roof system, warm facade	A, C	CdTe	Modules provided already with installation system attached to modules and compatible rubber sealant elements	https://ennogie.com/documentation_uk-2/
Solitek		Solar cell glazing	solar glazing/sky light	E	Bi-facial		https://www.solitek.eu/en/products

5. Conclusions

The building-integrated photovoltaic (BIPV) market is expected to expand drastically in the coming years. The first BIPV standard EN 50583-1 and 2 “Photovoltaics in buildings. Part 1: BIPV modules” and “Photovoltaics in buildings. Part 2: BIPV systems” is a major step toward a standardized BIPV market with better structure, as this standard defines five different integration categories of BIPV, depending on the intended way of application. This categorization complements already existing BIPV categorization by product type and system type. However, EN 50583 is not yet widely known in the building industry. Unfortunately, the number of BIPV market actors that are simultaneously aware of the needs and standard procedures of the building industry is limited. Therefore, with the development of BIPV standards and the availability of corresponding BIPV products, the next step is to create widely available sources of the BIPV products’ representations for the building sector such as a database of BIPV modules and systems. Such database may be integrated into computer-aid design (CAD) and building information modelling (BIM) software that will ease the inclusion of BIPV in the early design phase of the construction process. Building elements that are not part of the available databases have a limited chance to be considered in sophisticated construction projects. As soon as BIPV modules are available as database objects, including all the information needed in the construction process, BIPV systems will be able to take the step from a niche market to a standardized commodity product. Despite the fact that a variety of BIPV products and their compilation in systems that exist today on the market give many choices and possibilities to designers and construction project actors, there are still several obstacles on the way for this young but fast-growing field. The first obstacle is a specific BIPV standardization. Even though EN 50583 has created a solid base for BIPV standardization, there is still a need for more harmonized standards which include testing concerning BIPV systems as climate screen and durability along with other additional examination to existing testing from PV field. When applying BIPV products in specific countries national standards should also be considered. The last aspect here is standards related to the building industry, as there is still a question which of these standards must be obligatory and which should be voluntary. Standards concerning various aspects of safety and resistance to load impact must be of high priority. Also, the service life prediction could be especially challenging for innovative components, like the BIPV products.

Testing of BIPV systems is yet another aspect of the BIPV market. Right now, BIPV systems are tested according to the main standards for PV modules, assessing modules quality, safety, and durability to some extent. Additional testing that will evaluate BIPV systems as building components should be developed and implemented. Various aspects may be tested, like durability and reliability, examination of a performance as a climate screen, including ability to withstand rain with measuring a degree of water tightness of BIPV systems.

Further BIPV market development is dependent on finding solutions to cope with the barriers such as cost, reliability (including performance, output guarantee and product warranty), availability, aesthetics, maintenance, application of BIPV in renovation of existing buildings and new constructions. BIPV products’ cost could be improved by producing a vast number of specially designed BIPV products in a highly automated production line that allows differences in size, shape, colour, and power output. Availability may be improved by development of standardized BIPV products for selected building categories, which should be carried out in collaboration with specialists representing all the involved fields such as engineers and architects, as well as manufacturers, project developers and building owners. Another approach to improve the BIPV market is to identify building classes with standard constructions and dimensions by detailed analysis of the building stock. The resulting comprehensive data base will allow the definition of standardized modules that can be prefabricated, and which may be designed to be equipped with plug-and-play technologies. Provision of the same BIPV products and systems during their service life must be ensured. Cases when components of the BIPV systems need to be replaced (during 25-30 years’ service life of products), but with the actual manufacturers disappearing from the market, should be minimized. Aesthetical aspect may be improved by BIPV products of various colours and shapes. Most of the latest technologies allow inherently different colours and semitransparency, which give them a great design potential. The use of the immense design potential

may open and boost new market segments for BIPV products focusing on the design. The main concern for the maintenance aspect is the use of sealant elements made of rubber materials, which may need replacement during the BIPV system lifetime of 25-30 years.

Acknowledgement(s)

This work has been supported by the Research Council of Norway within the ENERGIX program and several partners through the research project “Building Integrated Photovoltaics for Norway” (BIPV Norway, project no. 244031).

References

- [1] UNEP 2009 annual report, U. N. Environ. Programme. (2009).
- [2] IECRE System - rules of procedure for the certification of photovoltaic systems according to the IECRE-PV schemes, Int. Electrotech. Comm. (2016).
- [3] BEAR-iD, NOBATEK, Film Optics, Tecnalia, Nearly zero-energy building concepts for the application of BIPV elements, PVSITES. (2016).
- [4] The European Parliament and the European Union, Directive 2010/31/EU of the European Parliament and of the Council of 19 May 2010 on the energy performance of buildings, (2010).
- [5] F. Noris, J.M. Espeche, BIPV market and stakeholder survey: summary of results, PVSITES. (2016).
- [6] the United Nations, the Sustainable Development Goals, (2015).
<https://www.un.org/sustainabledevelopment/sustainable-development-goals/>.
- [7] K. Berger, A. Cueli Belen, S. Boddaert, M. Del Buono, V. Delisle, A. Fedorova, F. Frontini, P. Hendrick, H. Ishii, K. Kapsis, J.-T. Kim, P. Kovacs, N.M. Chivelet, L. Maturi, M. Machado, A. Schneider, H.R. Wilson, International definitions of “BIPV”. Report IEA-PVPS T15-04: 2018, Int. Energy Agency. (2018).
- [8] K. Berger, S. Boddaert, M. Del Buono, A. Fedorova, F. Frontini, S. Inoue, H. Ishii, K. Kapsis, J.-T. Kim, P. Kovacs, M. Machado, N.M. Chivelet, A. Schneider, H.R. Wilson, Analysis of requirements, specifications and regulation of BIPV. Report IEA-PVPS T15-08: 2019, Int. Energy Agency. (2019).
- [9] CEA, Tecnalia, CTCV, Standardization needs for BIPV, PVSITES. (2016).
- [10] European Committee for Electrotechnical Standardization, EN 50583-1. Photovoltaics in buildings - Part 1: BIPV modules, (2016).
- [11] European Committee for Electrotechnical Standardization, EN 50583-2. Photovoltaics in buildings. Part 2: BIPV systems, (2016).
- [12] P. Bonomo, A. Chatzipanagi, F. Frontini, Overview and analysis of current BIPV products: new criteria for supporting the technological transfer in the building sector, *Vitr. - Int. J. Archit. Technol. Sustain.* 0 (2015) 67–85.
- [13] ISO 18178. Glass in buildings - Laminated solar PV glass for use in buildings, International Organ. Stand. (2018).
- [14] Acceptance criteria (AC 365) for building-integrated photovoltaic (BIPV) roof covering systems, Int. Code Counc. Eval. Serv. (2011).
- [15] F. Rehde, T. Szacsavay, A. Peppas, Review of standards for integrating BIPV-modules in building facade and roof, Fraunhofer ISE. (2016).
- [16] B.P. Jelle, Building integrated photovoltaics: a concise description of the current state of the art and possible research pathways, *Energies.* 9 (2015).
- [17] IEC 61215-1. Terrestrial photovoltaic (PV) modules - Design qualification and type approval - Part 1: Test requirements, Int. Electrotech. Comm. (2016).
- [18] IEC 61215-1-1. Terrestrial photovoltaic (PV) modules - Design qualification and type approval - Part 1-1: Special requirements for testing of crystalline silicon photovoltaic (PV) modules, Int. Electrotech. Comm. (2016).

- [19] IEC 61215-1-2. Terrestrial photovoltaic (PV) modules - Design qualification and type approval - Part 1-2: Special requirements for testing of thin-film Cadmium Telluride (CdTe) based photovoltaic (PV) modules, Int. Electrotech. Comm. (2016).
- [20] IEC 61215-1-3. Terrestrial photovoltaic (PV) modules - Design qualification and type approval - Part 1-3: Special requirements for testing of thin-film amorphous silicon based photovoltaic (PV) modules, Int. Electrotech. Comm. (2016).
- [21] IEC 61215-1-4. Terrestrial photovoltaic (PV) modules - Design qualification and type approval - Part 1-4: Special requirements for testing of thin-film Cu(In,Ga)(S,Se) (CIGS) based photovoltaic (PV) modules, Int. Electrotech. Comm. (2016).
- [22] IEC 61730-1. Photovoltaic (PV) module safety qualification - Part 1: Requirements for construction, Int. Electrotech. Comm. (2016).
- [23] IEC 61730-2. Photovoltaic (PV) module safety qualification - Part 2: Requirements for testing, Int. Electrotech. Comm. (2016).
- [24] UL 1703. UL standard for safety flat-plate photovoltaic modules and panels, Underwrit. Lab. (2002).
- [25] ISO 12543. Glass in building — Laminated glass and laminated safety glass, International Organ. Stand. (2011).
- [26] IEC TR 63226. Solar photovoltaic energy systems - Managing fire risk related to photovoltaic (PV) systems on buildings, Int. Electrotech. Comm. (2020).
- [27] ISO 15392. Sustainability in building construction – general principals, International Organ. Stand. (2008).
- [28] ISO 15686-1. Buildings and construction assets – service life planning – part 1: general principals and framework, International Organ. Stand. (2011).
- [29] the European Parliament and of the Council, the European Construction Product Regulation (CPR) 305/2011, Off. J. Eur. Union. (2011).
- [30] S. Boddaert, J. Benson, P. Bonomo, V. Delisle, C. Erban, A. Fedorova, F. Frontini, S. Inoue, H. Ishii, K. Kapsis, J.-T. Kim, P. Kovacs, M. Machado, N.M. Chivelet, E.R. Medina, A. Schneider, H.R. Wilson, Compilation and analysis of user needs for BIPV and its functions. Report IEA PVPS T15-06: 2019., Int. Energy Agency. (2019).
- [31] C. Ferrara, H.R. Wilson, W. Sprenger, The performance of photovoltaic (PV) systems. Modelling, measurement and assessment. Part three: Maximising photovoltaic (PV) system performance. 8 - Building-integrated photovoltaics (BIPV), Woodhead Publ. (2017).
- [32] the Swiss BIPV Competence Centre at the University of Applied Science and Arts of Southern Switzerland (SUPSI), Online catalogue of BIPV modules and fastening systems <http://www.bipv.ch/index.php/en/products-en-top/bipv-modules>, (2005).
- [33] C. Renken, Strategies to increase the deployment of PV in façades, Proc. 10th Conf. Adv. Build. Ski. (2015).
- [34] F. Frontini, P. Bonomo, A. Chatzipanagi, M. van den Donker, K. Sinapis, W. Folkerts, Building Integrated Photovoltaics. Report 2015, SUPSI. (2015).
- [35] K. Fath, A. Hartmann, H.R. Wilson, C. Hemmerle, T.E. Kuhn, J. Stengel, F. Schultmann, B. Weller, Life-cycle cost assessment of photovoltaic facade panels, Conf. Proc. ENERGY FORUM Sol. Build. Ski. (2011).
- [36] B.P. Jelle, C. Breivik, H.D. Røkenes, Building integrated photovoltaic products: A state-of-the-art review and future research opportunities, Sol. Energy Mater. Sol. Cells. 100 (2012) 69–96.
- [37] A. Røyset, T. Kolås, B.P. Jelle, Coloured building integrated photovoltaics: Influence on energy efficiency, Energy Build. 208 (2020).
- [38] S. Philipps, W. Warmuth, Photovoltaics report, updated: 18 May 2020, Fraunhofer Inst. Sol. Energy Syst. ISE Support PSE GmbH. (2020).
- [39] G. Verberne, P. Bonomo, F. Frontini, M.N. van den Donker, A. Chatzipanagi, K. Sinapis, W. Folkerts, BIPV products for facades and roofs: a market analysis, 29th EU-PVSEC Amst. (2014).

III. “A TESTING METHODOLOGY FOR QUANTIFICATION OF WIND-DRIVEN RAIN INTRUSION FOR BUILDING-INTEGRATED PHOTOVOLTAIC SYSTEMS”

Anna Fedorova, Bjørn Petter Jelle, Bozena Dorota Hrynyszyn, Stig Geving.
Buildings and Environment, 199, 2021.



A testing methodology for quantification of wind-driven rain intrusion for building-integrated photovoltaic systems

Anna Fedorova^{*}, Bjørn Petter Jelle, Bozena Dorota Hrynyszyn, Stig Geving

Norwegian University of Science and Technology (NTNU), Department of Civil and Environmental Engineering, NO-7491, Trondheim, Norway

ARTICLE INFO

Keywords:

Test method
Building integrated photovoltaics
BIPV
Wind driven rain
WDR
Watertightness

ABSTRACT

Wind-driven rain (WDR) exposure is a crucial impact factor to consider for building envelope components and systems. The roof being a climate screen, shields inner structures from various precipitations preventing most of the water from intruding. Although WDR exposure tests are quite common, there is a lack of studies that explore a quantification of water intrusion during such an experiment. Novel technologies such as e.g. building-integrated photovoltaic (BIPV) systems have been steadily more used as the building envelope components, and majority of BIPV systems are designed for roof integration. Such systems are mainly viewed as electricity generators, consequently, the power output and parameters that affect them are usually in focus when these systems are evaluated, whereas little information is available on the weather protection performance of BIPV systems. To address this gap, a series of experiments were conducted to improve the testing methodology of WDR exposure for BIPV systems where quantification of water intrusion was implemented. As a result, a novel framework is presented, which includes a step-by-step test methodology and a detailed description of the construction of a water collection system. Selected BIPV system for roof integration was tested according to the methodology and collected water amounts were provided. The findings in this study demonstrate that quantification of water intrusion is feasible and provides performance-based information that will help improving the design of BIPV systems as climate screens.

1. Introduction

1.1. Wind-driven raintightness test of building envelope components

The primary function of the building envelope is to compile a weather screen protecting the inner building structures and environment from various climate exposures. One of the main climate exposures that affect the building envelope is precipitation. All kinds of precipitation such as horizontal rain, wind-driven rain (WDR), hail, and snow significantly affect the hygrothermal performance of the building envelope.

A relatively young technology that has been introduced to the building industry and that steadily gains more attention is building-integrated photovoltaics (BIPV). BIPV systems are designed for integration into the building envelope along or instead of conventional building envelope components. Additionally to the weather screen function such systems produce electricity on-site [1].

To ensure that components and systems of the building envelope can sufficiently withstand exposure to various precipitations they are

subjected to numerous testing, both in laboratories and at outdoor fields. Outdoor testing may require significantly more resources, both economical and timewise, while testing in a laboratory could be done in shorter periods. Testing conducted in laboratories has an unbeatable advantage as climate parameters may easily be controlled under laboratory conditions. Watertightness testing of the building envelope components is usually conducted in laboratories.

One aspect of watertightness testing, including raintightness, in the building industry is that such testing is not a part of Construction products regulation No 305/2011 [2], which specifies harmonized rules for the marketing of construction products in the EU. The watertightness testing for the building envelope systems is therefore voluntary and is not required for them to be sold on the market. Such test may provide valuable information that might be further used either to predict product performance, to compare different products in the same product range or for future product development. The primary layer of a sloped ventilated roof structure, viewed from the outside, is compiled of various roof coverings, for example shingles or tiles, whose main function is to keep as much precipitation out of the inner roof structure as

^{*} Corresponding author. Høgskoleringen 7A, 7491, Trondheim, Norway.
E-mail address: anna.fedorova@ntnu.no (A. Fedorova).

<https://doi.org/10.1016/j.buildenv.2021.107917>

Received 4 February 2021; Received in revised form 20 April 2021; Accepted 20 April 2021

Available online 28 April 2021

0360-1323/© 2021 The Authors. Published by Elsevier Ltd. This is an open access article under the CC BY license (<http://creativecommons.org/licenses/by/4.0/>).

possible. Under this layer first lies a ventilated air cavity, and then the underroof. The underroof is a secondary water barrier - a layer of a wind and waterproof membrane, which ensures that the water that went through the primary layer would not enter into the next layers of the roof structure [3].

Rain penetration into the building envelope can create problems that affect the durability of building materials, such as material degradation, mould growth, and wood decay. Rainwater can reach inner roof structures through the areas where the roofing underlayment is fastened by nails and staples. To predict moisture damage quantification of rain penetration through roof tiles may be utilized [4]. Several studies investigated WDR exposure on building facades in different countries [5–9], which shows the importance of risk mitigation associated with moisture-related problems. However, limited information is available on studies focusing on WDR exposure on roofing systems. Investigation of how roofing systems respond to WDR exposure can provide information on design parameters that influence the watertightness of various roof coverings. The design may be improved to minimize water intrusion. Fasana and Nelva [10] found the following aspects of the design of the roof coverings that affect watertightness: the value of the overlap of the roof slates and dimension of the side joint between the roof slates. It was also highlighted that the inclination of the installed roof system plays a critical role and an angle at which the system is the most watertight can be found [10].

Another crucial aspect is that it is often not feasible to access information on the methodology and results used for watertightness testing of the building envelope components and systems. Laboratory investigations are usually carried out by laboratories on assignment by manufacturers, where the results usually are not available for public. Thus, the building envelope components and systems cannot be compared according to their watertightness quality. In international standards watertightness is mostly addressed on material or component level [11]. Therefore, a testing methodology that includes the quantification of water intrusion for roof systems would give the opportunity to compare (a) various conventional roof systems with each other, (b) BIPV systems with traditional (non-BIPV) roof systems, and (c) different BIPV systems with each other. Also, development of new BIPV systems may be challenging without a knowledge base of documented performance of such systems, as well as the same information on conventional roof systems. Therefore, this study focuses on laboratory investigation of BIPV systems and development of a WDR exposure testing methodology that utilizes a quantitative method.

1.2. Principals of watertightness testing

When it comes to WDR exposure testing both the watertightness and raintightness terminology are used to describe the quality of the building envelope components and systems to withstand WDR. The term watertightness is mostly used both in international standards and scientific work, while the term raintightness rarely appears. Even though raintightness may seem as a better description of the quality of the roof systems, the terms watertightness, water leakage and WDR intrusion will be used in this study.

The principal of the watertightness test for roof coverings is to apply a certain quantity of water spray at various ranges of air pressure differences at various slopes at defined conditions with respect to the exterior surface of a roof specimen to observe if water leakages occur [11–13]. The air pressure loads at which water leakages occur and their locations, along with corresponding water leakage intensities, have so far been recorded with the main aim to identify a qualitative description of the water leakages and the limit of watertightness for the tested building envelope systems. However, to be able to classify tested systems, additional test parameters and measurements should be included. More specifically, the watertightness could be characterized by a measured quantity of the water leakages, which will enable a comparison between a large range of different roof (and facade) products in

general and BIPV systems in particular. Thus, in the testing methodology of WDR intrusion for BIPV systems presented herein, a water leakage quantification method is proposed and evaluated.

The limit for the amount of water leakage intruding through the system is hardly specified for the building envelope systems. For BIPV systems intended for roof integration, this aspect is mentioned in the standard EN 50583–2 “Photovoltaics in buildings. Part 2: BIPV systems” [14] in annex A “Resistance to wind-driven rain of BIPV roof coverings with discontinuously laid elements – test method”:

- “A water collector shall be provided, capable of recording the amount of leakage water during any pressure step in the test”.
- “Reference leakage rate ($10 \text{ g/m}^2/5 \text{ min}$, 5 min being the duration of a single test step in the sub-test”.
- “The cases, in which leakages exceeding fine spray and wetting on the underside occur, are considered as being too severe for the application. In any case, the reference leakage rate of ($10 \text{ g/m}^2/5 \text{ min}$) shall not be surpassed”.

Test parameters from watertightness test standards are spray rate, air pressure and the duration of these two parameters [15]. Standards mainly focus on manipulation of air pressure ranges, while water spray rate is usually kept constant. It could be beneficial to manipulate both parameters to simulate WDR exposure more closely to the one that occurs in real conditions. However, this manipulation may be challenging, and more research is needed.

To thoroughly test the building envelope systems as the climate screen it is crucial to test a large-scale model, as the most vital here is to investigate how connection of elements of such systems affect the performance. There are three basic experimental methods that can be used in building science: (a) full-scale models, (b) test cells or (c) experimental modules and large-scale model tests [16]. By the full-scale model it is meant that a whole building in full-scale is taken as a model for test, which usually is performed outdoors [3]. The goal of such test is to collect data on the building performance in real outdoor conditions. By the test cells it is meant that a part of a building, a cell, is tested in outdoor conditions, while the necessary indoor conditions are controlled [17], while outdoor conditions are present as they are. The test cells test may be a connecting point between the full-scale test and the scale model test. By the large-scale model it is meant a model constructed of elements and modules of real size, but the tested fragment of the building envelope fitted to a test specimen. The large-scale model test enables evaluation of various building envelope systems under close-to-identical laboratory conditions as these conditions can be easily replicated in indoor laboratories using similar equipment and methodology.

Compared to the other two basic experimental methods the large-scale model test (c) has both economical and time related advantages, but the exact scale is to be chosen for each specific test case. While full scale and test cells testing of the building envelope systems can provide extensive information and understanding on how various building envelope components work together [3], for the purpose of the present study the large-scale model test was found most appropriate and thus employed in the investigations. Data collected from all mentioned methods may be utilized for future computer simulations.

1.3. Background of WDR tightness experiments for BIPV systems

BIPV, being normally a component of the exterior building skin, must comply with requirements for conventional building envelope components. Primarily coming from the PV industry BIPV systems are subjected to tests and certifications of the electrical power industry, while requirements of the building industry are often neglected [18,19].

Previous laboratory investigations carried out by Breivik et al. [20] and Andenæs et al. [21] utilized a dynamic air pressure test methodology, and showed the feasibility and importance of conducting

large-scale experiments with WDR exposure for the BIPV systems. For easier reference they are named Study 1 (experiments done by Breivik et al. [20]) and Study 2 (experiments done by Andenaes et al. [21]). Both studies were based on the test method standard NT BUILD 421 "Roofs: watertightness under pulsating air pressure" [22]. NT BUILD 421 was mainly used in the present study as this is the only standard for evaluating WDR exposure on roofs. This method applies to all components and sections of roofs made of any material to be fitted in roofs at any slope between 0° (horizontal) and 90° (vertical) at their normal operating conditions for which they were designed and installed according to the manufacturers' recommendations in a finished building.

In Study 1 the underlayment, a transparent polycarbonate (Lexan) board, was used under the BIPV system. Areas between the steel roofing and steel fitting were sealed with a self-adhering siliconized paper.

Throughout the duration of the test, the differential air pressure occurred over the underlayment. The test required that the differential air pressure occurred over the BIPV roof sample, so a hole (37 cm × 43 cm) was cut in the underlayment (2.75 m × 2.75 m). During testing, difficulties in maintaining the desired level of air pressure difference were encountered. As a solution to this problem, it was decided to seal the initial hole and to cut a smaller hole (7 cm × 43 cm). However, the same differential air pressure levels were not reached and hence this test phase was terminated.

Compared to Study 1 no underlayment was used in Study 2 [21] that was due to time constraints. The underlayment provides a certain amount of resistance against WDR intrusion due to an air cushion accumulating in the ventilated air gap behind the elements of a real roof or façade structure. Therefore, water leakages were expected to occur quite early in the test and a test procedure with lower load levels was used. In Study 2 the BIPV systems did not cover the whole test frame area thus areas between these BIPV systems, roof tiles and the rest of the frame were sealed using duct tape and a 0.15 mm thick polyethylene foil.

In Study 1 the inclination angle was changed more times during the test than in the present study and Study 2. It was found more time-efficient to adjust the inclination angle once from 30° in phase 1–15° in phase 2. Additionally, the drying time of the test systems between test phases could be shortened. In Study 1 heating fans were used; in Study 2 the test systems were left to air-dry overnight.

2. Methodology

2.1. Equipment

In the present study and previous studies [20,21] WDR was

simulated in a specially designed rain and wind (RAWI) box (Fig. 1) at the NTNU and SINTEF Community laboratory in Trondheim in Norway. WDR is simulated by dynamic air pressure and a set of nozzles that spray water on the mounted frame where a test specimen is installed. The RAWI box allows stepless tilting between 0 and 95° from the horizontal plane, controlled pulsating air pressure across the test specimen and run-off water at a constant rate 1.7 L/(m × min) at the top of the test area. A horizontal boom (row) with water nozzles is mounted on rails inside the box and moves up and down at a velocity of 0.2 m/s along the sample 0.6 m above the exterior roof surface spraying WDR at a rate 0.3 L/(m² × min). The run-off water and WDR spray rates are the same in NT BUILD 421 [22]. The nozzle boom sprays water and air pressure is supplied in pulses onto a test sample, simulating gusts of wind and rain.

The boom inside the RAWI box, which delivers WDR across the sample area, consists of tubes that supply water down to transparent vertical cylinders where it hits the air stream that blows out of horizontal air tubes and is blown onto the sample area [20].

The duration of the water spray and air pressure exposure are combined in NT BUILD 421 [22] and lasts for 10 min for each increase of air pressure, while the water spray rate stays constant. The parameters given in NT BUILD 421 [22] and the parameters used in the present study and in Study 1 are given in Table 1. The load level 0 (0 Pa air pressure, run-off water) was added along additional levels 6 (600 Pa) and 7 (750 Pa) compared to parameters given in NT BUILD 421 [22]. Pulsating air pressure intervals used in Study 2 were in a lower range and are given in Table 3. As test methodologies used by authors of the present study, and in Studies 1 and 2 differ from each other, a

Table 1 Test parameters of NT BUILD 421 [22] compared to parameters used in BIPV systems testing (present study and Study 1 (Table 2)).

NT BUILD 421 [22]			Present study and Study 1 [20] (Table 2)		
Angle of slope		39°–0°	Angle of slope		30° and 15°
Load level	Duration (min)	Pulsating air pressure intervals (Pa)	Load level	Duration (min)	Pulsating air pressure intervals (Pa)
1	10	0–100	0	10	0 Run-off water
2	10	0–200	1	10	0–100
3	10	0–300	2	10	0–200
4	10	0–400	3	10	0–300
5	10	0–550	4	10	0–400
			5	10	0–500
			6	10	0–600
			7	10	0–750



Fig. 1. Large-scale turnable box for rain and wind tightness testing of sloping building surfaces (RAWI box), while test is running (left) [20] and RAWI box without a test sample (right) [21]. Schematic drawing of RAWI box is shown in Fig. 12.

Table 2
Qualitative observations of water leakages during wind-driven raintightness testing in the RAWI box for the BIPV system Study 3.

Load level	Maximum wind speed (m/s)	Pulsating air pressure (Pa)	Colour mark	Inclination 30° (Fig. 13a)	Inclination 15° (Fig. 13b)
0	0	0 (run-off water)		No water leakages	No water leakages
1	12.9	0–100		No water leakages	No water leakages
2	18.2	0–200		No water leakages	No water leakages
3	22.3	0–300		No water leakages	No water leakages
4	25.8	0–400		Leakages occurred	New leakages occurred
5	28.8	0–500		New leakages occurred	New leakages occurred
6	31.6	0–600		New leakages occurred	New leakages occurred
7	35.3	0–750		No new leakages	New leakages occurred

comparison of these three methodologies is given in Table 3.

The test is initiated at load level 0, during which the nozzle boom is inactive and only run-off water is applied. At load levels 1–7 (between 100 Pa and 750 Pa, depending on the load level) air pressure inside the box is increased and decreased in cycles (pulses) lasting 5 s, for a period of 10 min.

2.2. Investigated BIPV system

In this study, a BIPV system for roof integration was chosen as the




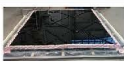
test system. The system was constructed by fish-scale solar shingles. Each solar shingle is a glass-glass module that is compounded by two layers of safety glass with solar cells laminated between them. Fig. 2a shows an outline of the front view of the BIPV system. Fig. 2b presents a range of solar shingles that were used to construct the system: (1) basic solar shingle; (2) solar shingle bottom; (3) solar shingle top; (4) solar shingle left. Fig. 2c shows the placement of rubber elements that were attached to each solar shingle. Reverse anchor-like components are attached to the upper part of the BIPV shingles, with a line of rubber sealing the gap between the shingles. Additionally, rubber gaskets are used under each screw. If needed, the BIPV system can be complimented to fit the roof shape using colour-matching aluminium composite plates, which can be cut to various sizes and forms.

2.3. Test arrangement

In NT BUILD 421 [22] the structural details of a test system are not specified. The test system should be installed according to the manual, using materials that will be used on the actual roof. A structure under roof coverings was built using wooden battens. The BIPV system was installed on a wooden structure according to the manufacturer’s manual, and the WDR test was performed in the RAWI box.

The focus of the present methodology was to implement quantification of water intrusion during the WDR test. For this matter it was crucial to find a solution to cover the areas around the tested system in such a way that it would be watertight. Another aspect was to find the optimal solution for utilizing an underlayment for the water collection, which included development and implementation of the water collection system. When the water collection system was ready, trial tests were run to ensure that the system worked correctly. Then the WDR test was performed according to Table 1 right. Acquired data included the limit of watertightness for the tested BIPV system (maximum level of differential air pressure before water leakages occur), amount of water that went through the tested BIPV system, locations where water intrusion occurred and corresponding levels of differential air pressure.

Table 3
Comparison of wind-driven rain exposure test methodologies used for the tested BIPV systems for roof integration.

Study reference	Tested system	Photo of the BIPV system	Pulsating (dynamic) air pressure intervals	Underlayment (Lexan plate)	Water intrusion quantification	Test procedure
Study 1 [20]	DuPont HexWrap NF		Run-off water (0 Pa), 100 Pa, 200 Pa, 300 Pa, 400 Pa, 500 Pa, 600 Pa, 750 Pa	Yes	No	3 phases of test: 1. run-off water applied at 30°–15° inclinations; 2. Range of pulsating air pressure applied to underlayment at 30° then the system was dried, and range of pulsating air pressure was applied at 15°; 3. An attempt to apply pulsating air pressure to BIPV system (terminated)
Study 2a [21]	Heda Solar 8 W solar tile		Run-off water (0 Pa), 10 Pa, 20 Pa, 30 Pa, 40 Pa, 50 Pa, 60 Pa, 70 Pa, 80 Pa, 90 Pa, 100 Pa, 120 Pa, 150 Pa	No	No	2 phases of test: 1. run-off water and lower range of pulsating air pressure applied to BIPV system at 30° inclination; 2. run-off water and lower range of pulsating air pressure applied to BIPV system at 15° inclination. Phase 2 was carried out on the next day after phase 1.
Study 2b [21]	GS Integra Line SP		Run-off water (0 Pa), 100 Pa, 120 Pa, 150 Pa	No	No	2 phases of test: 1. run-off water and a range of pulsating air pressure applied to BIPV system at 30° inclination; 2. run-off water and a range of pulsating air pressure applied to BIPV system at 15° inclination. Phase 2 was carried out on the same day after phase 1.
Study 3 (present study)	Sunstyle roof shingle		Run-off water (0 Pa), 100 Pa, 200 Pa, 300 Pa, 400 Pa, 500 Pa, 600 Pa, 750 Pa	Yes	Yes	2 phases of test: 1. run-off water and a range of pulsating air pressure applied to BIPV system at 30° inclination; 2. run-off water and a range of pulsating air pressure applied to BIPV system at 15° inclination. Phase 2 was carried out on the same day after phase 1.

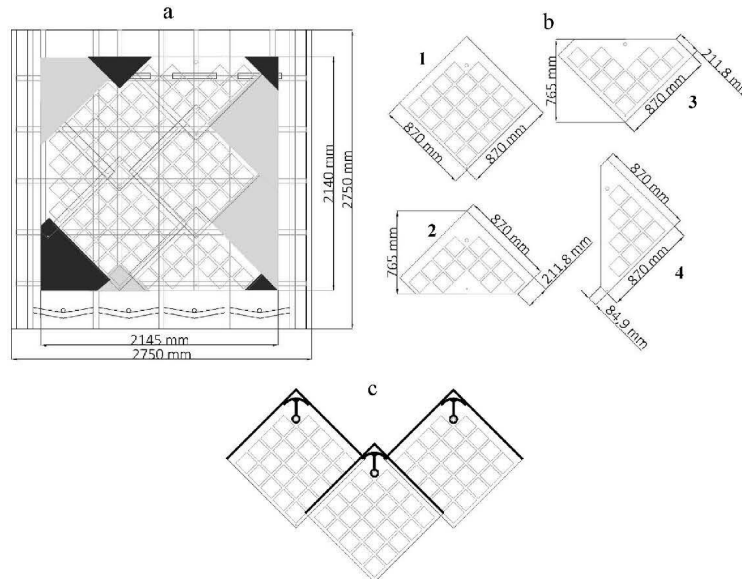


Fig. 2. (a) Front view of the outline of BIPV system in present study (to distinguish components of the system and to make connecting points better visible, BIPV shingles are left transparent, grey parts are metal plates, and black parts are glass-glass parts without PV cells). (b) Range of BIPV shingles: (1) basic solar shingle; (2) solar shingle bottom; (3) solar shingle top; (4) solar shingle left. (c) Rubber element on upper part of the solar shingle schematically shown on the drawing.

2.4. Development of a testing methodology for quantification of wind-driven rain intrusion for BIPV

After analyzing previous studies, planning to use the same RAWI box equipment, several improvement possibilities were identified. Firstly, the underlayment must be used along finding an optimal hole size cut into it, so that the desired air pressure difference can be achieved. The underlayment was also needed for water collection, i.e. a quantification of the water leakages. A water collection system was used for the first time in the RAWI box WDR exposure test. Thus, it took many trials and fails to make this system work properly, at the end the system proved to be feasible to build and use. A transparent polycarbonate (Lexan) board was applied as the underlayment so water leakages could be observed (and collected). The underlayment was fitted into the frame (2.75 m × 2.75 m) and was mounted on the wooden structure secured by screwing wooden battens to it. The wooden battens were spaced 0.6 m from each other and formed four separate sections. As the main frame of the test specimen was wider than the width of these four sections, two small sections were left along section 4 and section 1 (Fig. 3). The two smaller sections were not a part of the water collection system, as water was only collected from the four main sections.

At the bottom of the frame a water collection system was built. Following the already built four sections, four water collection sections were formed, where one round hole was cut in each section and a tube was connected to each hole. A triangle profile made of wooden battens was built near each hole and taped to the underlayment with duct tape. From Study 1 [20] it was found that the underlayment must be punctured so that the air pressure will be applied to tested system and the desired levels of air pressure difference could be reached. Hence, four holes (each with a size 5 cm × 40 cm) were cut in the upper part of the

underlayment. During the underlayment evaluation prior to testing an idea to cover these holes with a breathable waterproof material was assessed. If water that would go through the connecting points of a tested system would be drained through holes in the upper part of the underlayment, they must have been covered to collect all the water. After first test trials no water was draining through the holes in the underlayment, and they were left uncovered for the duration of the experiments. An outline of the water collection system is shown on Fig. 3. The present study will be further referred as Study 3.

To create a watertight barrier around the BIPV systems, the remaining fragments of the surrounding frame were covered with duct tape and a 0.15 mm thick polyethylene foil. Pretesting had shown a need of a better taping around the systems, as water leakages occurred at the points connecting the duct tape and the BIPV system, as well as between the duct tape and the polyethylene foil, already at 0 load level. The next step included finding a better sealing tape. It was decided to try to apply sealing tapes, which are usually used in underroof structures, as they had proven to be durable enough for prolonged periods [23]. Sealing tapes from Halotex along polyethylene foil were used to create a waterproof cover around the BIPV system. The polyethylene foil was sealed to the test frame using duct tape. Edges of the BIPV system were sealed using three types of sealing tape. The first layer was Halotex Flex Tape 60 mm following the polyethylene foil. Then Halotex Delta Tape 60 mm was placed over the plastic foil, following Halotex Delta Tape 100 mm (Figs. 4 and 5).

Examples of a complete taping are depicted in Fig. 6, from the front point of view before a trial testing and from the back-side point of view during testing.

As mentioned earlier, in the first trial run only duct tape was used, and it was changed to sealing tapes both around the BIPV system and in

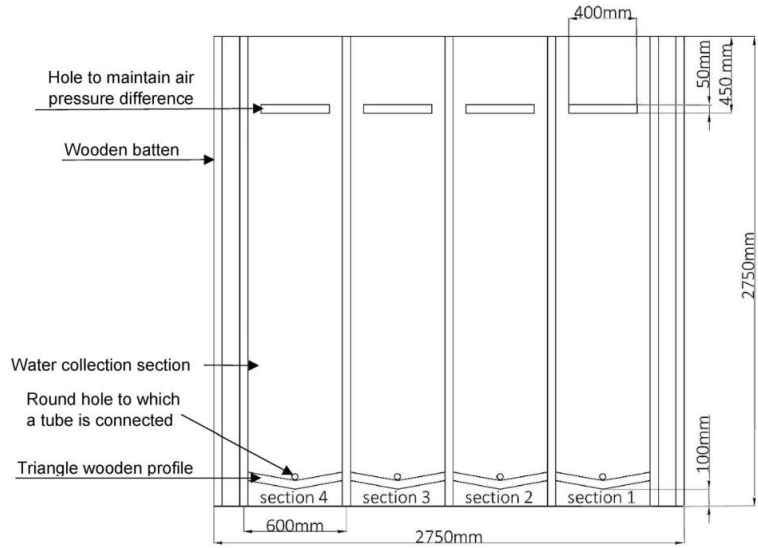


Fig. 3. Outline of the water collection system. Study 3 (Table 3).

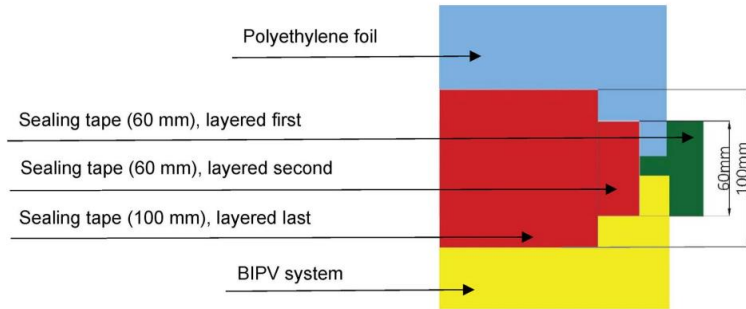


Fig. 4. Schematic drawing of sealing tapes layering.



Fig. 5. Sealing the edges of the BIPV system using sealing tapes and polyethylene foil (view from the frontside). On the right photo a tube used to measure the differential air pressure is visible lying on the black module. Study 3 (Table 3).



Fig. 6. View of a complete taping from the frontside (left) and from the backside (right). Study 3 (Table 3).

the water collection system. Wooden triangle profiles were then covered on the top and on the bottom side with duct tape (marked with number 1 on Fig. 7), while on the side part of each triangle profile where they were connected to the underlayment, Halotex multi xtreme flex tape was attached (marked with number 2 on Fig. 7) to seal the gap and ensure that all the water would be collected. Then double-sided sealing tape was attached to the upper part of each triangle profile. Later, plastic foil was attached to this double-sided tape (marked with number 3 on Fig. 7). Step by step procedure of the present methodology is summarized in Fig. 8.

2.5. Evaluation of the developed methodology

After taping of the BIPV system was completed (Fig. 9) several trial runs were conducted (Fig. 10), starting from 0 load level (no air pressure, run-off water only), and increasing load levels according to Table 1 (right). The focus at this point was to monitor areas with taping to ensure that water leakages did not occur there. Hence, only water going through joints in the BIPV system, including joints between BIPV tiles and non-PV tiles (dummies), was collected. Taping had to be fixed in various places across the edges with small fragments of Halotex Delta Tape 60 mm. Taping at the bottom side of the BIPV system also had to be fixed. Here water should drain away, but the sealing tape was stopping this drainage at a few points and subsequently this water erroneously went to the water collector system, which was observed during trial run. Before water leakages were collected for recording, some parts of the sealing tape in the drainage areas were cut and plasticine was added underneath some locations between the tiles. After such adjustments were done, water leakages occurred only between tiles and the rest of the water was draining as it would on an actual roof.

The four water collection sections were numbered and respective

containers for water collection were placed at the end of each tube connected to their section. The tubes were partially filled with water so that the air pressure measurements would not be interfered. The four sections with the water collection system at the bottom of the sections are shown in Fig. 10 (except the water collection containers), with some details depicted in Fig. 11. See also Figs. 12 and 13 which show the water collection containers. In Fig. 10 left, one of the four holes that are cut in the upper part of the underlayment is marked with a white rectangle.

At this point the taping was fixed and the test was run up to load level 4 (400 Pa), and as there were no leakages it was decided to run the first main test for this BIPV system. The test continued further with load levels 5, 6 and 7. One of the important aspects in WDR testing when using scale models is to make sure that the air pressure is evenly distributed across the whole area of the test system. In the RAWI box the air pressure is measured automatically, but usually there is no underlayment underneath the test system and the air pressure difference is set with respect to the ambient air pressure in the laboratory.

As in case of this test method, the air pressure difference must be set with respect to the air pressure underneath the tested BIPV system, hence a tube (Figs. 12 and 13) was placed under the BIPV system in the upper left corner and the other end of the tube then connected to the RAWI box. Along with this measurement, it was decided to measure the air pressure difference externally. For this matter one tube of the same diameter was installed during the taping stage on top of the BIPV system in the upper right corner (Fig. 5 right). Later this tube was connected to the external micromanometer (Figs. 12 and 13). Another tube of the same diameter was placed underneath the BIPV system. This tube was consistently moved across five points: each of the corners of the BIPV system and the middle part. Measurements were taken at each load level at the beginning of each of them and compared to the level of air

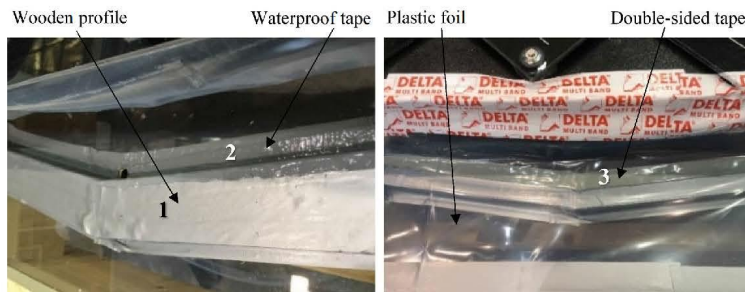


Fig. 7. Triangle wooden profile covered by duct tape (1) built on the underlayment. Waterproof tape sealing the gap between the underlayment and the triangle wooden profile (2), and double-sided tape sealing area between the triangle wooden profile and plastic foil (3). Study 3 (Table 3).

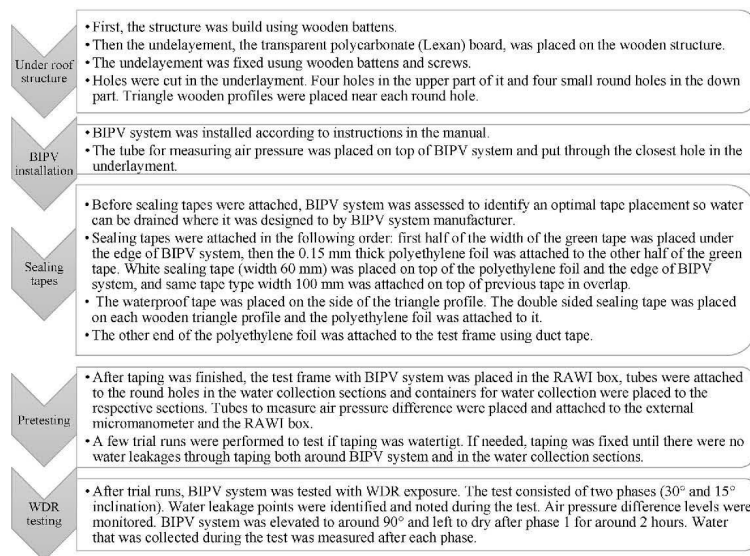


Fig. 8. Summary of the present test methodology.

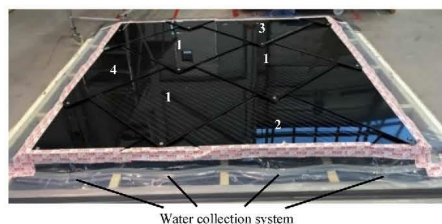


Fig. 9. The BIPV system with completed taping before testing. Study 3 (Table 3). Range of BIPV shingles: (1) basic solar shingle; (2) solar shingle bottom; (3) solar shingle top; (4) solar shingle left.

pressure measured by the RAWI box. All load levels during all test runs reached the desired values with minor error margins.

3. Results and discussion

3.1. The watertightness performance of tested BIPV system

The test was conducted in 2 phases, similar to the phases in Study 2. Phase 1 for the system inclined at 30° and phase 2 for the system inclined at 15°. Each phase started at load level 0 and then steadily continued up to load level 7 (Table 1, right and Table 3). The amount of water collected during each load level was low, and it was therefore decided to measure the water leakage once all load levels were applied. Even though it was proposed to measure the amount of water collected during each load level, it was not performed for this test. After the test for 30° inclination was over, the BIPV system was elevated and left to dry in air

so that the water collection measurements during the next test would be more accurate.

It was decided to conduct phase 2 on the same day as phase 1. Partially because the sealing tape was already tested and no water leakages through it were expected to appear, but also to shorten the time when the tested system was installed in the RAWI box. A few water droplets that remained on the underlayment prior phase 2 of the test were not distracting observations of water leakages occurring during phase 2, as all points of water leakages were clearly visible and marked consequently with an erasable marker. The remaining droplets were also considered not significant to influence the water measurements. At the end of 2 phases of the test it was concluded that it was not obligatory to use heat fans to dry the underlayment or the inner side of the tested system, neither to leave it to dry during a long time. It was enough to lift the system to a steeper angle and leave it in this position for few hours.

Observations are summarized in Table 2 and water leakage points are marked in Fig. 14. The results of collected water from testing of the Sunstyle BIPV system is presented in Fig. 15. The BIPV system showed a high watertightness level. During the test at 30° inclination leakages started to occur at 400 Pa (load level 4). Then new leakages continued to occur at 500 Pa (load level 5) and 600 Pa (load level 6). No new leakages occurred at 750 Pa (load level 7). Compared with the results of the test at 30° inclination, at 15° inclination leakages occurred one load level earlier, at 300 Pa (load level 3). New leakages continued to occur at each next load level applied (load levels 4, 5, 6, and 7). It may indicate that the tested system experienced higher WDR impact at the lower angle of inclination. The limit of watertightness for the tested BIPV system is at 300 Pa at 30° inclination and at 200 Pa at 15° inclination.

The main points where leakages occurred are in areas of metal plates overlapping BIPV shingles. The width of the metal plates is 2–3 times less than the width of the BIPV shingles. Already at low load levels, the metal plates were slightly bending that later lead to creating points of water leakage. Along with BIPV modules, metal plates were used to



Fig. 10. The BIPV system during trial runs viewed from the outside (left) and inside (right) of the RAWI box. Study 3 (Table 3).

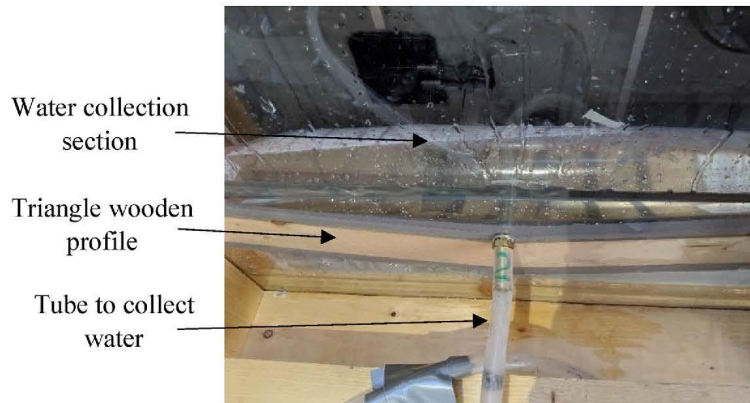


Fig. 11. The water collection sections viewed from the back side of the BIPV system. Study 3 (Table 3).

complete the system. Water leakages occurred mostly at points where the metal plates overlapped the BIPV modules. Even though the metal plates were only partially placed on water collection section 3 and mostly on section 4, most water leakages were collected in section 3. The amount of water collected from sections 4, 2, and 1 at the 30° inclination did not exceed 500 g, which is very low, considering that air pressure levels up to hurricane weather conditions were applied. During the mounting of this BIPV system, it was observed that the system would be very watertight as modules of the system were screwed to each other tightly, and various rubber sealant elements were used.

WDR test is quite a usual way to assess design quality of roof coverings. However, only after quantification of the water leakages, an actual watertightness of the system can be identified, thus enabling quantified comparisons with other systems. Conventional roof elements do not usually use sealant elements but are designed with openings for water drainage. Therefore, the watertightness level of traditional roof systems is expected to be significantly lower than roof systems with sealant elements. It might be beneficial to test more roof systems using

quantification of water leakages to collect data on how the design of roof system is correlated with the system watertightness.

3.2. Comparison of the present methodology and previous methodologies

The present test methodology and methodologies from Study 1 and 2 are summarized in Table 3. The main distinctions of Study 3 can be highlighted as follow:

- Water intrusion quantification using the underlayment was implemented.
- Holes of optimal size that were cut in the underlayment were found.
- Layering of sealing tapes was used to cover areas around the BIPV systems.
- Time between test phases was shortened.

The main aim of Study 3 was to implement quantification of water intrusion during WDR testing in the RAWI box. This aim was

17

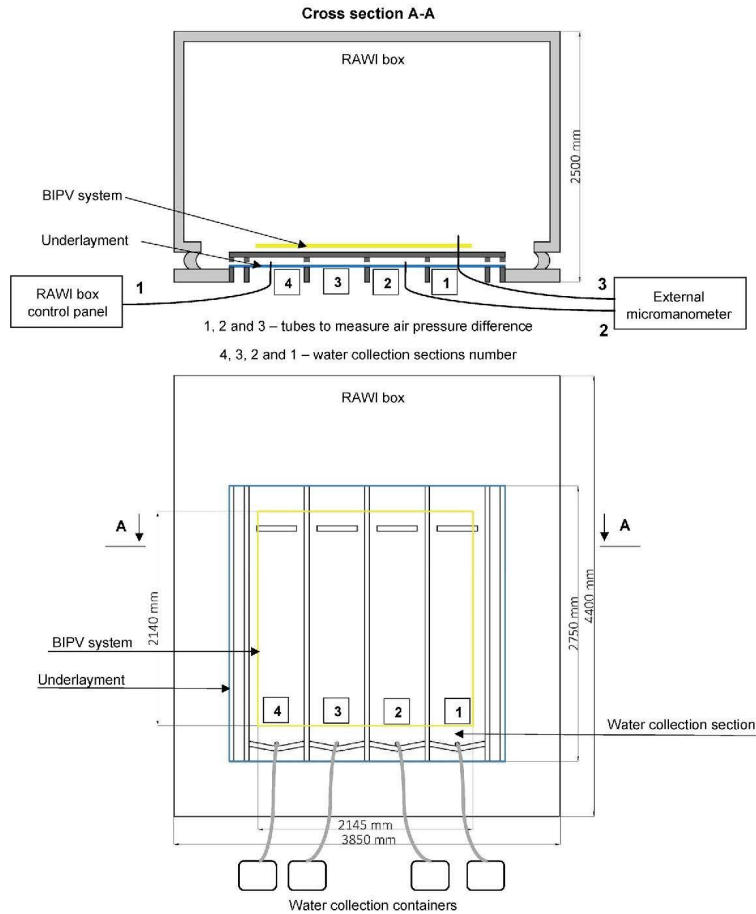


Fig. 12. Schematic drawing of raintightness test setup with four water collecting sections connected by tubes to four containers where the leakage water was collected. Additionally, a set of 3 tubes was used to measure air pressure difference. Tube 1 for measuring the differential air pressure by the RAWI box, and tubes 2 and 3 for measuring the differential air pressure connected to the external micromanometer. Study 3 (Table 3). Dimensions of the water collection system are given in Fig. 3. Upper sketch depicts a cross section top view of the RAWI box, whereas the lower sketch shows the front face of the RAWI box (see e.g. right photo in Fig. 1 and left photo in Fig. 13 for front face of the RAWI box with additional details).

successfully achieved. The underlayment was used as a part of the water collection system, the optimal size of holes was found, and water was collected during WDR experiments. While Study 1 also used underlayment, it was found difficult to find the right size of holes to cut in it so the differential air pressure could be applied to the tested BIPV system and maintain the desired level of air pressure. Even though air pressure intervals of the same magnitude as in Study 3 were applied in Study 1, differential air pressure was applied to the underlayment and not to the tested BIPV system. Qualitative data on placement of water intrusion obtained in Study 1 may differ from data that can be obtained if the same

system is tested according to the test methodology from Study 3. Therefore, data from Study 1 cannot be compared to data from Study 3. Data obtained in Study 2 also cannot be compared to data from Study 3. No underlayment was used in Study 2 and air pressure intervals of a lower range were used. Therefore, qualitative data on placement of water intrusion obtained in Study 2 (a and b) may differ from data that can be obtained if the same systems are tested according to the test methodology from Study 3. In conclusion, qualitative data from Study 1 and Study 2 cannot be compared to qualitative data from Study 3. However, testing methodologies can be compared (Table 3) and this



Fig. 13. Raintightness test setup in the laboratory. The set of 3 tubes to measure air pressure difference are marked. Tube 1 for measuring the differential air pressure by the RAWI box, and tubes 2 and 3 for measuring the differential air pressure connected to the external micromanometer. Study 3 (Table 3).

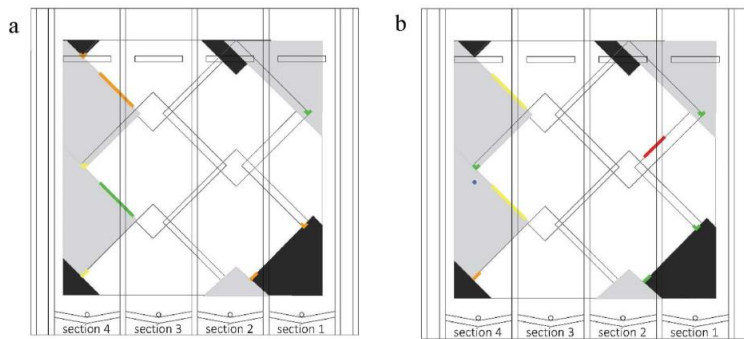


Fig. 14. Location of water leakage points for the BIPV system Study 3 with corresponding colours as given in Table 2. (a) First test phase (inclination 30°); (b) second test phase (inclination 15°). View from the backside of the BIPV system. (For interpretation of the references to colour in this figure legend, the reader is referred to the Web version of this article.)

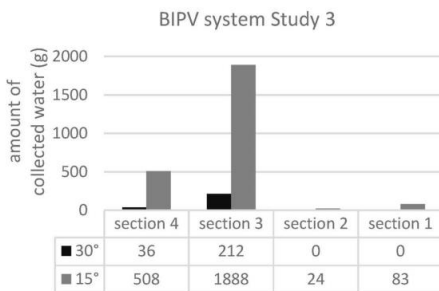


Fig. 15. The results of water collection from testing of BIPV system Study 3.

comparison helped to improve the present methodology. It must be noted that in the present study the preparation time before the test and trial testing took a considerable amount of time. Taping a large area with sealing tapes was challenging, and the tape had to be fixed multiple times during trial tests. Then once the tape was fixed, the test procedure

was straightforward.

4. Conclusions

The wind-driven rain (WDR) research field is complex and broad. It spreads from a micro-scale, covering the investigation of WDR exposure itself, its intensity, field measurements, etc. to a macro scale, when the subject of study explores how WDR affects the building envelope systems or the whole building. The present study focused on development and evaluation of a test methodology for assessing building-integrated photovoltaic (BIPV) systems ability to withstand WDR. The main novelty of the methodology is quantification of water intrusion collected during testing.

Critical aspects of the present methodology can be summarized as follow.

- 1) An underlayment must be used to enable water collection and replicate conditions of a real roof installation when an air cushion accumulates in the ventilated air gap behind the elements and makes the roof system more watertight. Four holes each with a size 5 cm × 40 cm for a test area of 2.75 m × 2.75 m were enough to reach the desired air pressure load levels. These holes are also needed so that the air pressure difference will be applied to the test system. If no

wholes are cut in the underlayment, the air pressure difference is applied to the underlayment. The underlayment is also a vital part of the water collection system.

- 2) To collect water from underneath the tested systems, edges around each system must be sealed. For that matter, a range of waterproof sealant tapes can be used.
- 3) The water collection system can be constructed using sections formed by wooden battens of the under-roof structure. At the bottom of each section, simple triangle profiles can be built for a more accessible water collection.
- 4) During the test, it is advised to measure the air pressure difference under the test system. Measurements applying an external micromanometer can be used to ensure that the air pressure distribution is even across the system. Two tubes connected to the micromanometer may be used when one is placed on top of the system, and the other one thoroughly moved under the system.
- 5) The test system areas should preferably be of the same size, and/or with a representative joint length amount, so that the water collection results could easily be compared.

The present test methodology may be further improved by implementation of automatic measurement of the amount of water leakages that can be applied at each level of air pressure. Then the duration of application of each air pressure load level (the duration of a single test step in the sub-test) may be shortened down from 10 min to 5min, i.e. so that water leakage measurements can be compared to a reference leakage rate of (10 g/m²)/5 min. More systems should be tested according to the presented methodology, BIPV systems, and conventional roof systems. When choosing an outline of systems to test it should be of the same size so the WDR exposure will be applied to the same area.

Test parameters used in this study are standard for the WDR test. Ideally, parameters should be calculated from information on driving rain intensities, wind pressure rates, water droplet sizes that are likely to occur for climate conditions at a specific location where the tested systems will be installed and used. Suppose several systems of the same specimen size will be tested according to this methodology. In that case, it will be possible to collect and create a database of the tested systems' watertightness level and forthcoming ones. This information can be useful for both the BIPV market and the scientific community, and roof and facade products in general. Firstly, as the methodology can be used by certifying institutions giving quality assurance for products available on the market. Secondly, such data may provide some directions for manufacturers and designers developing the products. Then these systems could become more accessible for customers and resellers to choose better-suited systems for a particular location. Simultaneously, data from performance-based tests may be used for computer simulations and future system upgrades and developments.

Declaration of competing interest

The authors declare that they have no known competing financial interests or personal relationships that could have appeared to influence the work reported in this paper.

Acknowledgements

This work was supported by the Research Council of Norway within

the ENERGIX program and several partners through the research project "Building Integrated Photovoltaics for Norway" (BIPV Norway, project no. 244031).

References

- [1] B.P. Jelle, C. Breivik, H.D. Raknes, Building integrated photovoltaic products: a state-of-the-art review and future research opportunities, *Sol. Energy Mater. Sol. Cells* 100 (2012) 69–96.
- [2] The European Parliament and the European Council, the Construction Product Regulation (CPR) 305/2011, Off. J. Eur. Union, 2011.
- [3] G.T. Bitsouniak, A. Gan Chowdhury, D. Sambare, Application of a full-scale testing facility for assessing wind-driven-rain intrusion, *Build. Environ.* 44 (2009) 2430–2441.
- [4] H. Saito, Application of the wood degradation model to an actual roof assembly subjected to rain penetration, *Energy Procedia* 132 (2017) 399–404.
- [5] M. Abuku, B. Bloeker, S. Rods, Moisture response of building facades to wind-driven rain: field measurements compared with numerical simulations, *J. Wind Eng. Ind. Aerod.* 97 (2009) 197–207.
- [6] J.M. Pérez-Bella, J. Domínguez-Hernández, B. Rodríguez-Soria, J.J. del Coz-Díaz, E. Cano-Suñén, Combined use of wind-driven rain and wind pressure to define water penetration risk into building facades: the Spanish case, *Build. Environ.* 64 (2013) 46–56.
- [7] C. Giarna, D. Aravanitinos, On building components' exposure to driving rain in Greece, *J. Wind Eng. Ind. Aerod.* 125 (2014) 133–145.
- [8] J. Domínguez-Hernández, J.M. Pérez-Bella, M. Alonso-Martínez, E. Cano-Suñén, J. J. del Coz-Díaz, Assessment of water penetration risk in building facades throughout Brazil, *Build. Res. Inf.* 45 (2016) 492–507.
- [9] T. Qian, H. Zhang, Assessment of long-term and extreme exposure to wind-driven rain for buildings in various regions of China, *Build. Environ.* 189 (2021).
- [10] S. Fasana, R. Nerva, Improvement of the performance of traditional stone roofs by wind driven rain experimental tests, *Construct. Build. Mater.* 25 (2011) 1491–1502.
- [11] N. Van Den Bossche, M.A. Lacasse, A. Janssens, A uniform methodology to establish test parameters for watertightness testing: Part I: a critical review, *Build. Environ.* 63 (2013) 145–156.
- [12] N. Van Den Bossche, M.A. Lacasse, A. Janssens, A uniform methodology to establish test parameters for watertightness testing: Part II: pareto front analysis on co-occurring rain and wind, *Build. Environ.* 63 (2013) 157–167.
- [13] J.M. Pérez-Bella, J. Domínguez-Hernández, E. Cano-Suñén, J.J. del Coz-Díaz, F. J. Suárez-Domínguez, A comparison of methods for determining watertightness test parameters of building facades, *Build. Environ.* 78 (2014) 145–154.
- [14] European Committee for Electrotechnical Standardization, EN 50583-2, Photovoltaics in Buildings, vol. 2, BIPV systems, 2016.
- [15] N. Sahal, M.A. Lacasse, Proposed method for calculating water penetration test parameters of wall assemblies as applied to Istanbul, Turkey, *Build. Environ.* 43 (2008) 1250–1260.
- [16] J.M. Lirio, E. Castañeda, B. Lauret, M. Khayet, A review on experimental research using scale models for buildings: application and methodologies, *Energy Build.* 142 (2017) 72–116.
- [17] G. Cattarin, F. Gausone, A. Kindiris, L. Pagliano, Outdoor test cells for building envelope experimental characterisation – a literature review, *Renew. Sustain. Energy Rev.* 54 (2016) 606–625.
- [18] CEA, Tecnalia, CTCV, Standardization Needs for BIPV, PVSTIES, 2016.
- [19] P. Bonomo, A. Chatzapanagis, F. Frontini, Overview and analysis of current BIPV products: new criteria for supporting the technological transfer in the building sector, *Vitr. - Int. J. Archit. Technol. Sustain.* (2015) 67–85.
- [20] C. Breivik, B.P. Jelle, B. Tømme, Ø. Holmberget, J. Nygård, E. Bergheim, A. Dalehaug, Large-scale experimental wind-driven rain exposure investigations of building integrated photovoltaics, *Sol. Energy* 90 (2013) 179–187.
- [21] E. Andersen, Wind-driven Rain Exposure and Assessment of Building Integrated Photovoltaic Systems, MSc thesis, Norwegian University of Science and Technology, Trondheim, 2016.
- [22] Nordtest Standard, NT BUILD 421, Roofs: Watertightness under Pulsating Air Pressure, 1993.
- [23] S.M. Fufa, N. Labonnote, S. Frank, P. Rütter, B.P. Jelle, Durability evaluation of adhesive tapes for building applications, *Construct. Build. Mater.* 161 (2018) 528–538.

IV. “QUANTIFICATION OF WIND-DRIVEN RAIN INTRUSION IN BUILDING-INTEGRATED PHOTOVOLTAIC SYSTEMS”

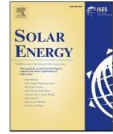
Anna Fedorova, Bjørn Petter Jelle, Bozena Dorota Hrynyszyn, Stig Geving

Solar energy, 230, 376-389, 2021.



Contents lists available at ScienceDirect

Solar Energy

journal homepage: www.elsevier.com/locate/solener

Quantification of wind-driven rain intrusion in building-integrated photovoltaic systems

Anna Fedorova^{*}, Bjørn Petter Jelle, Bozena Dorota Hrynyszyn, Stig Geving

Norwegian University of Science and Technology (NTNU), Department of Civil and Environmental Engineering, NO-7491 Trondheim, Norway

ARTICLE INFO

Keywords:

Building integrated photovoltaics
BIPV
Wind-driven rain
Quantification
Test
Watertightness

ABSTRACT

Wind-driven rain (WDR) impact is a serious exposure that affects performance of the building envelope components and systems. This study presents results from a laboratory investigation of a testing methodology of WDR intrusion in building-integrated photovoltaic (BIPV) systems. The major aspect proposed in this work is a quantification of water intrusion through BIPV systems. For that matter, a water collection system was designed and tested. When water intrusion is quantified, it may enable categorisation and comparison of various BIPV systems according to their watertightness level. This methodology was applied to three BIPV systems designed for roof integration. The methodology can also be modified and used for various building envelope systems, including traditional roof and facade systems without PV or BIPV systems. As the methodology was developed with climate conditions in northern Europe in mind, WDR exposure of extreme levels was applied. Wind speed ranges from 12.9 m/s (strong breeze) to 35.3 m/s (hurricane) were used. When it comes to newly developed and not well-studied building envelope systems, such as various BIPV systems, they should be subjected to a more extensive investigation. The proposed testing methodology could become an extension of the standard investigations of BIPV systems carried out at accredited laboratories.

1. Introduction

Building-integrated photovoltaics (BIPV) are photovoltaic modules designed to be integrated into parts of the building envelope, such as roofs or facades (Jelle et al., 2012). One of the building envelope functions is to keep as much precipitation (rain, wind, hail, snow, etc.) as possible from entering through a building's exterior weather protective skin. When various precipitations occur simultaneously, they have a more complex impact on the building envelope systems. Climate exposure, known as wind-driven rain (WDR), is a co-occurrence of rain and wind that causes an oblique rain intensity vector (Blocken and Carmeliet, 2004). Currently, watertightness testing in building science intends to assess the resistance of the building envelope elements and systems against WDR. On the one hand, before the building envelope systems are installed, they may be examined to withstand WDR exposure. However, this testing is not obligatory for the building envelope systems to be sold on the market as such a test is not a part of The Construction Product Regulation (CPR) No 305/2011 of the European Parliament and the European Council (The European Parliament and the European Council, 2011), which specifies harmonized rules for the marketing of

construction products in the EU. On the other hand, even though the WDR exposure test is quite common, there is a lack of appropriate quantitative data (Blocken and Carmeliet, 2004). Arce-Recatala et al. investigated weathertightness of rear-ventilated façade systems by quantifying WDR intrusion (Arce-Recatala et al., 2020). However, there are no adequate information available on the watertightness level of the building envelope systems in general and BIPV systems in particular. BIPV systems are still mostly seen as electricity generators. Therefore their evaluation focuses on testing and verification according to the International Electrotechnical Commission (IEC) standards (CEA et al., 2016; Wohlgemuth, 2012) IEC 61215 "Terrestrial photovoltaic (PV) modules - Design qualification and type approval" (International Electrotechnical Commission, 2016a, 2016b, 2016c, 2016d, 2016e) and IEC 61730 "Photovoltaic (PV) module safety qualification" (International Electrotechnical Commission, 2016f, 2016g). After a BIPV system has been tested and approved according to these two IEC standards, the system is expected to safely function without design failures during a service life of approximately 25–30 years with a decline in electricity production of no more than 1% per year (Wohlgemuth, 2012). However, BIPV systems are not usually evaluated as components of the building

^{*} Corresponding author.

E-mail address: anna.fedorova@ntnu.no (A. Fedorova).

<https://doi.org/10.1016/j.solener.2021.10.030>

Received 24 November 2020; Received in revised form 24 June 2021; Accepted 9 October 2021

Available online 21 October 2021

0038-092X/© 2021 The Author(s). Published by Elsevier Ltd on behalf of International Solar Energy Society. This is an open access article under the CC BY

license (<http://creativecommons.org/licenses/by/4.0/>).

skin, as a weather screen, and requirements are yet to be stated by the building industry (Pellegrino et al., 2013; Rehde et al., 2016). Requirements for roof and façade systems vary as their testing methodologies are varying. The testing standard NT BUILD 421 “Roofs: Watertightness under pulsating air pressure” (Nordtest Standard, 1993) describes a methodology for assessing roof systems’ ability to withstand WDR. A similar methodology but for façade systems is given in the European standard EN 12155 “Curtain walling. Watertightness. Laboratory test under static pressure” (European Committee for Standardization, 2000) and EN 13050 “Curtain walling. Watertightness. Laboratory test under dynamic condition of air pressure and water spray” (European Committee for Standardization, 2011).

As mentioned earlier, one possible influential aspect that can be determined during WDR testing is the amount of water leakage intruding through the tested system. While quantification of water intrusion is hardly specified for the building envelope systems, for BIPV systems intended for roof integration, this aspect is mentioned in the standard EN 50583-2 “Photovoltaics in buildings. Part 2: BIPV systems” (European Committee for Electrotechnical Standardization, 2016a) in annex A “Resistance to wind-driven rain of BIPV roof coverings with discontinuously laid elements – test method”. It must be noted that no requirements on WDR testing for BIPV façade systems are given in this standard. The following information on water leakage quantification is provided in the standard EN 50583-2 (European Committee for Electrotechnical Standardization, 2016a):

- “A water collector shall be provided, capable of recording the amount of leakage water during any pressure step in the test”.
- “Reference leakage rate ($10 \text{ g/m}^2/5 \text{ min}$, 5 min being the duration of a single test step in the sub-test”.
- “The cases, in which leakages exceeding fine spray and wetting on the underside occur, are considered as being too severe for the application. In any case, the reference leakage rate of ($10 \text{ g/m}^2/5 \text{ min}$ shall not be surpassed”.

There are four sub-tests (A, B, C, and D) defined in the standard EN 50583-2 (European Committee for Electrotechnical Standardization, 2016a), each specifies a WDR combination appropriate to specific climate zones. Sub-test A: low wind speed with severe rainfall rate; Sub-test B: low wind speed with high rainfall rate; Sub-test C: severe wind speed with low rainfall rate; Sub-test D: maximum rainfall rate with no wind (deluge).

In the present study, the water collection system was successfully designed, built, and applied for water leakage quantification for BIPV roof systems. As no structural details or drawings of the water collection system are given in EN 50583-2 (European Committee for Electrotechnical Standardization, 2016a), it is unclear how such a water collection should be executed. If data on quantified water leakages is available, it may be used to evaluate various systems and rank them according to their watertightness level. It might be especially useful for BIPV systems that are planned to be used in areas with harsher climates, and where wind speeds and precipitation levels are excessively varying. So far, watertightness testing of BIPV systems, and in general roof and façade systems, has been carried out without quantification of water intrusion. Hence, there is no appropriate method to quantitatively compare the watertightness of various roof and façade systems.

Thus, the objective of this study is to present the results from a test methodology of quantification of the wind-driven rain intrusion in BIPV systems for roof integration. In the first part of the paper, information on the applied test methodology and equipment is given. Then a short overview of tested BIPV systems presented. As the BIPV systems’ design can significantly vary, information on the design of the tested BIPV systems is also provided. Next, WDR test results are split into three parts, each part dedicated to one of the tested BIPV systems. Each part includes data on water leakage points, wind load levels at which leakages occurred, and the amount of water collected during the testing. The

paper ends with a comparative analysis of the tested BIPV systems.

2. Wind-driven rain testing methodology

Shortly, WDR testing can be described as follows. A constant supply of water (water spray) is applied to the test specimen. It is usual to apply a combination of run-off water applied on an upper side of the tested system and water spray that is distributed along the test specimen surface area. Simultaneously, a specific level of air pressure difference (ΔP) is reached between the outer and inner surfaces of the tested specimen (Perez-Bella et al., 2014). A range of air pressure is applied and increased stepwise. The test specimen is inspected for water passages into its inner surface and water leakage points are registered. As a result, a limit of watertightness can be identified for the tested systems. The limit of watertightness may be described as the maximum level of air pressure applied simultaneously with water spray when no water leakages occur on the tested system’s inner side.

Testing of the present study was executed according to NT BUILD 421 (Nordtest Standard, 1993) with minor modifications, and was mainly based on two studies (Andenaes, 2016; Breivik et al., 2013) carried out with the same large-scale apparatus, i.e. a rain and wind (RAWI) box (Fig. 1) at the NTNU and SINTEF Community laboratory in Trondheim, Norway. The RAWI box allows a step-less variable inclination, controlled differential air pressure applied across the test specimen, run-off water at the top of the test area, and WDR exposure across the test area.

The present test methodology consisted of 2 phases. The test system was first inclined to 30° and thereafter to 15° , where run-off water was applied for 10 min. Inclinations 30° and 15° were chosen because they represent typical ventilated pitched roof angles. In addition, these rather low inclination angles represent worst case scenarios with the potential of large wind-driven rain intrusion, thus they are better suited for testing of watertightness. Inclination angle of 30° was tested before 15° as normally there was expected more water intrusion at lower inclinations. To simulate WDR exposure, a pulsating dynamic air pressure was applied in steps (load levels), starting from load level 0, where no air pressure was used, only run-off water was applied for 10 min. During each load level, the dynamic air pressure was increased by 100 Pa (by 150 Pa for the last load level 7), applied in impulses, each load level lasting for 10 min. In NT BUILD 421, air pressure and run-off water are applied simultaneously from the beginning of the test, and the last air pressure level applied is 550 Pa compared to 750 Pa used in the current study. A summary of the applied test methodology and a comparison of the air pressure levels from NT BUILD 421 are given in Table 1. All parameters that were used in the current study are presented in Table 2.

The main aim of the current study was to quantify water leakages during wind-driven rain testing. An outline of the water collection system that was constructed for the experiments is depicted in Fig. 2.

The water collection system consisted of four equally sized sections (sections 1 – 4 on Fig. 2), but as the main frame ($2.75 \text{ m} \times 2.75 \text{ m}$) was larger than initially planned, two small sections were left along the Section 4 and Section 1. These two sections were not part of the water collection system. Water was collected from the four main sections in four respective containers. During testing of BIPV system 1, 5 L containers were used, whereas during testing of BIPV systems 2 and 3 10 L containers were used. It was decided to use 5 L and 10 L containers as they were weighed on scales during testing and had to be of a suitable size, manageable to lift and carry.

A transparent polycarbonate (Lexan) board was applied as an underlayment, which is correspondent to the roof secondary water barrier. Water collection points were formed at the bottom of the four vertical sections, where one round hole was cut in each section, and a tube was connected to each hole. A triangle profile made of wooden battens was built near each hole. Furthermore, four holes (each with a size of $5 \text{ cm} \times 40 \text{ cm}$) were cut in the underlayment’s upper part as shown in Fig. 2. Firstly, the underlayment must be punctured so that the desired levels of



Fig. 1. Large-scale turnable box for rain and wind tightness testing of sloping building surfaces (RAWI box). Test running with a test sample (left) (Breivik et al., 2013), and RAWI box without a test sample (right) (Andenas, 2016).

Table 1
Pulsating air pressure intervals used in the present study (compared to NT BUILD 421) including description of the test phases.

Air pressure intervals		Test phases used in the present study	
NT BUILD 421	Present study		
	0 (run-off water)	Test phase 1–30° inclination.	Test phase 2–15° inclination.
100 Pa	100 Pa	Run-off water and a range of pulsating air pressures (from 0 Pa to 750 Pa) applied to BIPV system at 30° inclination.	Run-off water and a range of pulsating air pressures (from 0 Pa to 750 Pa) applied to BIPV system at 15° inclination.
200 Pa	200 Pa		Phase 2 was carried out on the same day after phase 1.
300 Pa	300 Pa		
400 Pa	400 Pa		
550 Pa	500 Pa		
	600 Pa		
	750 Pa		

Table 2
Parameters used during wind-driven rain testing.

Load level	Colour mark	Pulsating (dynamic) air pressure intervals (Pa)	Weather condition description	Maximum wind speed (m/s)	Duration (min)
0	Yellow	0, run-off water	–	0	10
1	Light blue	0–100	Strong breeze	12.9	10
2	Blue	0–200	Fresh gale	18.2	10
3	Dark blue	0–300	Strong gale	22.3	10
4	Green	0–400	Storm	25.8	10
5	Yellow-green	0–500	Violent storm	28.8	10
6	Orange	0–600	Violent storm	31.6	10
7	Red	0–750	Hurricane	35.3	10

air pressure difference could be reached and applied to the BIPV system, and not to the underlayment itself. Secondly, the underlayment replicates conditions of a real roof installation when an air cushion accumulates in the ventilated air gap behind the elements and makes the roof system more watertight. And finally, the underlayment is needed to enable the water collection. Moreover, it must be transparent so that the

water leakages can be observed. The tested systems were mainly observed from outside the RAWI box (view depicted on Fig. 1 left), i.e., the BIPV system’s interior side. As the RAWI box has small windows on the opposite side, the systems were also inspected from time to time from that viewpoint (i.e., the exterior side of the BIPV systems) and photographed (photos can be viewed in Section 5).

After the application of the last level of air pressure (750 Pa) was finished, the test system was elevated so water droplets remaining on the underlayment could be collected. After a couple of hours, the underlayment was inspected, and as most water droplets were drained, containers with the collected water were weighed, and the results were recorded. The containers were then placed back to the water collection sections. In the second phase, the same procedure was applied to the test system inclined to 15°. Both phases were carried out on the same day.

During the experimental work, along with measuring the water amounts that went through the tested BIPV systems, the points where the water leakages occurred were registered (data is provided in Section 5). The water leakages were marked with colours according to the load level at which they had first appeared. Colour mark for each load level is given in Table 3. According to EN 50583-2 (European Committee for Electrotechnical Standardization, 2016a), the amount of water leakage should be registered at each load level. Unfortunately, due to a few aspects, it was not feasible to record the intensity of water leakages at each load level during the current study’s experiment. The amount of water leakages was not measured automatically and had to be done manually. Due to time constraints and a limited number of people involved in the experiments, it was not feasible to carry and weigh containers as often as needed for each load level. During testing of BIPV system 1, water leakages were relatively scarce, whereas during testing of the second and third systems the leakages were more severe. Another reason was that during each load level, not only the BIPV system must have been monitored, but also the sealing tapes all around the system must have been inspected. For future investigations it could be beneficial to organize the experiment so that either water would be measured automatically for each load level or that more people could be involved in the running of the laboratory experiments. Then one person could be responsible for operating the equipment, a second person could be monitoring the tested system and sealing tapes around it, and a third person could be responsible for the water leakage collection measurements.

3. Overview of tested BIPV systems

Three BIPV systems were tested in this study. BIPV system 1 was

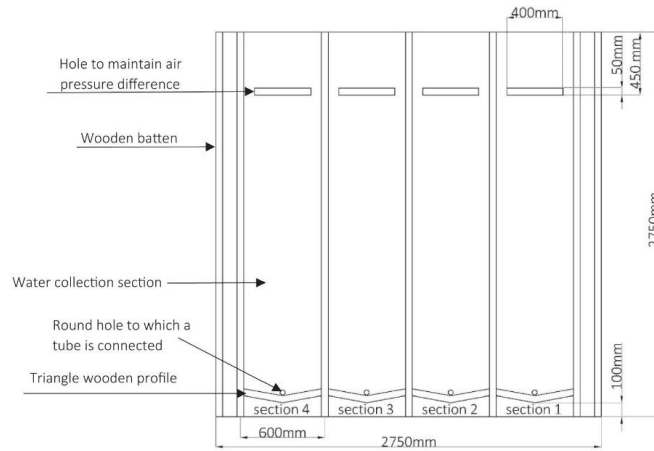





Fig. 2. Outline of the water collection system with four separate water collection sections. View from the interior BIPV system side (backside).

Table 3
Parameters of tested BIPV systems.

Number of system	Type of PV	Illustration	BIPV product category (Jelle et al., 2012)	BIPV system category (Verberne et al., 2014)	BIPV integration category (Fig. 1)	Weight (kg/m ²)	Materials	Producer
BIPV system 1	mono c-Si		Solar tile	Roofing: solar tiles-shingles	A	19.5	Laminated glass-glass module without a frame.	Sunstyle
BIPV system 2	mono c-Si		Solar tile	Roofing: solar tiles-shingles	A	17.1	Tile is made of a ceramic compound; solar cells are covered with glass.	Heda Solar
BIPV system 3	CdTe		BIPV module	In-roof system/warm facade	A, C	18	Laminated glass-glass module with steel profile on the left and right side of each module.	Ennogie

constructed by fish-scale solar shingles resembling the skin of a fish. Each solar shingle is a compound of two layers of safety glass with solar cells laminated between them. Therefore, such modules are called glass-glass modules. The full product range is given in Fig. 4 in sub-Section 4.1. If needed, the BIPV system can be complimented to fit the roof shape using colour-matching aluminium composite plates, which can be cut to various sizes and forms. Solar shingles are available in three colours: black, brick red, and slate grey, which are typical, neutral colours and can match most of the traditional roof systems when used as supplements. BIPV system 2 was composed of flat solar tiles and their matching tiles. Rectangular-shaped tiles are made of a ceramic compound, and the tiles with solar cells are covered with tempered glass. The matching tile is half of the size of the solar tile. These tiles are available only in black

colour, but manufacturer produces a variety of colours for other tiles. Finally, BIPV system 3 was constructed by large size BIPV modules, reminiscent standard PV modules. They are glass-glass modules installed on coated steel rails attached to each module's left and right side, which eases the installation. Only black coloured modules are available.

All BIPV systems can be categorized (Fedorova et al., 2020) by the type of BIPV products (Jelle et al., 2012); by the type of BIPV systems and the way of integration into the building envelope (Verberne et al., 2014); and by the BIPV categories given in the standard EN 50583 (Fig. 3) (European Committee for Electrotechnical Standardization, 2016a, 2016b). BIPV system 1 solar shingles and BIPV system 2 solar tiles are designed for roof integration. Therefore, they are categorized as roofing BIPV systems, while modules of BIPV system 3 can be integrated

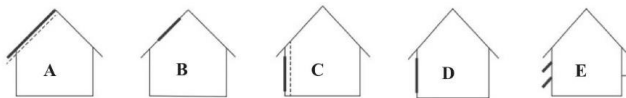


Fig. 3. BIPV categories as defined in EN 50583 (European Committee for Electrotechnical Standardization, 2016a, 2016b). (A) Sloped, roof-integrated, not accessible from within the building. (B) Sloped, roof-integrated, accessible from within the building. (C) Non-sloped (vertically) mounted, not accessible from within the building. (D) Non-sloped (vertically) mounted, accessible from within the building. (E) Externally integrated, accessible or not accessible from within the building (Fedorova et al., 2020).

into the roof or the façade. The weight of all three systems is remarkably close to each other. The lightest is BIPV system 2 with 17.1 kg/m^2 , then BIPV system 3 with 18 kg/m^2 , and BIPV system 1 with 19.5 kg/m^2 . The parameters of these BIPV systems are summarized in Table 3.

4. Installation of BIPV systems

The tested BIPV systems were installed according to the manufacturers' manuals. The manuals are available on the manufacturers' websites or could be requested from the manufacturers or BIPV system resellers. The same frame, $2.75 \text{ m} \times 2.75 \text{ m}$ (Fig. 2), built of wooden beams, was used for all the tested BIPV systems. The following information is presented in this chapter: photos of BIPV systems installed on actual building roofs, BIPV systems design and installation details that the authors find beneficial to mention, images of the BIPV systems installed in the laboratory, and the technical outline of the BIPV installations.

4.1. BIPV system 1 details

BIPV system 1 installation on an actual building roof is depicted in Fig. 4 (left). Glass-glass BIPV shingles of four shapes are presented on the market (marked with 1, 2, 3, and 4 on Fig. 4 (right)) and can cover the roof of various sizes using only solar shingles and additional triangle glass-glass parts (Fig. 5 (middle), marked with 5).

When needed, this system can be complemented by metal plates. However, these metal plates have a significantly smaller thickness and different stiffness from their BIPV counterparts and could thus cause additional water leakages as anticipated and demonstrated during testing. It must also be noted that it was not obvious how these metal plates should be installed. The manufacturer provided only BIPV shingles and small glass-glass triangle parts, made of the same materials. The metal plates are provided when the BIPV system is purchased from a reseller. Thus, no specific manuals and clear details are given for installing metal plates with the BIPV system. In Fig. 4 (middle) the metal plates are fixed using small screws, which differ from the screws used for BIPV system 1. When the system was delivered to the laboratory, both types of screws were provided. The final recommendation was to use the same screws as used for BIPV system 1. However, that led to metal plates not being screwed as tight as they would when screwed with the smaller screws.

A few rubber elements provided with BIPV system 1 are attached to each solar shingle (Fig. 5). Reverse anchor-like components are attached to the upper part of the BIPV shingles, with a line of rubber sealing the gap between shingles (Fig. 5, illustrated on the left picture and shown on the middle photo, marked with white rectangles). Additionally, rubber gaskets are used under each screw (Fig. 5 (right)).

The tested BIPV system 1 consisted of three whole and three half BIPV shingles (one solar shingle top, one solar shingle bottom and one

solar shingle left), four glass-glass elements, which were shaped to the system profile and provided with the system. Four metal plates, also shaped to fit the remaining parts of the profile, were cut in the laboratory. After the installation was finished, parts around the system were covered with a 0.15 mm thick polyethylene foil and connected to the BIPV system using sealing tapes. Then, the polyethylene foil was attached to the wooden frame using duct tape. BIPV system 1 with completed taping is depicted in Fig. 6. The same procedure of covering the surrounding wooden frame was used for all three BIPV systems tested in this study. The system outline (Fig. 6) shows how the solar shingles and complementing elements are connected.

4.2. BIPV system 2 details

An installation of flat solar tiles and matching tiles on an actual building roof is depicted in Fig. 7. The number of roof tiles with solar cells used on the roof will depend on the building's electricity demand, where the rest of the roof area can be covered with the matching tiles. Solar tiles have a unique design that provides drainage of water. Their mounting is similar to the mounting of conventional roof tiles. Tiles are placed on wooden beams and secured with hurricane clip nails (hooks) on each tile's right side, which is also standard for the conventional roof tiles. Additionally, solar tiles are secured with three screws, and matching tiles with two screws, on top of each tile.

Manufacturer produces an extensive range of solar tiles, varying in shape (wave tiles, flat tiles, flat tiles with borders) and colours. A variety of solar tiles may provide more accessible solutions to suit a particular built environment.

BIPV system 2 consisted of four BIPV roof tiles with eight matching tiles (one of which was cut in two). An outline of BIPV system 2, which shows how the tiles are connected, and the system with completed taping are depicted in Fig. 8. Solar tiles are coloured in dark grey with black rectangles with stripes illustrating the solar cells, whereas matching non-solar tiles are coloured in light grey for visualization purposes, in reality they have the same colour.

4.3. BIPV system 3 installed with metal roof plates details

BIPV system 3 was constructed with glass-glass modules, which can be installed in two ways: orientated vertically or horizontally. In this study modules were installed vertically. Most of the realized projects utilize BIPV modules only, covering the roof's whole area. Depending on the energy need of a particular building, it may not be necessary to cover the roof's entire area with solar modules. BIPV modules might be installed along metal roofing plates.

In the current study, BIPV system 3 was integrated with steel roof plates that have no PV elements on them (Fig. 10). These two roof systems have not been designed to be installed together but were used for our experimental purpose. Example of real-life installation of steel roof

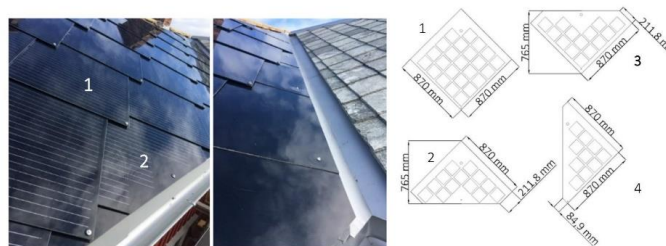


Fig. 4. BIPV system 1 installed on an actual building roof (left). Metal plates completing the BIPV system 1 at edges (middle). Range of BIPV shingles (right): 1 – basic solar shingle; 2 – solar shingle bottom; 3 – solar shingle top; 4 – solar shingle left.



Fig. 5. Rubber element on upper part of the solar shingle (schematically shown on the drawing to the left and how they are attached on the real roof shown on the photo in the middle) and lower part of the solar shingle (right). 1 – basic solar shingle, 3 – solar shingle top and 5 – matching glass-glass triangle element on an actual building roof.

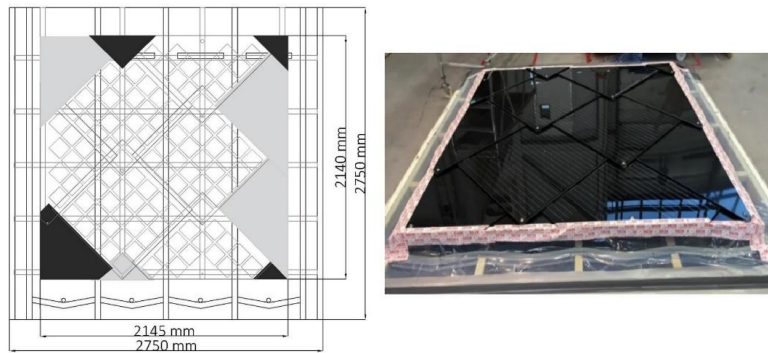


Fig. 6. Front view of the outline of BIPV system 1. To distinguish components of the system and to make connecting points better visible, BIPV shingles are left transparent, grey parts are metal plates, and black parts are glass-glass parts without PV cells. BIPV system 1 with completed taping before laboratory testing. View from the bottom of the exterior BIPV system side.

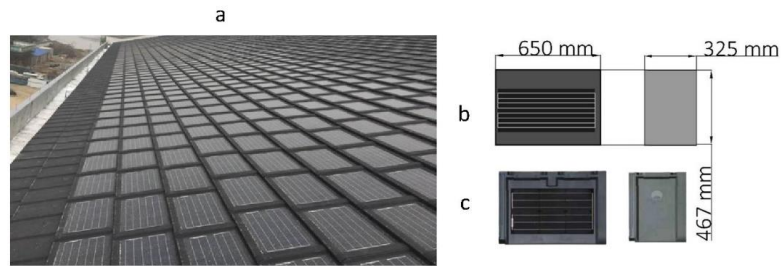


Fig. 7. (a) Complete solar tile system on an actual building roof, (b) solar tile and matching non-solar tile with dimensions, and (c) actual solar tile and dummy tile. The matching tile may seem more of a greyish colour here, but in reality, it is the same black colour as solar tile (“Heda Solar product catalogue,” 2017).

plates is shown in Fig. 9.

Steel rails attached to each module’s left and right side were not only helpful to ease the installation of the BIPV modules, but also made it uncomplicated to couple them with steel roof plates. Both BIPV modules and steel roof plates were fixed to the wooden beams with screws.

BIPV system 3 consisted of four BIPV modules with six rows of steel roof plates. The system outline and completed taping is depicted in Fig. 10. The BIPV modules are coloured in dark grey, whereas the steel

roof plates are coloured in light grey, similar to systems’ colours in real life.

5. Results and discussion

Before data on the water collection was aggregated, several trial tests were conducted to ensure that the water collection system was ready for testing. The data sets gathered are presented in the order the BIPV

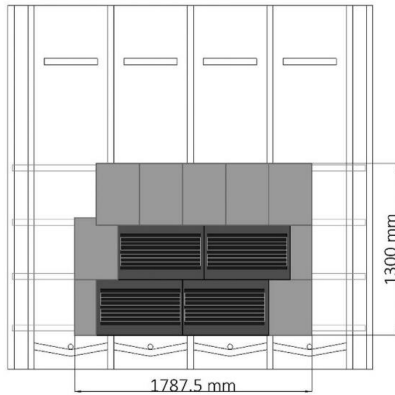


Fig. 8. Front view of the outline of BIPV roof tile system. To distinguish solar tiles from matching tiles they are coloured in dark grey and black (solar tiles) and light grey (matching tiles). As depicted on the picture on the right, in reality both types of tiles have the same black colour. Here BIPV roof tile system shown with completed taping before laboratory testing. Front view of the exterior BIPV system side.



Fig. 9. Isola Powertekk steel roof plates (non-PV) installed on an actual building roof ("<https://www.isola.com/>").

systems were tested: first, BIPV system 1, then BIPV system 2, and finally BIPV system 3 installed with steel roof plates.

5.1. Testing of BIPV system 1

The WDR tightness test of BIPV system 1 started with the system being inclined at 30° (Fig. 11) and load level 0. After 10 min of applying run-off water, a differential air pressure of 100 Pa (load level 1) was used, moving in 10 min periods to load levels 2 and 3. No water leakages were detected up to load level 4 (400 Pa). Water droplets started to occur in two areas where BIPV full shingles overlapped with the metal plates (all points of water leakages are shown in Fig. 12). New points of water droplets occurred at load levels 5 (500 Pa) and 6 (600 Pa). No new leakages were detected at the last load level 7 (750 Pa). Leakages that occurred had been intensifying at each next load level. When the test for 30° inclination was over, the system was elevated to nearly 90° inclination and left to dry.

For the next stage of the test, the system was inclined to 15°. The same procedure was followed, starting at load level 0, and finishing with load level 7 (750 Pa). Water leakages began to occur one load level earlier than at the previous stage, but only at the point where the metal plates were screwed together. A small amount of droplets occurred at

load level 4 (400 Pa) at the points where the BIPV shingles overlapped with the metal plates, following water leakages along the overlapping area at load level 5 (500 Pa) (the same area where water leakages occurred at load levels 4 (400 Pa) and 6 (600 Pa) at the previous stage). Small water leakages were visible on the overlap of the BIPV half-shingle lower tile, glass-glass triangle, and metal plate. The first water leakage between the BIPV shingles (the whole shingle and the half-shingle right tile) occurred at the last load level. Observations are summarized in Table 4 and water leakage points are marked in Fig. 12. After this stage was finished, the system was again lifted to nearly 90° to dry.

BIPV system 1 was initially tested at two inclinations (30° and 15°). As the system showed a high level of watertightness, it was decided to conduct an additional testing stage as a possible worst-case scenario where screws were loosened by three full turns each. The system was inclined to 15° angle, as the impact of the WDR is expected to be more forceful on lower inclined roof systems. During this stage of the test, no water leakages occurred until load level 2 (200 Pa). Water droplets appeared at the points where metal plates were screwed together and at the overlapping point of them, and where the half-shingle right was screwed with the glass-glass part. At the next load level, new points with water leakages emerged at overlaps of whole shingles and metal plates. Following new leakage points at load levels 4 (400 Pa) and 5 (500 Pa) (various overlapping points of shingles, glass-glass parts, and metal plates). At the last load level, 7 (750 Pa), droplets appeared on the glass-glass part where it overlapped with the metal plate. During the first two WDR testing at 30° and 15° inclination, before the test where the fastening screws were loosened, it was observed that the metal plates were slightly bending from the BIPV shingles when the air pressure was pulsating due to a difference in stiffness in the metal plates and their BIPV counterparts (and possible differences in distance between fastening screws), thus causing larger water leakages at these locations, which lead to considerably larger water leakages collected in Sections 3 and 4 as compared with Sections 1 and 2 for both inclinations as depicted in Fig. 14.

Water collected from the respective four sections was weighed on a scale after each test phase. As the amount of water did not exceed 3 L (5 L containers for each collection section were used when BIPV system 1 was tested), it could be measured once per the test phase. The quantified results of these water leakage measurements for BIPV system 1 are collected in Fig. 14.

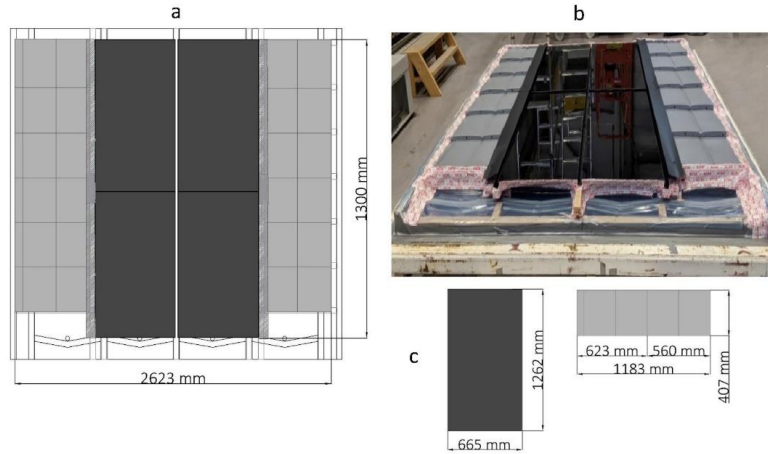


Fig. 10. Front view of the outline of BIPV system 3 and steel roof plates. The BIPV modules are coloured in dark grey, whereas steel roof plates are coloured in light grey. BIPV system 3 integrated with steel roof plates with completed taping before laboratory testing. View from the bottom of the exterior BIPV system side.



Fig. 11. BIPV system 1 during wind-driven rain testing in the RAWI box. Interior BIPV side (left) and exterior BIPV side (right).

5.2. Testing of BIPV system 2

BIPV system 2 did not cover the whole testing frame. Due to time and economic constraints, it was not feasible to obtain more tiles from the manufacturer, and the testing was thus run, as shown in Fig. 16. Two stages of WDR tightness testing were conducted for 30° and 15° angle inclinations, following the same procedure as for BIPV system 1 testing. BIPV system 2 during testing is shown in Fig. 15. Before the experiment with water collection started, a few trials to test the sealing tape were carried out. More severe water leakages occurred already at load level 1 (100 Pa), compared to the leakages in BIPV system 1, and hence 5 L containers were changed to 10 L containers for each collection section.

At the first phase (30° inclination), water leakages appeared at load level 1 (100 Pa) at four locations: two leakage points between matching tiles and two leakage points between solar tiles connected to matching tiles. During the next load level, more leakages started to appear with higher intensities. Only one more leakage point occurred during load

level 3 (300 Pa). During the following load levels, no new leakages occurred. All earlier appeared leakage points remained, and each water leakage's intensity was increasing with each next load level. At the second test phase (15° inclination), leakages occurred at the same load levels and approximately at the same points but at a higher rate. At load level 1 (100 Pa), six water leakage points occurred (compared to the four leakage points at the first phase) and at load level 2 (200 Pa), thirteen leakage points occurred (compared to the six points at the first phase). More leakages appeared at load level 3 (300 Pa), all of them, along the downside of the lower row of tiles of the BIPV system. Observations of both phases of the test are summarized in Table 5. All leakage points are shown in Fig. 16 A and 16B.

During testing of BIPV system 2, it was first attempted to weigh the leakage water amount at each load level. It was then decided to proceed with weighing the water amount from each water collection section summarized for each phase. The quantified results of these water leakage measurements for BIPV system 2 are collected in Fig. 17. As

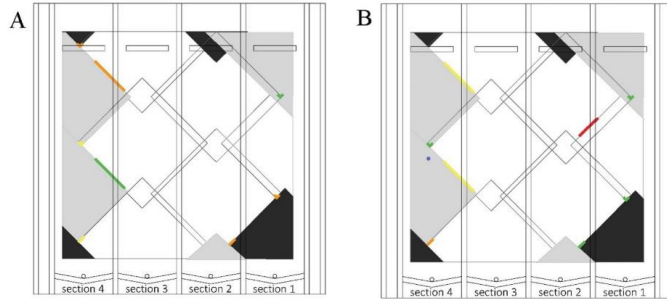


Fig. 12. Location of water leakage points for BIPV system 1 with corresponding colours as given in Table 4. A – first test phase (inclination 30°); B – second test phase (inclination 15°). View from the backside of the BIPV system.

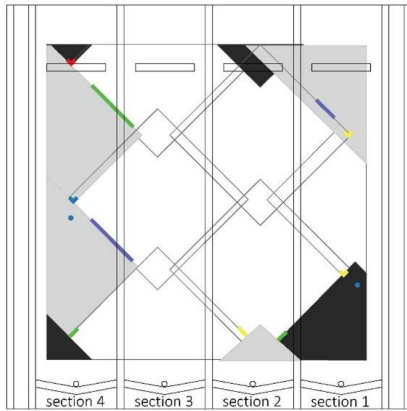


Fig. 13. Location of water leakage points for BIPV system 1 with corresponding colours as given in Table 4. Second test phase ran for the second time with the BIPV system inclined to 15°. All screws were loosened by three turns each. View from the backside of the BIPV system.

shown in Fig. 17, the amounts of water collected at the 30° inclination from Sections 4 and 3 are higher than the amounts collected from the same sections at the 15° inclination. However, data collected for sections 2 and 1 showed the opposite, i.e., the water amounts collected at the 15° inclination were slightly higher than at the 30° inclination, where the observed differences are larger than the estimated uncertainties in the water collection measurements.

5.3. Testing of BIPV system 3 and steel roof plates

The third tested system was constructed with BIPV modules installed along with steel roof plates. The BIPV system consisted of two pairs of modules (four modules in total). One module overlapped with the second module in each pair, and a rubber sealant profile was placed between them to fill in the gap. The two lower modules were installed first, then pieces of the rubber profile were placed on top of each module, followed by the installation of the two upper modules. The rubber sealant profile was not visible from the front side of the BIPV system and

Table 4
Qualitative observations of water leakages during wind-driven rain tightness testing in the RAWI box for BIPV system 1.

Load level	Pulsating air pressure (Pa)	Colour mark	Inclination 30° (Fig. 12 A)	Inclination 15° (Fig. 12 B)	Inclination 15°* (Fig. 13)
0	0 (run-off water)	Yellow	No water leakages	No water leakages	No water leakages
1	0–100	Light blue	No water leakages	No water leakages	No water leakages
2	0–200	Blue	No water leakages	No water leakages	Leakages occurred
3	0–300	Dark blue	No water leakages	Leakages occurred	New leakages occurred
4	0–400	Green	Leakages occurred	New leakages occurred	New leakages occurred
5	0–500	Yellow-green	New leakages occurred	New leakages occurred	New leakages occurred
6	0–600	Orange	New leakages occurred	New leakages occurred	No new leakages
7	0–750	Red	No new leakages	New leakages occurred	New leakages occurred

*All screws of the tested system were loosened by three turns.

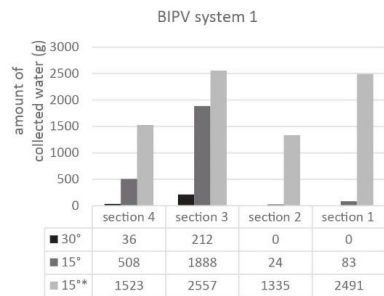


Fig. 14. Quantitative measurements of water amounts collected during wind-driven rain testing in the RAWI box for BIPV system 1.



Fig. 15. BIPV system 2 during wind-driven rain testing in the RAWI box. Interior BIPV side (upper photo) and exterior BIPV side (bottom photo).

Table 5
Qualitative observations of water leakages during wind-driven rain tightness testing in the RAWI box for the BIPV system 2.

Load level	Pulsating air pressure (Pa)	Colour mark	Inclination 30° (Fig. 16 A)	Inclination 15° (Fig. 16 B)
0	0 (run-off water)	Yellow	No water leakages	No water leakages
1	0–100	Light blue	Leakages occurred	Leakages occurred
2	0–200	Blue	New leakages occurred	New leakages occurred
3	0–300	Dark blue	New leakages occurred	New leakages occurred
4	0–400	Green	No new leakages	No new leakages
5	0–500	Light green	No new leakages	No new leakages
6	0–600	Orange	No new leakages	No new leakages
7	0–750	Red	No new leakages	No new leakages

could therefore not be inspected for correct placement during installation. When the system was later placed in the RAWI box and inclined at 30° for the test, it was possible to observe the rubber sealant profiles. However, no visible difference in the placement of the sealant profile between the left pair and the right pair of modules was observed.

At the first test phase (30° inclination) of the WDR testing, no water leakages were detected at load levels 0 and 1. However, the rubber profile between the right pair of modules had started to move/dislocate,

and at load level 2 (200 Pa), water began to run through it. New leakages occurred at load level 4 (400 Pa) at points where the metal plates overlapped, the parts close to the BIPV modules. A small number of water droplets appeared on the rubber profile between the left pair of modules. Water leakage points remained the same during all the next load levels, increasing in intensity with each next load level.

At the second test phase (15° inclination), water leakages appeared at the same locations, but at lower load levels: between the right pair of modules at load level 1 (100 Pa), at metal plate overlaps, and between the left pair of modules at load level 3. As the BIPV system was mounted and sealed with waterproof tapes, it was not feasible to correct the sealing profile placement between the right pair of BIPV modules. Therefore, it was decided to run the test as it was and investigate how much leakages would occur if the sealing profile was dislocated. Additionally, moderate water leakages occurred between the upper modules at the last load level. The difference in the amount of water leakage through the rubber profile between the left and right pair of BIPV modules at 30° and 15° inclinations can be observed in Fig. 22. A comparison of the rubber profile between the left and right pairs of the modules during testing is shown in Figs. 18 and 19, and after the WDR test was fully finished is shown in Fig. 20.

Observations of both phases of the test are summarized in Table 6. All water leakage points are shown in Fig. 21A and 21B. The quantified results of these water leakage measurements for BIPV system 3 integrated with steel roof plates are collected in Fig. 22.

Even though data on leakage water collected during WDR testing of

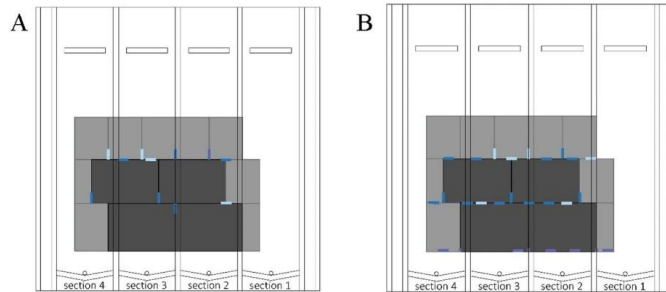


Fig. 16. Location of water leakage points for BIPV system 2 with corresponding colours as given in Table 5. A – first test phase (inclination 30°); B – second test phase (inclination 15°). View from the backside of the BIPV system.

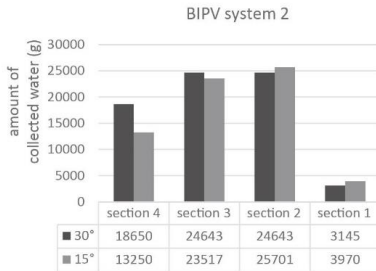


Fig. 17. Quantitative measurements of water amounts collected during wind-driven rain testing in the RAWI box for BIPV system 2.

BIPV system 3 is provided, it must be noted that an utterly watertight tape sealing was not achieved for this system (see Fig. 10). Thus, the amount of water included in Fig. 22 also contains some amount of water that ran through the sealing tape system. The test was run anyway to study the behaviour of this system under WDR exposure. The amount of water collected from Section 3 corresponds to a small water leakage between the left pair of BIPV modules. In contrast, the water amount collected in Section 2 is approximately 21 and 16 (for 30° and 15° inclination, respectively) times larger than in Section 3.

Such a large difference occurred due to the rubber sealant profile's displacement between the right pair of the BIPV modules. Therefore, it can be advisable to include in the installation manual information about the importance of the proper placement of the sealant profile. Additionally, a solution for fixing this rubber profile on the module may be found to avoid the displacement. In water collection sections 4 and 1, the water leakage was collected from the points connecting the BIPV system with steel roof plates. The steel rails attached to the left and right side of

BIPV modules are designed for water drainage, and steel roof plates on both sides of the BIPV system were placed over the steel rails. The distance from the roof plates placed to the right pair of BIPV modules was wider than the distance from the left pair of BIPV modules to the roof plates. Consequently, the amount of leakage water on the right side of the BIPV modules (Section 1) was approximately 3.5–3.6 times larger than on the left side of the BIPV modules (Section 4), for inclination 30° and 15°, respectively. Therefore, it can be concluded that the steel roof plates should be placed closer to the BIPV modules to minimize water leakage.

5.4. Comparison of tested BIPV systems

As was anticipated before the experiment, test results showed that the most watertight BIPV system among the tested ones was BIPV system 1, with respect to short-time wind-driven rain exposure tests. Multiple rubber sealing elements used during the system installation provided a reliable waterproofing. However, if after installation, the BIPV system needs adjustment or the cabling needs to be checked, it should be advised to change the used sealing elements to new ones. The BIPV shingles are screwed quite tightly, and sealing elements are hence squeezed. Thus, they might be deformed, and thereby loose waterproofing ability to some degree. Careful use of a rubber sealing profile was also necessary for BIPV system 3. If the sealing profile is placed correctly and stays in place, the watertightness level is quite close to BIPV system 1. However, more investigations of the long-term performance of the rubber sealing profiles should be carried out, as the durability of these materials may be much shorter than the service lifetime of the BIPV system. BIPV system 2 resembles conventional roof tiles and was expected to be less watertight than the other two BIPV systems. As no sealing materials were used in BIPV system 2, it should be compared to data on the watertightness of conventional roof tiles. From the graph in Fig. 17 it can be concluded that BIPV system 2 has an advantage when it comes to a lower inclination angle. BIPV system 2 performed almost as good or even better at 15° than at 30° inclination,

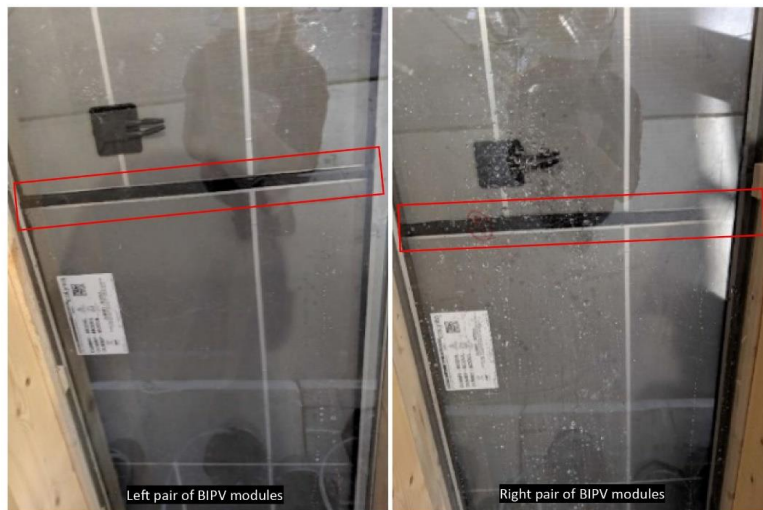


Fig. 18. The rubber sealant profile (marked with white rectangles) between pairs BIPV modules during wind-driven rain testing in the RAWI box with 30° inclination. A major difference in water leakage intensity between left pairs (no leakage) and right pairs (intense leakage) of the BIPV modules could be observed.

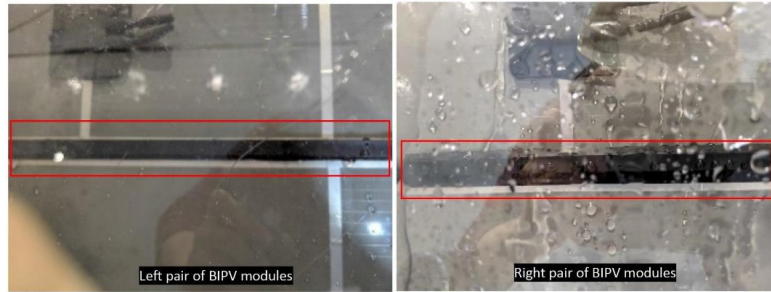


Fig. 19. The rubber sealant profiles (marked with white rectangles) between BIPV modules during wind-driven rain testing in the RAWI box with 15° inclination. A major difference in water leakage intensity between left pairs (no leakage) and right pairs (intense leakage) of the BIPV modules could be observed.



Fig. 20. The rubber profile between the pairs of BIPV modules (marked with white rectangles) inspected after wind-driven rain testing in the RAWI box for BIPV system 3 installed with steel roof plates. The rubber profile between right pair of modules was dislocated and had lost its sealing function, while the rubber profile between the left pair of modules was still in place and thus no water leaked through it.

Table 6
Qualitative observations of water leakages during wind-driven rain tightness testing in the RAWI box for BIPV system 3 installed with steel roof plates.

Load level	Pulsating air pressure (Pa)	Colour mark	Inclination 30° (Fig. 21 A)	Inclination 15° (Fig. 21 B)
0	0 (run-off water)	Yellow	No water leakages	No water leakages
1	0–100	Light blue	No water leakages	Leakages occurred
2	0–200	Blue	Leakages occurred	No new leakages
3	0–300	Dark blue	No new leakages	New leakages occurred
4	0–400	Green	New leakages occurred	No new leakages
5	0–500	Light yellow	No new leakages	No new leakages
6	0–600	Orange	No new leakages	No new leakages
7	0–750	Red	No new leakages	New leakages occurred

whereas the two other BIPV systems were less watertight at 15° than at 30° when compared to themselves. The watertightness level of the tested BIPV systems is provided in Table 7.

Even though the watertightness level may be identified without quantification of the water leakage, it is an influential parameter that can support a more precise classification of the tested BIPV systems. In this study, both BIPV systems 1 and 3 are watertight at 300 Pa at 30° inclination and at 200 Pa at 15° inclination. However, without additional data on the amount of water that go through each system it is not possible to quantitatively compare and identify which of these systems are the more watertight ones.

6. Conclusions

The aim of this study was to quantify the water intrusion during wind-driven rain test in building-integrated photovoltaic (BIPV) systems. A test methodology for testing the watertightness of roof and facade systems was presented and applied utilizing a water collection

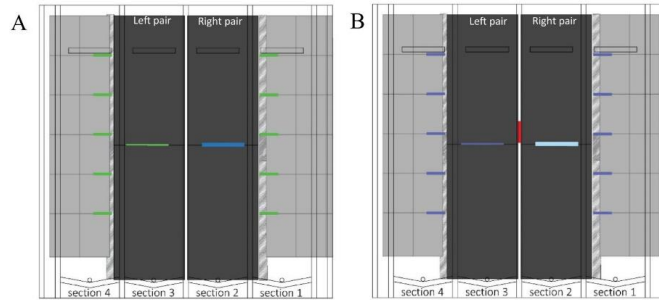


Fig. 21. Location of water leakage points for BIPV system 3 installed with steel roof plates with corresponding colours as given in Table 6. A – first test phase (inclination 30°); B – second test phase (inclination 15°). View from the backside of the BIPV system.

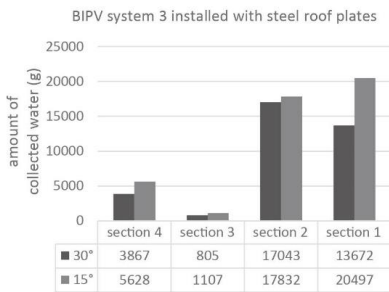


Fig. 22. Quantitative measurements of water amounts collected during wind-driven rain testing in the RAWI box for BIPV system 3 installed with steel roof plates. Note that some of the water collected here has erroneously run through the sealing tape system.

Table 7
Watertightness level of tested BIPV systems.

	Angle of inclination		Weather condition equivalent of air pressure	
	30°	15°		
BIPV system	Watertight at air pressure level		200 Pa ≡ fresh gale	
BIPV system 1	300 Pa	200 Pa	18.2 m/s	
BIPV system 2	300 Pa	200 Pa	300 Pa ≡ strong gale	
Metal roof plates	300 Pa	200 Pa	22.3 m/s	
BIPV system 3	0 Pa (run-off water)	0 Pa (run-off water)		

system. The test methodology was applied to three different BIPV systems for roof integration.

The study’s principal finding is the design of a successfully functioning water collection system and results from these laboratory investigations with quantified water leakages from different BIPV systems.

Acquired data on the amount of water leakages collected during the test provides the ground for comparing different systems. The systems can be ranked according to their watertightness level, i.e., the maximum level of air pressure applied simultaneously with water spray when no water leakages occur on the tested system’s inner side. Quantification of the amount of water that go through the tested systems can provide additional valuable information for a more precise classification, identifying the causes for the different water leakages and their magnitudes, and hence providing the necessary information for further improving the BIPV systems. The watertightness level is determined for all the tested systems. Such a ranking may be helpful when choosing which BIPV system is the most suitable for a particular climate.

Declaration of Competing Interest

The authors declare that they have no known competing financial interests or personal relationships that could have appeared to influence the work reported in this paper.

Acknowledgements

This work has been supported by the Research Council of Norway within the ENERGIX program and several partners through the research project “Building Integrated Photovoltaics for Norway” (BIPV Norway, project no. 244031).

References

Audenates, E., 2016. Wind-driven rain exposure and assessment of building integrated photovoltaic systems. MSc thesis. Norwegian University of Science and Technology, Trondheim.

Arce-Recatala, M., Garcia-Morales, S., Van Den Bossche, N., 2020. Quantifying wind-driven rain intrusion - a comparative study on the water management features of different types of rear-ventilated facade systems. E3S Web Conf., NSB 2020: 12th Symposium on Building Physics 172.

Blocken, B., Carmeliet, J., 2004. A review of wind-driven rain research in building science. J. Wind Eng. Ind. Aerodyn. 92, 1079–1130.

Breivik, C., Jelle, B.P., Tjøne, B., Holmberget, Ø., Nygård, J., Bergheim, E., Dalehaug, A., 2013. Large-scale experimental wind-driven rain exposure investigations of building integrated photovoltaics. Sol. Energy 90, 179–187.

CEA, Tecnelia, CTCV, 2016. Standardization needs for BIPV. PVSITES.

European Committee for Electrotechnical Standardization, 2016a. EN 50583-2. Photovoltaics in buildings. Part 2: BIPV systems.

European Committee for Electrotechnical Standardization, 2016b. EN 50583-1. Photovoltaics in buildings - Part 1: BIPV modules.

European Committee for Standardization, 2011. EN 13050:2011. Curtain walling. Watertightness. Laboratory test under dynamic condition of air pressure and water spray.

European Committee for Standardization, 2000. EN 12155. Curtain walling. Watertightness. Laboratory test under static pressure.

- Fedorova, A., Hrynyszyn, B.D., Jelle, B.P., 2020. Building integrated photovoltaics from products to system integration – a critical review. *IOP Mater. Sci. Eng.*
- Heda Solar product catalogue, 2017. <https://www.isola.com/> [WWW Document], (accessed 9.15.20).
- International Electrotechnical Commission, 2016a. IEC 61215-1. Terrestrial photovoltaic (PV) modules - Design qualification and type approval - Part 1: Test requirements.
- International Electrotechnical Commission, 2016b. IEC 61215-1-1. Terrestrial photovoltaic (PV) modules - Design qualification and type approval - Part 1-1: Special requirements for testing of crystalline silicon photovoltaic (PV) modules.
- International Electrotechnical Commission, 2016c. IEC 61215-1-2. Terrestrial photovoltaic (PV) modules - Design qualification and type approval - Part 1-2: Special requirements for testing of thin-film Cadmium Telluride (CdTe) based photovoltaic (PV) modules.
- International Electrotechnical Commission, 2016d. IEC 61215-1-3. Terrestrial photovoltaic (PV) modules - Design qualification and type approval - Part 1-3: Special requirements for testing of thin-film amorphous silicon based photovoltaic (PV) modules.
- International Electrotechnical Commission, 2016e. IEC 61215-1-4. Terrestrial photovoltaic (PV) modules - Design qualification and type approval - Part 1-4: Special requirements for testing of thin-film $\text{Cu}(\text{In,Ga})(\text{S,Se})$ (CIGS) based photovoltaic (PV) modules.
- International Electrotechnical Commission, 2016f. IEC 61730-1. Photovoltaic (PV) module safety qualification - Part 1: Requirements for construction.
- International Electrotechnical Commission, 2016g. IEC 61730-2. Photovoltaic (PV) module safety qualification - Part 2: Requirements for testing.
- Jelle, B.P., Breivik, C., Røkenes, I.L.D., 2012. Building integrated photovoltaic products: A state of the art review and future research opportunities. *Sol. Energy Mater. Sol. Cells* 100, 69–96.
- Nordtest Standard, 1993. NT BUILD 421. Roofs: watertightness under pulsating air pressure.
- Pellegrino, M., Flaminio, G., Graditi, G., 2013. Testing and standards for new BIPV products. *IECON 2013 - 39th Annu. Conf. IEEE Ind. Electron. Soc.* 8127–8132.
- Perez-Bella, J.M., Domínguez-Hernández, J., Cano Sutiñi, E., del Coz Díaz, J.J., Suárez-Domínguez, F.J., 2014. A comparison of methods for determining watertightness test parameters of building façades. *Build. Environ.* 78, 145–154.
- Rehde, F., Szacsavay, T., Peppas, A., 2016. Review of standards for integrating BIPV-modules in building facade and roof. Fraunhofer ISE.
- The European Parliament and the European Council, 2011. the Construction Product Regulation (CPR) 305/2011. Off. J. Eur. Union.
- Verberne, G., Bonomo, P., Frontini, F., van den Donker, M.N., Chatzipanagi, A., Sinapis, K., Folkerts, W., 2014. BIPV products for facades and roofs: a market analysis. 29th EU-PVSEC. Amst.
- Wohlgemuth, J.H., 2012. Standards for PV modules and components - recent developments and challenges. 27th Eur. Photovolt. Sol. Energy Conf. Exhib.

ISBN 978-82-326-7556-2 (printed ver.)
ISBN 978-82-326-7555-5 (electronic ver.)
ISSN 1503-8181 (printed ver.)
ISSN 2703-8084 (online ver.)



NTNU

Norwegian University of
Science and Technology